Novel Ruthenium Complexes and Their Applications as Catalysts and Anticancer Agents

Andrea Rodríguez Bárzano

Submitted in accordance with the requirements for the degree of Doctor of Philosophy

The University of Leeds

School of Chemistry

May 2013

The candidate confirms that the work submitted is her own and that appropriate credit has been given where reference has been made to the work of others.

This copy has been supplied on the understanding that it is copyright material and that no quotation from the thesis may be published without proper acknowledgement.

The right of Andrea Rodríguez Bárzano to be identified as Author of this work has been asserted by her in accordance with the Copyright, Designs and Patents Act 1988.

Acknowledgements

Firstly, I thank Patrick for giving me the opportunity of spending these years in his lab, for sharing his knowledge, for his invaluable guidance, help and support and, no less importantly, for making my time with the McGowan group such an enjoyable experience. Thank you to TSB for the funding and to all the members of the Cp* project. Particularly, thank you to John, for all the meetings and advice and to Tom and Ben for their help with the hydrogenations.

Many thanks to Christopher Pask for basically everything, from very constructive discussions to disgusting pump-oil changing. We miss you upstairs. Special thanks go to the technical staff at Leeds, including Colin Kilner, Simon Barrett, Tanya Marinko-Covell and Ian Blakeley, who provided analyses and characterisation data. Chapter 6 would not have been possible without the efforts of our "Bradford team": Rianne and Aida, I cannot thank you enough. Thank you also to the iPRD members, mainly Peter Baldwin for testing some of my compounds against racemisations and James Tunstall for his patience with the "delicate" GC machine.

Thanks to all the people in the McGowan and Halcrow groups (past and present) for the fun. I will probably forget someone, but I have to mention Joel and Alun (for sharing the "ruthenium joy"), Chris, Felix (endless knowledge of everything technology-related), Steph, Rianne, Aida, Carlo, Andrew, Zary, Ben, Jonathan, Laurence, Amedeo, Rufeida, Tom, and many masters students. Outside the lab, for their help with X-ray crystallography, I would like to thank James and Ben, and all the people involved in the McGowan-Willans-Kee group meetings for listening and sharing ideas.

Leo, thank you for your affection, for your constant encouragement and for many beautiful moments. You have given these years the best possible soundtrack. Finally, I have to thank my family and, above all, my parents for their unconditional support and for being always present despite the distance. For so much effort... Gracias.

Abstract

This thesis concerns the synthesis and characterisation of arene, Cp* and functionalised Cp* complexes of ruthenium for their use as transfer hydrogenation catalysts and anticancer agents. As catalysts, the compounds have been tested, principally, against the redox neutral alkylation of *tert*-butylamine with phenethyl alcohol and the reduction of benzaldehyde. As anticancer agents, the compounds have been tested *in vitro* against the cell lines HT-29 and A2780.

Chapter 1 is a review of transfer hydrogenations using ruthenium, iridium and rhodium complexes, immobilisation alternatives and research into metal-containing anticancer drugs.

Chapter 2 describes the synthesis and characterisation of functionalised η^6-arene complexes of ruthenium and a brief investigation into their immobilisation possibilities.

Chapter 3 describes the synthesis and characterisation of pyridine-containing *p*-cymene complexes of ruthenium.

Chapter 4 describes the synthesis and characterisation of Cp*, functionalised Cp* and tetramethylfulvene complexes of ruthenium.

Chapter 5 describes the homogeneous catalytic testing of the compounds discussed in Chapters 2-4 for transfer hydrogenations.

Chapter 6 describes the *in vitro* IC_{50} results obtained for compounds selected among those discussed in Chapter 4 against two cell lines.

Chapter 7 gives the experimental details and the characterisation data for the processes and compounds discussed in Chapters 2-6.

Table of Contents

Glossary of Terms

δ	Chemical shift
η	Hapticity
μ	Bridging ligand
Å	Angstrom, 1×10^{-10} m
A2780	Ovarian carcinoma
Acac	Acetylacetonate
A2780cis	Ovarian carcinoma with inbuilt resistance to cisplatin
API	Active pharmaceutical ingredient
Ar	Aryl
ATH	Asymmetric transfer hydrogenation
atm	Atmospheres
ATRA	Atom-transfer radical addition
bdpp	2,4-Bis(diphenylphosphino)pentane
BINAP	2,2'-Bis(diphenylphosphino)-1,1'-binaphthyl
Bn	Benzyl
br.	Broad
^{t}Bu	Tertiary butyl
^{o}C	Degrees Celsius
CALB	*Candida Antarctica* lipase B
Cp	Cyclopentadienyl ligand
Cp*	Pentamethylcyclopentadienyl ligand
$Cp^{\#}$	$C_5(CH_3)_4(CH_2)_5OH$
CPG	Controlled-pore glass
cod	1,5-Cyclooctadiene
COSY	Correlation spectroscopy
cot	1,3,5,7-Cyclooctatetraene
CsDPEN	N-camphorsulfonyl-1,2-diphenylethylenediamine
CTR1	Copper transporter-1

Cy	Cyclohexyl
DEPT	Distortionless enhancement by polarisation transfer
DIC	N,N'-Diisopropylcarbodiimide
dippf	1,1'-Bis(diisopropylphosphino)ferrocene
DKR	Dynamic kinetic resolution
DMSO	Dimethylsulfoxide
DNA	Deoxyribose nucleic acid
DPEN	1,2-Diphenylethylenediamine
DPEphos	Bis(2-diphenylphosphinophenyl)ether
dppe	1,2-Bis(diphenylphosphino)ethane
dppf	1,1'-Bis(diphenylphosphino)ferrocene
dppm	1,1-Bis(diphenylphosphino)methane
dppp	1,3-Bis(diphenylphosphino)propane
EAT	Ehrlich ascites tumour
e.e.	Enantiomeric excess
e.g.	*Exempli gratia,* for example
en	Ethylenediamine
ES MS	Electrospray mass spectrometry
Et	Ethyl
Et al.	*Et alia,* and others
Exo	External
FDA	Food and drug administration
FT-IR	Fourier transform infrared spectroscopy
5-FU	5-Fluorouracil
GC	Gas chromatography
$\{^1H\}$	^1H decoupled
HL-60	Human promyelocytic leukemia
HMBC	Heteronuclear multiple bond correlation
HMQC	Heteronuclear multiple quantum correlation

HT-29	Human colon adenocarcinoma
IC_{50}	Concentration at which 50% growth is inhibited
ICP	Inductively coupled plasma
i.e.	*Id est*, that is
In situ	In position
In vacuo	Under vacuum
In vitro	In glass
In vivo	In life
IPA	Isopropanol
J	Spin-spin coupling constant
K	Kelvin
L	2-Electron donor
L.G.	Leaving group
$[M]^+$	Parent molecular ion
MCM-41	Mesoporous silica
Me	Methyl
MPa	Megapascal
MPV	Meerwein-Ponndorf-Verley
MTT	3-(4,5-Dimethylthiazol-2-yl)-2,5-diphenyl tetrazolium bromide
m/z	Mass to charge ratio
nbd	Norbornadiene
NN	Diamine ligand
PEG	Poly(ethyleneglycol)
Ph	Phenyl
PP	Diphosphine ligand
^{i}Pr	Isopropyl
psi	Pound per square inch
pta	1,3,5-Triaza-7-phosphatricyclo[3.3.1.1]decane
py	Pyridine

Q	Quaternary
R	General organic substituent
RCC	Renal-cell carcinoma
r.t.	Room temperature
[Ru]	Ruthenium complex
SBA-15	Mesoporous silica
S/C	Substrate to catalyst ratio
SLP	Supported liquid phase
s.u.s.	Standard uncertainties
TBAB	Tetrabutylammonium bromide
TEAF	Triethylammonium formate
tert	Tertiary
Tf	Triflyl
THF	Tetrahydrofuran
Ts	Tosyl, 4-toluenesulfonyl
TsCYDN	N-(4-Toluenesulfonyl)-1,2-cyclohexanediamine
TsDPEN	N-(4-Toluenesulfonyl)-1,2-diphenylethylenediamine
UV	Ultraviolet
v/v	Volume/volume
X	1-Electron donor
Xantphos	4,5-Bis(diphenylphosphino)-9,9-dimethylxanthene

Chapter 1

Introduction

1.1 Introduction

This chapter presents an introduction to current and previous research on catalytic transfer hydrogenation reactions and chemotherapy with transition metal complexes. In the first part, different types of transfer hydrogenation reactions are explained and examples given where, principally ruthenium, but also iridium and rhodium complexes have been used as catalysts. Some investigations on mechanistic aspects of these reactions are introduced, as well as immobilisation techniques that have been utilised to adapt the use of the mentioned complexes to heterogeneous processes. The second part of this chapter offers a brief summary of metal compounds with anticancer activity, including those already in the clinic and others, still under study, with the most promising activities.

1.2 Transfer Hydrogenation Reactions

1.2.1 Introduction

Transfer hydrogenation reactions involve the interchange of hydrogen atoms between substrates or reactants, that can be either oxidised or reduced during the process, and a metal catalyst. A general scheme of this type of reactions is presented in **Scheme 1.2.1**. For instance, alcohols or amines can be oxidised to ketones/aldehydes or imines in a dehydrogenation process where the metal catalyst takes their hydrogens, generally forming metal hydride species. These hydrogens might be then transferred to an organic hydrogen acceptor which, in turn, gets reduced. In the reverse reactions or hydrogenations, the metal first binds the hydrogens given by a hydrogen donor and then transfers them to the double bond of the corresponding substrate.

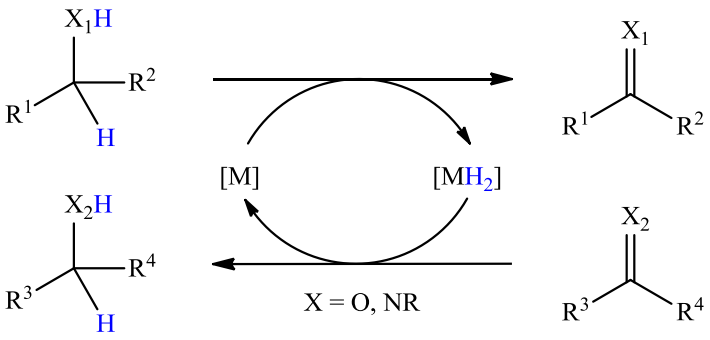

Scheme 1.2.1 General scheme for transfer hydrogenation reactions

In contrast to hydrogenations using molecular H_2, transfer hydrogenation reactions are less hazardous (H_2 is very flammable) and avoid the use of the high pressures associated with the manipulation of gaseous H_2. They are, thus, milder and more desirable transformations.

Despite transition metal complexes being the catalysts most broadly employed nowadays for transfer hydrogenations, reactions of this kind were traditionally carried out using aluminium alkoxides. These processes with aluminium are known as Meerwein-Ponndorf-Verley (MPV) reductions[1-3] or Oppenauer oxidations,[4] and they are generally thought to proceed through a cyclic six-membered ring transition state (**Scheme 1.2.2**).[5] The major drawback of these reactions is that stoichiometric amounts of the metal complex are required, and the final alcohols in the case of reductions have to be liberated by aqueous acidification.[5]

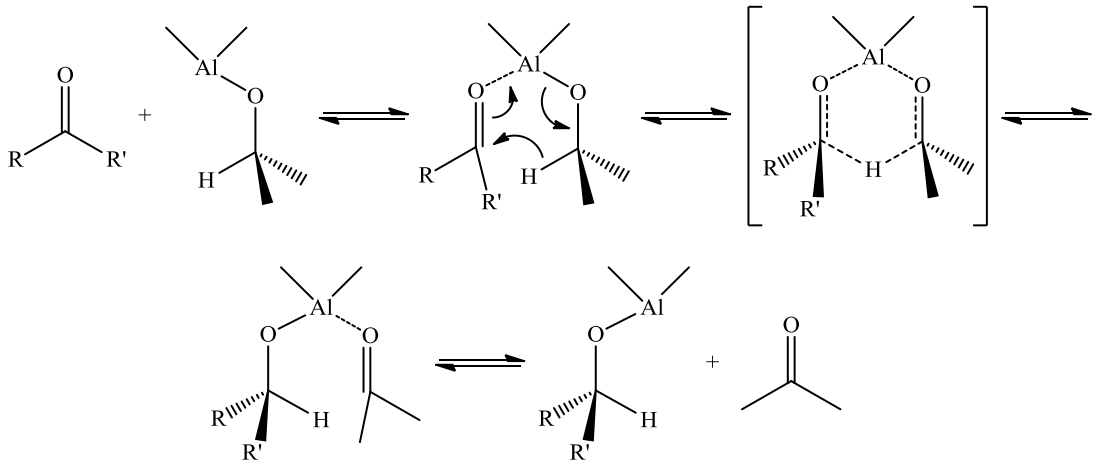

Scheme 1.2.2 Mechanism of the MPV reduction of a ketone with aluminium isopropoxide

This chapter focuses on the utilisation of ruthenium for a series of transfer hydrogenations. The first examples of ruthenium-catalysed transfer hydrogenations were reported in 1971 by Sasson and Blum, using $RuCl_2(PPh_3)_3$ at high temperatures (180-200ºC),[6, 7] which were later reduced (82ºC) for reactions performed in the presence of NaOH.[8]

1.2.2 Redox Neutral Alkylations

Redox neutral alkylations or N-alkylations are reactions between alcohols (primary alcohols are the most commonly used) and amines in which, after initial oxidation of the alcohol, a condensation of the amine with the generated aldehyde

produces an imine, and this is finally reduced to yield an N-alkylated amine. They consist, thus, of three parts: oxidation of the alcohol, formation of the imine and reduction to an amine. The first and the third parts are aided by a transition metal catalyst that "borrows" the hydrogens from the starting alcohol and then transfers them to the imine (**Scheme 1.2.3**). The mechanism is generally referred to as "hydrogen borrowing" or "hydrogen autotransfer" process.[9, 10]

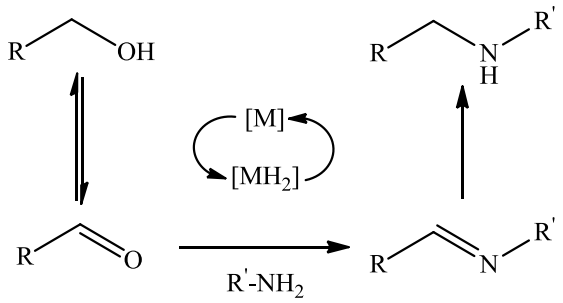

Scheme 1.2.3 General scheme for the N-alkylation of amines with alcohols

These transformations are good examples of atom economy because the only by-product generated is water, from the condensation between the aldehyde and the amine. Other traditional methods for the alkylation of amines include the use of toxic alkyl halides that, apart from producing salts as by-products, hinder the control of mono-alkylations,[11-13] and the reductive amination of carbonyl compounds.[14, 15] The advantages of using alcohols as alkylating agents are their low toxicity, high availability and stability, and low costs.

Some of the first examples of N-alkylations catalysed by ruthenium complexes were reported by Watanabe *et al*.[16-21] They investigated the N-alkylation of 2-aminopyridine with ethanol (**Scheme 1.2.4**).[21] 49% yield of **2** was obtained selectively with $RuCl_2(PPh_3)_3$, while [Ru(cod)(cot)] (cod = 1,5-cyclooctadiene; cot = 1,3,5,7-cyclooctatetraene) produced 79% of **1**. In general, it was concluded that the ratio of mono-alkylated and di-alkylated products depended on both the molar ratio of amine to alcohol and the type of ruthenium complex used, and generally the presence of phosphines favoured the di-alkylation.

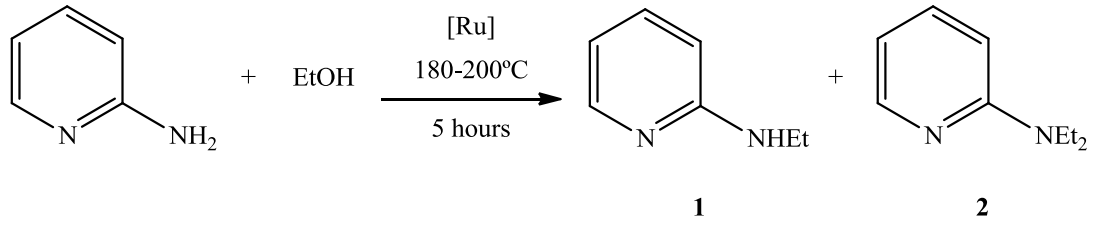

Scheme 1.2.4 N-alkylation of 2-aminopyridine with ethanol

Watanabe also studied N-heterocyclisations, like the ones summarised in **Scheme 1.2.5**,[17] to produce quinoline, indole, piperidine, morpholine and piperazine derivatives from a variety of amines and alcohols. The most successful catalyst in the majority of the trials was $RuCl_2(PPh_3)_3$, and the importance of phosphine ligands was demonstrated, but high temperature conditions were normally required.

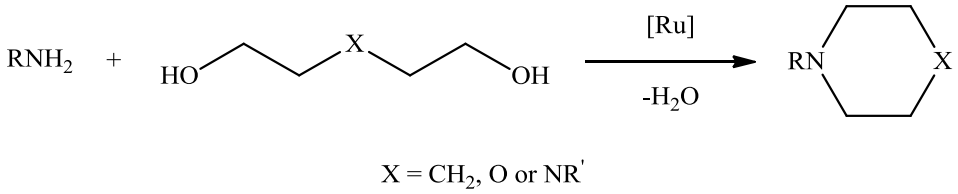

Scheme 1.2.5 N-heterocyclisations studied by Watanabe and co-workers

The synthesis of arylpiperazines (X = NR' and R = aryl in **Scheme 1.2.5**) was also tried with PNP and NN'N (neutral tridentate ligands) complexes of ruthenium(II) (**Figure 1.2.1**) by van Koten *et al*.,[22] and they managed comparable or better activities than those obtained with $RuCl_2(PPh_3)_3$. The presence of PPh_3 ligands in the complexes was essential. In another article, Marsella related a higher PPh_3:Ru ratio with a higher selectivity towards mono-alkylation in similar reactions.[23]

The group of Rigo analysed the N-methylation of primary (RNH_2) and secondary (R_2NH) alkylamines by methanol to yield $RN(CH_3)_2$ and R_2NCH_3 species respectively.[24] They used methanol as the solvent, at reflux, and tested several ruthenium complexes. The best activities were obtained with [Ru(η^5-C_5H_5)Cl(PPh_3)$_2$] (**Figure 1.2.2**) and, proving the borrowing hydrogen mechanism, both imine and mono-methylated derivatives were detected as intermediates.

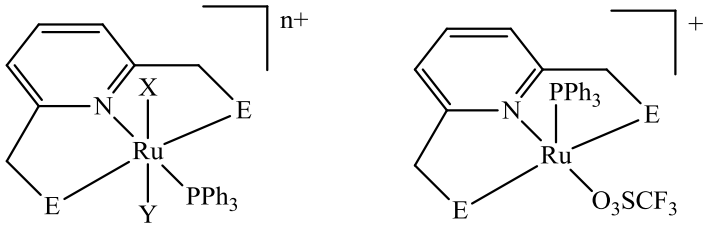

n = 0-2; E = PPh_2 or NMe_2; X, Y = Cl or MeCN

Figure 1.2.1 Ruthenium complexes studied by van Koten *et al*. for the synthesis of arylpiperazines

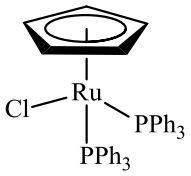

Figure 1.2.2 [Ru(η^5-C_5H_5)Cl(PPh_3)$_2$] complex employed by Rigo *et al*. for N-methylation

More recently, Williams and co-workers discovered the favourable combination of [$RuCl_2$(*p*-cymene)]$_2$ and diphosphines at reflux in toluene for the N-alkylation of primary or secondary amines.[25, 26] The optimum conditions were obtained with dppf (1,1'-bis(diphenylphosphino)ferrocene) or DPEphos (bis(2-diphenylphosphinophenyl)ether) as ligands, after reaction times of 24 hours. The system was also successful in reactions between primary amines and diols, producing N-heterocycles, between secondary alcohols and amines, and between primary alcohols and sulfonamides, but in these two last cases, temperatures of 150ºC in xylene were needed to give complete conversion.[27] One example of the efficient application of [$RuCl_2$(*p*-cymene)]$_2$ + diphosphine is the synthesis of Piribedil, a drug used in the treatment of Parkinson's disease.[27] The compound can be obtained in 87% isolated yield with the conditions specified in **Scheme 1.2.6**. In a later article, Williams' group reported the possibility of carrying out the same reactions using microwave heating instead of thermal heating, which largely reduced the reaction times and, as an added advantage, removed the need for a solvent.[28] Using microwaves, Piribedil can be prepared in 89% yield at 115ºC in 90 minutes, using 5 mol% of Ru and DPEphos.

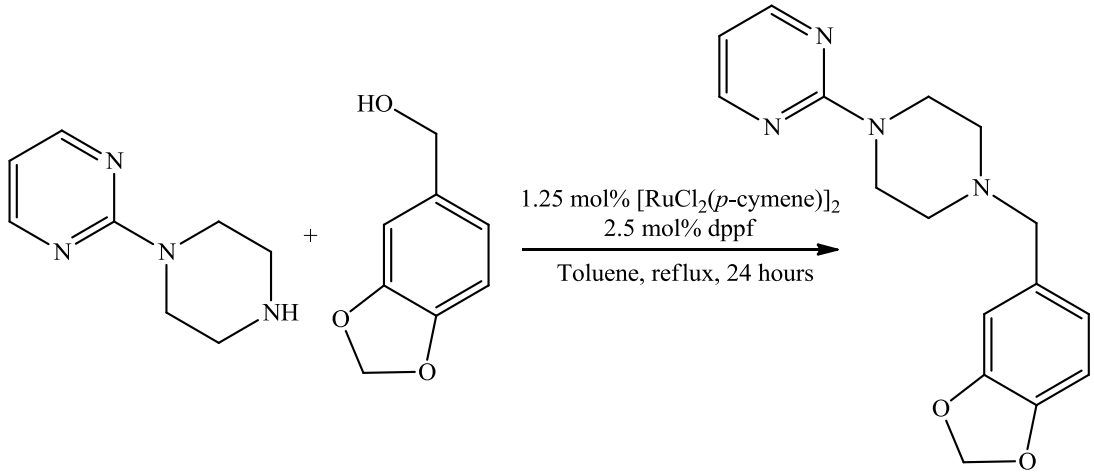

Scheme 1.2.6 Williams' conditions for the synthesis of Piribedil

According to Xu and co-workers, in contrast to the typical borrowing hydrogen reaction conducted under an inert atmosphere, N-alkylations in air work more efficiently.[29] They reported various N-alkylations, including those of sulfonamides (**Scheme 1.2.7**), using simple Ru, Ir or Rh complexes without added ligands (*e.g.* $RuCl_3$, $IrCl_3$ or $RhCl_3$), in air and with no solvent. They proposed that, in air (oxygen), the oxidation of the alcohol to an aldehyde is more favourable, and that the hydrogen transfer proceeds without the formation of MH or MH_2 species.

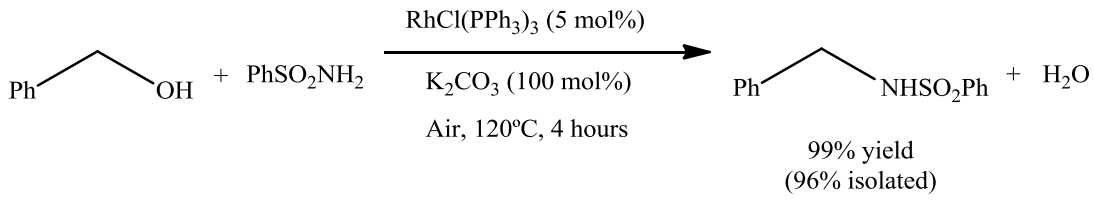

Scheme 1.2.7 N-alkylation of phenyl sulfonamide in air with Wilkinson's catalyst ($RhCl(PPh_3)_3$)

N-alkylations have also been successful using iridium catalysts, like the ones employed by the groups of Williams[30-32] and Yamaguchi.[33-40] For instance, Williams reported the use of $[Ir(cod)Cl]_2$ with dppf in toluene at reflux for the synthesis of tryptamine derivatives (**Scheme 1.2.8**).[32] The same group also published the use of the SCRAM catalyst $[Cp^*IrI_2]_2$ (Cp^* = pentamethylcyclopentadienyl) for the alkylation of amines with alcohols in water (**Scheme 1.2.9**) or ionic liquids.[31] The use of water was found favourable for the formation of secondary amines, while ionic liquids were a better medium for obtaining tertiary amines, probably because they ease the iminium reduction step.

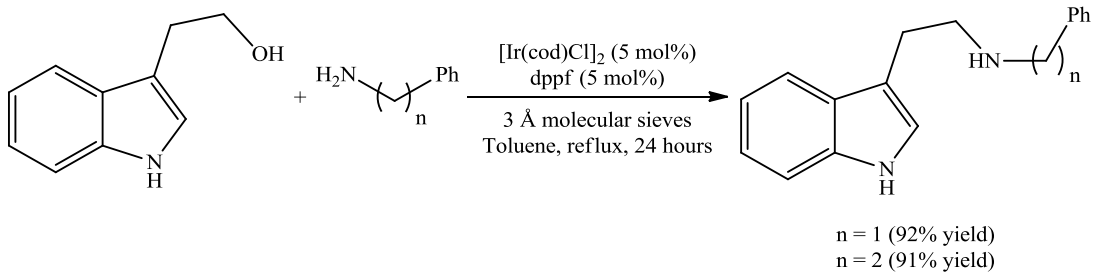

Scheme 1.2.8 Williams' conditions for the synthesis of tryptamine derivatives

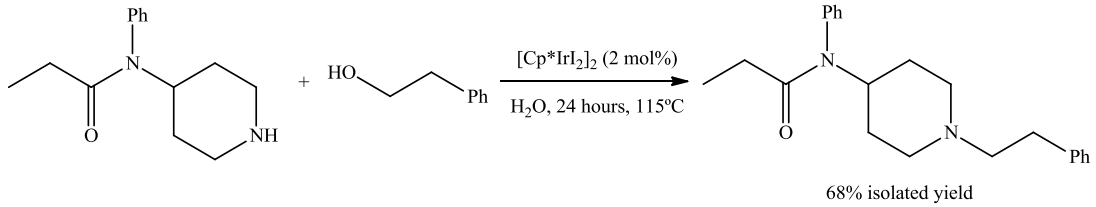

Scheme 1.2.9 Williams' conditions for the synthesis of fentanyl

Yamaguchi and co-workers prepared a highly water soluble and air stable ammine complex of iridium (**Figure 1.2.3**) and used it for the N-alkylation of aqueous ammonia with alcohols (**Scheme 1.2.10**).[40] This catalyst could be recycled two times by addition of dichloromethane at the end of the catalytic reaction, so the product could be extracted into the organic phase and the catalyst recovered into the aqueous phase.

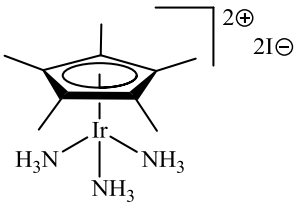

Figure 1.2.3 Water soluble iridium complex used by Yamaguchi *et al*. for N-alkylation

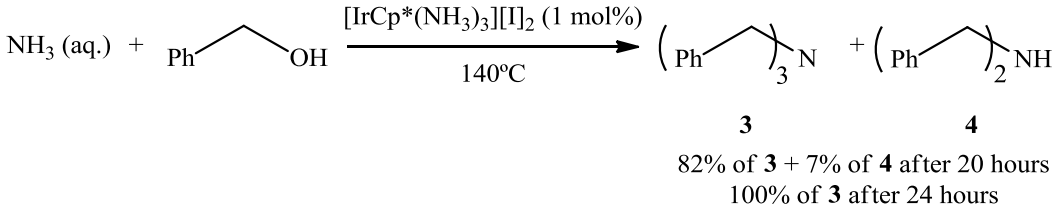

Scheme 1.2.10 Yamaguchi's conditions for the N-alkylation of aqueous ammonia

An alternative to the normal N-alkylation, entailing an aza-Wittig reaction with an iminophosphorane, was also reported by Williams using an iridium catalyst

(**Scheme 1.2.11**).[41] The combination of $[Ir(cod)Cl]_2$ (2.5 mol%) with dppf (5 mol%) and K_2CO_3 (5 mol%) at 110ºC for 24 hours was found to give quantitative conversions. A drawback of this approach is the difficult removal of the triphenylphosphine oxide formed during the reaction.

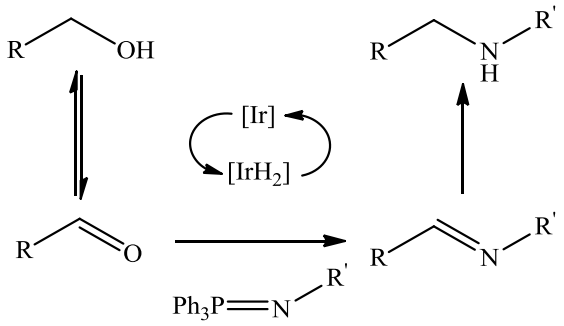

Scheme 1.2.11 General scheme for the N-alkylation using aza-Wittig reactions with iminophosphoranes

1.2.3 Hydrogenations and Dehydrogenations

Transfer hydrogenations and dehydrogenations need an auxiliary organic molecule as hydrogen donor or acceptor respectively. The most commonly used hydrogen donor systems are isopropanol and formic acid.

Isopropanol (IPA) is an effective hydrogen donor that produces acetone during catalytic transfer hydrogenations (**Scheme 1.2.12**).[42, 43] In this system, the product is in equilibrium with the starting materials so, initially, the reaction is kinetically controlled, but when the concentrations of product and acetone increase, the rate of the reverse reaction also increases and the process becomes thermodynamically controlled. This reversibility affects both the yield and the optical purity of the product, but can be easily overcome by using IPA in high concentrations (as the solvent) or by continuously distilling and removing the acetone by-product. The IPA system can be used to reduce aldehydes, ketones and iminium salts, and it is a convenient hydrogen donor because it is readily available, safe and cheap. While isobutanol is also a good hydrogen donor (but generally less active), primary alcohols such as methanol or ethanol produce aldehydes that might interfere in the catalytic reaction. Acetone is the hydrogen acceptor normally used for the reverse transformations (dehydrogenations).

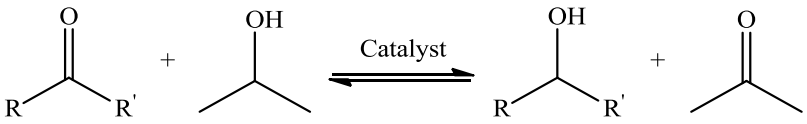

Scheme 1.2.12 Catalytic transfer hydrogenation with isopropanol as hydrogen donor

The other important hydrogen donor system is the mixture of formic acid with triethylamine (**Scheme 1.2.13**).[44, 45] Molar mixtures of a 5:2 ratio form an azeotrope,[44] which, at room temperature, is a single phase, soluble in most solvents, although other molar ratios may form biphasic solutions.[42, 43] This triethylammonium formate system (TEAF) can be used to reduce aldehydes, ketones, imines and iminium salts, and decomposes producing gaseous CO_2, which prevents the reverse reaction (the process is always kept under kinetic control). The actual hydrogen donor in this system is the formate anion, so, in water, hydrogenation reactions only take place above pH 3.6 (the aqueous pK_a of formic acid). The role of the Et_3N in the TEAF system is believed to be the buffering of the pH while formic acid is consumed. An excess of formic acid over substrate is often used, and the 5:2 TEAF system is acidic, which might make it incompatible with some catalysts or substrates. In such an acidic medium, imines can get protonated (the pK_a of imines is approximately 6 in water) forming iminium salts, which are much more reactive. This possibly explains why IPA, being a neutral system, cannot reduce imines. In aqueous catalytic reactions, the formate salts HCO_2Na or HCO_2K are commonly used, and the CO_2 generated ends up trapped as bicarbonate.

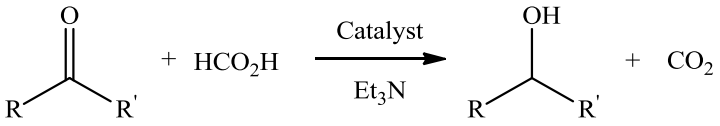

Scheme 1.2.13 Catalytic transfer hydrogenation with formic acid-triethylamine as hydrogen donor

1.2.3.1 Ketone and Aldehyde Reductions

The most notable ruthenium catalytic system for asymmetric transfer hydrogenations (ATH) is the one developed by Noyori (**Figure 1.2.4**),[45] who won the Nobel Prize in 2001 for his work on chirally catalysed hydrogenation reactions.

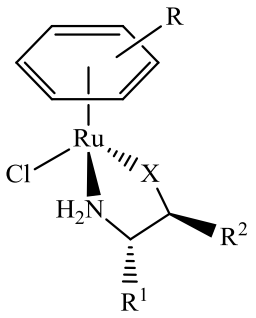

X = O or NTs
Ts = $SO_2(C_6H_4$-*p*-$CH_3)$

Figure 1.2.4 Noyori's arene-ruthenium catalysts

In 1995, Noyori first published the use of N,N-ligand catalysts, prepared *in situ*, for the asymmetric reduction of prochiral aromatic ketones in isopropanol, like the example with acetophenone in **Scheme 1.2.14**.[45] Due to some reversibility observed, to maintain the enantiomeric purity throughout the reaction, the substrate concentration had to be low (0.1 M) and long exposures of the product to the catalyst had to be avoided. Without the diamine ligand, $[RuCl_2(mesitylene)]_2$ gave (S)-1-phenylethanol in 8% yield. With the addition of TsDPEN (N-(*p*-toluenesulfonyl)-1,2-diphenylethylenediamine), the yield reached 95% and 97% e.e. was obtained.

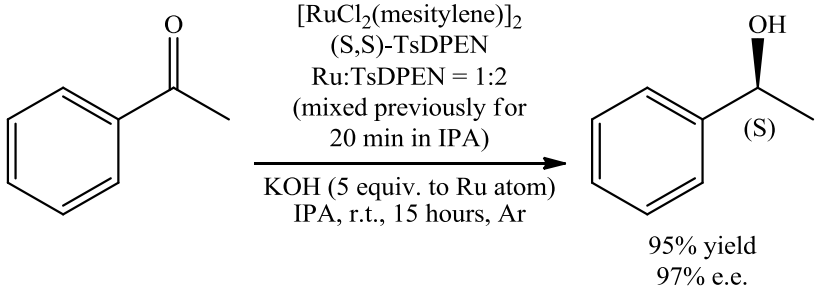

Scheme 1.2.14 Noyori's conditions for the ATH of acetophenone in IPA with [RuCl(mesitylene)(TsDPEN)] (mesitylene = 1,3,5-trimethylbenzene; TsDPEN = N-(*p*-toluenesulfonyl)-1,2-diphenylethylenediamine). S/C = 200

When N,N-ligands are replaced by N,O-ligands, the reaction rates are much faster, but the enantioselectivity decreases.[46, 47] In the model reaction with acetophenone (0.1 M) (**Scheme 1.2.15**), 94% yield was obtained after only 1 hour at room temperature in isopropanol, using a catalyst prepared *in situ* from $[RuCl_2(hexamethylbenzene)]_2$ and (S,S)-2-methylamino-1,2-diphenylethanol. With

both types of N,N- or N,O-ligands, the presence of a primary or secondary amine at one end is crucial, and dimethylamino groups have proven inactive.

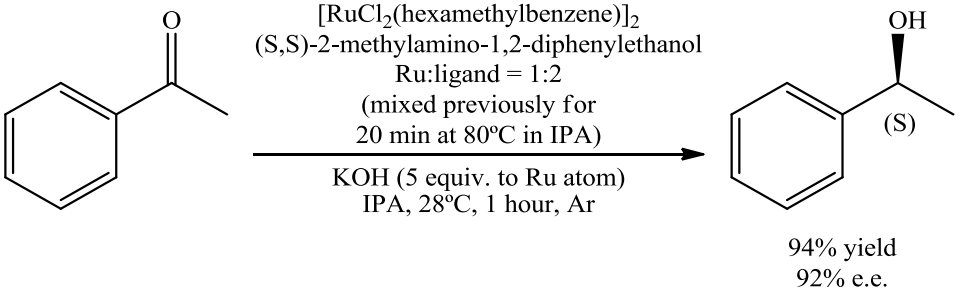

Scheme 1.2.15 Noyori's conditions for the ATH of acetophenone in IPA with [RuCl(hexamethylbenzene)(aminoalcohol)] (aminoalcohol = 2-methylamino-1,2-diphenylethanol). S/C = 1000

To avoid the deterioration of optical purity observed during reactions in isopropanol, the same group also tested the N,N-Ru-arene catalytic system using the 5:2 azeotropic mixture of formic acid and triethylamine.[47, 48] This allowed a much higher substrate concentration, between 2 and 10 M, while maintaining the enantioselectivity. In the model reduction of acetophenone (**Scheme 1.2.16**), using a 2 M initial concentration of the substrate, complete conversions and very good enantioselectivities could be obtained at room temperature. The same reaction at 60ºC proceeded up to ten times faster, but with 2% decrease in the e.e. This acetophenone hydrogenation with [RuCl(mesitylene)(TsDPEN)] also worked with 10 M solutions and S/C ratios of 1000. With regard to the arene ligands, for all of these hydrogenations, the reactivity decreases in the order benzene > *p*-cymene = mesitylene > hexamethylbenzene, probably due to steric reasons, but *p*-cymene and mesitylene give the best enantioselectivities.

The ATH of benzaldehyde to deuterated benzyl alcohol has also been studied by Noyori's group under the series of different conditions mentioned earlier.[49] **Table 1.2.1** gives a summary of the best results.

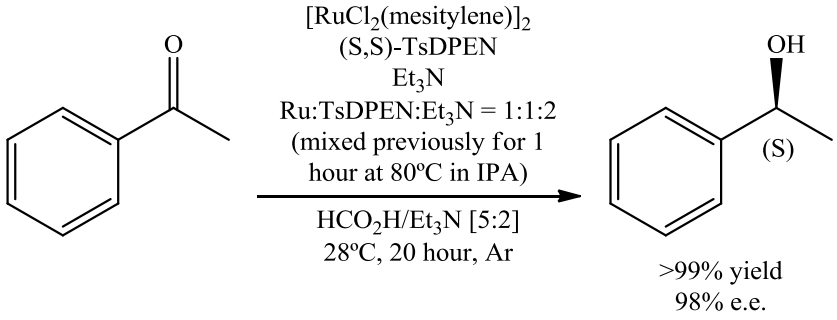

Scheme 1.2.16 Noyori's conditions for the ATH of acetophenone in formic acid/Et_3N with [RuCl(mesitylene)(TsDPEN)]. S/C = 200

	N,N-ligand in IPA	**N,O-ligand in IPA**	**N,N-ligand in TEAF**
Substrate	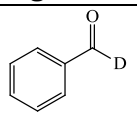	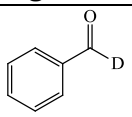	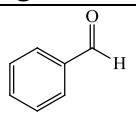
[Substrate] (M)	0.1	0.1	0.1 in acetonitrile
Hydrogen donor	Isopropanol	Isopropanol	DCO_2D-Et_3N (1:1)
Catalyst	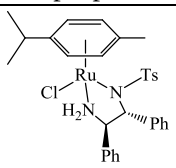	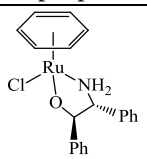	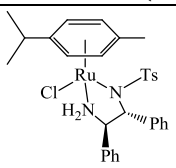
Base (equiv. to Ru)	^{t}BuOK (5)	^{t}BuOK (4)	None
S/C	200	200	200
Temperature (ºC)	22	28	28
Time (hours)	0.5	1	4
Product	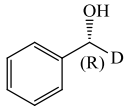	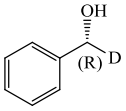	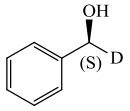
Conversion (%)	100	49	93
e.e. (%)	98	45	98

Table 1.2.1 Noyori's results for the ATH of benzaldehyde to deuterated benzyl alcohol

Noyori and co-workers also isolated three different species involved in the asymmetric transfer hydrogenation catalysis (**Figure 1.2.5**).[50, 51] The halogenated species (**A**) acts as a pre-catalyst and needs to lose HCl in order to become the actual catalyst (**B**). This is facilitated in most of the cases with the presence of a base, such as KOH or ^{t}BuOK. During the catalytic cycle, the sixteen electron complex **B** is transformed into **C**, which is the active species in the hydrogenation of substrates. **C** can interact with a C=O bond through both the hydride and one N-H, forming a six-membered ring transition state and promoting the hydrogen transfer (see section **1.3**).

Both compounds **B** and **C** can catalyse dehydrogenations and hydrogenations respectively in the absence of a base.

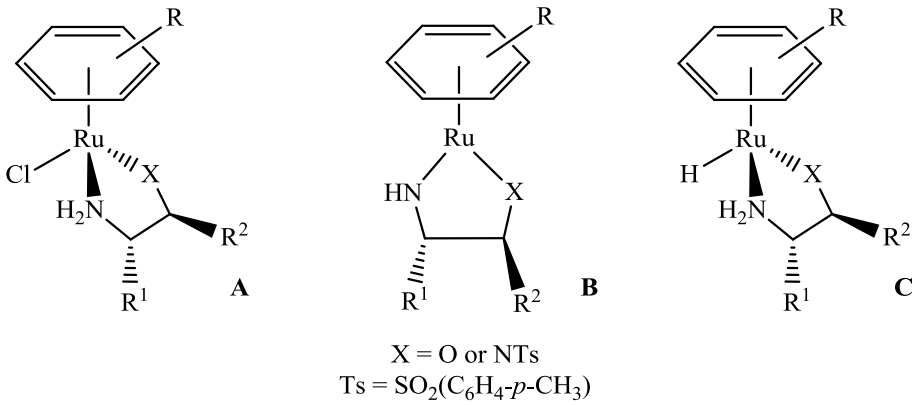

Figure 1.2.5 A) Pre-catalyst; **B)** catalyst and **C)** reactive intermediate in Noyori's ATH

An increased stability and longevity of Noyori-type catalysts has been obtained through the linking of the N,N- or N,O-ligands to the η^6-arene moiety, giving what are called "tethered" complexes (**Figure 1.2.6**).[52-54] The ligands, thus, are attached to the metal at three points, and this locks the free rotation of the arene, permitting in most cases a better control over enantioselectivity. For instance, complex **6**, synthesised by Wills and co-workers, is able to completely reduce acetophenone in less than 3 hours at 28ºC in HCO_2H-Et_3N, giving 96% e.e. (S/C = 200), or in 100 minutes at 40ºC.[55] The untethered equivalent, in contrast, needs overnight reactions to yield similar results. Moreover, catalyst **6** maintains its effectiveness after several new additions of substrate. Later on, the same group optimised the length of the tethered chain to four atoms, which further accelerated the reductive transformations.[56] Ether-tethered complexes (such as **7**) have also been prepared by both Wills' and Ikariya's groups with very promising results.[57, 58]

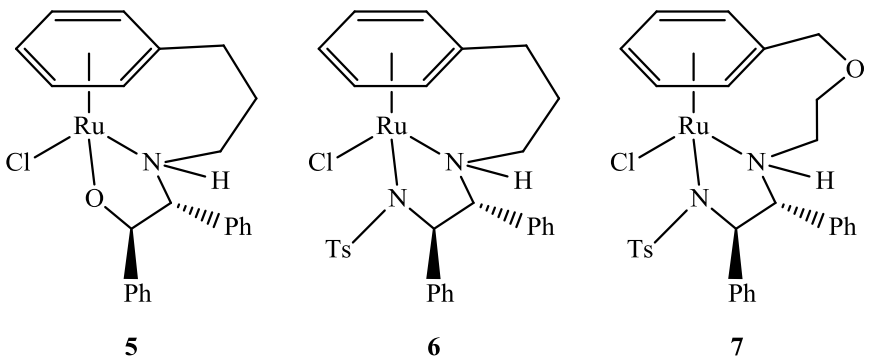

Figure 1.2.6 Some of the tethered catalysts published by Wills *et al*.

Other ligands employed with ruthenium in transfer hydrogenations with IPA include diaminoferrocenyl derivatives[59] and phosphinites.[60] In this latter case, the phosphinite ligands form dimeric complexes (**Figure 1.2.7**), which act as pre-catalysts in the acetophenone reduction in the presence of NaOH, giving good conversions and moderate enantioselectivities. These catalysts are believe to operate via the formation of a Ru-alkoxide, facilitated by the base.

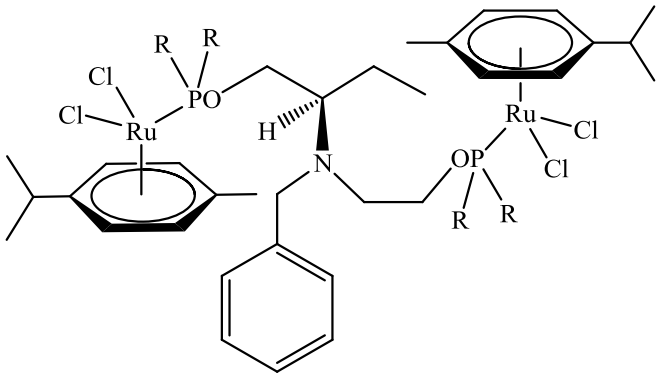

Figure 1.2.7 Phosphinite-Ru catalyst used for ATH of aromatic ketones in IPA. R = Ph or Cy (Cyclohexyl)

Pentamethylcyclopentadienyl (Cp*) complexes of iridium and rhodium with the ligands TsDPEN and TsCYDN (N-(*p*-toluenesulfonyl)-1,2-cyclohexanediamine) have also been tested for ATH of aromatic ketones.[61] The catalysts can be prepared by reacting $[Cp^*MCl_2]_2$ (M = Ir or Rh) with the ligand and triethylamine at room temperature in a molar ratio 1:2:4.2. For the reduction of acetophenone (0.1 M) in isopropanol (**Scheme 1.2.17**), the complexes with TsCYDN give higher reactivities, and those with Rh are more active than the Ir analogues. Despite good results, Ru-TsDPEN provides faster reactions with comparable enantioselectivities. With functionalised acetophenones as substrates, electron-withdrawing substituents give excellent yields and high optical purities, whereas electron-donating groups slow the reactions down, but maintain good enantioselectivities. Bulky alkyl substituents in the aromatic ketones both slow the hydrogenations and reduce the final enantiomeric excesses.

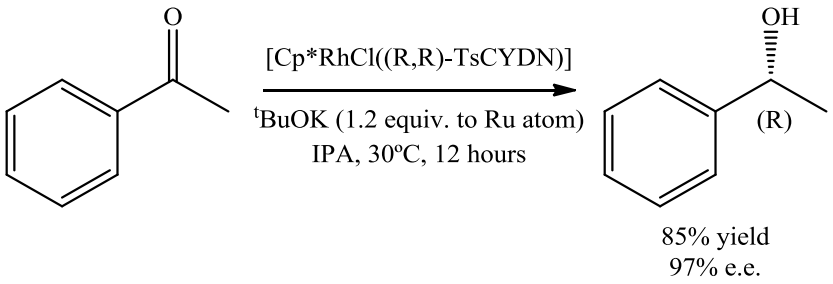

Scheme 1.2.17 Noyori's conditions for the ATH of acetophenone in IPA with [Cp*RhCl(TsCYDN)]. S/C = 200

Growing interest in greener reactions has driven research towards asymmetric transfer hydrogenations in water. In 2001, Williams *et al*. prepared some water-soluble ligands based on Noyori's TsDPEN and Knochel's TsCYDN by addition of a sulfonic acid group (**Figure 1.2.8**).[62] The corresponding catalysts were obtained by reacting $[RuCl_2(p\text{-cymene})]_2$ with each ligand in the presence of a base at 40ºC, and used for ATH of aromatic ketones. The model reaction with acetophenone is shown in **Scheme 1.2.18**. Isopropanol was used as co-solvent and hydrogen donor.

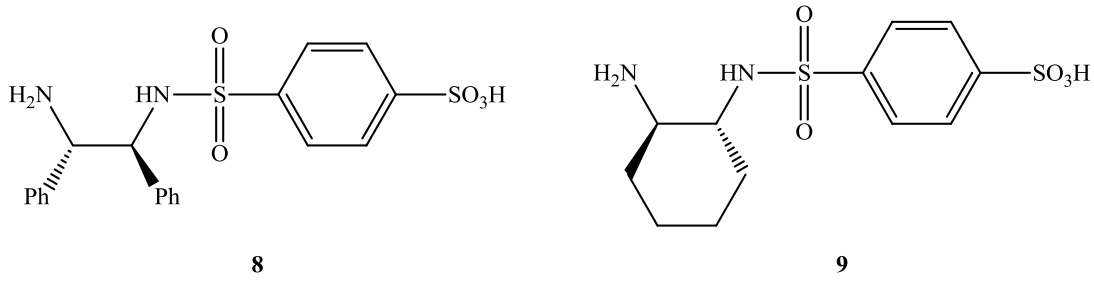

Figure 1.2.8 Water-soluble ligands modified with $-SO_3H$ from **8**) TsDPEN and **9**) TsCYDN

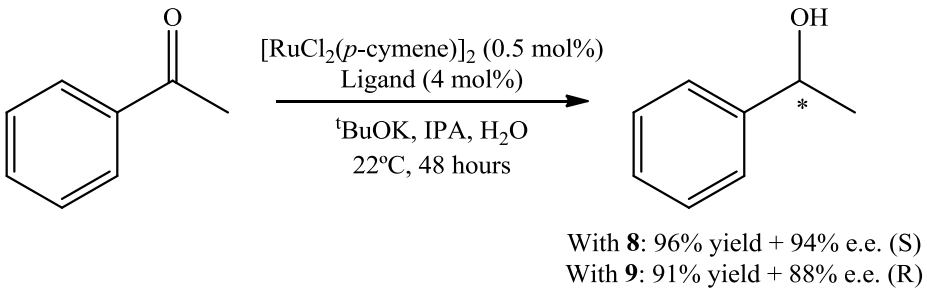

Scheme 1.2.18 Williams' conditions for the ATH of acetophenone in IPA-H_2O with water-soluble TsDPEN- or TsCYDN-derived ligands

More recently, Xiao's group demonstrated that Noyori's catalysts do not need to be modified for reactions in water.[63] They showed that the reduction of

acetophenone can proceed in water, using HCO_2Na as a hydrogen donor and [RuCl(*p*-cymene)(TsDPEN)] at S/C = 100 or higher. In 1 hour, a complete conversion was obtained with 94% e.e., without the need for a co-solvent. When the system was compared to the one using HCO_2H-Et_3N as both solvent and reductant, only 2% conversion was managed with the latter in 1 hour. It is believed that, as ketones are not soluble in water, in fact the reaction takes place in the substrate phase, where the catalyst is more soluble.

Another useful ligand for water reactions is CsDPEN (N-camphorsulfonyl-1,2-diphenylethylenediamine), which has been shown to form efficient catalysts with Ru, Rh and, mainly, Ir.[64] In the reduction of acetophenone (**Scheme 1.2.19**), the rhodium and iridium catalysts obtained from $[Cp^*MCl_2]_2$ (M = Rh or Ir) and CsDPEN give faster rates than the one from $[RuCl_2(p\text{-cymene})]_2$ and CsDPEN. Ir-CsDPEN is the best of the three catalysts when the substrate to catalyst ratio is increased to 1000.

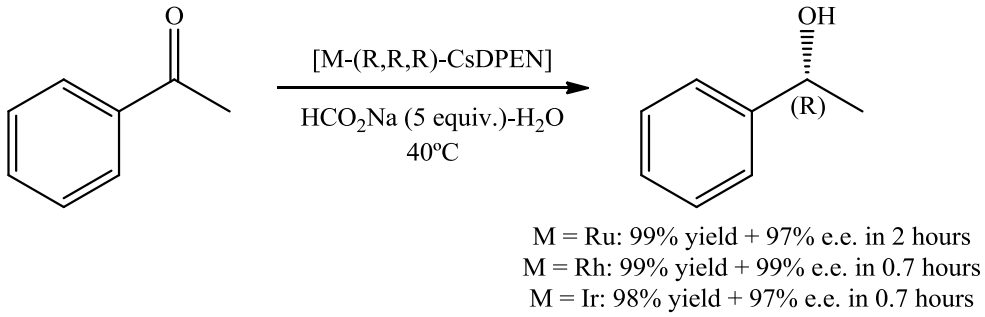

Scheme 1.2.19 Xiao's conditions for the ATH of acetophenone in water using Ru-, Rh- or Ir-CsDPEN complexes. S/C = 100

1.2.3.2 Imine Reductions

In 1996, Noyori reported the reduction of imines with [Ru(*p*-cymene)Cl(TsDPEN)], using the 5:2 azeotropic mixture of formic acid-triethylamine.[65] An example with 6,7-dimethoxy-1-methyl-3,4-dihydroisoquinoline is shown in **Scheme 1.2.20**. This substrate was quantitatively reduced at a substrate to catalyst ratio of 200 using acetonitrile as co-solvent. At S/C = 1000, the reaction took 12 hours and gave 97% yield and 94% e.e. Isopropanol could not be used as a hydrogen source but, with the formic acid azeotrope, imines were much more

reactive than ketones, being reduced even in the presence of acetone, which remained unchanged.

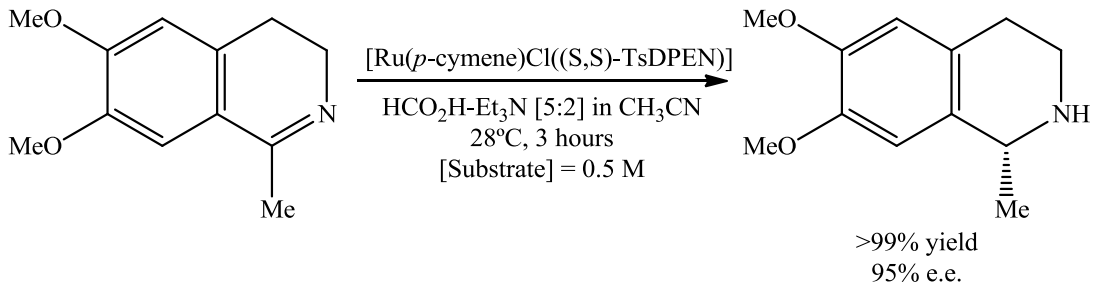

Scheme 1.2.20 Noyori's conditions for the ATH of imines in HCO_2H-Et_3N/CH_3CN with [Ru(*p*-cymene)Cl(TsDPEN)]. S/C = 200; HCO_2H/substrate = 6

The use of N'-alkylated TsDPEN complexes of ruthenium for the reduction of imines has been investigated by the group of Wills,[66, 67] and an N'-methylated version was discovered to be even more active than the original non-substituted complex reported by Noyori. This methylated complex was able to completely reduce 6,7-dimethoxy-1-methyl-3,4-dihydroisoquinoline with 75% e.e. in less than 2 hours at 28ºC and S/C = 100.

It is generally accepted that the mechanism for the reduction of imines differs to that of ketones and does not involve a six-membered ring transition state.[68] Instead, an ionic hydrogenation is more likely, where the imine is protonated and becomes activated and non-coordinative prior to the hydride transfer. This theory is supported by Bäckvall's investigations, which proved that Ru-hydride TsDPEN species do not react with imines unless in the presence of an acid.[69] This explains why isopropanol alone cannot be used in these transformations and suggests that a concerted pathway does not operate for imines.

1.2.3.3 Alcohol and Amine Oxidations

The dehydrogenation of secondary alcohols can be successfully catalysed by $RuCl_2(PPh_3)_3$, using acetone as hydrogen acceptor and solvent, as published by Bäckvall.[70, 71] As an example, the optimised conditions for the oxidation of 1-phenylethanol are depicted in **Scheme 1.2.21**.

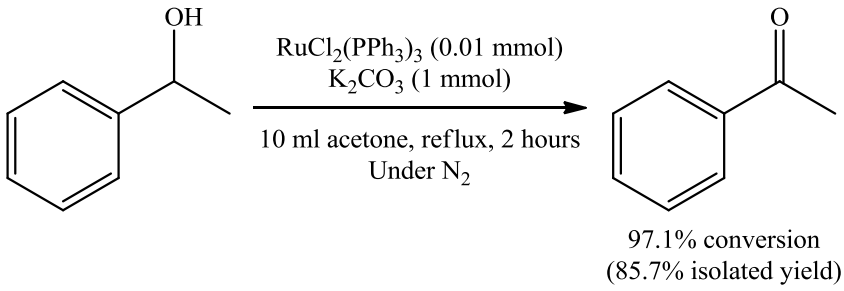

Scheme 1.2.21 Bäckvall's conditions for the oxidation of 1-phenylethanol in acetone using $RuCl_2(PPh_3)_3$. S/C = 1000

Despite the good results with secondary alcohols, Bäckvall's system does not work for primary alcohols. However, these other conversions are possible with some iridium-Cp* catalysts reported by Yamaguchi and Fujita (**Figure 1.2.9**).[72-74] The dimer **10** catalyses the oxidation of benzyl alcohol at room temperature in acetone (**Scheme 1.2.22**), whilst **12** performs the same transformation in the absence of hydrogen acceptor (**Scheme 1.2.23**).

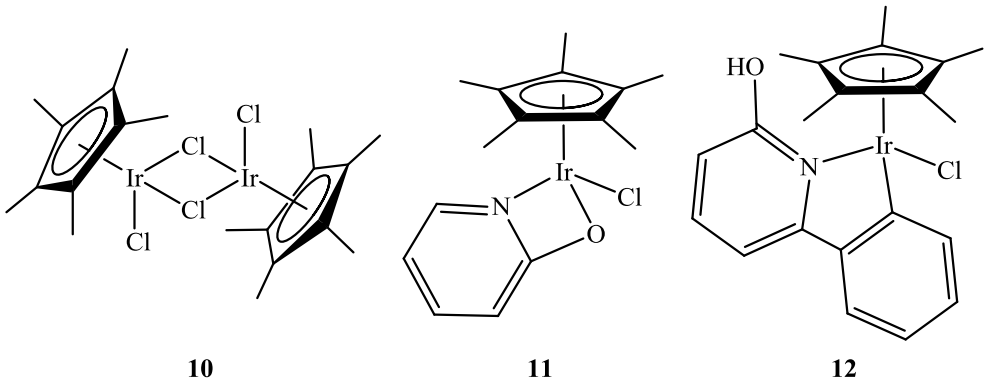

10 **11** **12**

Figure 1.2.9 Iridium-Cp* complexes used as oxidation catalysts by Fujita

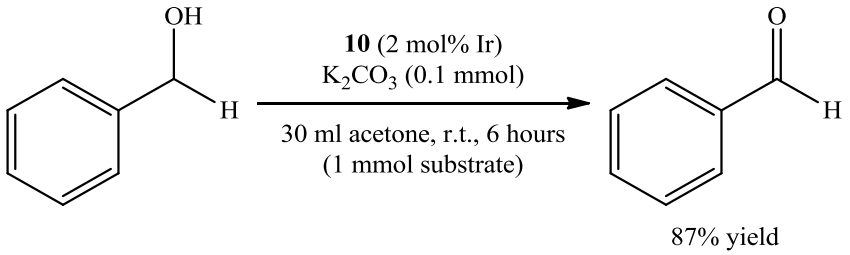

Scheme 1.2.22 Fujita's conditions for the oxidation of benzyl alcohol in acetone using $[Cp^*IrCl_2]_2$

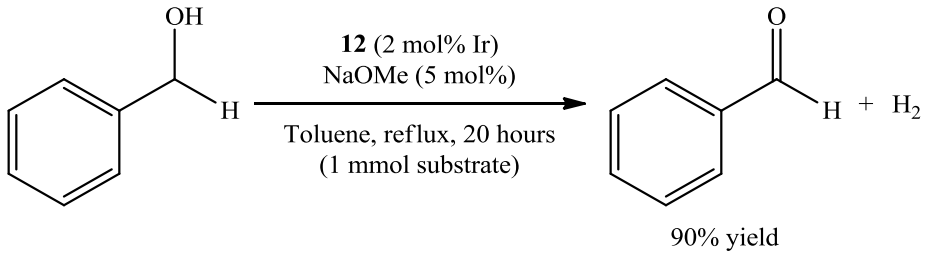

Scheme 1.2.23 Fujita's conditions for the oxidant-free dehydrogenation of benzyl alcohol

A modification of catalyst **11** in **Figure 1.2.9** has also been used for the dehydrogenation of cyclic amines with good results.[75] The 5-CF_3 substituted pyridonate complex is able to oxidise tetrahydroquinolines to quinolines (**Scheme 1.2.24**) and, furthermore, the hydrogen generated can be reused for the reverse reactions.

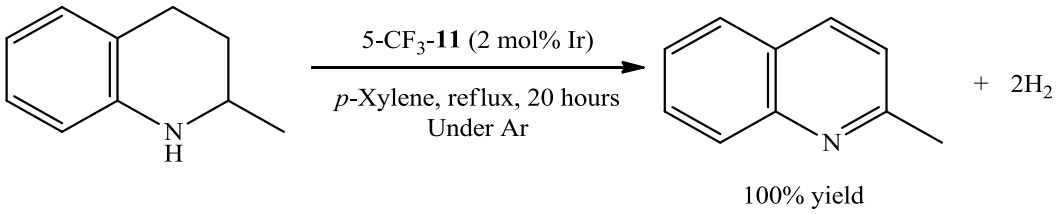

Scheme 1.2.24 Fujita's conditions for the oxidant-free dehydrogenation of 1,2,3,4-tetrahydroquinoline

1.2.4 Racemisations and Dynamic Kinetic Resolutions

In racemisations, an optically pure alcohol or amine is converted into a racemic mixture via an intermediate ketone or imine through hydrogen transfer with a metal catalyst. Several ruthenium complexes are active for these transformations. The racemisation of phenylethanol has been successful with [Ru(η^5-indenyl)Cl(PPh_3)$_2$] (**Scheme 1.2.25**),[76] with [Cp*RuCl(cod)] and $Ph_2P(CH_2)_2NH_2$ (**Scheme 1.2.26**),[77] or with [Ru(η^5-C_5Ph_5)Cl$(CO)_2$] (**Scheme 1.2.27**).[78]

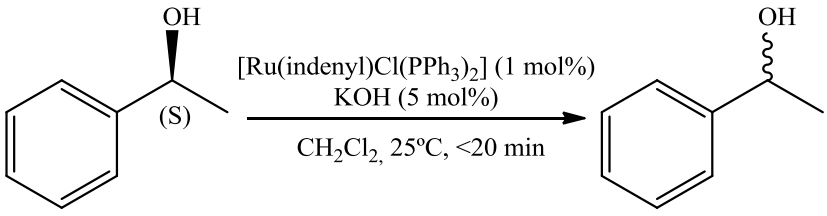

Scheme 1.2.25 Park's conditions for the racemisation of (S)-phenylethanol

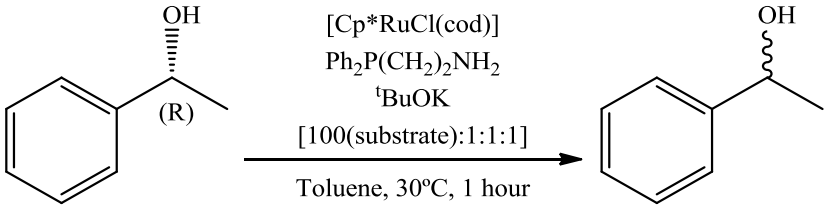

Scheme 1.2.26 Ikariya's conditions for the racemisation of (R)-phenylethanol

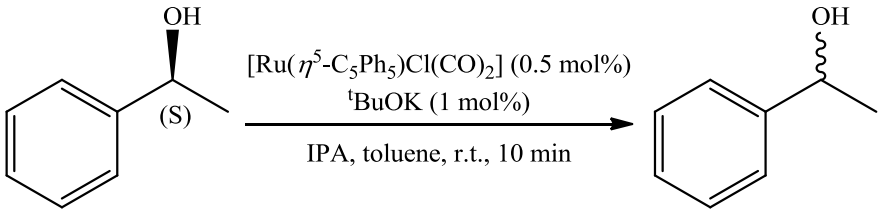

Scheme 1.2.27 Bäckvall's conditions for the racemisation of (S)-phenylethanol

Racemisations play a fundamental part in dynamic kinetic resolutions (DKR), which combine the resolution of a racemic mixture by, for example, chemical modification using an enzyme or selective crystallisation, with the racemisation of the unwanted isomer (**Scheme 1.2.28**). These processes permit, in theory, a full conversion to the isomer of interest, in contrast to the common diastereomeric crystallisation, where only a maximum 50% of the desired isomer can be recovered.

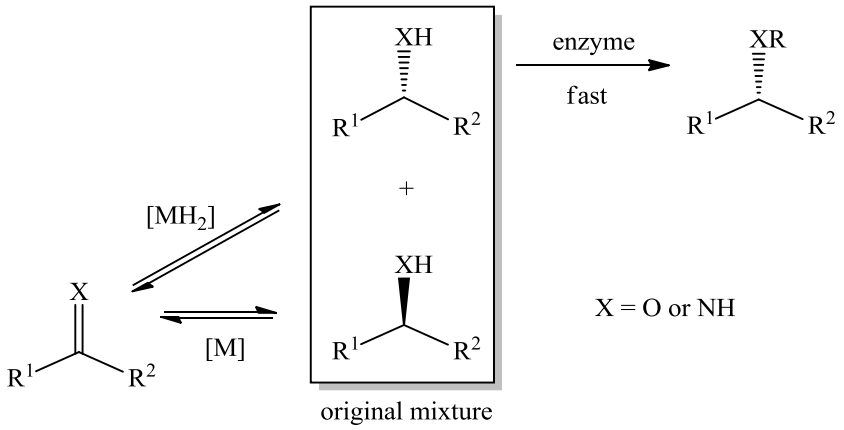

Scheme 1.2.28 General scheme for dynamic kinetic resolutions of alcohols or amines

The ruthenium Shvo-type catalyst in **Figure 1.2.10** has been used for the DKR of amines with *Candida Antarctica* lipase B (CALB) as the enzyme and isopropyl acetate as acylating agent for resolution (**Scheme 1.2.29**).[79] Also efficiently, the iridium SCRAM catalyst $[Cp^*IrI_2]_2$ has been demonstrated to catalyse these transformations, such as the one in **Scheme 1.2.30**,[80] and has been

employed for the preparation of sertraline, the active pharmaceutical ingredient (API) in Pfizer's antidepressant Zoloft.[81]

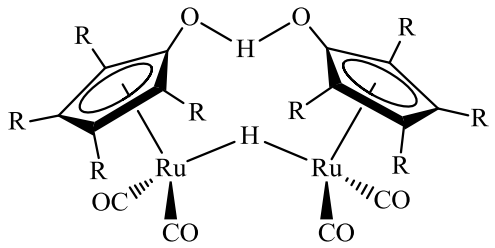

R = *p*-MeO-C_6H_4

13

Figure 1.2.10 Shvo-type catalyst used for the dynamic kinetic resolution of amines

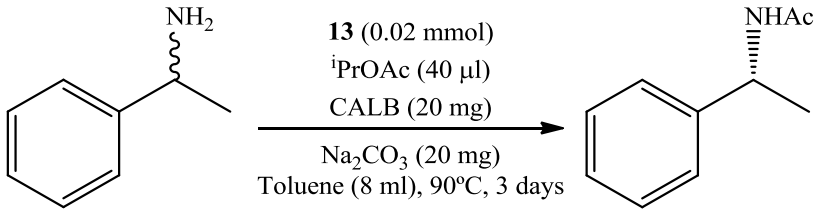

Scheme 1.2.29 Bäckvall's conditions for the DKR of racemic methylbenzylamine

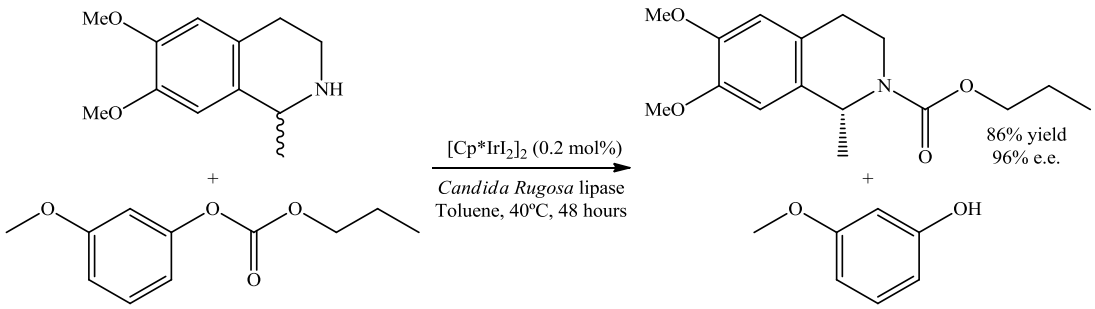

Scheme 1.2.30 Page's conditions for the DKR of racemic 6,7-dimethoxy-1-methyl-1,2,3,4-tetrahydroisoquinoline

1.2.5 Other Transfer Hydrogenation Reactions

1.2.5.1 Reductive Aminations

Reductive aminations are coupling reactions between ketones or aldehydes and amines in the presence of a reducing agent, so the imine formed can be

converted into a final amine. They only differ to redox neutral alkylations in that the latter start with an alcohol and include one more step.

Xiao and co-workers have demonstrated the possible use of air stable cyclometalated imido iridium complexes (**Figure 1.2.11**) to carry out non-chiral reductive aminations under transfer hydrogenation conditions.[82] An example is the reaction between acetophenone and *p*-anisidine in **Scheme 1.2.31**.

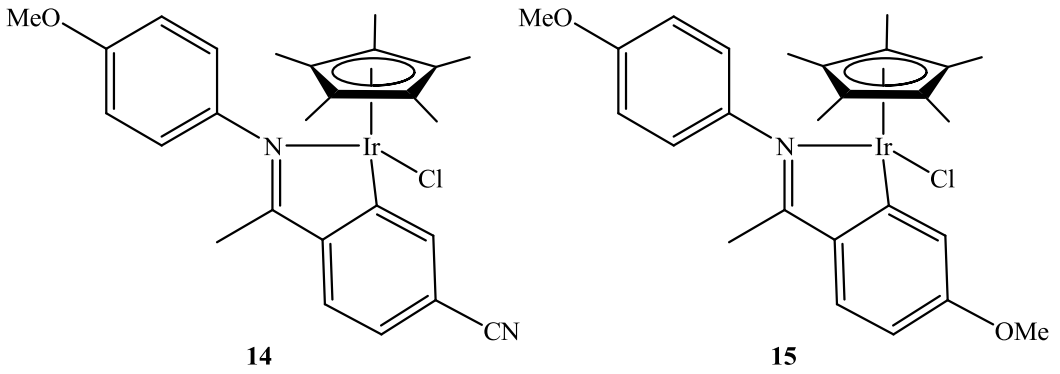

Figure 1.2.11 Cyclometalated imido Ir(III) complexes used by Xiao for reductive amination

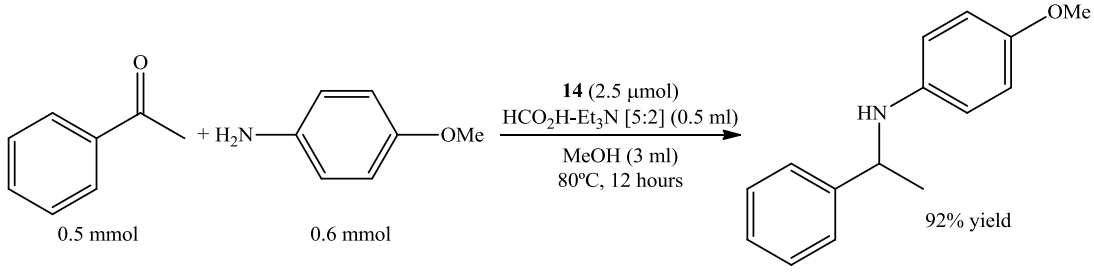

Scheme 1.2.31 Xiao's reductive amination between acetophenone and *p*-anisidine

A chiral example of intramolecular reductive amination is shown in **Scheme 1.2.32**, by Wills *et al*.[83]

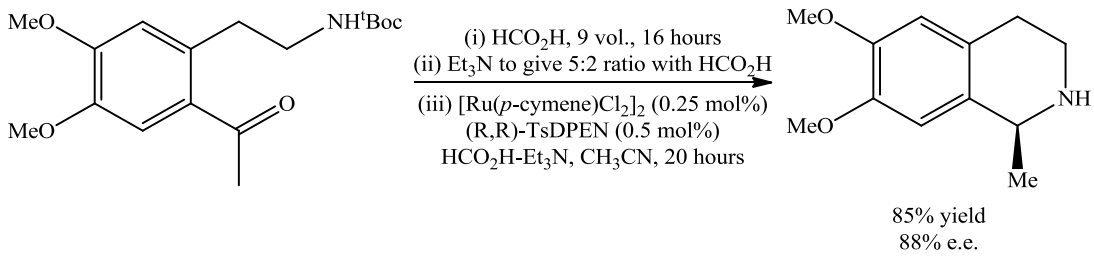

Scheme 1.2.32 Wills' conditions for intramolecular reductive amination

1.2.5.2 C-C Bond Forming Reactions

In a similar process to that of redox neutral alkylations between alcohols and amines, Williams developed a hydrogen borrowing system to form C-C bonds from alcohols. The alcohol is initially oxidised to a ketone or aldehyde, which then undergoes an olefination, and finally the alkene is reduced to an alkane without the need of an external hydrogen donor (**Scheme 1.2.33**). One possible method to obtain the intermediate alkene involves the use of active methylene compounds (**Scheme 1.2.34**).[84] A more common method employs indirect Wittig reactions with phosphorane ylide nucleophiles (**Scheme 1.2.35**).[85, 86]

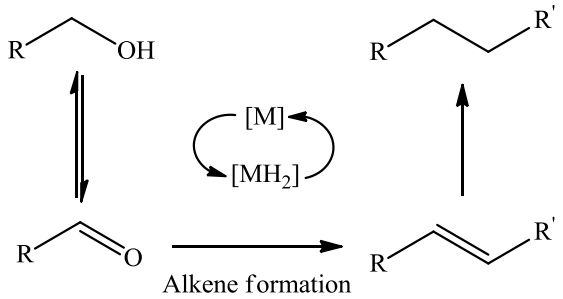

Scheme 1.2.33 General scheme for C-C bond forming reactions from alcohols

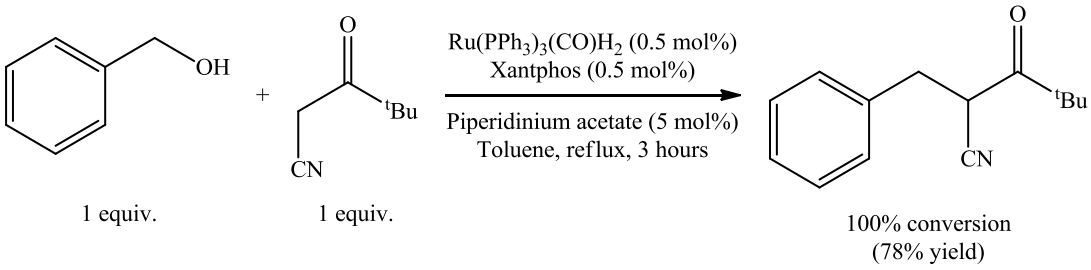

Scheme 1.2.34 Williams' conditions for the C-C bond formation between benzyl alcohol and a ketonitrile. Xantphos = 4,5-bis(diphenylphosphino)-9,9-dimethylxanthene

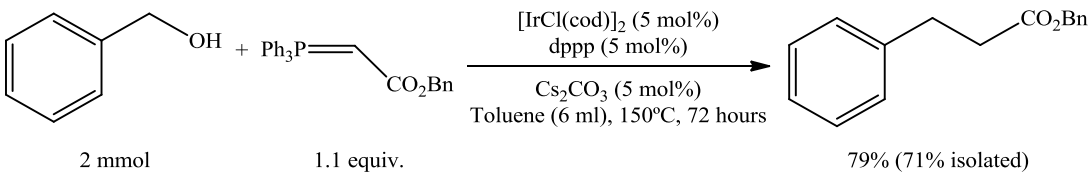

Scheme 1.2.35 Williams' conditions for the C-C bond formation between benzyl alcohol and benzyl(triphenylphosphoranylidene)acetate. dppp = 1,3-bis(diphenylphosphino)propane

1.2.6 Reactions Involving H_2

Hydrogenations using molecular H_2 and transition metal catalysts are extensively employed and constitute a vast area of research. This section only aims to, very briefly, present some examples of such reactions with relevant ruthenium, rhodium and iridium complexes.

Several ruthenium systems have served as efficient catalysts for non-asymmetric hydrogenations. One example is the dimer $[RuCl_2(p\text{-cymene})]_2$ which, together with I_2, is able to facilitate the reduction of quinolines in tetrahydrofuran (**Scheme 1.2.36**).[87] On publishing their results, Zhou and co-workers stated that the presence of I_2 was fundamental, and even $[RuI_2(p\text{-cymene})]_2$ produced only 48% conversion when I_2 was not included in the reaction.

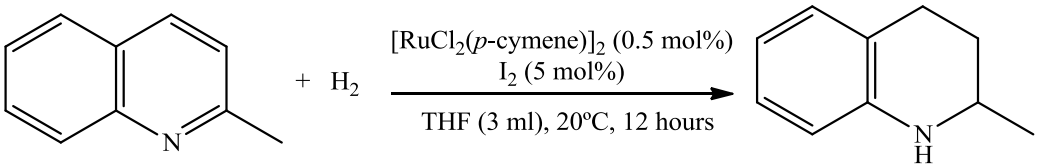

Scheme 1.2.36 Zhou's conditions for the hydrogenation of 2-methylquinoline. S/C = 100

The use of DPEphos (bis(2-diphenylphosphinophenyl)ether) as ligand for cyclopentadienyl or *p*-cymene complexes of ruthenium (**Figure 1.2.12**) permits the reduction of styrene to ethylbenzene in good yields, as detailed in **Scheme 1.2.37**.[88] However, more common is the utilisation of N-NH_2 or P-NH_2 ligands, for which Ikariya has found a wide range of applications, such as the hydrogenation of carboxylic esters (**Scheme 1.2.38**)[89] or imides (**Scheme 1.2.39**).[90]

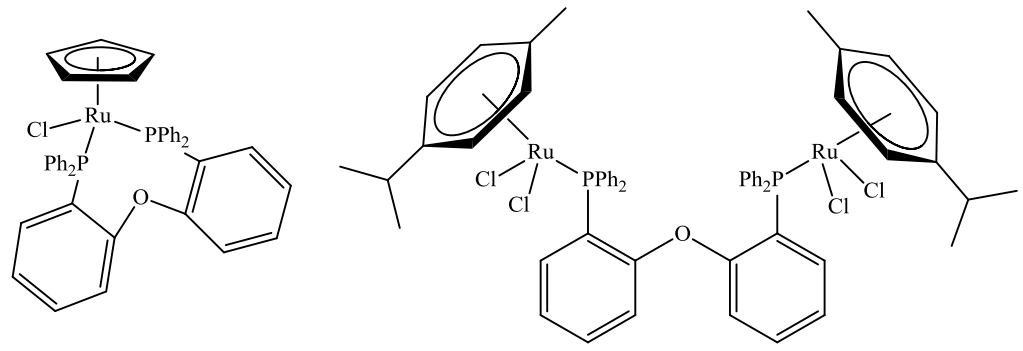

16 **17**

Figure 1.2.12 DPEphos complexes of ruthenium used for the hydrogenation of styrene

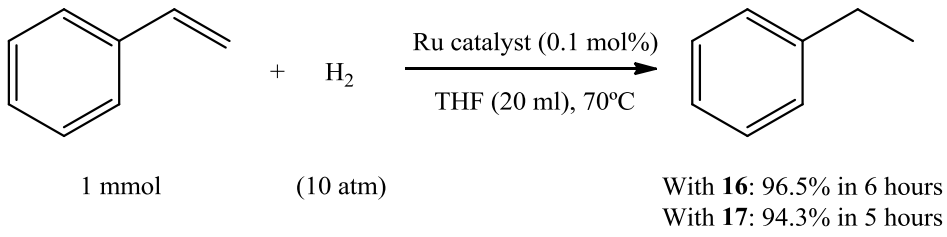

Scheme 1.2.37 Balakrishna's conditions for the hydrogenation of styrene

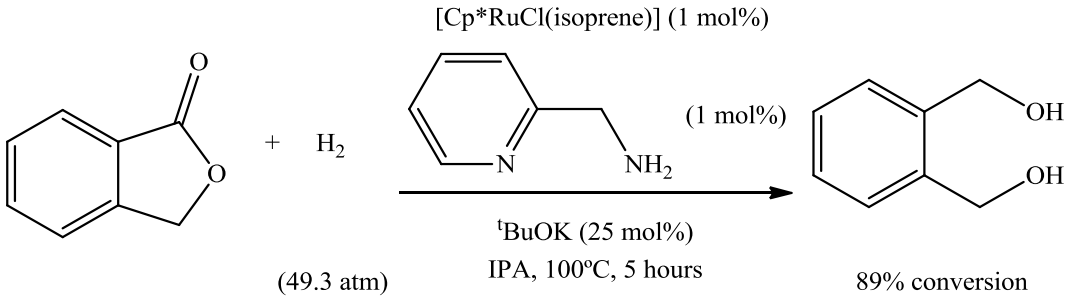

Scheme 1.2.38 Ikariya's conditions for the hydrogenation of phthalide

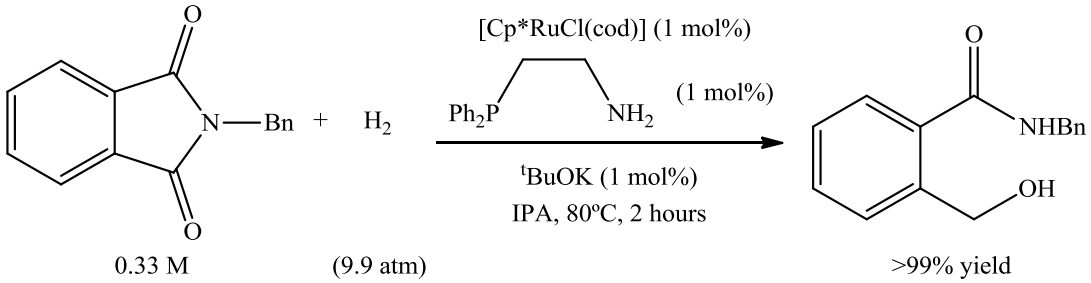

Scheme 1.2.39 Ikariya's conditions for the hydrogenation of N-benzylphthalimide

Ikariya's group has also worked on asymmetric hydrogenations, initially with similar systems to the ones employed in the non-asymmetric reactions, but including chiral ligands (**Scheme 1.2.40**).[91] Later on, this group developed triflylamide (NTf)-tethered metal-(DPEN) complexes of Ru[92] and Rh or Ir,[93] all performing well in the asymmetric hydrogenation of acetophenone. Under identical conditions (H_2 pressure = 30 atm, MeOH, 30ºC, 24 hours, S/C = 100), the three complexes in **Figure 1.2.13** yielded 1-phenylethanol in >94% conversions and 93% enantiomeric excesses. In all of these latest examples where the solvent utilised was an alcohol, it was demonstrated that the reactions did not proceed without a specified H_2 pressure, so the role of isopropanol or methanol was not that of a hydrogen donor. In the Noyori-type catalysts **18**, **19** and **20**, the NTf tether somehow switches the catalytic activity from asymmetric transfer hydrogenation to asymmetric hydrogenation.

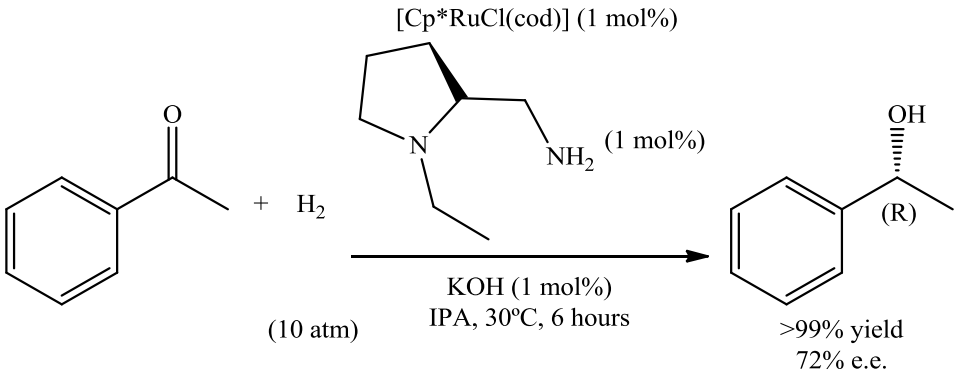

Scheme 1.2.40 Ikariya's conditions for the hydrogenation of acetophenone using [Cp*RuCl(cod)] and a chiral N-NH_2 ligand

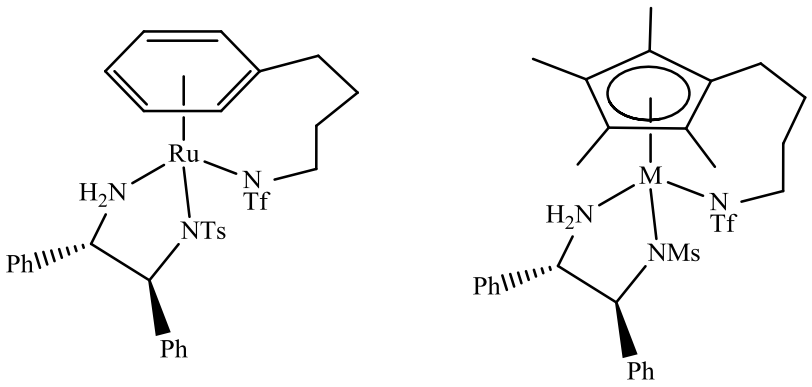

18

19 M = Rh
20 M = Ir

Figure 1.2.13 Triflylamide (NTf)-tethered complexes used by Ikariya for asymmetric hydrogenations

1.3 Mechanistic Investigations

The different possible mechanisms for transfer hydrogenations have been reviewed by Brandt *et al.*[94] Initially, they can be divided into two main categories: direct hydrogen transfer mechanism or hydridic mechanism. A direct hydrogen transfer does not involve metal hydride intermediates and typically operates in reactions catalysed by main group metals, such as the Meerwein-Ponndorf-Verley (MPV) reduction (see above, **Scheme 1.2.2**). The hydridic route is associated with transition metals and entails the formation of hydride intermediates. It can be further classified into either a dihydride or a monohydride pathway. In a dihydride mechanism, the two hydrogens from an alcohol or amine become equivalent, both behave as hydrides during the metal-catalysed process (**Scheme 1.3.1**). In a

monohydride mechanism, only the C–H from the donor forms a hydride with the metal, whilst the proton in –OH or –NRH keeps its identity (**Scheme 1.3.2**).

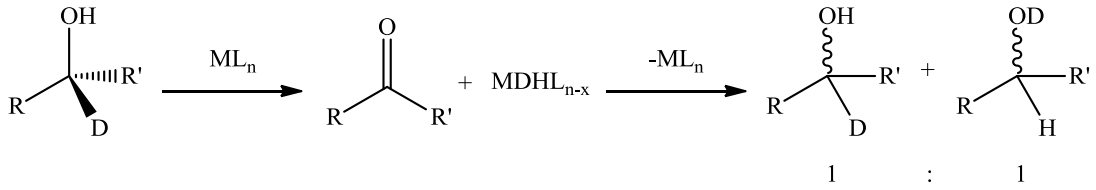

Scheme 1.3.1 Dihydride route in the dehydrogenation of a monodeuterated alcohol and later hydrogenation of the resultant ketone

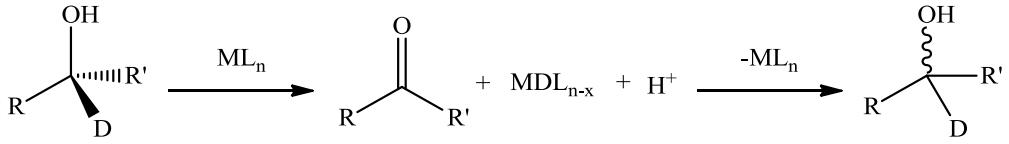

Scheme 1.3.2 Monohydride route in the dehydrogenation of a monodeuterated alcohol and later hydrogenation of the resultant ketone

Dihydride mechanisms are common with ruthenium dichloride complexes, such as $RuCl_2(PPh_3)_3$.[95] In the presence of a base and isopropanol, $RuCl_2(PPh_3)_3$ first gives $RuHCl(PPh_3)_3$ and then $RuH_2(PPh_3)_3$ in two consecutive steps through alkoxide formation and β-elimination. The latter is the active species in hydrogen transfer reactions, which follow the mechanism depicted in **Scheme 1.3.3**.[96]

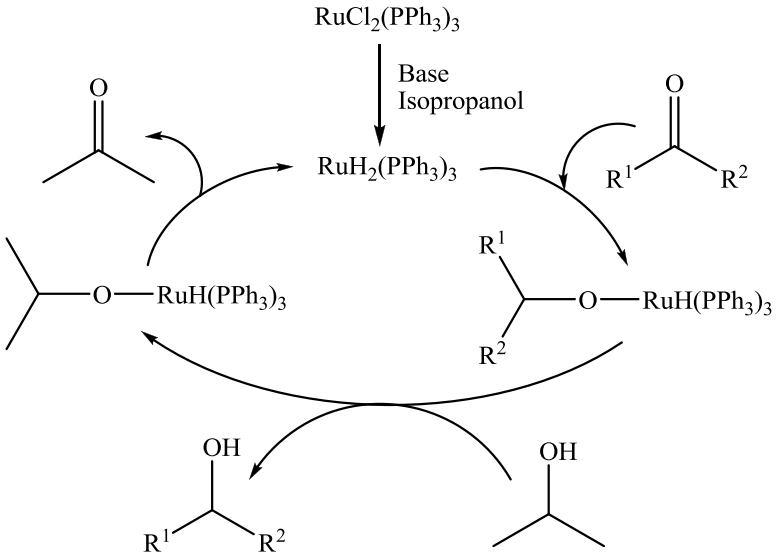

Scheme 1.3.3 Mechanism for transfer hydrogenation with $RuCl_2(PPh_3)_3$

Monohydride mechanisms generally operate in rhodium- or iridium-catalysed reactions, and also with ruthenium monochloride species.[94] They proceed by either inner sphere or outer sphere pathways.

1.3.1 Inner Sphere Mechanisms

These processes involve the formation of an alkoxide with the transition metal, followed by β-elimination to produce the metal hydride. **Scheme 1.3.4** shows the inner sphere mechanism originally proposed for transfer hydrogenations with transition metals in isopropanol.[51]

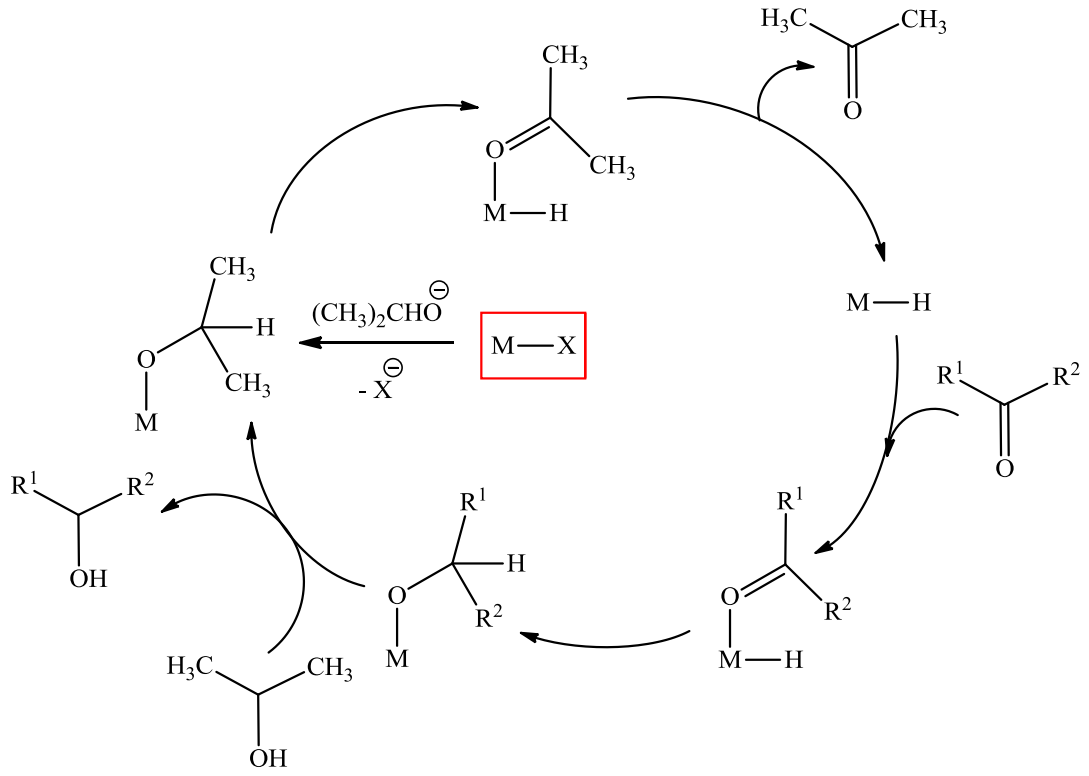

Scheme 1.3.4 Inner sphere mechanism for transfer hydrogenations with transition metals in isopropanol

A particular example of a monohydride inner sphere mechanism is the one proposed by Fujita for his oxidant-free oxidation of alcohols with a 2-hydroxypyridine Cp*Ir complex (**Scheme 1.3.5**).[73] This mechanism has been supported by the detection of the H_2 formed during the reaction and the fact that species **11** has been isolated and shows high catalytic activity.

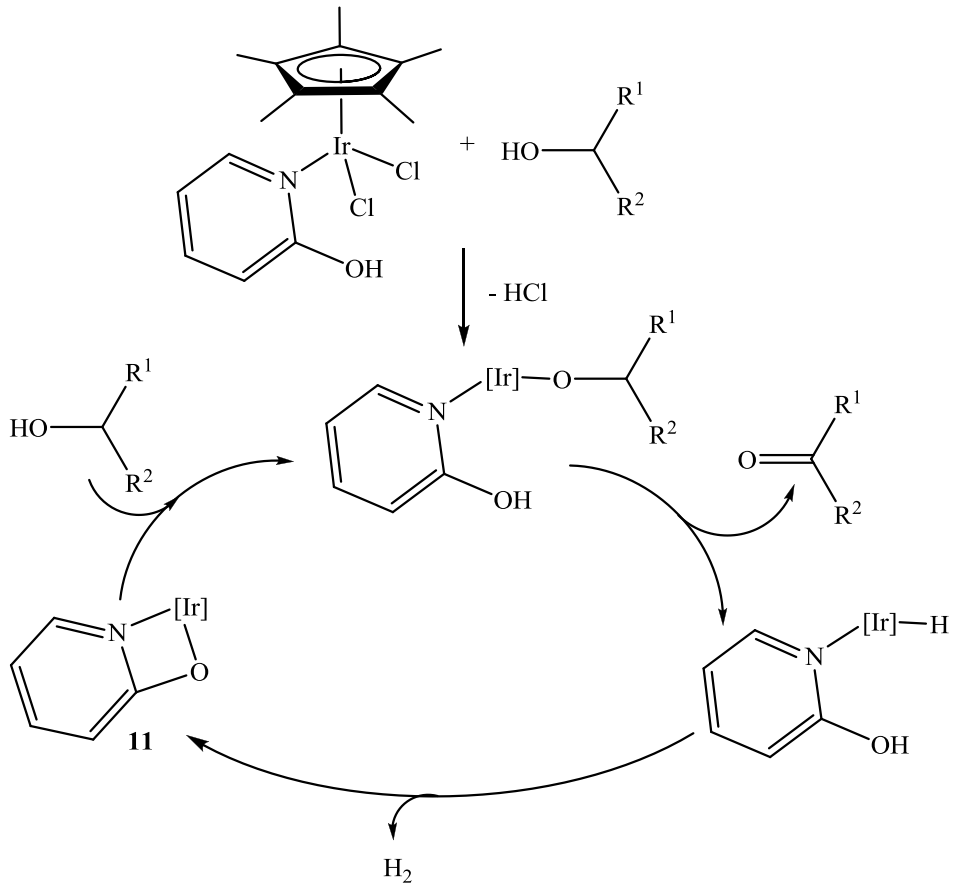

Scheme 1.3.5 Mechanism proposed by Fujita for the oxidant-free oxidation of alcohols with a 2-hydroxypyridine Cp*Ir complex

1.3.2 Outer Sphere Mechanisms

In these mechanisms, there is no direct coordination of any substrate to the metal and, with help from a ligand, the hydrogen transfer can take place either in a concerted or stepwise manner.

1.3.2.1 Concerted Mechanisms

A concerted mechanism has been proposed for the transfer hydrogenation with the dimeric Shvo catalyst, which is in equilibrium with two monomers **21** and **22** (**Scheme 1.3.6**).[94] **21** can hydrogenate double bonds in hydrogen acceptors (**Scheme 1.3.7**), while **22** is able to dehydrogenate a hydrogen donor, so the two monomers interconvert.

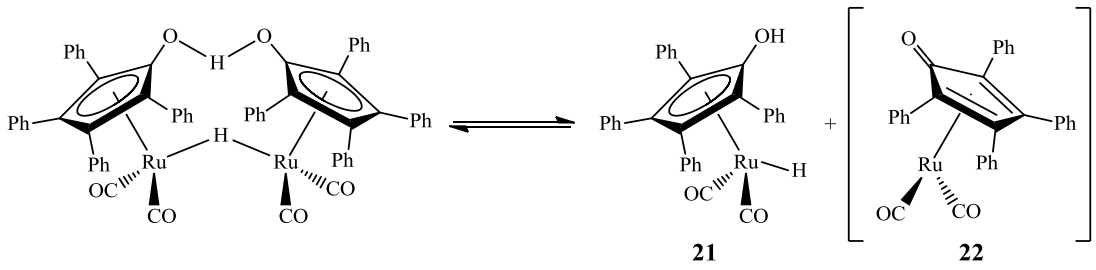

Scheme 1.3.6 Shvo's catalyst equilibrium with monomers **21** and **22**

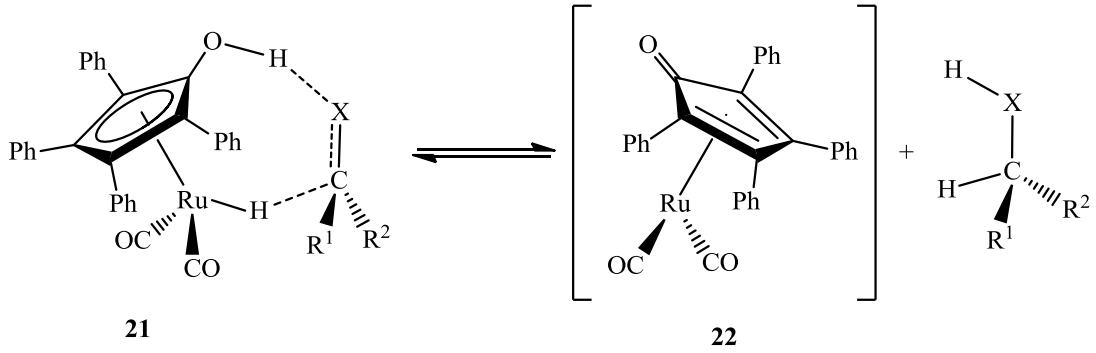

Scheme 1.3.7 Transfer hydrogenation with the monomer **21** from the Shvo catalyst

The metal ligand bifunctional catalysis, as Noyori denominated those transfer hydrogenations with [Ru(η^6-arene)Cl(N,N- or N,O-ligand)] complexes, is another example of a concerted process.[51, 94] The chelating ligands involved contain an NH_2 or NRH group, which interacts through a hydrogen bond with the carbonyl oxygen in ketones. This assists the formation of an ordered six-membered transition state, from where the hydride and proton transfers occur simultaneously (**Scheme 1.3.8**). A strong base is needed, firstly to generate the catalyst *in situ* from [$RuCl_2(\eta^6$-arene)]$_2$ and the chelating ligand, and also to generate the 16 electron species **B** from the pre-catalyst **A**. Both species **B** and **C** have been isolated and characterised by X-ray crystallography,[50, 51] but also similar intermediates in reactions with aminoindanol ligands have been detected by electrospray ionisation mass spectroscopy.[97] Not only experimental but also computational methods provide evidence for this mechanism.[51, 98-100] With aryl ketones, a transition state in which the aromatic substituent is close to the η^6-arene ligand of the complex is favoured due to CH/π attractive interactions, and greatly contributes to an enrichment of the enantioselectivity (**Figure 1.3.1**).[100, 101]

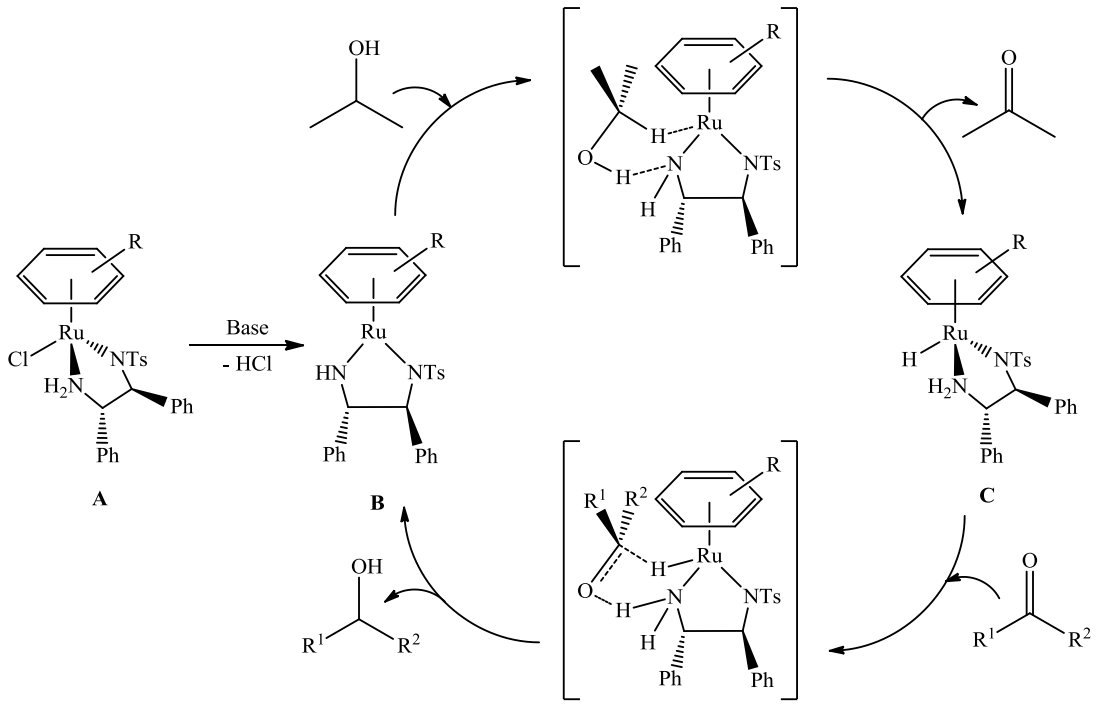

Scheme 1.3.8 Noyori's metal ligand bifunctional catalysis mechanism

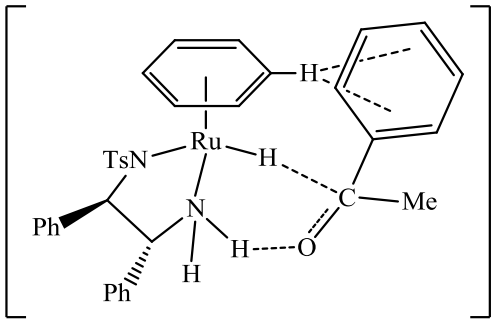

Figure 1.3.1 CH/π interaction between the η^6-arene ligand and the aryl substituent of a ketone

Xiao and co-workers have provided a modified version of Noyori's mechanism for reactions that proceed in water with HCO_2Na, where H_2O is the proton donor and HCO_2^- is the hydride donor.[102] Under these conditions, H_2O can behave as hydrogen-bond donor and interact with the carbonyl oxygen of a ketone during hydrogen transfer, which greatly improves the rate of the reaction. However, in aqueous media, the transformation depends largely on the pH. In acidic medium, TsDPEN can get protonated and de-coordinate, reducing the catalytic activity, and in basic medium, H_2O can coordinate to Ru and deactivate the catalyst (**Scheme 1.3.9**).

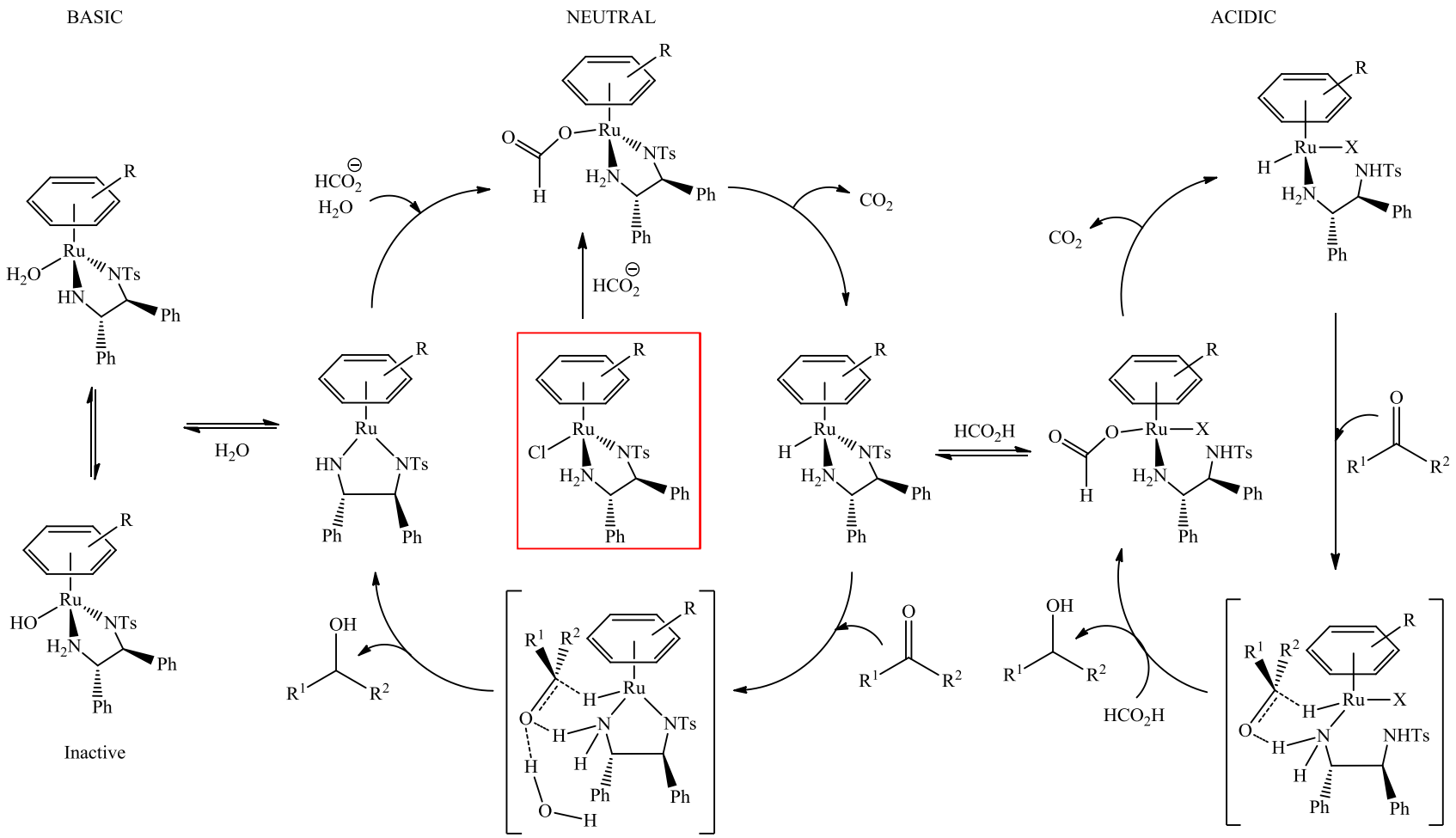

Scheme 1.3.9 Xiao's mechanism for transfer hydrogenation in water at different pH conditions

1.3.2.2 Stepwise Mechanisms

In a stepwise mechanism, the transfer of the proton and that of the hydride occur in separate steps. For example, this happens in ionic hydrogenations, where a rapid and reversible protonation of the substrate precedes and facilitates the hydride transfer from the metal. This mechanism is the one believed to operate in the hydrogenation of imines.[69, 94, 103]

1.4 Immobilisation Techniques

1.4.1 Introduction

The main advantage of heterogeneous catalytic processes is the ease of recovery of the metal catalysts employed. This is very important when the metals used are expensive and limited and recycling becomes a priority for the industry in order to reduce economic costs and unnecessary pollutant residues. Besides, in specific cases such as the production of pharmaceuticals, the removal of the catalysts is essential to avoid or minimise the metal content in the final products. In spite of these conveniences, heterogeneous catalysts are still, generally, less active and less selective than homogeneous ones. This is explained by the fact that homogeneous catalysts dissolve in the reaction media, facilitating the access of the substrates to the catalyst. On the other hand, in heterogeneous systems, the access to catalytically active sites is commonly restricted, and maximising the surface-area-to-volume ratio of the catalysts is a fundamental need. A desirable combination of both types of catalysis might be obtained through the immobilisation of homogeneous complexes, which can be carried out by either covalent or non-covalent interactions with the chosen support. This way, the catalysts can be recovered and recycled by, for example, simple filtration or decantation or, more efficiently, adapted for flow chemistry.

1.4.2 Covalent Immobilisation

Covalent tethering of metal complexes to a solid support through coordinated ligands is one of the most common and favoured immobilisation techniques (**Figure 1.4.1**). It has the advantage of generating more stable and stronger interactions, but generally requires previous modification of the ligands/complexes and/or supports.

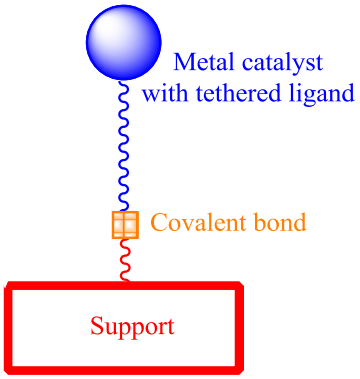

Figure 1.4.1 Covalent bond between a functionalised metal catalyst and a support

Both organic and inorganic matrices have been used for covalent immobilisation, including silica, alumina, polymers, dendrimers, etc.[104-106] Organic supports might be soluble (linear polymers, dendrimers) or insoluble (cross-linked polymers). Soluble polymer-attached complexes allow catalytic reactions to proceed under homogeneous conditions and, when the reaction is complete, can be separated by, for example, solvent precipitation or membrane filtration. In the case of insoluble polymers, an important characteristic is their swellability in organic solvents, which may be beneficial and favour a more homogeneous-like behaviour or detrimental and incite aggregation and deactivation of the catalysts. Inorganic oxides, on the other hand, are always insoluble and present very high thermal and mechanical stabilities, large surface areas and a rigid structure that prevents the aggregation of active catalysts. Probably the most widely utilised inorganic oxide is silica, principally in the form of mesoporous silica (*e.g.* MCM-41), with well defined pore structures and pore diameters between 2 and 50 nm. Silica and alumina contain silanol groups on their surfaces which ease the covalent attachment of potential ligands (**Scheme 1.4.1**).

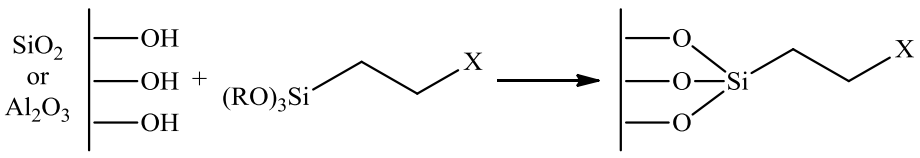

Scheme 1.4.1 Typical covalent bonding to silanol groups

To avoid metal leaching, both the covalent bond between the ligand and the support and the coordinative bond between the ligand and the metal have to be stable enough under catalytic conditions. To this end, the immobilisation through an arene

or cyclopentadienyl ligand is an attractive approach, because these ligands coordinate to the metal centre with several carbon atoms and this is expected to offer very high stabilities against dissociation. η^x-Coordinated rings (x = 5 or 6) are π-acid ligands which, apart from donating electron density to the metal, also receive certain back-bonding into their π^* empty orbitals.[107, 108] One example of this technique is the immobilised version of the SCRAM catalyst $[Ir(\eta^5\text{-}C_5Me_5)I_2]_2$ where one of the methyl groups in each ring has been functionalised with a $(CH_2)_5OH$ chain and this, in turn, immobilised onto poly(ethyleneglycol) (**Figure 1.4.2**).[109] This heterogeneous catalyst has been used in transfer hydrogenation reactions such as the racemic resolution of sertraline, and survived three recycles.[81]

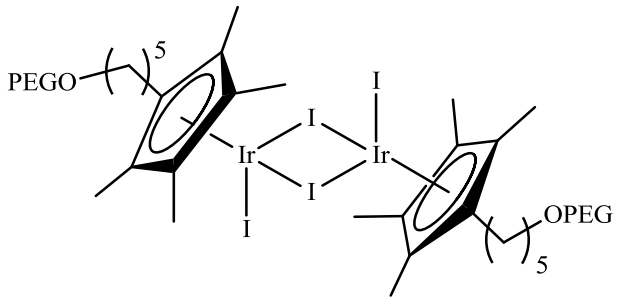

Figure 1.4.2 SCRAM catalyst immobilised onto poly(ethyleneglycol)

1.4.3 Non-Covalent Immobilisation

The different non-covalent methods employed for the immobilisation of metal complexes generally involve weak interactions with the supports. Consequently, the choice of reaction conditions and solvents play an important role in guaranteeing the stability and recovery of the catalysts. These methods represent a more straightforward approach than covalent immobilisation, with no or less previous modifications of the catalysts or supports needed. The four principal techniques for non-covalent immobilisation are adsorption, entrapment and electronic or coordinative interactions.[104, 106, 110]

1.4.3.1 Immobilisation by Adsorption

In the case of adsorption, the metal complex stays attached to the support relying on weak van der Waals interactions. The success of this method tends to be very limited, but improved approaches use the formation of hydrogen bonds with the matrix (*e.g.* silanol groups on silica) (**Figure 1.4.3**). These hydrogen bonds might

form between the surface of the support and a suitable ligand of the metal complex or a counterion of a charged catalyst.[104, 106, 110] Another version of adsorption is that of supported liquid phases (SLP). This involves a biphasic system in which a polar solvent adheres to a hydrophilic support and dissolves a hydrophilic catalyst, whilst the catalytic reaction takes place in an organic apolar solvent in contact with the polar one.[106, 110]

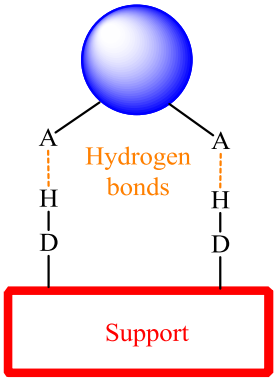

Figure 1.4.3 Adsorption of a catalyst through hydrogen bond formation with groups on the support

An example of SLP was reported by Wan and Davis in 1994.[111, 112] They presented a system in which [Ru(BINAP-4SO_3Na)(benzene)Cl][Cl] (BINAP = 2,2'-bis(diphenylphosphino)-1,1'-binaphthyl) was dissolved in highly polar ethylene glycol as the hydrophilic phase, supported on a controlled-pore glass (CPG) with an average pore size of 242 Å. A non-polar mixture of 1:1 cyclohexane/chloroform was used as the hydrophobic phase, where the reactants and products dissolved (**Figure 1.4.4**). The heterogeneous catalyst was tested in the hydrogenation of 2-(6'-methoxy-2'-naphthyl)acrylic acid (**Scheme 1.4.2**) under 94-101 MPa of H_2 and at 276 K. 100% conversion was obtained with an enantiomeric excess of 96%. The results were similar to those of the analogous homogeneous system in methanol, whereas the two-phase system without CPG gave a low conversion of < 2%. For the heterogeneous SLP system, recycling was successful without loss of enantioselectivity and with no leaching of ruthenium into the organic phase observed.

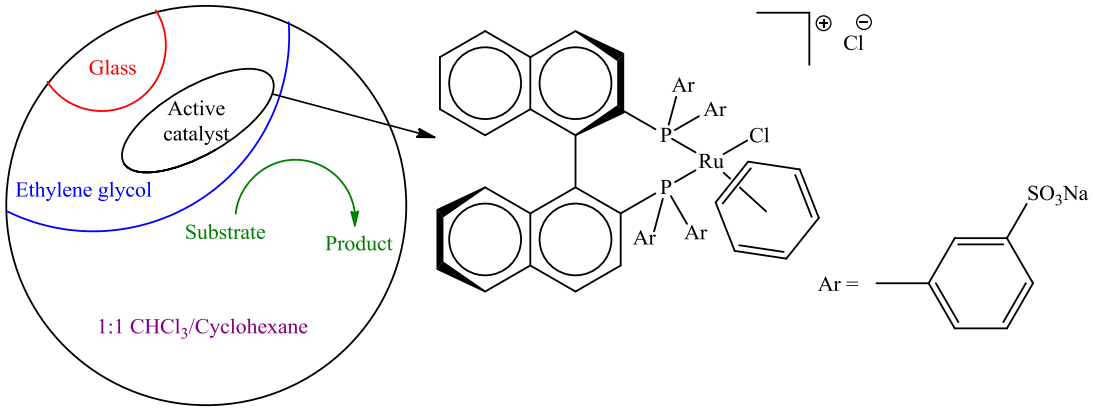

Figure 1.4.4 [Ru(BINAP-4SO_3Na)(benzene)Cl][Cl] in ethylene glycol supported on a controlled-pore glass

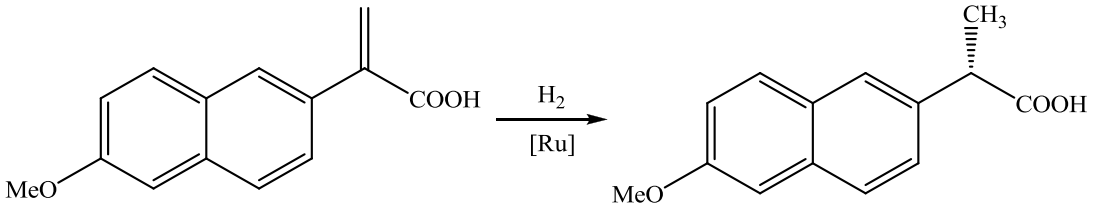

Scheme 1.4.2 Hydrogenation of 2-(6'-methoxy-2'-naphthyl)acrylic acid to (S)-naproxen

1.4.3.2 Immobilisation by Entrapment

The method of entrapment or encapsulation encloses the catalyst inside the pores of a support, which makes unnecessary the presence of additional complex-support interactions.[104, 106, 110] For this method to be successful, the apertures of the pores in the matrix have to be smaller than the size of the complex inside them, so the metal catalyst stays entrapped and leaching is avoided. The two techniques employed for this aim are either the assembling of parts of the catalyst together once inside the cages of the support or the assembling of the support around the pre-formed catalyst. The first case is known as the "ship-in-a-bottle" approach, and it is schematically depicted in **Figure 1.4.5**. The second case is achieved, normally, by polymerising the support around the catalyst, which tends to generate poorly defined pore openings and sizes. Depending on the technique of choice, the stabilities of either the support or the catalyst under the synthesis conditions need to be considered.

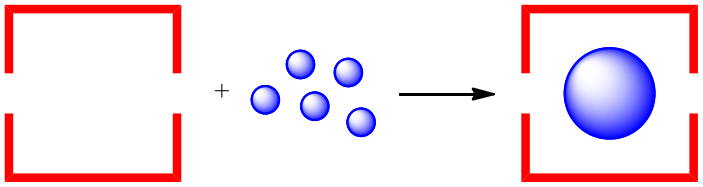

Figure 1.4.5 "Ship-in-a-bottle" entrapment by formation of the catalyst inside the pores of a support

Blum and co-workers managed to entrap the catalyst [Ru(*p*-cymene)Cl(BINAP)][Cl] inside a porous silica obtained by the sol-gel method of polymerising $Si(OMe)_4$.[113] This system was used for the hydrogenation of itaconic acid (R = H in **Scheme 1.4.3**) with a substrate/catalyst molar ratio of 30 at 80ºC and 10 atm. of H_2 in water, in the presence of NEt_3. The catalyst was recycled, with yields of 100, 98, 95 and 90% in the first four runs and optical purities of 52, 50, 46 and 41%, and no leaching was observed. The analogous homogeneous system was not active for this transformation due to insolubility in water.

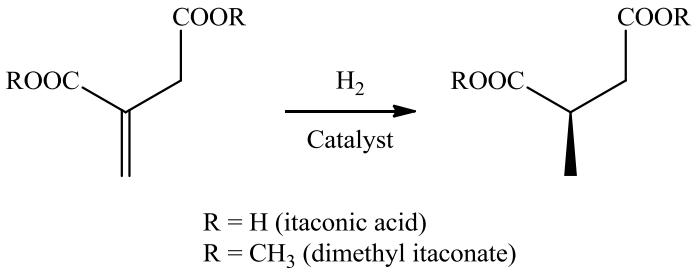

Scheme 1.4.3 Hydrogenation of itaconic acid (R = H) or dimethyl itaconate (R = CH_3)

1.4.3.3 Immobilisation by Electronic Interactions

This method relies on the ionic exchange capabilities of some inorganic materials (clays, zeolites, etc.) and polymeric resins. The most common case is that in which the support presents anionic charges that allow the interaction with cationic complexes by exchange with the initial counterion of the positively charged catalyst (**Figure 1.4.6**).[104, 106, 110] As a drawback, this immobilisation technique can only be applied if the catalyst is known to remain charged during the complete catalytic cycle. Natural or synthetic clays are the preferred supports. They are aluminosilicates where isomorphic substitutions among cations (Al/Si, Mg/Al, etc.) generate charge defaults and the subsequent anionic nature.

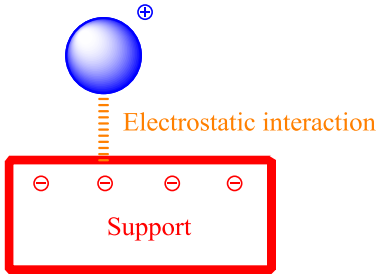

Figure 1.4.6 Electrostatic interaction between an anionic support and a cationic metal complex

One of the first examples of electrostatic immobilisation of rhodium complexes on clays was published by Uematsu and co-workers.[114] They reported the cationic exchange of [Rh(BINAP)(cod)][ClO_4] with sodium hectorites (clays) by intercalation of the complex between the clay sheets in a mixture of acetonitrile and water (**Figure 1.4.7**). The system was tested for the hydrogenation of itaconates (**Scheme 1.4.3**) and gave complete conversions in methanol in 2 hours, but with very poor enantioselectivities. The recycling of this catalyst was not reported.

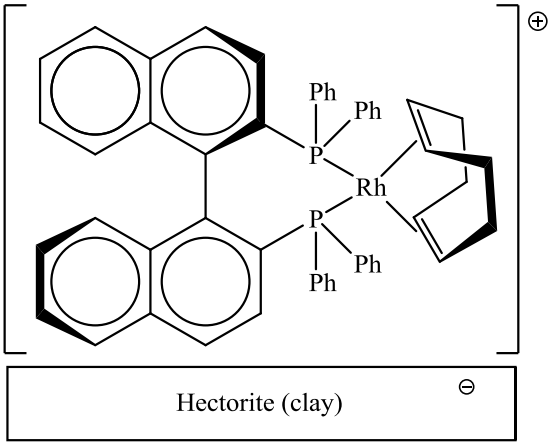

Figure 1.4.7 $[Rh(BINAP)(cod)]^+$ complex immobilised by electrostatic interaction with an anionic clay

1.4.3.4 Immobilisation by Coordinative Interactions

In this type of immobilisation, a group from the support coordinates to the metal centre of the catalyst (**Figure 1.4.8**).[110] This coordination can be direct or through a previous modification of the support with covalently grafted small molecules, *e.g.* aminopropyl silica.

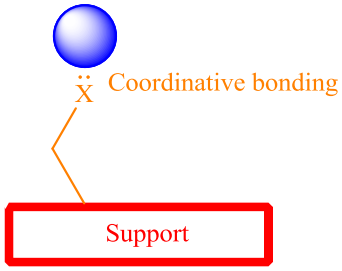

Figure 1.4.8 Coordinative interaction between a functionalised support and a metal catalyst

One example of this approach was the immobilisation of rhodium hydrogenation catalysts onto basic carbon by Stevenson *et al.*[115] Complexes of the type [Rh(nbd)(diphosphine)][BF_4] (nbd = norbornadiene) were anchored to unmodified carbon surfaces via Rh-O coordinative bonds (**Figure 1.4.9**) and tested in the hydrogenation of prochiral C=C bonds like that of dimethyl itaconate (R = CH_3 in **Scheme 1.4.3**). The results showed similar activities to those obtained with the homogeneous analogues (complete conversions reached within minutes) and improved enantioselectivities. When the diphosphine used was 2,4-bis(diphenylphosphino)pentane (bdpp), the enantiomeric excess was 78% (70% in the homogeneous system), with no leaching observed by ICP analysis after three reuses.

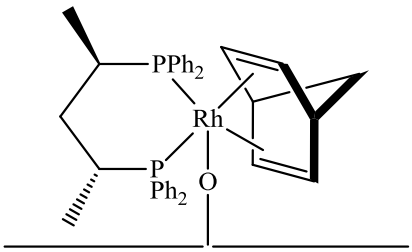

Figure 1.4.9 [Rh(nbd)(bdpp)]$^+$ complex immobilised on basic carbon through a Rh-O coordinative interaction

1.4.4 Examples of Immobilised Ruthenium Complexes

The Noyori-type TsDPEN ligand or derived ligands are probably the most frequently used for transfer hydrogenations with ruthenium, and numerous examples have been published where the Ru-TsDPEN moiety has been, to a higher or lower extent, successfully immobilised. For instance, Wang and co-workers studied the performance of complexes of ruthenium with the silica-supported TsDPEN ligand (**Figure 1.4.10**).[116] The complexes were prepared *in situ* by addition of [$RuCl_2$(*p*-

cymene)]$_2$ to the corresponding supported ligand, and the reduction of acetophenone was tested in water with HCO_2Na as the hydrogen donor (**Scheme 1.4.4**). The mixture of Ru-**23** (1 mol%) and tetrabutylammonium bromide (TBAB) as an additive gave > 99% yield with 96% e.e. after 2 hours for the first three runs, and the catalyst could be reused six times with maintained enantioselectivities and still quantitative yields. Various other ketones could be reduced with the same method, in some cases achieving eleven possible reuses, but no leaching information was reported. Ligands **24** and **25** (MCM-41 and SBA-15) gave worse results.

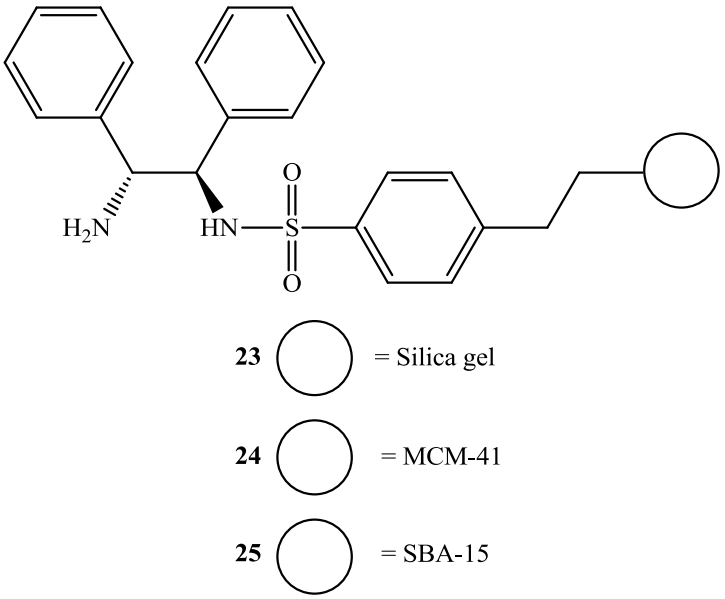

Figure 1.4.10 TsDPEN ligand supported on different types of silica

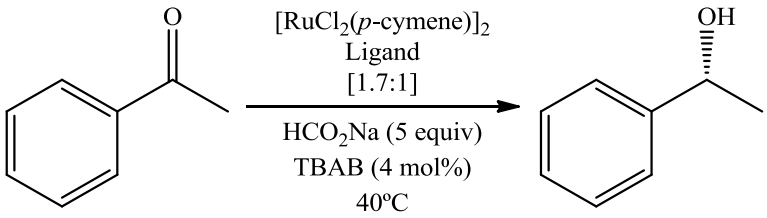

Scheme 1.4.4 Wang's conditions for the reduction of acetophenone. S/C = 100

In the same year, Xiao *et al*. reported the immobilisation of Ru-TsDPEN on poly(ethyleneglycol) (**Figure 1.4.11**).[117] The catalyst was tested in the asymmetric transfer hydrogenation of acetophenone in water with HCO_2Na (**Scheme 1.4.5**). 99% conversion was obtained after 1 hour, with 92% enantiomeric excess. Compared with the immobilised system in HCO_2H-Et_3N, the reaction in HCO_2Na-H_2O gave a much faster rate. At the end of each reduction, a solvent of low polarity such as

diethyl ether could be added to precipitate the PEG-supported Ru-TsDPEN, and the catalyst could be reused more than ten times with no loss in enantioselectivity, although 0.4% of leached Ru was detected by ICP analysis.

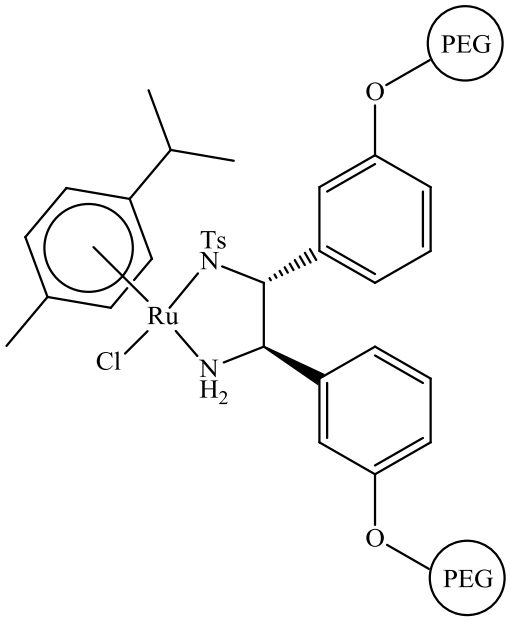

Figure 1.4.11 Poly(ethyleneglycol)-supported Ru-TsDPEN

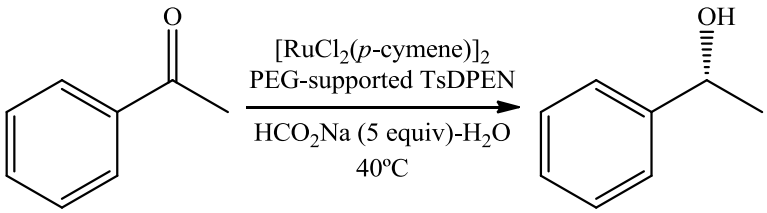

Scheme 1.4.5 Xiao's conditions for the reduction of acetophenone. S/C = 100

The group of Li developed a strategy to anchor Ru-TsDPEN to a mesoporous silica which had been previously modified with the introduction of magnetic nanoparticles, so the catalyst could be recovered with the aid of an external magnet.[118] After immobilisation of the ligand (**Figure 1.4.12**), the complex was generated *in situ* by addition of $[RuCl_2(p\text{-cymene})]_2$. The system was tested in the asymmetric reduction of substituted dihydroisoquinoline (**Scheme 1.4.6**), giving 98% yield and 94% e.e. in 1.5 hours, very similar results to those obtained with the corresponding homogeneous analogue. The supported catalyst could be reused nine times with enantioselectivities ranging from 90 to 94% and increasing reaction times

of 1.5-7 hours. A leaching of 11 mol% Ru was detected by ICP analysis after the nine runs.

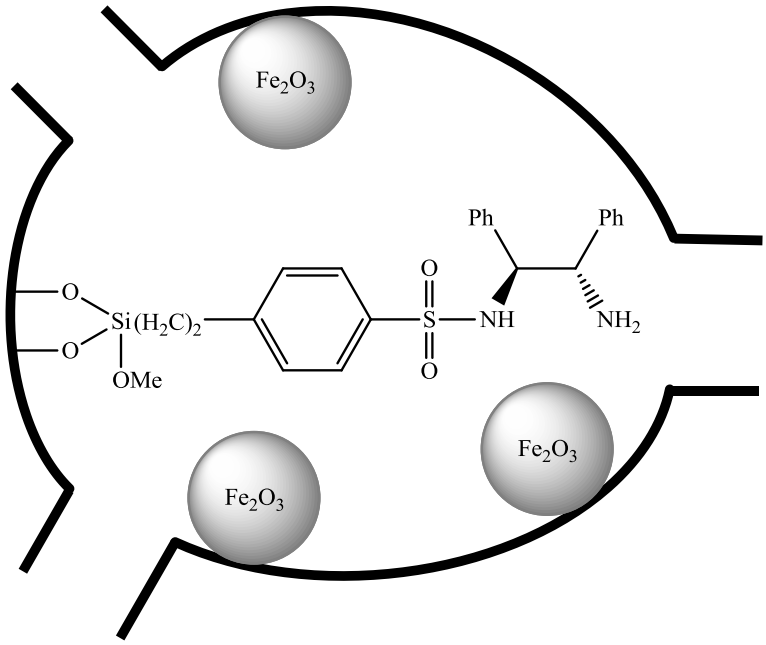

Figure 1.4.12 TsDPEN ligand immobilised onto magnetic mesoporous silica

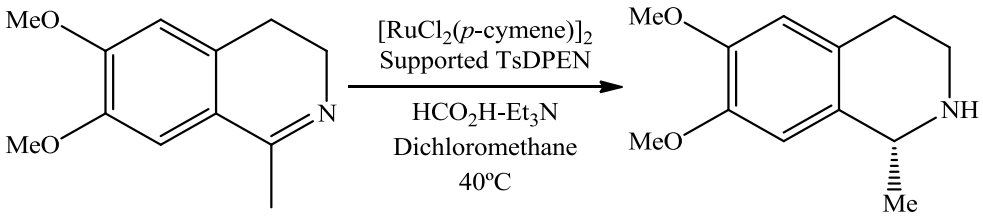

Scheme 1.4.6 Li's conditions for the reduction of substituted dihydroisoquinoline. S/C = 100

The same group also published an interesting example of encapsulated Ru-TsDPEN in SBA-16 silica.[119] They used silylating agents containing organic groups with different hydrophobic or hydrophilic properties in order to tune the microenvironment of the silica nanocages and enhance the diffusion rates of substrates and products. The two silylating agents that they tested are shown in **Figure 1.4.13**. Different systems with varied ratios of the two silylating agents were used in the asymmetric transfer hydrogenation of acetophenone and other substrates in HCO_2Na-H_2O. The best results were always obtained when the nanocages had been exclusively modified with amphiphilic groups.

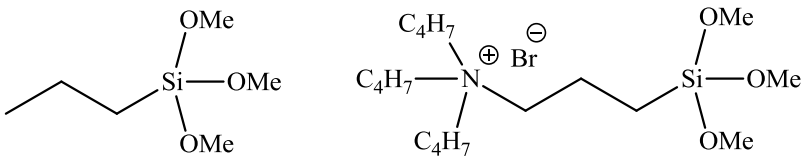

Figure 1.4.13 a) lipophilic propyltrimethoxysilane and b) amphiphilic N-trimethoxysilylpropyl-N,N,N-tri-*n*-butylammonium

Another example involving magnetic nanoparticles was that of Fan and co-workers.[120] They modified the arene in Ru-TsDPEN to include an ammonium salt (**Figure 1.4.14**), suitable to form a pseudorotaxane complex with dibenzo-24-crown-8-functionalised magnetic nanoparticles. In this case, the hydrogenation of 2-methylquinoline was examined (**Scheme 1.4.7**), which could take place homogeneously. Upon completion of the reaction, the functionalised magnetic nanoparticles could be added to form the insoluble pseudorotaxane, later separated from the product by decantation with the aid of an external magnet. The catalyst could be then disassembled and reused. A total of five runs were performed, with 2 mol% Ru, giving constant 89% e.e. and activities in the range 95-99%.

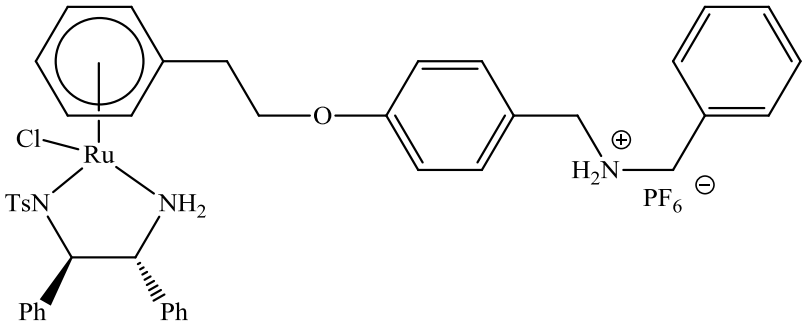

Figure 1.4.14 Ru-TsDPEN complex modified with a dialkylammonium salt in the arene

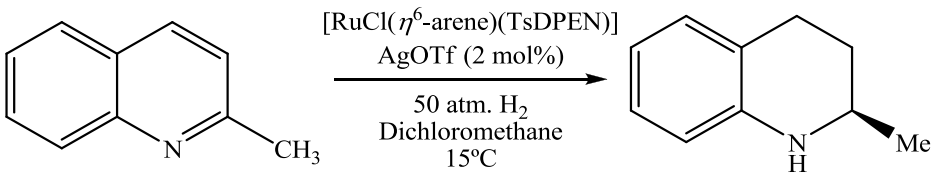

Scheme 1.4.7 Fan's conditions for the hydrogenation of 2-methylquinoline. S/C = 50

More recently, Liu *et al*. have reported the immobilisation of chiral N'-alkylated TsDPEN complexes of ruthenium, forming double-stranded hydrophobic

linear polystyrene, on zirconium phosphonate layers (**Figure 1.4.15**).[121] The heterogeneous catalysts were obtained by radical polymerisation of a TsDPEN-derived system, subsequent coordination with $[RuCl_2(p\text{-cymene})]_2$ and, finally, co-precipitation of the $[P(O)(OH)_2]$ functionalised polymer with NaH_2PO_4 and $ZrOCl_2$. This system gave, in the asymmetric transfer hydrogenation of acetophenone with HCO_2H-Et_3N, > 99% conversion with 94.9% e.e. in 16 hours, with a substrate to catalyst ratio of 100 and a temperature of 50ºC. Using only the polystyrene chains, abundant leaching of Ru was observed, but the further anchoring to the rigid porous backbone of the zirconium layers allowed five recycles of the catalyst.

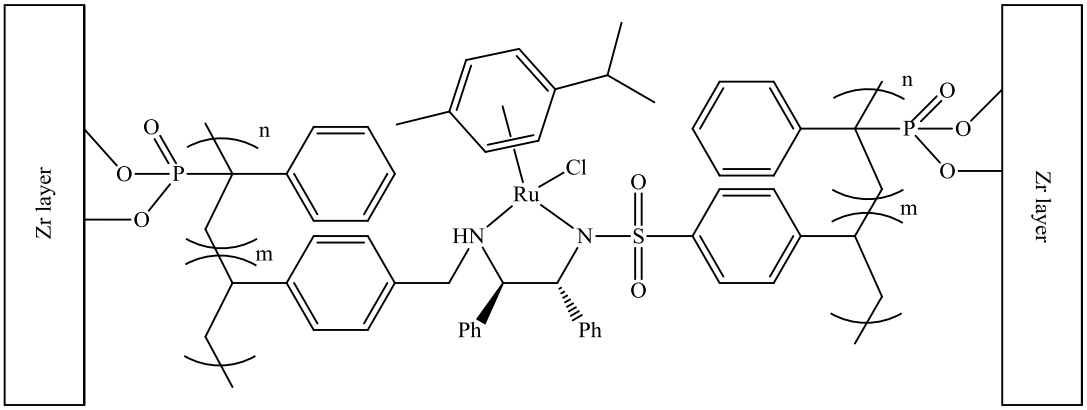

Figure 1.4.15 Polymeric Ru-TsDPEN complexes supported onto inorganic zirconium layers

1.5 Cancer

Cancer is the common name for a group of diseases that are characterised by excessive cell proliferation due to the loss of growth control by certain cells. Whereas most adult cells reach senescence and cease dividing, tumour cells are immortal and might divide without limit. There are two types of tumours: benign tumours, which rarely threaten life, and malignant tumours, which may become invasive and are life-threatening. The latter are those properly known as cancers. The causes of cancer are varied, but generally involve agents that damage DNA, such as chemical carcinogens, radiation or some viruses.[122] Such a cellular stress as DNA damage, in healthy cells, is normally dealt with by genes like the p53 transcription factor, whose function is to trigger biological responses for cellular suicide, including cell cycle arrest or cell death by apoptosis. However, in tumour cells, the p53 function is frequently inactivated, allowing the uncontrolled cell propagation.[123, 124] Besides the formation of primary tumours, most cancerous cells have the ability

to migrate, invading nearby or distant secondary sites where they can proliferate in a process called metastasis, probably the most lethal consequence of cancers.[125]

Within the United Kingdom, the most commonly diagnosed cancers are breast cancer in women and prostate cancer in men, with five-year survival rates of 84.3 and 80.2% respectively, according to data from 2010.[126] These two, together with lung and colorectal cancers, made up to 53% of the 268,758 cases of malignant tumours registered in England in 2010. The lowest five-year survival among both women and men (3.4 and 4.4%) is found in people diagnosed with pancreatic cancer. Universal treatments against cancer include surgery, radiotherapy (use of radiation, normally X-rays), hormone therapy (in some hormone sensitive cases like breast, prostate, ovarian or kidney cancers that grow in response to hormones, medicines are used to block the effects of these) or chemotherapy, used by themselves or in combinations.[127] The latter is the utilisation of cell killing or cytotoxic drugs for the treatment of the disease, and, among more than 100 compounds available, metallodrugs show promising prospects and are under continuous study, with a few examples already in the market and the clinic.

1.6 Platinum-Based Anticancer Drugs

1.6.1 Cisplatin

Cisplatin or *cis*-diamminedichloroplatinum(II) (**Figure 1.6.1**) was the first anticancer metal complex introduced in the clinic and is still broadly used in the treatment of, for example, testicular, head and neck, bladder and cervical cancers.[127] Its anticancer properties were discovered by Rosenberg in 1965 during an investigation of the effect of electrical fields on the growth of bacteria using platinum electrodes. These platinum electrodes were thought to be inert, but in fact gave rise to electrolysis products such as cisplatin, responsible for the observed elongation of the cells.[128] The drug was first tested *in vivo* with mice in 1969,[129] and used with patients in 1971,[130] but it did not obtain the approval of the US Food and Drug Administration (FDA) until 1978.[130]

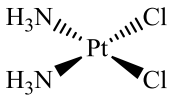

Figure 1.6.1 Structure of cisplatin

The primary target of cisplatin is commonly considered to be the chromosomal DNA. The drug can enter the cells either by passive diffusion or with the help of transporters like the copper transporter-1 (CTR1). Once inside the cell, cisplatin is activated by aquation (replacement of one or the two chlorides by water molecules), which is possible due to the low chloride concentrations in the cytoplasm (23 mM). Binding to DNA occurs predominantly at the N7 position of guanine (G) (**Figure 1.6.2**) and, occasionally, adenine (A), generating a series of different Pt-DNA adducts (**Scheme 1.6.1**)[130-132] that prevent DNA replication and transcription.

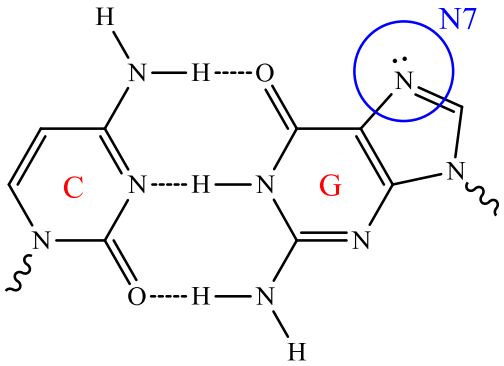

Figure 1.6.2 N7 position in guanine

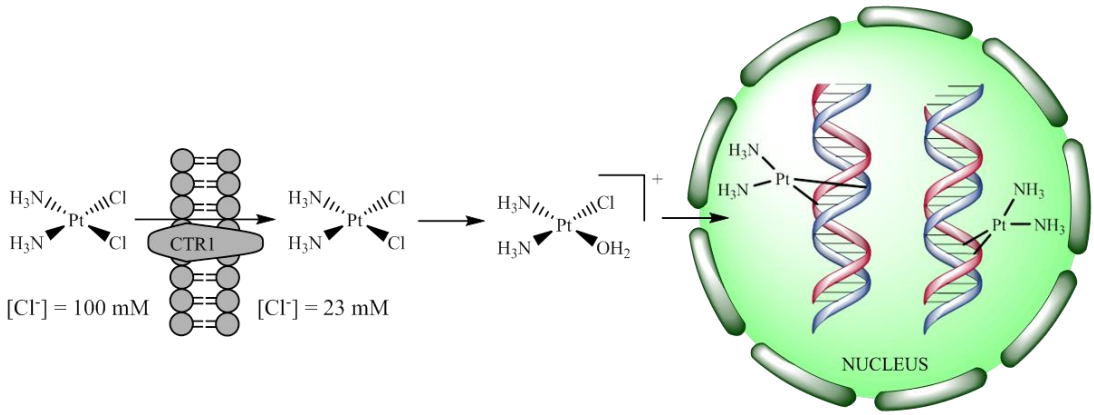

Scheme 1.6.1 Mechanism of action of cisplatin

Among the Pt-DNA adducts that might be formed, the more abundant one corresponds to a bifunctional intrastrand (on the same strand) crosslink between two

adjacent guanines (60-65%), considered to be the responsible factor for the antitumour activity of cisplatin. Other adducts include intrastrand crosslinks between guanine and adenine, between two guanines separated by a third base, monofunctional adducts on guanines or interstrand crosslinks on opposite DNA strands.[130, 133-135]

The three major problems derived from the use of cisplatin are its severe toxicity, mainly in the form of nephrotoxicity (damage to the kidneys), its lack of solubility, which prevents oral administration, and the acquired or intrinsic resistance to the drug observed in some tumours. The latter may be due to successful repair or tolerance after Pt-DNA adduct formation, or scarce DNA binding, this one derived from the loss of membrane transporters or the cytoplasmic detoxification via reactions with thiol-containing species.[130, 132] Platinum(II) is a soft Lewis acid and tends to bind sulfur atoms,[136] present in the amino acids cysteine and methionine. Since the discovery of cisplatin, research into new platinum- and, in general, metal-based anticancer drugs has tried to overcome the aforementioned drawbacks, and find improved physicochemical properties (stability and solubility in water) and therapeutic advantages (reduced toxicity and higher spectrum of activity).

1.6.2 Carboplatin

Carboplatin or *cis*-diammine-[1,1-cyclobutane-dicarboxylato]platinum(II) (**Figure 1.6.3**) was first administered to patients in 1982 and approved in 1989.[130] It was developed by substituting the very labile chloride groups in cisplatin with a bidentate dicarboxylate, a more stable leaving group, which provides it with a lower rate of aquation and, consequently, lower toxicity. Once carboplatin has been monoaquated, the dicarboxylate group becomes more labile, so, initially, the drug binds monofunctionally to DNA. Equal binding of cisplatin and carboplatin to DNA (which requires a 20- to 40-fold larger dose of the latter) results in similar lesions and, thus, cytotoxicity.[137] Carboplatin is used to treat ovarian and lung cancers,[127] showing no nephrotoxicity, but myelosuppression (reduced production of blood cells) as the dose-limiting side effect.[137]

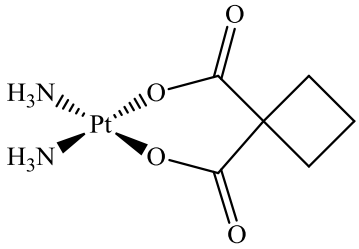

Figure 1.6.3 Structure of carboplatin

1.6.3 Oxaliplatin

Oxaliplatin or *cis*-(1R,2R)-diamminecyclohexane oxalatoplatinum(II) (**Figure 1.6.4**) was the third and last platinum drug to be approved by the FDA in 2002.[130] It was discovered by Kuretani and co-workers in 1978[138] and it introduces the advantages of a greater solubility than that of cisplatin,[138] and a broader spectrum of activity in comparison to cisplatin or carboplatin, being active against some cisplatin-resistant cells and colorectal cancers, principally in combination with 5-fluorouracil (5-FU).[139] While cisplatin adducts interact with some damage recognition proteins producing a signal transduction pathway that leads to cell cycle arrest and/or apoptosis, oxaliplatin adducts seem to be poorly recognised by these proteins. The mechanism of action and resistance of oxaliplatin is, thus, different, and this is believed to result from the type of DNA lesions induced by the diamminecyclohexane ligand.[139]

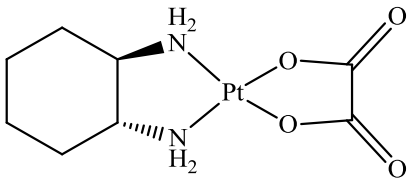

Figure 1.6.4 Structure of oxaliplatin

1.7 Metallocenes

The antitumour properties of Cp_2TiCl_2 or titanocene dichloride (**Figure 1.7.1**) were discovered in 1979 by Köpf and Köpf-Maier after *in vivo* studies on mice with transplanted Ehrlich ascites tumour (EAT) cells.[140] Subsequently, other metallocene dichlorides were tested against the same cancer type. Cp_2ZrCl_2 and Cp_2HfCl_2 showed no activity *in vivo*, which was initially considered a result of the larger distance between the chlorides in these complexes compared with the titanium

analogue.[141] The complexes Cp_2VCl_2 and Cp_2MoCl_2, on the other hand, proved active against EAT in mice, and this led to an investigation of the possible differences in the behaviour of all of the mentioned metallocenes against EAT cells *in vitro*.[142] While Cp_2VCl_2 is able to inhibit cellular growth *in vitro* at concentrations of 5×10^{-6} M, Cp_2TiCl_2 and Cp_2MoCl_2 are only active at concentrations 100 times those of vanadocene dichloride, and Cp_2ZrCl_2 or Cp_2HfCl_2 require concentrations of 5×10^{-3} M to kill *in vitro*-cultured cells.[142]

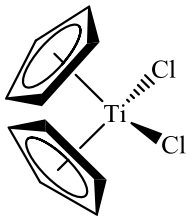

Figure 1.7.1 Structure of titanocene dichloride

Metallocene dihalides resemble cisplatin in that they share a *cis*-MX_2 structure where the halides can be hydrolysed to generate the active species that eventually binds to DNA. However, the chloride hydrolysis steps of Cp_2MCl_2 complexes are much faster than those of cisplatin.[143] This is probably due to the increased preference for H_2O (hard base) of hard metals such as Ti(IV) in comparison to the soft Pt(II).[136] Another feature of metallocene complexes is that they might suffer hydrolytic displacement of the η^5-cyclopentadienyl ligands, depending principally on the metal and the solution pH.[143] At physiological pH, the η^5-C_5H_5 hydrolysis of Cp_2ZrCl_2 is rapid and that of Cp_2TiCl_2 is also noticeable. Only Cp_2VCl_2 seems stable under the same conditions,[143] which relates to its higher *in vitro* activity (see above). For this reason and a poor solubility in water, Cp_2TiCl_2 was generally administered in 10% DMSO/90% saline solutions at low pH, despite a slightly faster rate of η^5-C_5H_5 hydrolysis in DMSO than in pure water (30% of the Cp rings hydrolyse in 100% DMSO solutions after 24 hours).[144]

Titanocene dichloride is 100 times less cytotoxic than cisplatin and 2 times less cytotoxic than carboplatin against A2780 ovarian tumour cells, but presents different side effects, hepatic toxicity being the most important one, while for cisplatin and carboplatin the dose-limiting side effects are nephrotoxicity and myelotoxocity respectively.[145] Cp_2TiCl_2 maintains its activity against cisplatin-

resistant A2780cis ovarian cancer cells: this cell line is 1.5-fold more resistant to Cp_2TiCl_2 than A2780, but the resistance increases to 12.7-fold in the case of cisplatin.[145]

Extensive studies and promising *in vitro* and *in vivo* results with mice made titanocene dichloride enter clinical trials. Rübben and co-workers, for example, analysed the responses to Cp_2TiCl_2 of a number of patients with renal-cell carcinoma (RCC) in a Phase II study, but none of them showed positive results at the end of the treatment.[146] Cp_2TiCl_2 was eventually discarded as an anticancer drug, but opened the way to the more recent evaluation of diverse metallocene derivatives that intend to increase the anticancer activity of the parent complex.

The most common modifications of Cp_2MCl_2 complexes involve substitution on the cyclopentadienyl rings, in order to improve factors such as solubility or rate of hydrolysis. The group of Tacke has reported, for instance, the synthesis of a series of bridged and unbridged titanocenes with methoxy-phenyl or benzodioxole substituents that exceed the cytotoxicity of the unsubstituted titanocene dichloride.[147] Within the McGowan group, a number of Cp_2MCl_2 compounds with ionised amino pendant arm substituents in one or the two η^5-C_5H_5 rings have been synthesised and published (**Figure 1.7.2**). These salts are soluble in polar solvents such as methanol or water, and are generally more potent than Cp_2TiCl_2 and cytotoxic against cisplatin-resistant cell lines.[148-150]

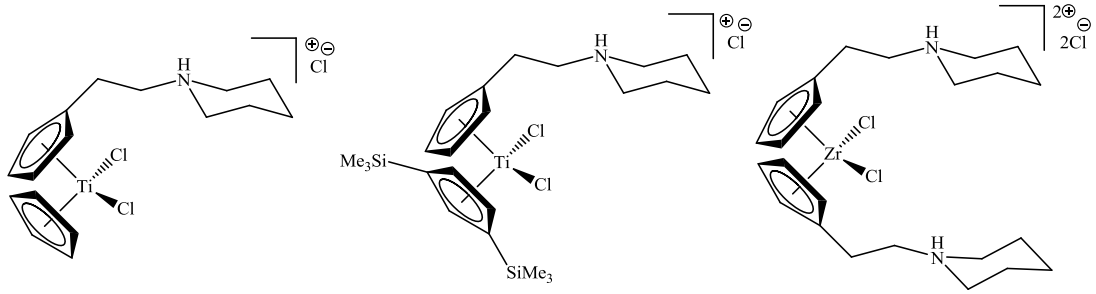

Figure 1.7.2 Examples of modified metallocenes published by the McGowan group

1.8 Ruthenium Complexes

1.8.1 NAMI-A

Imidazolium *trans*-[imidazoledimethylsulfoxide-tetrachlororuthenate(III)] or NAMI-A (**Figure 1.8.1**) is one of the two ruthenium complexes with anticancer properties that has entered clinical trials. It was originally synthesised by the group of Sava as an improvement to NAMI, which is the same complex with Na^+ as the cation instead of the protonated imidazole. NAMI, despite showing good antitumour and antimetastatic activity, co-crystallises with solvent molecules and degrades in air, while NAMI-A is stable and can be obtained in high purity.[151]

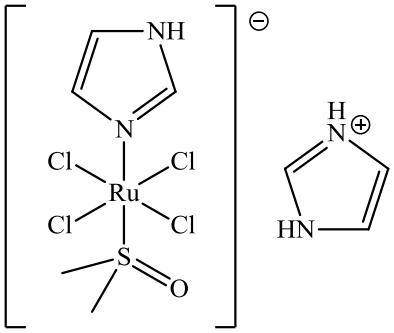

Figure 1.8.1 Structure of NAMI-A

The most singular characteristic of NAMI-A is its lack of direct cytotoxicity, observed in a number of studies with different cell lines *in vitro*.[152] Nevertheless, preclinical investigations *in vivo* showed that NAMI-A increased the lifetime expectancy of tumour-bearing mice due to its antimetastatic capabilities. Unlike, for example, cisplatin, NAMI-A did not reduce the growth of primary tumours, but once these had been surgically removed, the animals treated with NAMI-A presented better survival prospects.[153] The mechanism of action of NAMI-A has not been completely elucidated, but its antimetastatic behaviour responds to several factors: this complex salt has anti-angiogenic properties (reduces the formation of new blood vessels); it exerts a cytostatic effect (inhibition of cell growth and multiplication) by reversible arrest of cells in the premitotic phase, instead of a cytotoxic effect (cell killing); and prevents the invasion of the extracellular matrix by tumour cells.[154, 155]

NAMI-A, like the other anticancer drugs discussed here, seems to coordinate to DNA through the N7 atom of guanine or adenine, which has been proven in

studies with the 9-methyladenine model.[156] The hydrolysis of NAMI-A is pH and [Cl^-] dependent and, in the hypoxic environment of tumours (pH = 6.0-7.0), the aqua replacement of the DMSO moiety is favoured over the hydrolysis of one chloride. This means that, in water, the coordination site to DNA bases is the DMSO site of the parent compound.[156] The pharmacokinetics, toxicity and maximum tolerated dose of NAMI-A in patients have been investigated during Phase I clinical trials, and no severe toxicity has been found.[157] This advantage over platinum-based drugs is considered the result of the poor cytotoxicity of NAMI-A.

1.8.2 KP1019

Indazolium *trans*-[tetrachlorobis(indazole)ruthenate(III)] or KP1019 (**Figure 1.8.2**) was the second ruthenium-based anticancer agent to be considered for clinical trials. This complex is stable in the solid state but only moderately soluble in water, so, generally, it is prepared *in situ* from the corresponding sodium salt during clinical testing. The main advantages that KP1019 introduces with respect to cisplatin are its activity against colon carcinomas, which are not treatable with the platinum drug, and scarce levels of acquired resistance, apart from the absence of serious side effects that was concluded from Phase I clinical trials.[158]

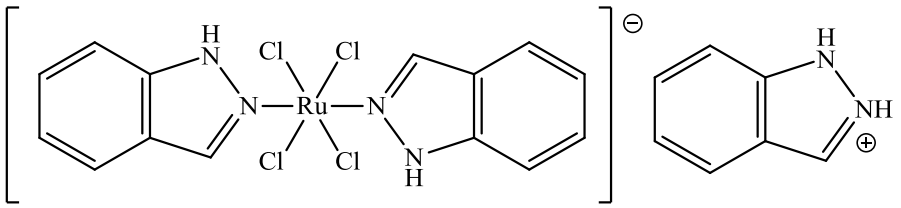

Figure 1.8.2 Structure of KP1019

KP1019 is transformed into the aqua species at physiological conditions, with a decomposition rate of less than 0.9% per hour and a half-life of 74.3 hours.[159] In the blood plasma, the drug reacts to a large extent with serum proteins such as albumin (80-90%) and transferrin (approx. 2%), which are thought to act as "reservoir" and transporter into cells respectively.[160] KP1019 is activated by reduction to ruthenium(II) species, which coordinate faster to biomolecules, in the hypoxic environments of tumours.[161]

1.9 Project Aims

The aims of this project were to:

- Synthesise and characterise novel complexes of ruthenium with arene or pentamethylcyclopentadienyl (Cp*) ligands (**Figure 1.9.1**).

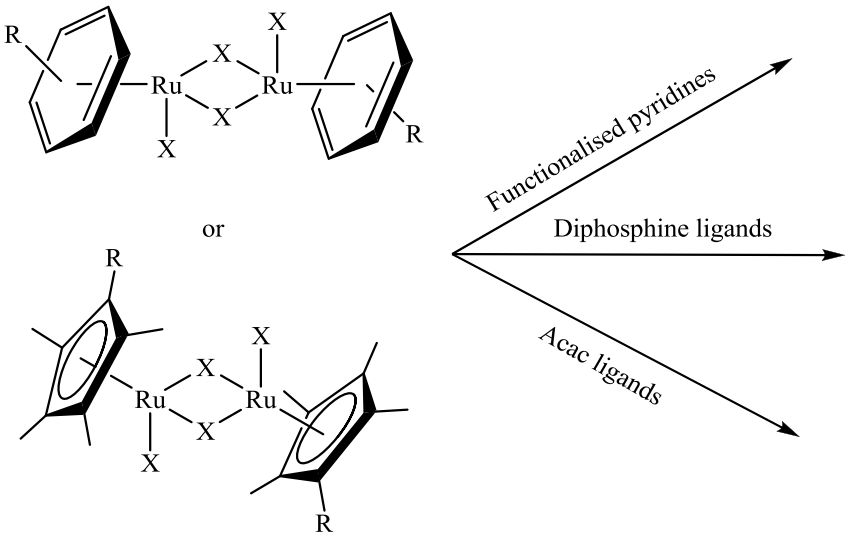

Figure 1.9.1 Summary of the synthetic strategies employed

- Investigate the alternatives for the immobilisation of functionalised arene- or Cp*-Ru complexes through covalent bonding to solid supports, so they can be used as heterogeneous catalysts (**Scheme 1.9.1**).

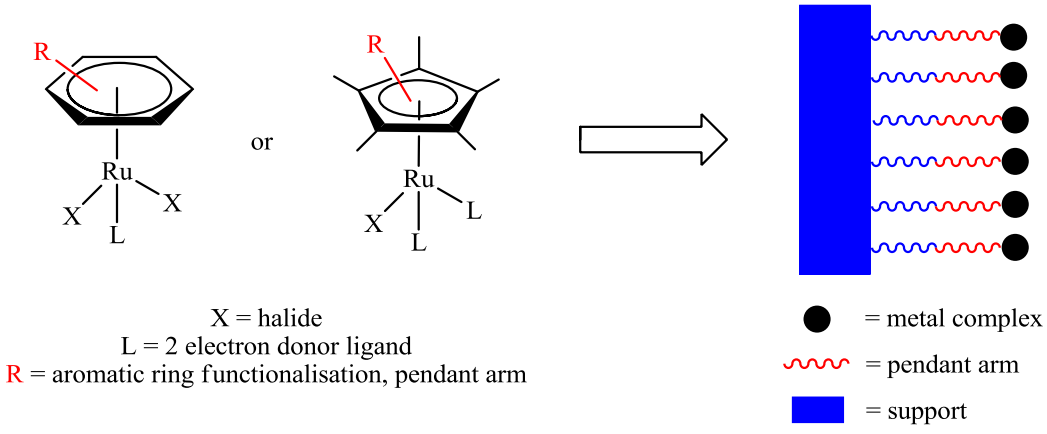

Scheme 1.9.1 General structures of the complexes synthesised and the intended immobilisation strategy

- Test the complexes as catalysts for homogeneous transfer hydrogenation reactions.
- Test the complexes as anticancer agents against the HT-29 and A2780 cell lines.

1.10 References

1. H. Meerwein and R. Schmidt, *Justus Liebigs Annalen der Chemie*, 1925, **444**, 221-238.
2. W. Ponndorf, *Angewandte Chemie*, 1926, **39**, 138-143.
3. A. Verley, *Bull. Soc. Chim. Fr.*, 1925, **37**, 537.
4. R. V. Oppenauer, *Recl. Trav. Chim. Pays-Bas*, 1937, **56**, 137-144.
5. C. F. de Graauw, J. A. Peters, H. van Bekkum and J. Huskens, *Synthesis*, 1994, **1994**, 1007-1017.
6. Y. Sasson and J. Blum, *Tetrahedron Letters*, 1971, **12**, 2167-2170.
7. Y. Sasson and J. Blum, *The Journal of Organic Chemistry*, 1975, **40**, 1887-1896.
8. R. L. Chowdhury and J.-E. Bäckvall, *Journal of the Chemical Society, Chemical Communications*, 1991, 1063-1064.
9. M. H. S. A. Hamid, P. A. Slatford and J. M. J. Williams, *Advanced Synthesis & Catalysis*, 2007, **349**, 1555-1575.
10. G. Guillena, D. J. Ramón and M. Yus, *Angewandte Chemie International Edition*, 2007, **46**, 2358-2364.
11. R. N. Salvatore, A. S. Nagle and K. W. Jung, *The Journal of Organic Chemistry*, 2002, **67**, 674-683.
12. C. Chiappe and D. Pieraccini, *Green Chemistry*, 2003, **5**, 193-197.
13. R. N. Salvatore, C. H. Yoon and K. W. Jung, *Tetrahedron*, 2001, **57**, 7785-7811.
14. S. Bhattacharyya, *Tetrahedron Letters*, 1994, **35**, 2401-2404.
15. A. K. Szardenings, T. S. Burkoth, G. C. Look and D. A. Campbell, *The Journal of Organic Chemistry*, 1996, **61**, 6720-6722.
16. Y. Watanabe, Y. Tsuji, H. Ige, Y. Ohsugi and T. Ohta, *The Journal of Organic Chemistry*, 1984, **49**, 3359-3363.

17. Y. Tsuji, K. T. Huh, Y. Ohsugi and Y. Watanabe, *The Journal of Organic Chemistry*, 1985, **50**, 1365-1370.
18. Y. Tsuji, K. T. Huh and Y. Watanabe, *Tetrahedron Letters*, 1986, **27**, 377-380.
19. Y. Tsuji, K. T. Huh and Y. Watanabe, *The Journal of Organic Chemistry*, 1987, **52**, 1673-1680.
20. Y. Tsuji, S. Kotachi, K. T. Huh and Y. Watanabe, *The Journal of Organic Chemistry*, 1990, **55**, 580-584.
21. Y. Watanabe, Y. Morisaki, T. Kondo and T.-A. Mitsudo, *The Journal of Organic Chemistry*, 1996, **61**, 4214-4218.
22. R. A. T. M. Abbenhuis, J. Boersma and G. van Koten, *The Journal of Organic Chemistry*, 1998, **63**, 4282-4290.
23. J. A. Marsella, *Journal of Organometallic Chemistry*, 1991, **407**, 97-105.
24. A. Del Zotto, W. Baratta, M. Sandri, G. Verardo and P. Rigo, *European Journal of Inorganic Chemistry*, **2004**, 524-529.
25. M. H. S. A. Hamid and J. M. J. Williams, *Chemical Communications*, 2007, 725-727.
26. M. H. S. A. Hamid and J. M. J. Williams, *Tetrahedron Letters*, 2007, **48**, 8263-8265.
27. M. H. S. A. Hamid, C. L. Allen, G. W. Lamb, A. C. Maxwell, H. C. Maytum, A. J. A. Watson and J. M. J. Williams, *Journal of the American Chemical Society*, 2009, **131**, 1766-1774.
28. A. J. A. Watson, A. C. Maxwell and J. M. J. Williams, *The Journal of Organic Chemistry*, 2011, **76**, 2328-2331.
29. C. Liu, S. Liao, Q. Li, S. Feng, Q. Sun, X. Yu and Q. Xu, *The Journal of Organic Chemistry*, 2011, **76**, 5759-5773.
30. O. Saidi, A. J. Blacker, M. M. Farah, S. P. Marsden and J. M. J. Williams, *Chemical Communications*, 2010, **46**, 1541-1543.
31. O. Saidi, A. J. Blacker, G. W. Lamb, S. P. Marsden, J. E. Taylor and J. M. J. Williams, *Organic Process Research & Development*, 2010, **14**, 1046-1049.
32. G. Cami-Kobeci, P. A. Slatford, M. K. Whittlesey and J. M. J. Williams, *Bioorganic & Medicinal Chemistry Letters*, 2005, **15**, 535-537.
33. K.-I. Fujita, K. Yamamoto and R. Yamaguchi, *Organic Letters*, 2002, **4**, 2691-2694.

34. K.-I. Fujita, Z. Li, N. Ozeki and R. Yamaguchi, *Tetrahedron Letters*, 2003, **44**, 2687-2690.
35. K.-I. Fujita, T. Fujii and R. Yamaguchi, *Organic Letters*, 2004, **6**, 3525-3528.
36. K.-I. Fujita, Y. Enoki and R. Yamaguchi, *Organic Syntheses*, 2006, **83**, 217-221.
37. K.-I. Fujita, Y. Enoki and R. Yamaguchi, *Tetrahedron*, 2008, **64**, 1943-1954.
38. K.-I. Fujita, A. Komatsubara and R. Yamaguchi, *Tetrahedron*, 2009, **65**, 3624-3628.
39. M. Zhu, K.-I. Fujita and R. Yamaguchi, *Organic Letters*, 2010, **12**, 1336-1339.
40. R. Kawahara, K.-I. Fujita and R. Yamaguchi, *Journal of the American Chemical Society*, 2010, **132**, 15108-15111.
41. G. Cami-Kobeci and J. M. J. Williams, *Chemical Communications*, 2004, 1072-1073.
42. A. J. Blacker, *Handbook of Homogeneous Hydrogenation*, WILEY-VCH Verlag GmbH & Co., Weinheim, 2007.
43. A. J. Blacker and P. Thompson, *Asymmetric Catalysis on Industrial Scale: Challenges, Approaches, and Solutions*, WILEY-VCH Verlag GmbH & Co., Weinheim, 2010.
44. K. Narita and M. Sekiya, *Chemical & Pharmaceutical Bulletin*, 1977, **25**, 135-140.
45. S. Hashiguchi, A. Fujii, J. Takehara, T. Ikariya and R. Noyori, *Journal of the American Chemical Society*, 1995, **117**, 7562-7563.
46. J. Takehara, S. Hashiguchi, A. Fujii, S.-I. Inoue, T. Ikariya and R. Noyori, *Chemical Communications*, 1996, 233-234.
47. R. Noyori and S. Hashiguchi, *Accounts of Chemical Research*, 1997, **30**, 97-102.
48. A. Fujii, S. Hashiguchi, N. Uematsu, T. Ikariya and R. Noyori, *Journal of the American Chemical Society*, 1996, **118**, 2521-2522.
49. I. Yamada and R. Noyori, *Organic Letters*, 2000, **2**, 3425-3427.
50. K.-J. Haack, S. Hashiguchi, A. Fujii, T. Ikariya and R. Noyori, *Angewandte Chemie International Edition in English*, 1997, **36**, 285-288.
51. M. Yamakawa, H. Ito and R. Noyori, *Journal of the American Chemical Society*, 2000, **122**, 1466-1478.

52. J. Hannedouche, G. J. Clarkson and M. Wills, *Journal of the American Chemical Society*, 2004, **126**, 986-987.

53. D. J. Morris, A. M. Hayes and M. Wills, *The Journal of Organic Chemistry*, 2006, **71**, 7035-7044.

54. J. E. D. Martins, D. J. Morris, B. Tripathi and M. Wills, *Journal of Organometallic Chemistry*, 2008, **693**, 3527-3532.

55. A. M. Hayes, D. J. Morris, G. J. Clarkson and M. Wills, *Journal of the American Chemical Society*, 2005, **127**, 7318-7319.

56. F. K. Cheung, C. Lin, F. Minissi, A. L. Crivillé, M. A. Graham, D. J. Fox and M. Wills, *Organic Letters*, 2007, **9**, 4659-4662.

57. V. Parekh, J. A. Ramsden and M. Wills, *Catalysis Science & Technology*, 2012, **2**, 406-414.

58. T. Touge, T. Hakamata, H. Nara, T. Kobayashi, N. Sayo, T. Saito, Y. Kayaki and T. Ikariya, *Journal of the American Chemical Society*, 2011, **133**, 14960-14963.

59. K. Püntener, L. Schwink and P. Knochel, *Tetrahedron Letters*, 1996, **37**, 8165-8168.

60. M. Aydemir, N. Meric, A. Baysal, Y. Turgut, C. Kayan, S. Şeker, M. Toğrul and B. Gümgüm, *Journal of Organometallic Chemistry*, 2011, **696**, 1541-1546.

61. K. Murata, T. Ikariya and R. Noyori, *The Journal of Organic Chemistry*, 1999, **64**, 2186-2187.

62. C. Bubert, J. Blacker, S. M. Brown, J. Crosby, S. Fitzjohn, J. P. Muxworthy, T. Thorpe and J. M. J. Williams, *Tetrahedron Letters*, 2001, **42**, 4037-4039.

63. X. Wu, X. Li, W. Hems, F. King and J. Xiao, *Organic & Biomolecular Chemistry*, 2004, **2**, 1818-1821.

64. X. Li, J. Blacker, I. Houson, X. Wu and J. Xiao, *Synlett*, 2006, **2006**, 1155-1160.

65. N. Uematsu, A. Fujii, S. Hashiguchi, T. Ikariya and R. Noyori, *Journal of the American Chemical Society*, 1996, **118**, 4916-4917.

66. J. E. D. Martins, G. J. Clarkson and M. Wills, *Organic Letters*, 2009, **11**, 847-850.

67. J. E. D. Martins, M. A. Contreras Redondo and M. Wills, *Tetrahedron: Asymmetry*, 2010, **21**, 2258-2264.

68. C. Wang, B. Villa-Marcos and J. Xiao, *Chemical Communications*, 2011, **47**, 9773-9785.
69. J. B. Åberg, J. S. M. Samec and J.-E. Bäckvall, *Chemical Communications*, 2006, 2771-2773.
70. G. Z. Wang and J.-E. Bäckvall, *Journal of the Chemical Society, Chemical Communications*, 1992, 337-339.
71. M. L. S. Almeida, M. Beller, G.-Z. Wang and J.-E. Bäckvall, *Chemistry – A European Journal*, 1996, **2**, 1533-1536.
72. K.-I. Fujita, S. Furukawa and R. Yamaguchi, *Journal of Organometallic Chemistry*, 2002, **649**, 289-292.
73. K.-I. Fujita, N. Tanino and R. Yamaguchi, *Organic Letters*, 2006, **9**, 109-111.
74. K.-I. Fujita, T. Yoshida, Y. Imori and R. Yamaguchi, *Organic Letters*, 2011, **13**, 2278-2281.
75. R. Yamaguchi, C. Ikeda, Y. Takahashi and K.-I. Fujita, *Journal of the American Chemical Society*, 2009, **131**, 8410-8412.
76. J. H. Koh, H. M. Jeong and J. Park, *Tetrahedron Letters*, 1998, **39**, 5545-5548.
77. M. Ito, A. Osaku, S. Kitahara, M. Hirakawa and T. Ikariya, *Tetrahedron Letters*, 2003, **44**, 7521-7523.
78. G. Csjernyik, K. Bogár and J.-E. Bäckvall, *Tetrahedron Letters*, 2004, **45**, 6799-6802.
79. L. K. Thalén, D. Zhao, J.-B. Sortais, J. Paetzold, C. Hoben and J.-E. Bäckvall, *Chemistry - A European Journal*, 2009, **15**, 3403-3410.
80. A. J. Blacker, M. J. Stirling and M. I. Page, *Organic Process Research & Development*, 2007, **11**, 642-648.
81. A. J. Blacker, S. Brown, B. Clique, B. Gourlay, C. E. Headley, S. Ingham, D. Ritson, T. Screen, M. J. Stirling, D. Taylor and G. Thompson, *Organic Process Research & Development*, 2009, **13**, 1370-1378.
82. C. Wang, A. Pettman, J. Bacsa and J. Xiao, *Angewandte Chemie International Edition*, 2010, **49**, 7548-7552.
83. G. D. Williams, R. A. Pike, C. E. Wade and M. Wills, *Organic Letters*, 2003, **5**, 4227-4230.

84. P. A. Slatford, M. K. Whittlesey and J. M. J. Williams, *Tetrahedron Letters*, 2006, **47**, 6787-6789.
85. M. G. Edwards and J. M. J. Williams, *Angewandte Chemie International Edition*, 2002, **41**, 4740-4743.
86. P. J. Black, M. G. Edwards and J. M. J. Williams, *European Journal of Organic Chemistry*, 2006, **2006**, 4367-4378.
87. S.-M. Lu, X.-W. Han and Y.-G. Zhou, *Journal of Organometallic Chemistry*, 2007, **692**, 3065-3069.
88. R. Venkateswaran, J. T. Mague and M. S. Balakrishna, *Inorganic Chemistry*, 2007, **46**, 809-817.
89. M. Ito, T. Ootsuka, R. Watari, A. Shiibashi, A. Himizu and T. Ikariya, *Journal of the American Chemical Society*, 2011, **133**, 4240-4242.
90. M. Ito, A. Sakaguchi, C. Kobayashi and T. Ikariya, *Journal of the American Chemical Society*, 2007, **129**, 290-291.
91. M. Ito, M. Hirakawa, K. Murata and T. Ikariya, *Organometallics*, 2001, **20**, 379-381.
92. M. Ito, Y. Endo and T. Ikariya, *Organometallics*, 2008, **27**, 6053-6055.
93. M. Ito, Y. Endo, N. Tejima and T. Ikariya, *Organometallics*, 2010, **29**, 2397-2399.
94. J. S. M. Samec, J.-E. Bäckvall, P. G. Andersson and P. Brandt, *Chemical Society Reviews*, 2006, **35**, 237-248.
95. Y. R. S. Laxmi and J.-E. Bäckvall, *Chemical Communications*, 2000, 611-612.
96. A. Aranyos, G. Csjernyik, K. J. Szabo and J.-E. Bäckvall, *Chemical Communications*, 1999, 351-352.
97. J. A. Kenny, K. Versluis, A. J. R. Heck, T. Walsgrove and M. Wills, *Chemical Communications*, 2000, 99-100.
98. C. P. Casey and J. B. Johnson, *The Journal of Organic Chemistry*, 2003, **68**, 1998-2001.
99. D. A. Alonso, P. Brandt, S. J. M. Nordin and P. G. Andersson, *Journal of the American Chemical Society*, 1999, **121**, 9580-9588.
100. R. Noyori, M. Yamakawa and S. Hashiguchi, *The Journal of Organic Chemistry*, 2001, **66**, 7931-7944.

101. M. Yamakawa, I. Yamada and R. Noyori, *Angewandte Chemie International Edition*, 2001, **40**, 2818-2821.

102. X. Wu, J. Liu, D. Di Tommaso, J. A. Iggo, C. R. A. Catlow, J. Bacsa and J. Xiao, *Chemistry – A European Journal*, 2008, **14**, 7699-7715.

103. M. P. Magee and J. R. Norton, *Journal of the American Chemical Society*, 2001, **123**, 1778-1779.

104. P. McMorn and G. J. Hutchings, *Chemical Society Reviews*, 2004, **33**, 108-122.

105. Q.-H. Fan, Y.-M. Li and A. S. C. Chan, *Chemical Reviews*, 2002, **102**, 3385-3466.

106. M. Heitbaum, F. Glorius and I. Escher, *Angewandte Chemie International Edition*, 2006, **45**, 4732-4762.

107. E. L. Muetterties, J. R. Bleeke, E. J. Wucherer and T. Albright, *Chemical Reviews*, 1982, **82**, 499-525.

108. M. Stebler-Roethlisberger, W. Hummel, P. A. Pittet, H. B. Buergi, A. Ludi and A. E. Merbach, *Inorganic Chemistry*, 1988, **27**, 1358-1363.

109. J. Blacker, K. Treacher and T. Screen, *International Patent*, 2009, WO 2009/093059 A2.

110. J. M. Fraile, J. I. García and J. A. Mayoral, *Chemical Reviews*, 2008, **109**, 360-417.

111. K. T. Wan and M. E. Davis, *Nature*, 1994, **370**, 449-450.

112. K. T. Wan and M. E. Davis, *Journal of Catalysis*, 1995, **152**, 25-30.

113. F. Gelman, D. Avnir, H. Schumann and J. Blum, *Journal of Molecular Catalysis A: Chemical*, 1999, **146**, 123-128.

114. S. Shimazu, K. Ro, T. Sento, N. Ichikuni and T. Uematsu, *Journal of Molecular Catalysis A: Chemical*, 1996, **107**, 297-303.

115. C. F. J. Barnard, J. Rouzaud and S. H. Stevenson, *Organic Process Research & Development*, 2005, **9**, 164-167.

116. P. N. Liu, J. G. Deng, Y. Q. Tu and S. H. Wang, *Chemical Communications*, 2004, 2070-2071.

117. X. Li, X. Wu, W. Chen, F. E. Hancock, F. King and J. Xiao, *Organic Letters*, 2004, **6**, 3321-3324.

118. J. Li, Y. Zhang, D. Han, Q. Gao and C. Li, *Journal of Molecular Catalysis A: Chemical*, 2009, **298**, 31-35.

119. S. Bai, H. Yang, P. Wang, J. Gao, B. Li, Q. Yang and C. Li, *Chemical Communications*, 2010, **46**, 8145-8147.
120. L. Wu, Y.-M. He and Q.-H. Fan, *Advanced Synthesis & Catalysis*, 2011, **353**, 2915-2919.
121. R. Wang, J. Wan, X. Ma, X. Xu and L. Liu, *Dalton Transactions*, 2013, **42**, 6513-6522.
122. D. Voet and J. G. Voet, *Biochemistry*, 4th edn., Wiley, New York, 2011.
123. V. Bykov and K. Wiman, *Annals of Medicine*, 2003, **35**, 458-465.
124. J. J. Fuster, S. M. Sanz-González, U. M. Moll and V. Andrés, *Trends in molecular medicine*, 2007, **13**, 192-199.
125. D. R. Welch, *Breast Disease*, 2007, **26**, 3-12.
126. *Office for National Statistics: www.ons.gov.uk, accessed on February 2013*.
127. *Cancer Research UK: www.cancerresearchuk.org, accessed on February 2013*.
128. B. Rosenberg, L. Vancamp and T. Krigas, *Nature*, 1965, **205**, 698-699.
129. B. Rosenberg, L. Vancamp, J. E. Trosko and V. H. Mansour, *Nature*, 1969, **222**, 385-386.
130. L. Kelland, *Nature Reviews Cancer*, 2007, **7**, 573-584.
131. A. Pasini and F. Zunino, *Angewandte Chemie International Edition in English*, 1987, **26**, 615-624.
132. D. Gibson, *Dalton Transactions*, 2009, 10681-10689.
133. A. Eastman, *Biochemistry*, 1983, **22**, 3927-3933.
134. N. P. Johnson, A. M. Mazard, J. Escalier and J. P. Macquet, *Journal of the American Chemical Society*, 1985, **107**, 6376-6380.
135. A. M. J. Fichtinger-Schepman, P. H. M. Lohman and J. Reedijk, *Nucleic Acids Research*, 1982, **10**, 5345-5356.
136. R. G. Pearson, *Journal of Chemical Education*, 1968, **45**, 581-587.
137. R. J. Knox, F. Friedlos, D. A. Lydall and J. J. Roberts, *Cancer Research*, 1986, **46**, 1972-1979.
138. Y. Kidani, K. Inagaki, M. Iigo, A. Hoshi and K. Kuretani, *Journal of Medicinal Chemistry*, 1978, **21**, 1315-1318.
139. E. Raymond, S. Faivre, S. Chaney, J. Woynarowski and E. Cvitkovic, *Molecular Cancer Therapeutics*, 2002, **1**, 227-235.

140. H. Köpf and P. Köpf-Maier, *Angewandte Chemie International Edition in English*, 1979, **18**, 477-478.

141. P. Köpf-Maier, B. Hesse and H. Köpf, *Journal of Cancer Research and Clinical Oncology*, 1980, **96**, 43-51.

142. P. Köpf-Maier, W. Wagner and H. Köpf, *Cancer Chemotherapy and Pharmacology*, 1981, **5**, 237-241.

143. J. H. Toney and T. J. Marks, *Journal of the American Chemical Society*, 1985, **107**, 947-953.

144. G. Mokdsi and M. M. Harding, *Metal-Based Drugs*, 1998, **5**, 207-215.

145. C. V. Christodoulou, A. G. Eliopoulos, L. S. Young, L. Hodgkins, D. R. Ferry and D. J. Kerr, *British Journal of Cancer*, 1998, **77**, 2088-2097.

146. G. Lümmen, H. Sperling, H. Luboldt, T. Otto and H. Rübben, *Cancer Chemotherapy and Pharmacology*, 1998, **42**, 415-417.

147. N. J. Sweeney, J. Claffey, H. Müller-Bunz, C. Pampillón, K. Strohfeldt and M. Tacke, *Applied Organometallic Chemistry*, 2007, **21**, 57-65.

148. O. R. Allen, L. Croll, A. L. Gott, R. J. Knox and P. C. McGowan, *Organometallics*, 2003, **23**, 288-292.

149. O. R. Allen, A. L. Gott, J. A. Hartley, J. M. Hartley, R. J. Knox and P. C. McGowan, *Dalton Transactions*, 2007, 5082-5090.

150. O. R. Allen, R. J. Knox and P. C. McGowan, *Dalton Transactions*, 2008, 5293-5295.

151. G. Mestroni, E. Alessio and G. Sava, *International Patent*, 1998, PCT C 07F 15/00, A61K 31/28. WO98/00431.

152. A. Bergamo, R. Gagliardi, V. Scarcia, A. Furlani, E. Alessio, G. Mestroni and G. Sava, *Journal of Pharmacology and Experimental Therapeutics*, 1999, **289**, 559-564.

153. G. Sava, K. Clerici, I. Capozzi, M. Cocchietto, R. Gagliardi, E. Alessio, G. Mestroni and A. Perbellini, *Anti-Cancer Drugs*, 1999, **10**, 129-138.

154. A. Vacca, M. Bruno, A. Boccarelli, M. Coluccia, D. Ribatti, A. Bergamo, S. Garbisa, L. Sartor and G. Sava, *British Journal of Cancer*, 2002, **86**, 993-998.

155. S. Zorzet, A. Bergamo, M. Cocchietto, A. Sorc, B. Gava, E. Alessio, E. Iengo and G. Sava, *Journal of Pharmacology and Experimental Therapeutics*, 2000, **295**, 927-933.

156. M. Bacac, A. C. G. Hotze, K. van der Schilden, J. G. Haasnoot, S. Pacor, E. Alessio, G. Sava and J. Reedijk, *Journal of Inorganic Biochemistry*, 2004, **98**, 402-412.

157. J. M. Rademaker-Lakhai, D. van den Bongard, D. Pluim, J. H. Beijnen and J. H. M. Schellens, *Clinical Cancer Research*, 2004, **10**, 3717-3727.

158. C. G. Hartinger, S. Zorbas-Seifried, M. A. Jakupec, B. Kynast, H. Zorbas and B. K. Keppler, *Journal of Inorganic Biochemistry*, 2006, **100**, 891-904.

159. K.-G. Lipponer, E. Vogel and B. K. Keppler, *Metal-Based Drugs*, 1996, **3**, 243-260.

160. L. Trynda-Lemiesz, A. Karaczyn, B. K. Keppler and H. Kozlowski, *Journal of Inorganic Biochemistry*, 2000, **78**, 341-346.

161. E. Reisner, V. B. Arion, M. F. C. Guedes da Silva, R. Lichtenecker, A. Eichinger, B. K. Keppler, V. Y. Kukushkin and A. J. L. Pombeiro, *Inorganic Chemistry*, 2004, **43**, 7083-7093.

Chapter 2

2,5-Dihydrophenyl Carboxy Ligands and Functionalised η^6-Arene Ruthenium Complexes

2.1 Introduction

This chapter presents the synthesis of a library of functionalised η^6-arene ruthenium complexes which try to mimic the performance of the *p*-cymene ruthenium dimer, which is catalytically active towards hydrogen transfer reactions in the presence of diphosphine or diamine chelating ligands.[1-3] The functionalised dimers (**2.3** to **2.9**) have a similar general structure to the *p*-cymene dimer (**Figure 2.1.1**), but they include groups that, in principle, could be covalently attached to functionalised supports. The starting materials for the preparation of these complexes were two different 2,5-dihydrophenyl carboxy compounds (**2.1** and **2.2**). These have the same general structure but differ in their chain lengths: 2,5-dihydrophenylacetic acid (one carbon length chain) and 2,5-dihydro-4-phenylbutyric acid (three carbon length chain). **2.10** is a functionalised η^6-arene ruthenium monomer with a coordinated pyridine.

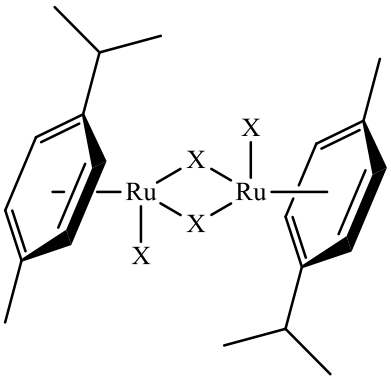

Figure 2.1.1 Ruthenium *p*-cymene dimer $[RuX_2C_6H_4(CH_3)(CH(CH_3)_2)]_2$. X = Cl or I

The routes to the two ligands (compounds **2.1** and **2.2**) had been previously developed,[4, 5] as well as those to the complexes **2.3**, **2.5** and **2.6**.[4, 5] The syntheses and characterisations of five novel compounds (**2.4** and **2.7** to **2.10**) are reported. All of the species discussed in this chapter are shown in **Figure 2.1.2**.

The functionalised η^6-arene ruthenium dimers were originally prepared to be immobilised through the arene ligand and used as heterogeneous catalysts for hydrogen transfer reactions. Their different functional groups (acids and esters) could give various possibilities when binding covalently to modified supports and the different chain lengths could be tested to see if dimers with longer pendant arms (more flexible) resembled the commonly more active homogeneous catalysts. The

variation of the halides used responded to an interest in analysing possible different activities.

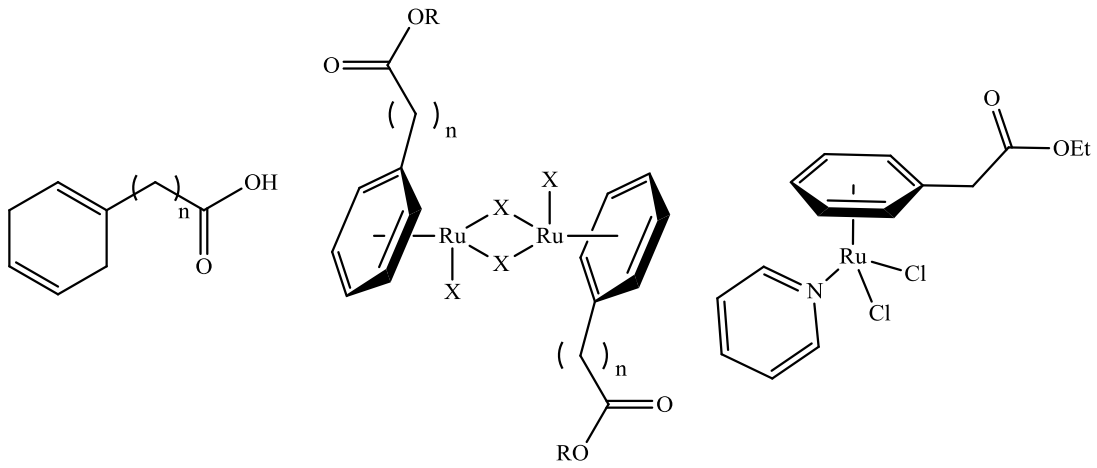

2.1 n = 1
2.2 n = 3

2.3 R = H, n = 1, X = Cl
2.4 R = H, n = 1, X = Br
2.5 R = H, n = 3, X = Cl
2.6 R = Et, n = 1, X = Cl
2.7 R = Et, n = 1, X = Br
2.8 R = Et, n = 3, X = Cl
2.9 R = Et, n = 1, X = I

2.10

Figure 2.1.2 General structures of the complexes discussed in Chapter 2

2.2 2,5-Dihydrophenyl Carboxy Ligands

The general process for the synthesis of ligands **2.1** and **2.2** was a Birch reduction starting from phenylacetic acid (n = 1) or 4-phenylbutyric acid (n = 3) respectively, using sodium, liquid ammonia and ethanol at -78°C under a nitrogen atmosphere (**Scheme 2.2.1**). This procedure had been reported previously by Sheldrick *et al.*[4] and it had also been used within the McGowan group.[5]

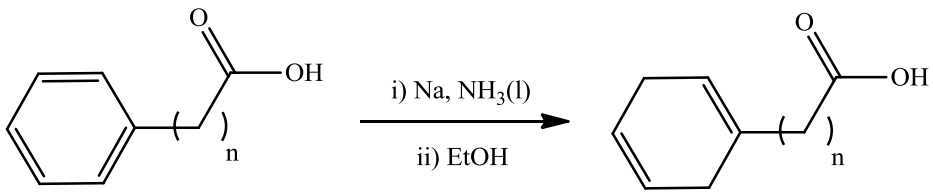

2.1 n = 1 (82%)
2.2 n = 3 (88%)

Scheme 2.2.1 General scheme for the synthesis of 2,5-dihydrophenyl carboxy ligands

Both compounds were obtained in high yields above 80% and, as they had been previously characterised in the literature,[4] only ^{1}H NMR analyses were recorded to confirm the formation of the products. Even with incomplete reactions the final mixtures were used in subsequent transformations because ruthenium sources of the type RuX_3 only react with the dihydrophenyl (reduced) compounds.

2.3 Functionalised η^6-Arene Ruthenium Complexes

2.3.1 Synthesis of $[RuX_2C_6H_5(CH_2)_nCOOR]_2$ (X = Cl, Br) (2.3−2.8)

The 2,5-dihydrophenyl carboxy ligands **2.1** and **2.2**, together with ruthenium sources, $RuCl_3 \cdot 3H_2O$ or $RuBr_3$, were the starting materials used for the synthesis of the complexes presented in this section (**2.3** to **2.8**). The general process taking place was a redox reaction in which ruthenium(III) was reduced to ruthenium(II) and the dihydrophenyl carboxy ligand was oxidised to its aromatic form, giving η^6-coordination to the metal (**Scheme 2.3.1**), as shown by Bennett and Smith.[6] The solvent varied depending on the functional group required in the final complex; a 5:1 mixture of acetone/water was employed to prepare acids while the use of ethanol resulted in the formation of esters.

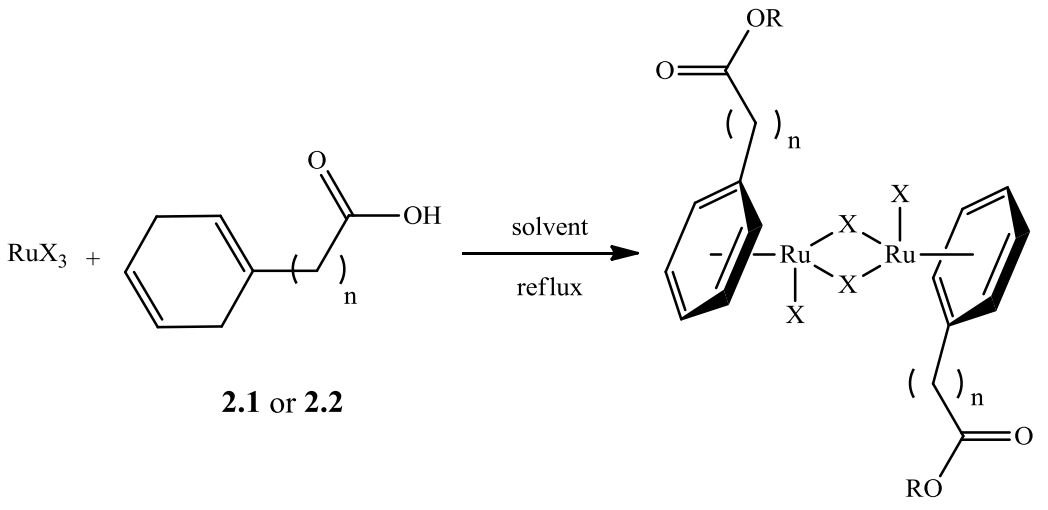

2.1 or **2.2**

2.3 R = H, n = 1, X = Cl (87%)
2.4 R = H, n = 1, X = Br (82%)
2.5 R = H, n = 3, X = Cl (58%)
2.6 R = Et, n = 1, X = Cl (56%)
2.7 R = Et, n = 1, X = Br (31%)
2.8 R = Et, n = 3, X = Cl (5%)

Scheme 2.3.1 General scheme for the synthesis of functionalised η^6-arene ruthenium dimers

Compounds **2.3**, **2.5** and **2.6** had been previously synthesised by Sheldrick *et al.* and analysed for both η^6- and N-terminal labelling of amino acids and peptides. In the first case, they tested the labelling of aromatic amino acids by formation of [(η^6-arene)$_2$Ru^{II}] sandwich complexes. The N-terminal coupling reactions were performed by a carbodiimide method.[4] Compounds **2.3** and **2.6** had also been prepared within the McGowan group as starting materials to possible anticancer ruthenium drugs.[5]

All of these functionalised η^6-arene dimers were obtained as orange or red powders in yields ranging from 5 to 87%, and they exhibited poor solubilities in non-coordinating solvents (particularly the acids **2.3** to **2.5**).

2.3.1.1 NMR Data for Compound 2.8

A labelled diagram of complex **2.8** is given in **Figure 2.3.1**. The assignment shown in **Table 2.3.1** corresponds to the data from the ^{1}H and ^{13}C{^{1}H} NMR spectra presented in **Figure 2.3.2** and **Figure 2.3.3** respectively. The ^{1}H NMR spectrum of this complex contains chemical shifts for the aromatic protons between 5.0 and 6.0 ppm, shifted upfield from the normal aromatic region due to coordination to ruthenium. This is a common factor for all of the arene and cyclopentadienyl complexes synthesised in this project. ^{1}J ^{1}H-^{13}C{^{1}H} HMQC (**Figure 2.3.4**) and ^{2,3}J ^{1}H-^{13}C{^{1}H} HMBC (**Figure 2.3.5**) NMR spectra for compound **2.8** are also given, and helped in the assignment of the aromatics and the CH_2 protons "e", "f" and "g".

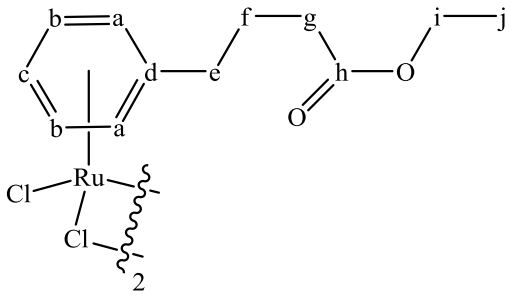

Figure 2.3.1 Labelled diagram of complex **2.8**

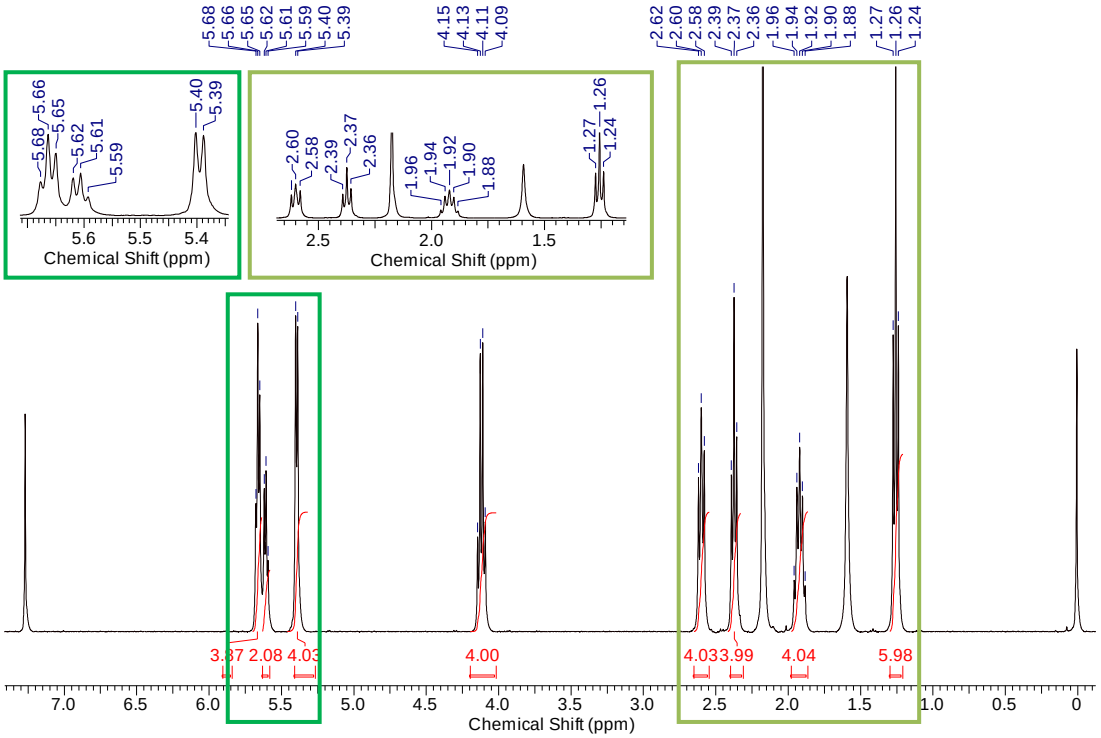

Figure 2.3.2 ^{1}H NMR spectrum of **2.8** in $CDCl_3$ at 400.13 MHz and 300.0 K.

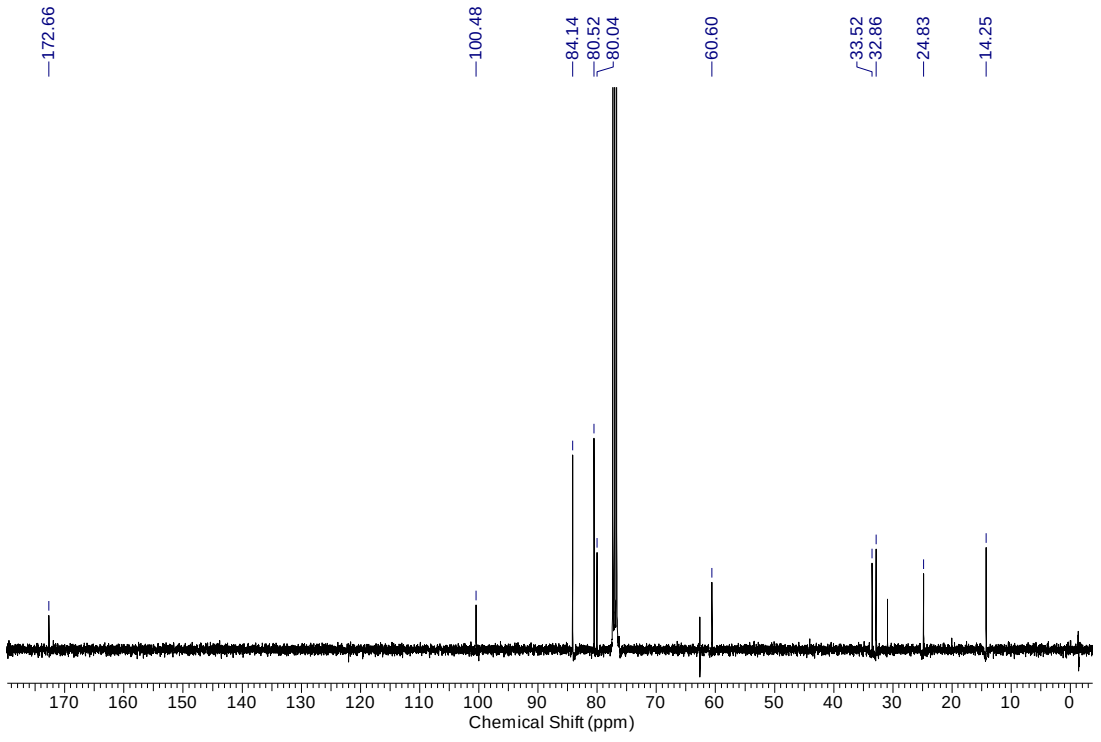

Figure 2.3.3 $^{13}C\{^{1}H\}$ NMR spectrum of **2.8** in $CDCl_3$ at 100.61 MHz and 300.0 K

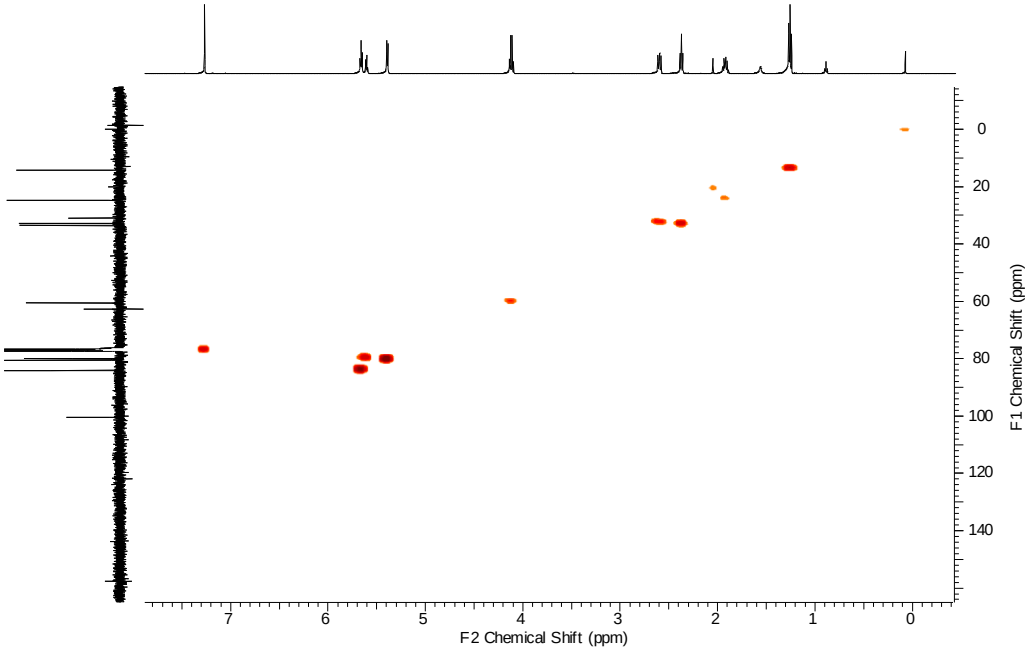

Figure 2.3.4 ^{1}J ^{1}H-$^{13}C\{^{1}H\}$ HMQC spectrum of **2.8** in $CDCl_3$ at 300.0 K

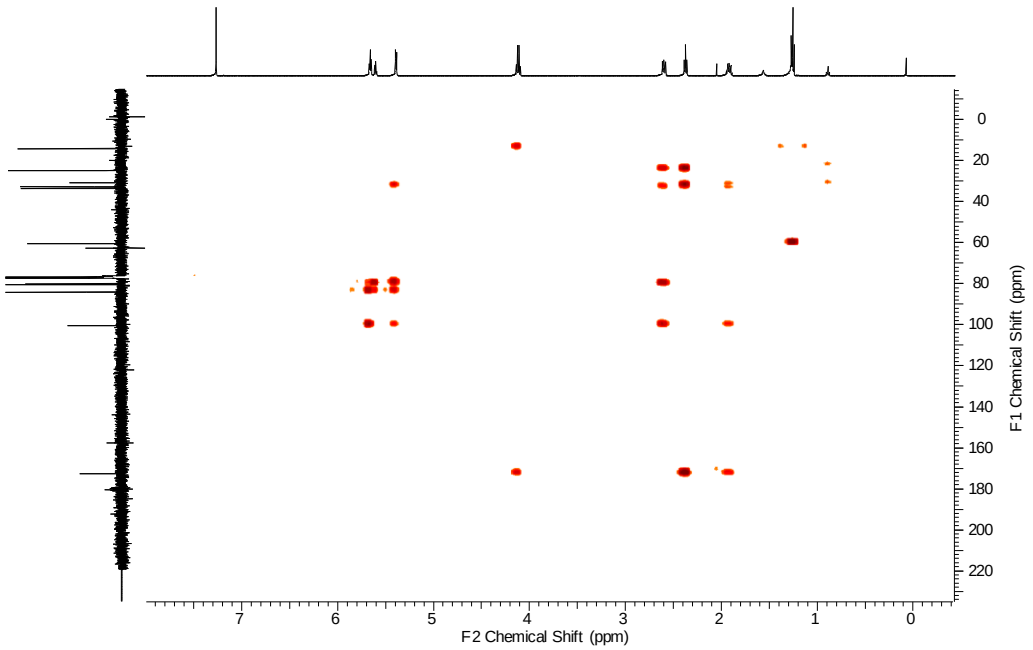

Figure 2.3.5 $^{2,3}J$ ^{1}H-$^{13}C\{^{1}H\}$ HMBC spectrum of **2.8** in $CDCl_3$ at 300.0 K

^{1}H Chemical Shift, δ (ppm)	**Assignment**
5.66 (t, $^{3}J_{(H-H)}$ = 5.4 Hz, 4H)	b
5.61 (t, $^{3}J_{(H-H)}$ = 5.3 Hz, 2H)	c
5.39 (d, $^{3}J_{(H-H)}$ = 5.6 Hz, 4H)	a
4.12 (q, $^{3}J_{(H-H)}$ = 7.1 Hz, 4H)	i
2.60 (m, 4H)	e
2.37 (t, $^{3}J_{(H-H)}$ = 7.3 Hz, 4H)	g
1.92 (quintet, $^{3}J_{(H-H)}$ = 7.5 Hz, 4H)	f
1.26 (t, $^{3}J_{(H-H)}$ = 7.0 Hz, 6H)	j
^{13}C{^{1}H} Chemical Shift, δ (ppm)	**Assignment**
172.7 (Q)	h
100.5 (Q)	d
84.1 (CH)	b
80.5 (CH)	a
80.0 (CH)	c
60.6 (CH_2)	i
33.5 (CH_2)	g
32.9 (CH_2)	e
24.8 (CH_2)	f
14.3 (CH_3)	j

Table 2.3.1 ^{1}H and ^{13}C{^{1}H} chemical shift assignment for complex **2.8**

2.3.2 Synthesis of $[RuI_2C_6H_5CH_2COOCH_2CH_3]_2$ (2.9)

Complex **2.9** was synthesised by halide exchange from complex **2.6** with NaI in chloroform (**Scheme 2.3.2**). This method was adapted from a similar procedure presented in the literature by Keppler *et al*.[7] and some previous work with iridium by one of the partner companies of this project.[8] The compound was obtained in 14% yield as a red solid.

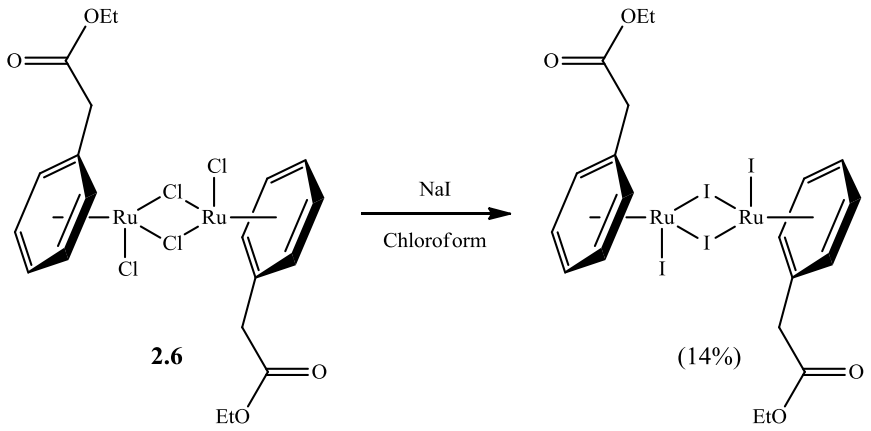

Scheme 2.3.2 Synthesis of complex **2.9** $[RuI_2C_6H_5CH_2COOEt]_2$

2.3.2.1 NMR Data for Compound 2.9

A labelled diagram of complex **2.9** is presented in **Figure 2.3.6**. The ^{1}H NMR spectrum of this compound is shown in **Figure 2.3.7**. **Table 2.3.2** gives the ^{1}H and ^{13}C{^{1}H} NMR data assignments.

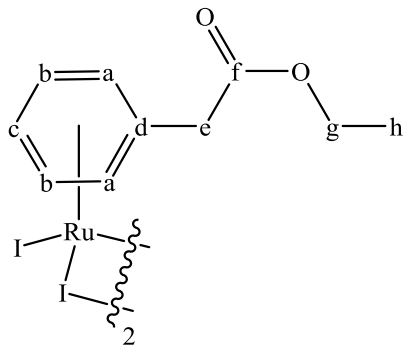

Figure 2.3.6 Labelled diagram of complex **2.9**

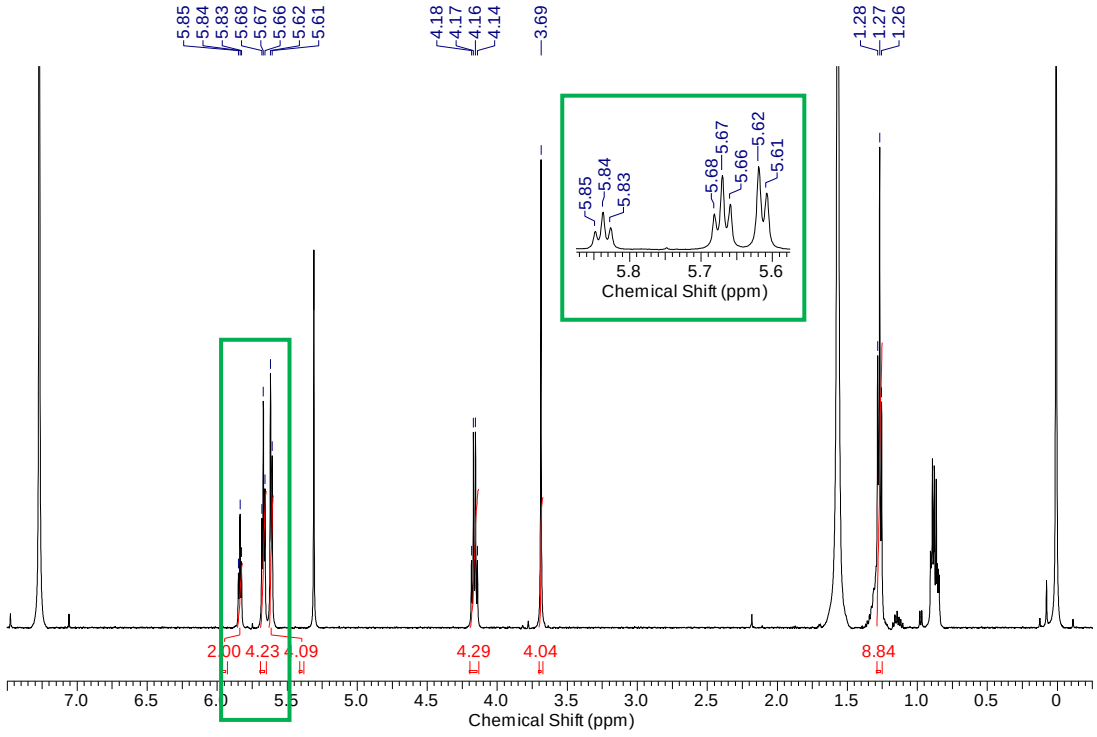

Figure 2.3.7 ^{1}H NMR spectrum of **2.9** in $CDCl_3$ at 500.23 MHz and 298.4 K.

^{1}H Chemical Shift, δ (ppm)	Assignment
5.84 (t, $^{3}J_{(H-H)}$ = 5.4 Hz, 2H)	c
5.67 (t, $^{3}J_{(H-H)}$ = 5.6 Hz, 4H)	b
5.61 (d, $^{3}J_{(H-H)}$ = 5.6 Hz, 4H)	a
4.16 (q, $^{3}J_{(H-H)}$ = 7.2 Hz, 4H)	g
3.69 (s, 4H)	e
1.27 (t, $^{3}J_{(H-H)}$ = 7.2 Hz, 6H)	h
^{13}C{^{1}H} Chemical Shift, δ (ppm)	**Assignment**
170.0 (Q)	f
96.8 (Q)	d
86.1 (CH)	a
84.0 (CH)	c
83.0 (CH)	b
61.7 (CH_2)	g
40.6 (CH_2)	e
14.1 (CH_3)	h

Table 2.3.2 ^{1}H and ^{13}C{^{1}H} chemical shift assignment for complex **2.9**

2.3.2.2 X-Ray Crystallographic Analysis of Compound 2.9

Red crystals of complex **2.9** suitable for X-ray crystallography were obtained by vapour diffusion of pentane into a saturated solution of the complex in dichloromethane. Complex **2.9** crystallised in a monoclinic cell, and structural solution was performed in the space group $P2_1/c$. The asymmetric unit is formed by half of the dimer, and there are 2 molecules in the unit cell. The molecular structure of compound **2.9** is shown in **Figure 2.3.8** and selected bond lengths and angles are given in **Table 2.3.3**.

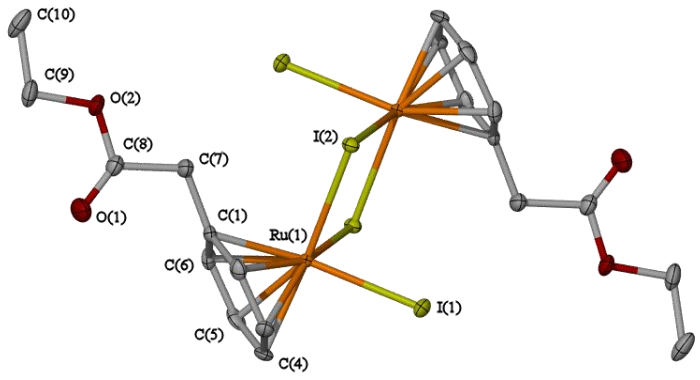

Figure 2.3.8 Molecular structure of complex **2.9**. Displacement ellipsoids are at the 50% probability level. Hydrogen atoms are omitted for clarity

Bond	Distance (Å)	Bond	Distance (Å)
I(1)-Ru(1)	2.7470(4)	C(8)-O(1)	1.204(4)
I(2)-Ru(1)	2.7402(4)	O(2)-C(8)	1.344(5)
C(1)-C(7)	1.512(5)	O(2)-C(9)	1.461(4)
C(7)-C(8)	1.527(4)	C(9)-C(10)	1.507(6)
Ru(1)-Ring	1.680	Ru(1)-$C_{(arene)}$	2.202
Bond	**Angle (°)**	**Bond**	**Angle (°)**
I(2)-Ru(1)-I(1)	87.474(12)	C(1)-C(7)-C(8)	113.9(3)
Ru(1)*-I(2)-Ru(1)	96.899(10)	O(2)-C(8)-C(7)	108.7(3)
I(2)*-Ru(1)-I(2)	83.101(10)	C(8)-O(2)-C(9)	116.5(3)
C(1)-Ru(1)-I(2)	91.06(9)	O(2)-C(9)-C(10)	107.5(3)
C(6)-Ru(1)-C(1)	37.45(12)	O(1)-C(8)-O(2)	125.4(3)

Table 2.3.3 Selected interatomic distances and angles for compound **2.9** with s.u.s. shown in parenthesis. * = Symmetry generated atoms

The distances Ru-I(1) and Ru-I(2), which are around 2.74 Å are, as expected, longer than the Ru-Cl distances (around 2.45 Å) in other complexes presented in this document. The average distance from ruthenium to the carbon atoms in the arene ring is 2.202 Å, and the ring centroid is 1.680 Å away from the metal centre. These two values are in accordance with those observed in the other arene complexes reported here. When packed in the solid state, complex **2.9** does not present any classic hydrogen bond or other type of significant interaction.

2.3.3 Synthesis of $[RuCl_2(C_6H_5CH_2COOCH_2CH_3)(NC_5H_5)]$ (2.10)

Compound **2.10** was prepared by stirring complex **2.6** and pyridine in dichloromethane at room temperature overnight (**Scheme 2.3.3**). It was isolated as an orange/yellow product in 71% yield.

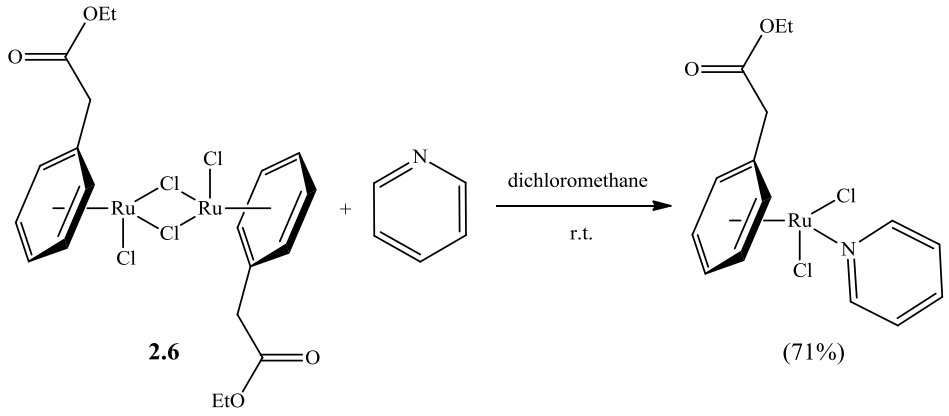

Scheme 2.3.3 Synthesis of complex **2.10** $[RuCl_2(C_6H_5CH_2COOEt)(NC_5H_5)]$

2.3.3.1 NMR Data for Compound 2.10

Figure 2.3.9 shows the labelled diagram of complex **2.10**. The ^{1}H and $^{13}C\{^{1}H\}$ NMR spectra of this compound are shown in **Figure 2.3.10** and **Figure 2.3.11**. **Table 2.3.4** gives the spectral assignments for this complex.

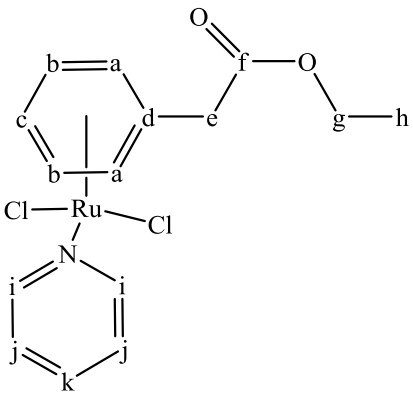

Figure 2.3.9 Labelled diagram of complex **2.10**

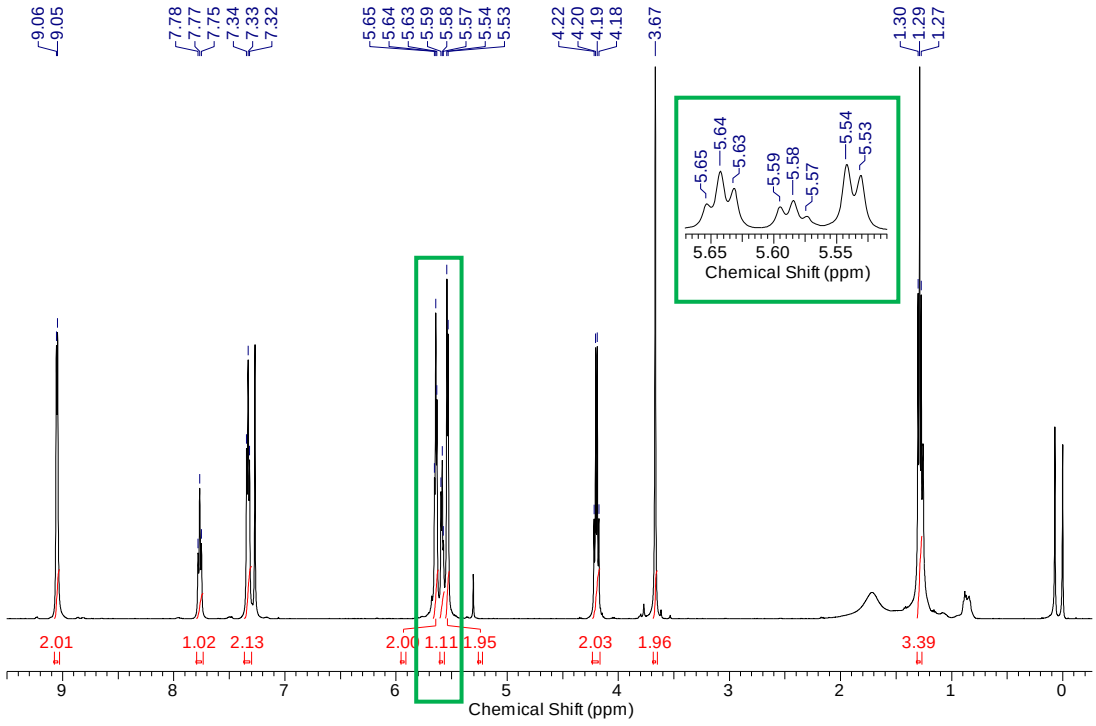

Figure 2.3.10 ^{1}H NMR spectrum of **2.10** in $CDCl_3$ at 500.23 MHz and 298.6 K

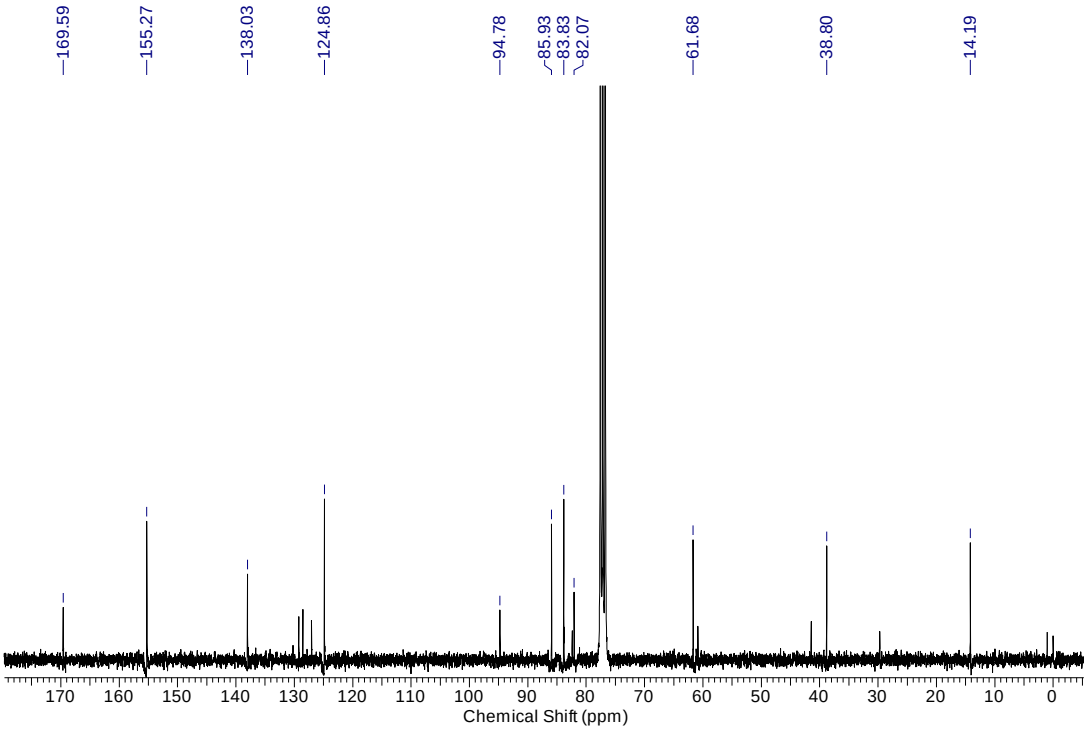

Figure 2.3.11 $^{13}C\{^{1}H\}$ NMR spectrum of **2.10** in $CDCl_3$ at 75.47 MHz and 300.0 K

^{1}H Chemical Shift, δ (ppm)	**Assignment**
9.05 (d, $^{3}J_{(H-H)}$ = 5.2 Hz, 2H)	i
7.77 (t, $^{3}J_{(H-H)}$ = 7.4 Hz, 1H)	k
7.33 (t, $^{3}J_{(H-H)}$ = 6.8 Hz, 2H)	j
5.64 (t, $^{3}J_{(H-H)}$ = 5.4 Hz, 2H)	b
5.58 (t, $^{3}J_{(H-H)}$ = 5.2 Hz, 1H)	c
5.54 (d, $^{3}J_{(H-H)}$ = 5.6 Hz, 2H)	a
4.20 (q, $^{3}J_{(H-H)}$ = 7.2 Hz, 2H)	g
3.67 (s, 2H)	e
1.29 (t, $^{3}J_{(H-H)}$ = 7.2 Hz, 3H)	h
$^{13}C\{^{1}H\}$ Chemical Shift, δ (ppm)	**Assignment**
169.6 (Q)	f
155.3 (CH)	i
138.0 (CH)	k
124.9 (CH)	j
94.8 (Q)	d
85.9 (CH)	b
83.8 (CH)	a
82.1 (CH)	c
61.7 (CH_2)	g
38.8 (CH_2)	e
14.2 (CH_3)	h

Table 2.3.4 ^{1}H and $^{13}C\{^{1}H\}$ chemical shift assignment for complex **2.10**

2.3.3.2 X-Ray Crystallographic Analysis of Compound 2.10

Orange crystals of complex **2.10** suitable for X-ray crystallography were obtained by vapour diffusion of diethyl ether into a saturated solution of the complex in chloroform. Compound **2.10** crystallised in a triclinic cell and structural solution was performed in the space group $P\bar{1}$. This compound and, in general, all of the ruthenium complexes synthesised and analysed by X-ray crystallography in this project exhibit the characteristic pseudo-tetrahedral geometry of η^6-arene or η^5-cyclopentadienyl ruthenium complexes ("piano stool" or "half sandwich" structure). The η^6 π-bonded arene occupies one vertex of the tetrahedron, with the other three ligands in the remaining three sites. The molecular structure of complex **2.10** is shown in **Figure 2.3.12**, and selected bond lengths and angles are given in **Table 2.3.5**. The average Ru-$C_{(arene)}$ bond distance is 2.209 Å, and the ring centroid is at 1.683 Å from the ruthenium atom, both comparable with previous ruthenium compounds.[9, 10] No classic hydrogen bonds have been found, but there are some π-π stacking interactions (3.622 Å) between the pyridine rings (**Figure 2.3.13**).

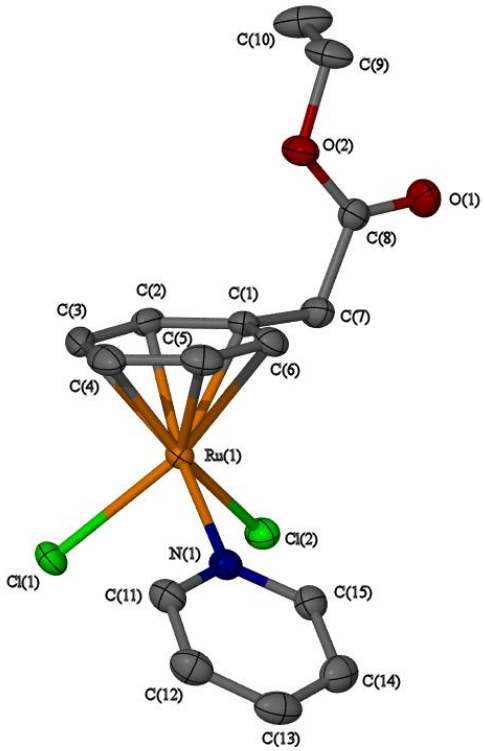

Figure 2.3.12 Molecular structure of complex **2.10**. Displacement ellipsoids are at the 50% probability level. Hydrogen atoms are omitted for clarity

Bond	Distance (Å)	Bond	Distance (Å)
Ru(1)-N(1)	2.156(3)	C(8)-O(1)	1.213(4)
Ru(1)-Cl(1)	2.4438(8)	C(8)-O(2)	1.344(4)
Ru(1)-Cl(2)	2.4308(8)	O(2)-C(9)	1.483(4)
C(1)-C(2)	1.439(4)	C(9)-C(10)	1.520(5)
C(1)-C(7)	1.519(4)	N(1)-C(11)	1.362(4)
C(7)-C(8)	1.527(4)	C(11)-C(12)	1.394(5)
Ru(1)-Ring	1.683	Ru(1)-$C_{(arene)}$	2.209
Bond	**Angle (°)**	**Bond**	**Angle (°)**
Cl(2)-Ru(1)-Cl(1)	86.47(3)	C(1)-Ru(1)-C(6)	37.54(11)
N(1)-C(11)-C(12)	122.9(3)	C(1)-C(7)-C(8)	114.9(2)
C(11)-N(1)-Ru(1)	119.2(2)	O(1)-C(8)-C(7)	122.1(3)
N(1)-Ru(1)-Cl(1)	84.75(7)	O(1)-C(8)-O(2)	124.5(3)
N(1)-Ru(1)-Cl(2)	87.00(7)	O(2)-C(9)-C(10)	110.4(3)

Table 2.3.5 Selected interatomic distances and angles for compound **2.10** with s.u.s. shown in parenthesis

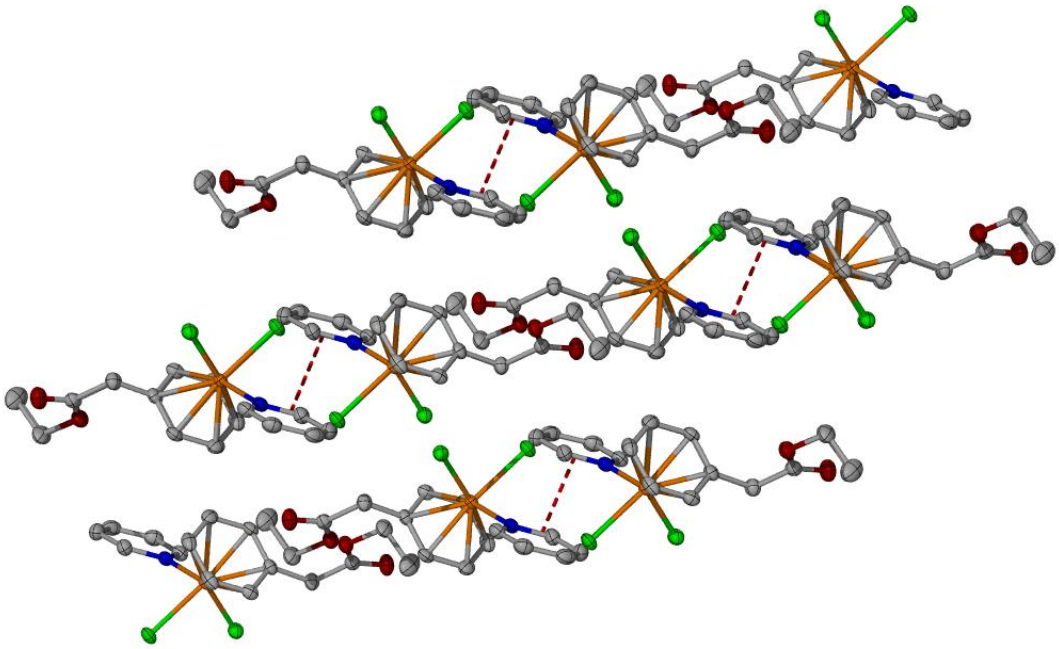

Figure 2.3.13 Compound **2.10** viewed along the c axis showing π-π stacking interactions (3.622 Å) between molecules. Hydrogen atoms omitted for clarity

2.4 General Observations and Comments

The functionalised η^6-arene ruthenium complexes synthesised in this chapter react in solutions of strongly nucleophilic coordinating solvents, despite being air stable. This is in accordance with previous observations reported in the literature.[11-15]

These reactions are photochemical, although they could be thermal with more unstable and reactive polycyclic aromatic ligands (with more delocalised π-electrons).[16] The result is the displacement of the arene, which can be proven by ^{1}H NMR with the appearance of peaks at around 7 ppm (non-coordinated aromatics).

Valerga and co-workers studied these reactions for dimers with bridging ligands with the general formula [{$RuCl_2(\eta^6$-arene)}$_2$(μ-L)], and suggested that the first mechanistic step is the cleavage of the dimer to give a monomer with a coordinated arene, two chlorides and the ligand L. This then reacts with a molecule of solvent, which replaces the ligand L, and finally, three other molecules of solvent displace the arene completely, resulting in the final product, with the general formula $RuCl_2(sol)_4$ (sol = coordinating solvent) (**Scheme 2.4.1**).[11] This product has already been characterised and displays tetragonal symmetry with trans linear chlorides.[15] Although the complexes presented in this chapter differ slightly in structure, the mechanism in which their reactions with coordinating solvents proceed could be similar to the one proposed by Valerga, but this has not been investigated further.

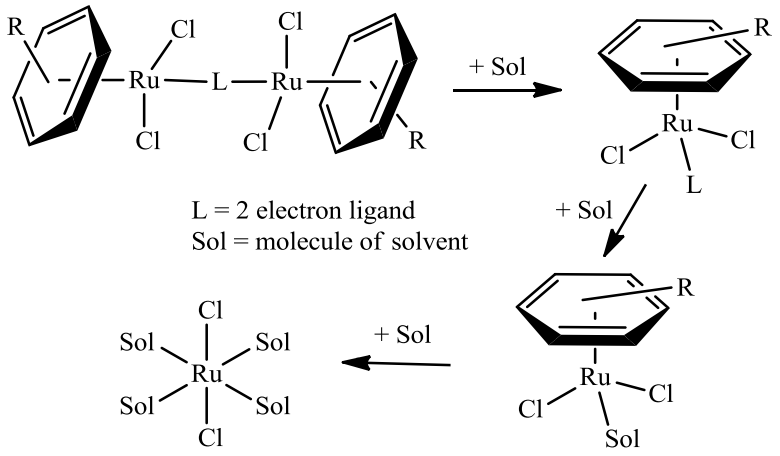

Scheme 2.4.1 Sequence suggested by Valerga *et al.* for the reaction with coordinating solvents[11]

The decomposition in solution of coordinating solvents is accelerated by exposing freshly prepared samples to UV lamps, which proves that these reactions are photochemical. With *p*-cymene ligands, these types of reactions have not been noticed during this project, which may indicate that electron withdrawing groups such as carboxylic acids and esters in the functionalised complexes make them less

stable. Arene exchange reactions in aromatic solvents have not been observed, although they are also suggested in the literature.[17]

The acid dimers **2.3**, **2.4** and **2.5** are only soluble in coordinating solvents such as acetonitrile or methanol, which ends up producing the above mentioned photochemical reactions with the solvents. However, the esters are generally more soluble, and also dissolve in non-coordinating solvents like chloroform, dichloromethane or toluene at its boiling point.

2.5 Immobilisation Attempts

The η^6-arene complexes presented in this chapter contain functionalities suitable, in principle, to react covalently with modified surfaces and give immobilised metal compounds that could be tested as heterogeneous hydrogen transfer catalysts. However, when different nucleophilic groups, mainly amines, were reacted with the carboxy dimers, the final mixtures were complex. This possibly indicates that both reactions with the carboxylic carbons and the ruthenium centres were taking place.

In a different attempt, instead of starting from a dimeric complex, ligand **2.1** was immobilised onto aminopropyl silica (amine loading of 2 mmol/g and moisture content of approx. 5%) (**Figure 2.5.1**), which was provided by an industrial partner to this project, Yorkshire Process Technology Ltd. (spin out of Reaxa Ltd.). A peptide coupling reagent, N,N'-diisopropylcarbodiimide (DIC) (**Figure 2.5.2**), was used for the formation of the corresponding amide.

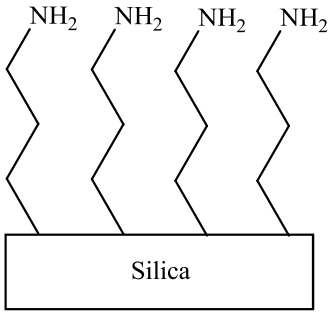

Figure 2.5.1 Aminopropyl silica

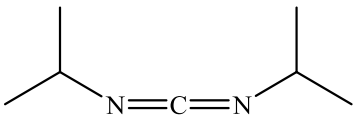

Figure 2.5.2 N,N'-Diisopropylcarbodiimide (DIC)

The resulting immobilised ligand was analysed by elemental analysis, with imprecise results, and solid state infrared spectroscopy, after drying it in a vacuum oven at 50-60°C to eliminate the infrared bands at 3400 and 1600 cm^{-1} from the silica support, assigned to the stretching and deformation vibrations of adsorbed water molecules.[18] The appearance of an intense peak at 1628 cm^{-1} indicated the formation of an amide (**Figure 2.5.3**).

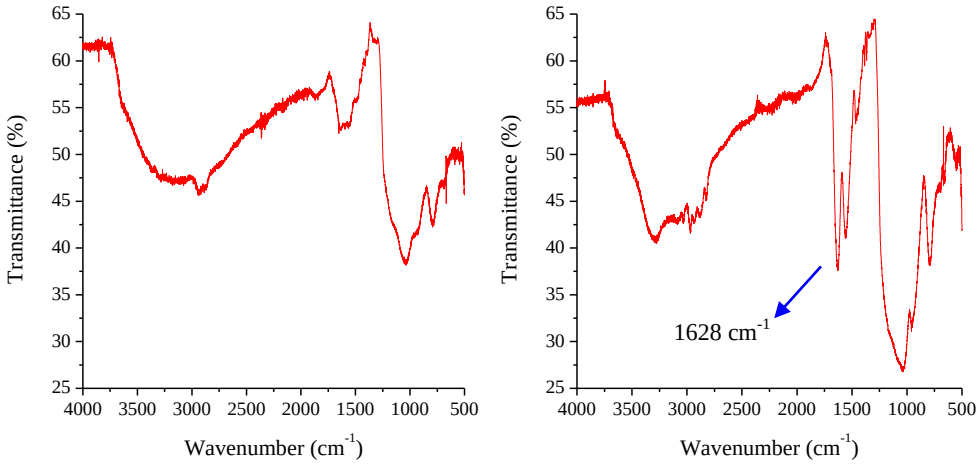

Figure 2.5.3 Infrared spectra (Transmittance % vs. cm^{-1}) of a) aminopropyl silica, b) immobilised ligand **2.1**

The immobilised ligand was then mixed with $RuCl_3 \cdot 3H_2O$ in refluxing ethanol. The resulting dark green powder has not been analysed, but was proven to be inactive against the N-alkylation of *tert*-butylamine with phenethyl alcohol. The loading of ruthenium within the supported material was believed to be very low.

2.6 Conclusions

Two 2,5-dihydrophenyl carboxy ligands and seven functionalised η^6-arene ruthenium complexes have been successfully synthesised. The aim was to investigate the possibilities for covalent immobilisation onto modified supports through pendant

chains in the arene ligands and utilisation of the heterogeneous complexes as catalysts for hydrogen transfer reactions. The arene coordination to ruthenium in all of these complexes has proven poorly stable, contrary to expectations, preventing the immobilisation objective.

2.7 References

1. X. Li, J. Blacker, I. Houson, X. Wu and J. Xiao, *Synlett*, 2006, **2006**, 1155-1160.
2. R. Noyori and S. Hashiguchi, *Accounts of Chemical Research*, 1997, **30**, 97-102.
3. M. H. S. A. Hamid and J. M. J. Williams, *Chemical Communications*, 2007, 725-727.
4. R. Stodt, S. Gencaslan, Iris M. Müller and William S. Sheldrick, *European Journal of Inorganic Chemistry*, 2003, **2003**, 1873-1882.
5. K. D. Camm, *PhD Thesis*, University of Leeds, 2004.
6. M. A. Bennett and A. K. Smith, *Journal of the Chemical Society, Dalton Transactions*, 1974, 233-241.
7. M. G. Mendoza-Ferri, C. G. Hartinger, A. A. Nazarov, R. E. Eichinger, M. A. Jakupec, K. Severin and B. K. Keppler, *Organometallics*, 2009, **28**, 6260-6265.
8. T. Screen, *Personal communication*.
9. R. Aronson, M. R. J. Elsegood, J. W. Steed and D. A. Tocher, *Polyhedron*, 1991, **10**, 1727-1732.
10. Z. Almodares, *PhD Thesis*, University of Leeds, 2010.
11. P. Valerga, M. C. Puerta and D. S. Pandey, *Journal of Organometallic Chemistry*, 2002, **648**, 27-32.
12. W. Lackner, C. M. Standfest-Hauser, K. Mereiter, R. Schmid and K. Kirchner, *Inorganica Chimica Acta*, 2004, **357**, 2721-2727.
13. T. Hayashida and H. Nagashima, *Organometallics*, 2002, **21**, 3884-3888.
14. A. M. Pizarro, M. Melchart, A. Habtemariam, L. Salassa, F. P. A. Fabbiani, S. Parsons and P. J. Sadler, *Inorganic Chemistry*, 2010, **49**, 3310-3319.
15. M. Bown and D. C. R. Hockless, *Acta Crystallographica Section C*, 1996, **52**, 1105-1106.

16. A. M. McNair and K. R. Mann, *Inorganic Chemistry*, 1986, **25**, 2519-2527.
17. B. Therrien, T. R. Ward, M. Pilkington, C. Hoffmann, F. Gilardoni and J. Weber, *Organometallics*, 1998, **17**, 330-337.
18. G. D. Chukin and V. I. Malevich, *Zhurnal Prikladnoi Spektroskopii*, 1977, **26**, 294-301.

Chapter 3

η^6-*p*-Cymene Ruthenium Complexes

3.1 Introduction

This chapter introduces the synthesis and characterisation of a library of pyridine η^6-*p*-cymene ruthenium monomers with general structure [RuX_2(*p*-cymene)(NC_5H_4R)] (R = different substituting groups in the pyridine ring) as potential hydrogen transfer catalysts (**3.4** to **3.13**). A *tert*-butylamine monomer (**3.3**) was also synthesised following the same general method, and the preparation of a complex with two pyridine ligands (**3.14**) is presented as well. The starting materials used for all of these syntheses were the ruthenium dimers with general structure [RuX_2(*p*-cymene)]$_2$ (X = Cl for complex **3.1** and X = I for complex **3.2**), also reported in this chapter. Six of the complexes described had been previously synthesised (**3.1** to **3.4**, **3.6** and **3.12**) by different methods. All of the species discussed in this chapter are shown in **Figure 3.1.1**.

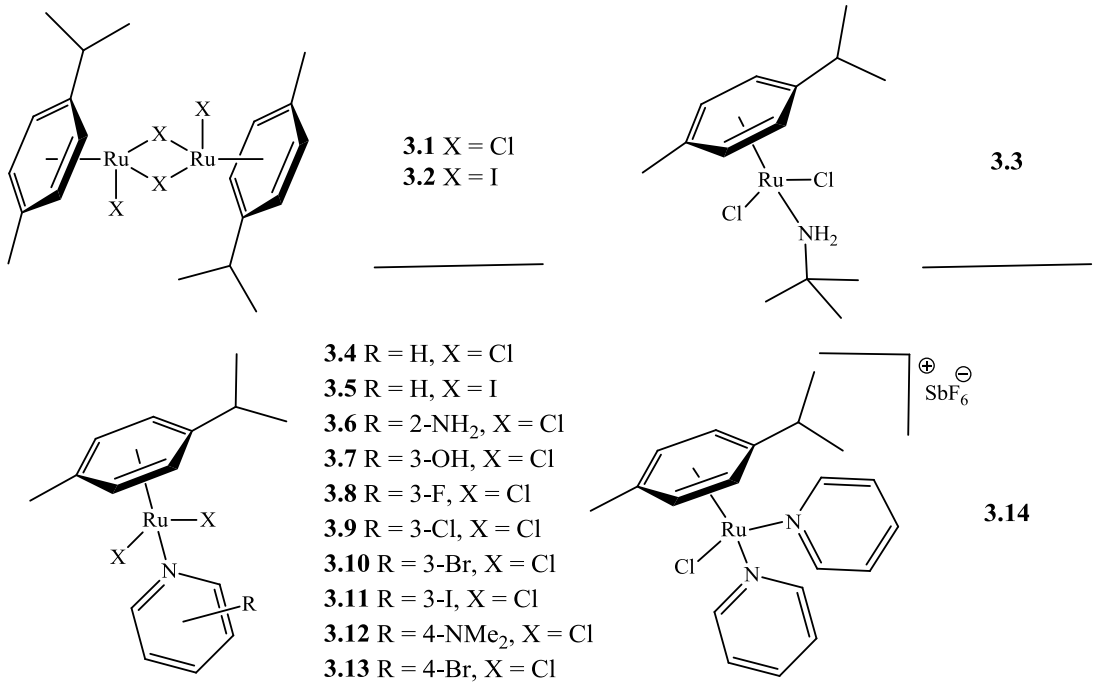

Figure 3.1.1 General structures of the complexes discussed in Chapter 3

The η^6-*p*-cymene ruthenium dimers **3.1** and **3.2** are commercially available. Nevertheless, during this project, they were synthesised because it was easy and cheap. Some methods previously published for their synthesis include those of Bennett and Smith,[1] Jensen *et al.*[2] and Keppler *et al.*[3] These two complexes have previously proven good pre-catalysts for the hydrogen transfer reactions of interest under homogeneous conditions. They generally need the presence of a nucleophilic

ligand to cleave the dimer and form the proposed active species, and this nucleophilic ligand is commonly a chelating diphosphine or diamine.[4-6] The monomers (**3.3** to **3.14**) presented in this chapter contain monodentate ligands instead, such as pyridines and *tert*-butylamine. The different functional groups in positions 2, 3 and 4 of the pyridines could influence the lability of the pyridine as coordinating ligand and, thus, the activity of the catalyst. Fujita and co-workers have already used some iridium pyridine (2-hydroxypyridine) complexes as catalysts for dehydrogenations of alcohols.[7]

3.2 η^6-*p*-Cymene Ruthenium Dimers

3.2.1 Synthesis of $[RuCl_2(C_{10}H_{14})]_2$ (3.1)

Compound **3.1** was obtained as a red microcrystalline powder in 89% yield from the reaction of α-terpinene with $RuCl_3 \cdot 3H_2O$ in refluxing ethanol (**Scheme 3.2.1**). This complex had already been synthesised within the McGowan group using the same procedure,[8] adapted from the publications mentioned above.

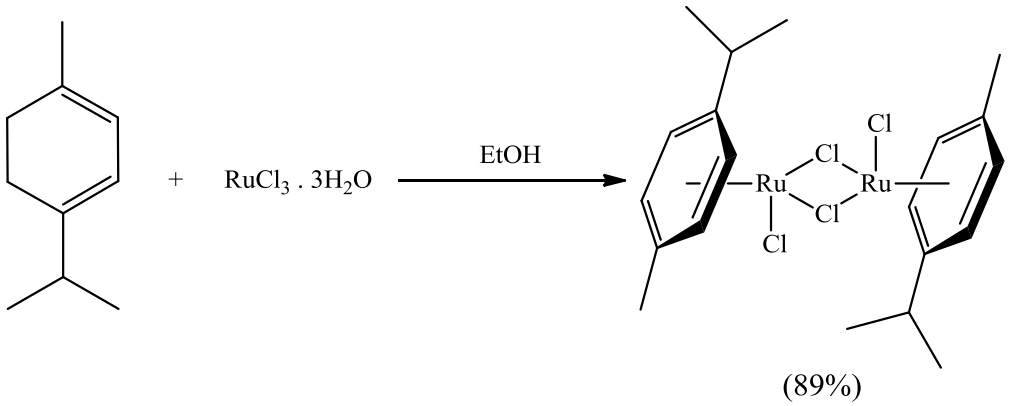

Scheme 3.2.1 Synthesis of complex **3.1** $[RuCl_2(p\text{-cymene})]_2$

3.2.2 Synthesis of $[RuI_2(C_{10}H_{14})]_2$ (3.2)

Compound **3.2** was obtained in 86% yield from the reaction of **3.1** with sodium iodide in chloroform/water (**Scheme 3.2.2**), which was a modification of previously published work[1, 3] and a method utilised for halide exchange reactions with iridium complexes that was personally communicated to the author.[9] It is a dark red microcrystalline powder, soluble in most common solvents. Characterisation data was compared with the literature to confirm product formation.[3]

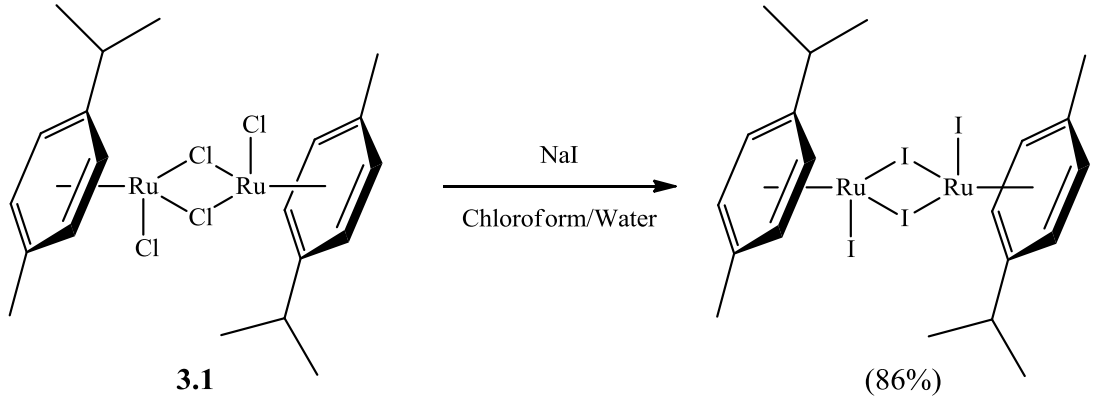

3.1 (86%)

Scheme 3.2.2 Synthesis of complex **3.2** $[RuI_2(p\text{-cymene})]_2$

When compound **3.1** was mixed with bromide salts in an attempt to prepare $[RuBr_2(p\text{-cymene})]_2$ using this method, the result was always a mixture of both the chloride and the bromide dimers that could not be separated. The bromide dimer is not commercially available.

3.3 η^6-*p*-Cymene Ruthenium Monomers

3.3.1 Synthesis of $[RuCl_2(C_{10}H_{14})(NH_2C(CH_3)_3)]$ (3.3)

Complex **3.3** was produced in 74% yield as an orange solid from compound **3.1** and *tert*-butylamine in dichloromethane (**Scheme 3.3.1**). It is an air and moisture stable, neutral, 18 electron complex. The characterisation data matched that previously reported by Wright *et al*., who synthesised this compound using ultrasound.[10]

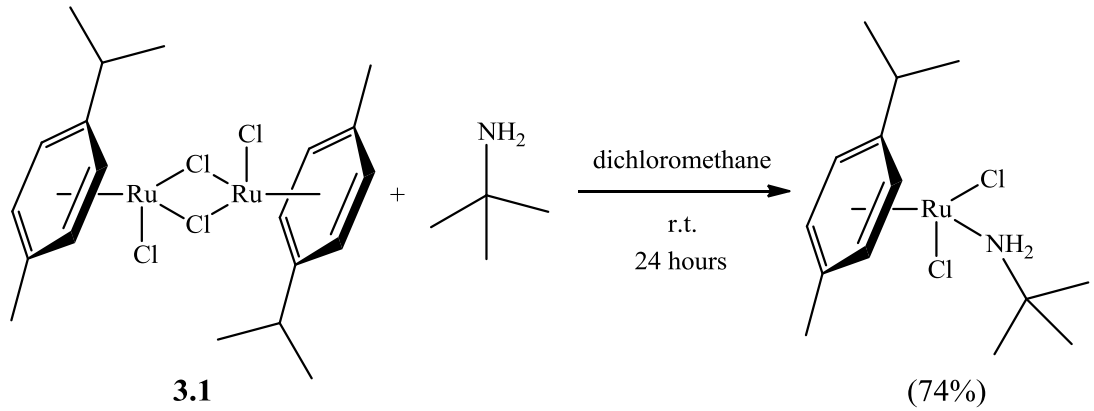

3.1 (74%)

Scheme 3.3.1 Synthesis of complex **3.3** $[RuCl_2(C_{10}H_{14})(NH_2C(CH_3)_3)]$

3.3.1.1 X-Ray Crystallographic Analysis of Compound 3.3

Orange crystals of complex **3.3** suitable for X-ray crystallography were obtained by vapour diffusion of pentane into a saturated solution of the complex in chloroform. Complex **3.3** crystallised in a monoclinic cell, and structural solution was performed in the space group $P2_1/c$. The asymmetric unit comprises one molecule of compound **3.3** and one molecule of disordered chloroform. This molecule of chloroform is disordered over two positions with an occupancy of 0.5. Some atoms in the molecule of the complex seemed also disordered, but the structure was solved without considering multiple occupancy in these cases. The molecular structure is shown in **Figure 3.3.1** and selected bond lengths and angles are shown in **Table 3.3.1**.

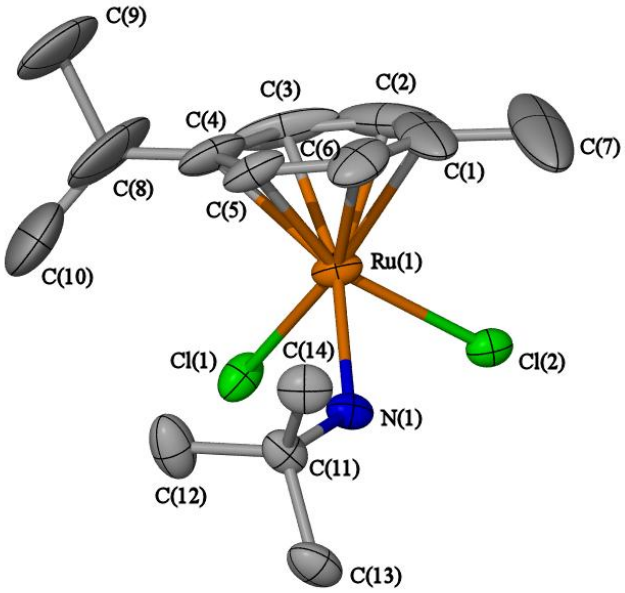

Figure 3.3.1 Molecular structure of complex **3.3**. Displacement ellipsoids are at the 50% probability level. Hydrogen atoms and the molecule of chloroform are omitted for clarity

The distance between the ruthenium centre and the arene ring centroid is 1.688 Å. The bond length Ru(1)-N(1) is 2.207(3) Å, and the average Ru-$C_{(arene)}$ is 2.202 Å, all comparable with previously published values.[11] Compound **3.3** shows intermolecular hydrogen bonding between N(1)-H and Cl(2) with an N...Cl distance of 3.602 Å and between C(3)-H and Cl(2) with a C...Cl distance of 3.616 Å. Each molecule interacts doubly with two neighbouring molecules in the solid state (**Figure 3.3.2**).

Bond	Distance (Å)	Bond	Distance (Å)
Ru(1)-N(1)	2.207(3)	C(4)-C(8)	1.422(11)
Ru(1)-Cl(1)	2.4483(12)	C(8)-C(9)	1.566(10)
Ru(1)-Cl(2)	2.4704(12)	C(8)-C(10)	1.555(5)
C(1)-C(2)	1.411(15)	N(1)-C(11)	1.516(6)
C(1)-C(7)	1.547(14)	C(11)-C(12)	1.539(7)
Ru(1)-Ring	1.688	Ru(1)-$C_{(arene)}$	2.202
Bond	**Angle (°)**	**Bond**	**Angle (°)**
Cl(1)-Ru(1)-Cl(2)	86.09(4)	C(6)-Ru(1)-C(1)	37.1(3)
N(1)-C(11)-C(12)	108.4(4)	C(6)-C(1)-C(2)	188.8(8)
C(11)-N(1)-Ru(1)	130.4(3)	C(5)-C(4)-C(8)	129.7(8)
N(1)-Ru(1)-Cl(1)	83.13(9)	C(4)-C(8)-C(9)	112.3(8)
N(1)-Ru(1)-Cl(2)	78.20(10)	C(10)-C(8)-C(9)	109.2(9)

Table 3.3.1 Selected interatomic distances and angles for compound **3.3** with s.u.s. shown in parenthesis

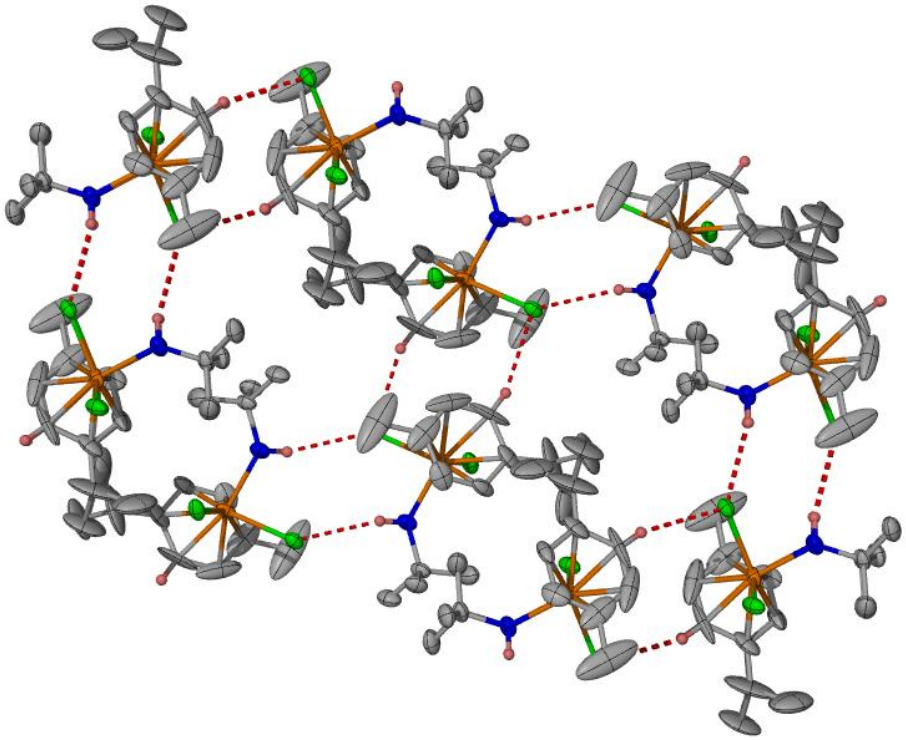

Figure 3.3.2 Compound **3.3** viewed along the c axis showing hydrogen bonding interactions. Only the hydrogen atoms involved in these interactions are shown. The molecules of chloroform are omitted for clarity

3.3.2 Synthesis of $[RuX_2(C_{10}H_{14})(NC_5H_4R)]$ (X = Cl, I) (3.4−3.13)

The general method for the synthesis of these pyridine complexes (**3.4** to **3.13**) is given in **Scheme 3.3.2**. They were all prepared as yellow, orange or brown solids under mild conditions from compounds **3.1** or **3.2** and the corresponding ligand in dichloromethane at room temperature, in yields above 70%. Some of these compounds had been previously synthesised and characterised; the pyridine monomer with chlorides (**3.4**) was prepared by Bennett and Smith,[1] the 2-aminopyridine complex (**3.6**) was reported by Aronson *et al*. and was characterised by X-ray crystallography,[11] and the 4-dimethylaminopyridine compound (**3.12**) was obtained by Köytepe and co-workers.[12] These published syntheses, though, involved high temperatures. All of the other pyridine monomers (**3.5**, **3.7** to **3.11** and **3.13**) are novel to the best knowledge of the author.

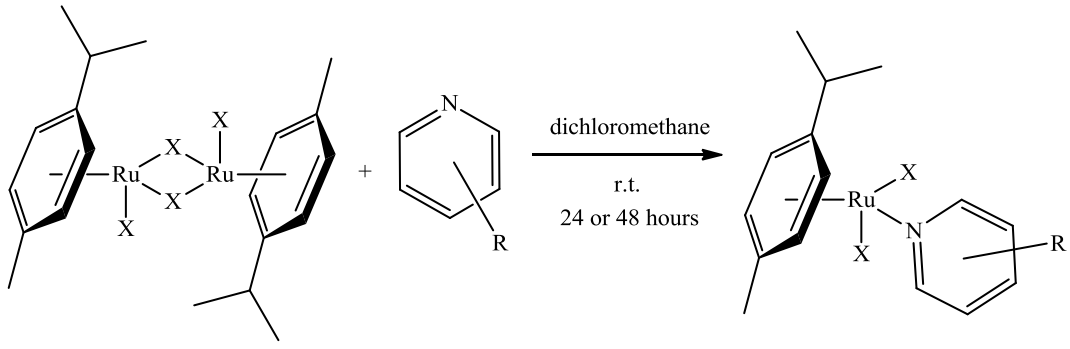

3.1 or **3.2**

3.4 R = H, X = Cl (89%)
3.5 R = H, X = I (88%)
3.6 R = 2-NH_2, X = Cl (85%)
3.7 R = 3-OH, X = Cl (74%)
3.8 R = 3-F, X = Cl (97%)
3.9 R = 3-Cl, X = Cl (96%)
3.10 R = 3-Br, X = Cl (90%)
3.11 R = 3-I, X = Cl (74%)
3.12 R = 4-NMe_2, X = Cl (70%)
3.13 R = 4-Br, X = Cl (100%)

Scheme 3.3.2 General scheme for the synthesis of the pyridine η^6-*p*-cymene ruthenium monomers

3.3.2.1 X-Ray Crystallographic Analysis of Compound 3.4

Orange crystals of complex **3.4** suitable for X-ray crystallography were obtained by vapour diffusion of pentane into a saturated solution of the complex in chloroform. Compound **3.4** crystallised in a monoclinic cell, and structural solution

was performed in the space group $P2_1/c$. The complex exhibits the typical "half-sandwich" structure of η^6-arene ruthenium complexes. The molecular structure of compound **3.4** is shown in **Figure 3.3.3**.

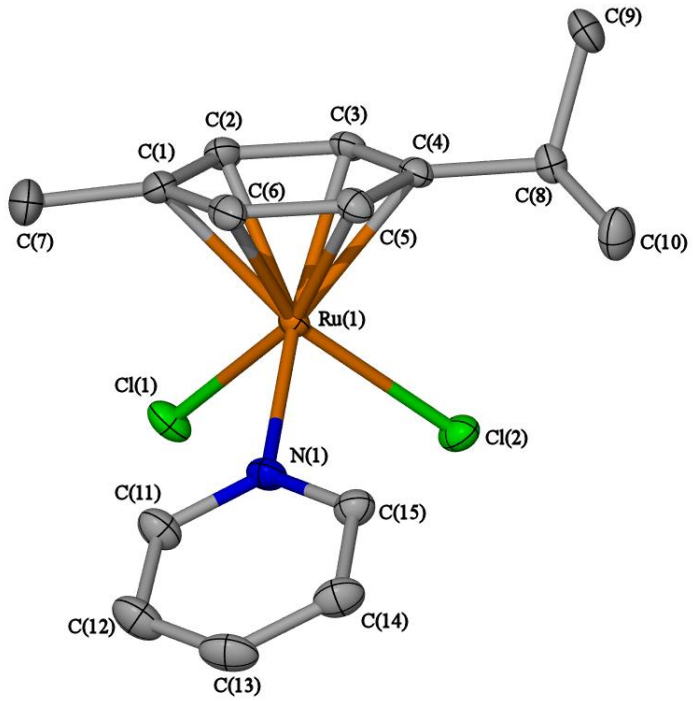

Figure 3.3.3 Molecular structure of complex **3.4**. Displacement ellipsoids are at the 50% probability level. Hydrogen atoms are omitted for clarity

Bond	**Distance (Å)**	**Bond**	**Distance (Å)**
Ru(1)-N(1)	2.1720(15)	C(4)-C(8)	1.537(2)
Ru(1)-Cl(1)	2.4382(5)	C(8)-C(9)	1.562(3)
Ru(1)-Cl(2)	2.4514(5)	C(8)-C(10)	1.546(3)
C(1)-C(2)	1.448(3)	N(1)-C(11)	1.372(2)
C(1)-C(7)	1.526(3)	C(11)-C(12)	1.407(3)
Ru(1)-Ring	1.686	Ru(1)-$C_{(arene)}$	2.219
Bond	**Angle (°)**	**Bond**	**Angle (°)**
Cl(1)-Ru(1)-Cl(2)	87.446(18)	C(6)-Ru(1)-C(1)	38.13(7)
N(1)-C(11)-C(12)	122.27(18)	C(6)-C(1)-C(2)	117.16(15)
C(11)-N(1)-Ru(1)	122.46(12)	C(5)-C(4)-C(8)	123.22(15)
N(1)-Ru(1)-Cl(1)	86.84(4)	C(4)-C(8)-C(9)	108.58(14)
N(1)-Ru(1)-Cl(2)	85.89(4)	C(10)-C(8)-C(9)	110.89(16)

Table 3.3.2 Selected interatomic distances and angles for compound **3.4** with s.u.s. shown in parenthesis

Table 3.3.2 gives selected bond lengths and angles of complex **3.4**. The average Ru-$C_{(arene)}$ distance for this complex is 2.219 Å, similar to other η^6-arene ruthenium complexes.[11] The distance between the metal atom and the arene ring centroid is 1.686 Å, also comparable with previously reported data.

3.3.2.2 NMR Data for Compound 3.7

The structure of complex **3.7** is represented and labelled in **Figure 3.3.4**. **Figure 3.3.5** shows the ^{1}H NMR spectrum of this complex together with those of free 3-hydroxypyridine, $[RuCl_2(p\text{-cymene})]_2$ (**3.1**) and free *p*-cymene. The region between 1.0 and 3.3 ppm includes the aliphatic *p*-cymene peaks, which are very distinctive and allow easy identification of the different compounds. The pyridine region between 6.7 and 8.8 ppm shows how the peaks of coordinated 3-hydroxypyridine in complex **3.7** differ from those of the free ligand; when coordinated, 3-hydroxypyridine presents four well separated and differentiable peaks. $^{13}C\{^1H\}$ (**Figure 3.3.6**), ^1H-^1H COSY (**Figure 3.3.7**), ^1J ^1H-$^{13}C\{^1H\}$ HMQC (**Figure 3.3.8**) and $^{2,3}J$ ^1H-$^{13}C\{^1H\}$ HMBC (**Figure 3.3.9**) NMR spectra are also given. The chemical shift assignment is shown in **Table 3.3.3**.

The ^1H-^1H COSY and ^1J ^1H-$^{13}C\{^1H\}$ HMQC spectra obtained for complex **3.7** are analogous to those of the rest of the 3-substituted pyridine complexes in this chapter, and, accordingly, similar assignments have been made.

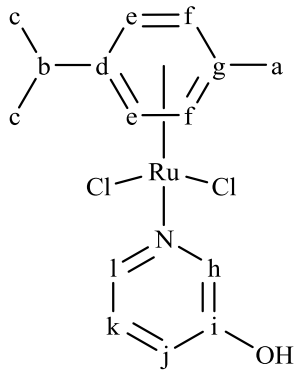

Figure 3.3.4 Labelled diagram of complex **3.7**

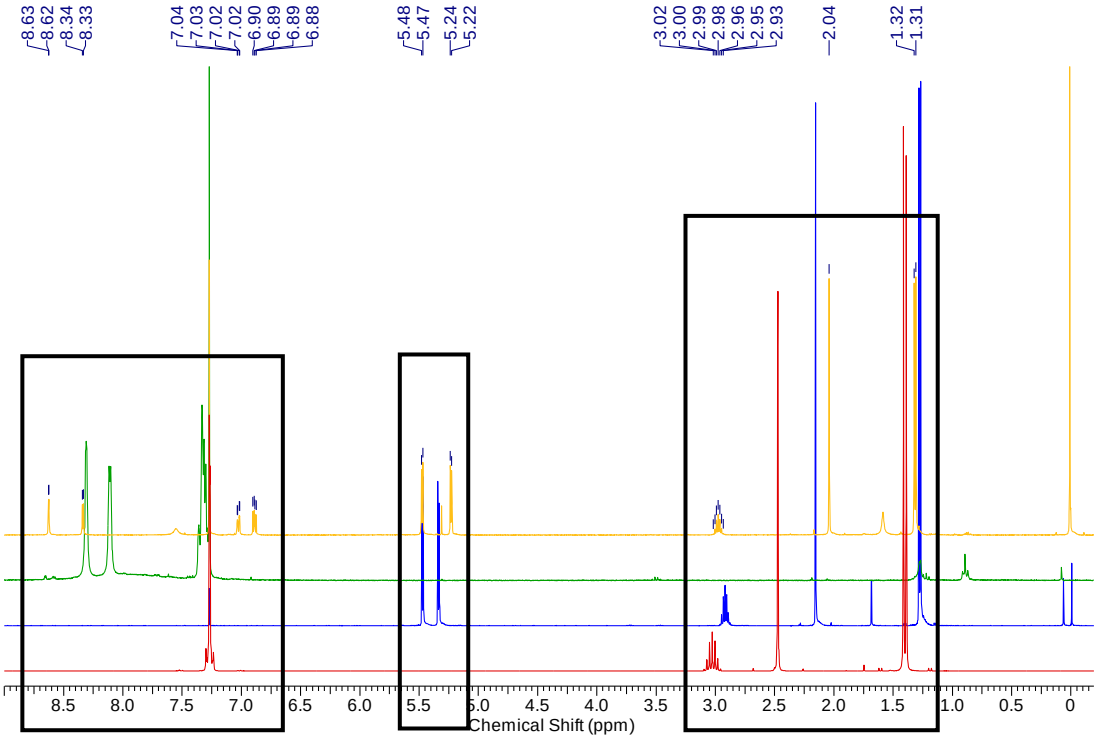

Figure 3.3.5 ^{1}H NMR spectra of **3.7** (yellow), free 3-hydroxypyridine (green), **3.1** (blue) and free *p*-cymene (red) in $CDCl_3$

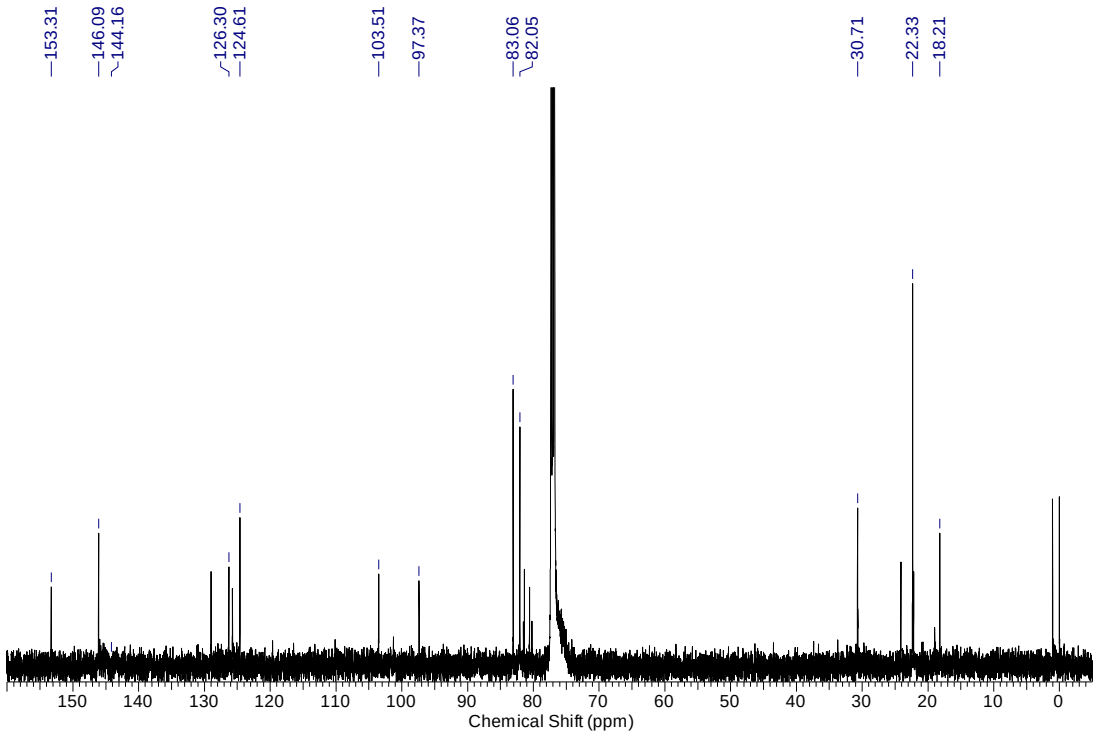

Figure 3.3.6 $^{13}C\{^{1}H\}$ NMR spectrum of **3.7** in $CDCl_3$ at 125.77 MHz and 299.2 K

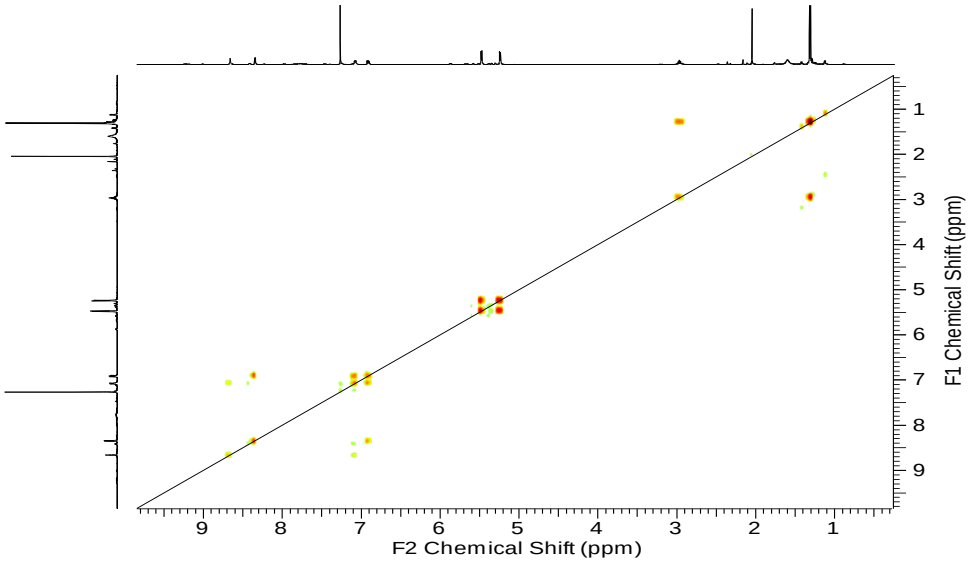

Figure 3.3.7 ^{1}H-^{1}H COSY spectrum of **3.7** in $CDCl_3$ at 300.0 K

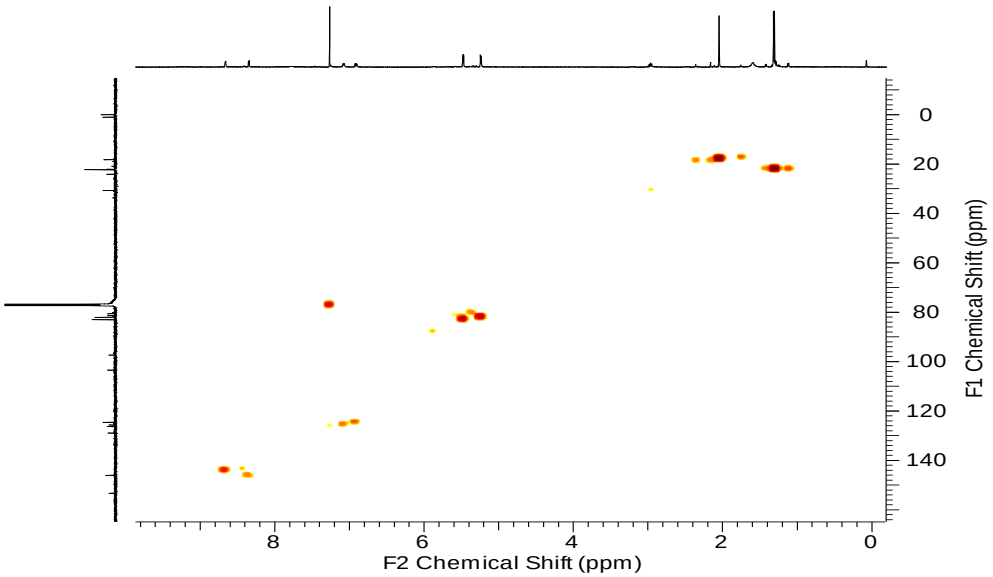

Figure 3.3.8 ^{1}J ^{1}H-^{13}C{^{1}H} HMQC spectrum of **3.7** in $CDCl_3$ at 300.1 K

From the ^{1}J ^{1}H-^{13}C{^{1}H} HMQC spectrum of compound **3.7**, it can be observed that carbon "h" is at a higher field than "l" in the ^{13}C{^{1}H} NMR spectrum of this complex. This is maintained in complex **3.8**, but reversed in complexes **3.9**, **3.10** and **3.11**. The quaternary carbon "i" gradually shifts from a lower to a higher field in the series **3.8** < **3.7** < **3.9** < **3.10** < **3.11**, which corresponds to the decreasing electronegativities of the substituents (F > O > Cl > Br > I).

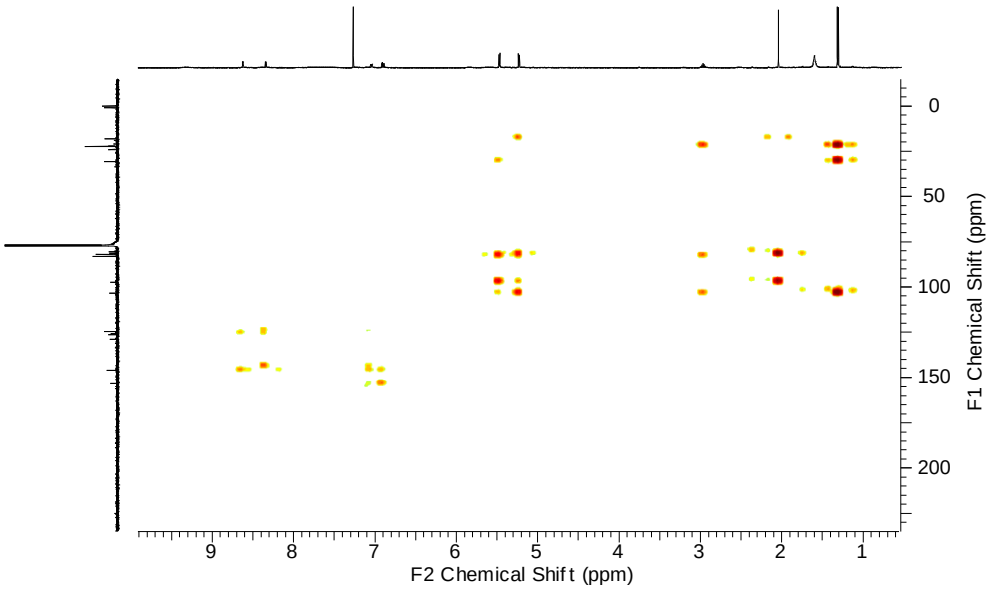

Figure 3.3.9 $^{2,3}J$ ^{1}H-$^{13}C\{^{1}H\}$ HMBC spectrum of **3.7** in $CDCl_3$ at 300.0 K

^{1}H Chemical Shift, δ (ppm)	**Assignment**
8.63 (m, 1H)	h
8.34 (d, $^{3}J_{(H-H)}$ = 5.1 Hz, 1H)	l
7.02 (dd, $^{3}J_{(H-H)}$ = 8.3, 1.5 Hz, 1H)	j
6.89 (dd, $^{3}J_{(H-H)}$ = 8.1, 5.6 Hz, 1H)	k
5.47 (d, $^{3}J_{(H-H)}$ = 5.1 Hz, 2H)	e
5.23 (d, $^{3}J_{(H-H)}$ = 6.0 Hz, 2H)	f
2.98 (m, 1H)	b
2.04 (s, 3H)	a
1.31 (d, $^{3}J_{(H-H)}$ = 6.8 Hz, 6H)	c
$^{13}C\{^{1}H\}$ Chemical Shift, δ (ppm)	**Assignment**
153.3 (Q)	i
146.1 (CH)	l
144.2 (CH)	h
126.3 (CH)	j
124.6 (CH)	k
103.5 (Q)	d
97.4 (Q)	g
83.1 (CH)	e
82.1 (CH)	f
30.7 (CH)	b
22.3 (CH_3)	c
18.2 (CH_3)	a

Table 3.3.3 ^{1}H and $^{13}C\{^{1}H\}$ chemical shift assignment for complex **3.7**

3.3.2.3 X-Ray Crystallographic Analysis of Compound 3.7

Orange crystals of compound **3.7** suitable for X-ray crystallography were obtained by vapour diffusion of pentane into a saturated solution of the complex in dichloromethane. Compound **3.7** crystallised in a monoclinic cell, and structural solution was performed in the space group $P2_1/c$. The molecular structure of this complex is shown in **Figure 3.3.10**.

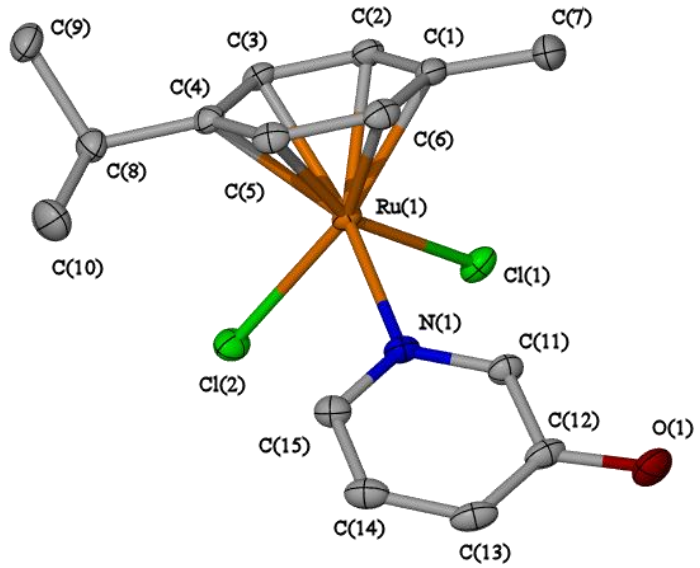

Figure 3.3.10 Molecular structure of complex **3.7**. Displacement ellipsoids are at the 50% probability level. Hydrogen atoms are omitted for clarity

Selected bond lengths and angles for complex **3.7** are given in **Table 3.3.4**. The average Ru-$C_{(arene)}$ distance for this complex is 2.201 Å and the distance between the metal atom and the arene ring centroid is 1.675 Å. The distance Ru-N(1) is 2.1505(17) Å.

Bond	Distance (Å)	Bond	Distance (Å)
Ru(1)-N(1)	2.1505(17)	C(4)-C(8)	1.525(3)
Ru(1)-Cl(1)	2.4389(5)	C(8)-C(9)	1.543(3)
Ru(1)-Cl(2)	2.4313(6)	C(8)-C(10)	1.531(3)
C(1)-C(2)	1.441(3)	N(1)-C(11)	1.349(3)
C(2)-C(3)	1.410(3)	C(11)-C(12)	1.410(3)
C(1)-C(7)	1.513(3)	O(1)-C(12)	1.369(3)
Ru(1)-Ring	1.675	Ru(1)-$C_{(arene)}$	2.201
Bond	**Angle (°)**	**Bond**	**Angle (°)**
Cl(2)-Ru(1)-Cl(1)	87.07(2)	C(6)-Ru(1)-C(1)	37.82(8)
N(1)-C(11)-C(12)	122.5(2)	C(6)-C(1)-C(2)	117.39(18)
C(11)-N(1)-Ru(1)	120.78(14)	C(5)-C(4)-C(8)	123.69(18)
N(1)-Ru(1)-Cl(1)	87.26(5)	C(10)-C(8)-C(9)	110.63(18)
N(1)-Ru(1)-Cl(2)	85.16(5)	O(1)-C(12)-C(11)	116.77(19)

Table 3.3.4 Selected interatomic distances and angles for compound **3.7** with s.u.s. shown in parenthesis

Compound **3.7** shows intermolecular hydrogen bonding between O(1)-H and Cl(1) with a O...Cl distance of 3.178 Å and between C(3)-H and Cl(1) with a C...Cl distance of 3.683 Å in the solid state. Each molecule interacts doubly with two neighbouring molecules (**Figure 3.3.11**).

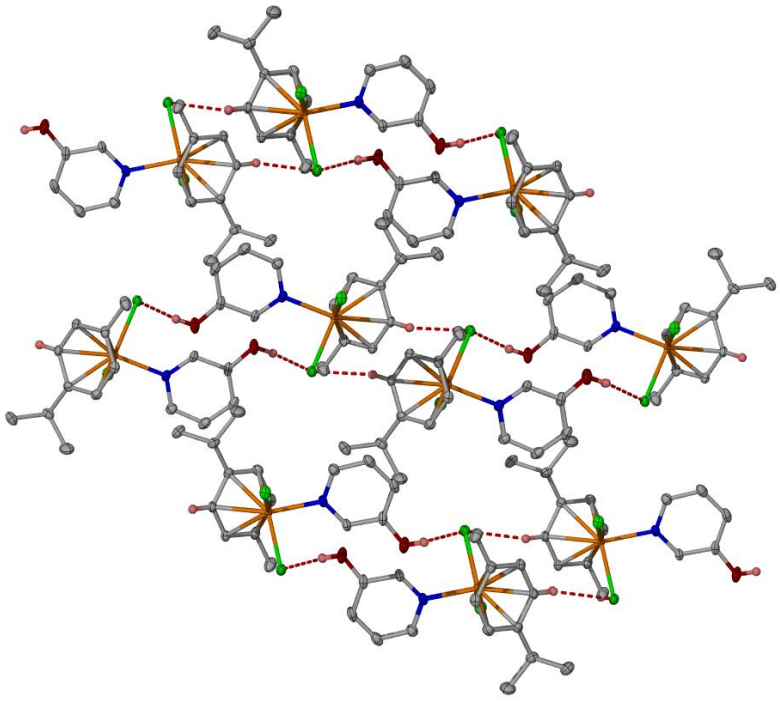

Figure 3.3.11 Compound **3.7** viewed along the a axis showing hydrogen bonding interactions. Only the hydrogen atoms involved in these interactions are shown

3.3.2.4 NMR Data for Compound 3.8

A labelled diagram of complex **3.8** is shown in **Figure 3.3.12** and its chemical shift assignment is given in **Table 3.3.5**. ^{13}C-^{19}F coupling can be observed for the pyridine carbons in the $^{13}C\{^{1}H\}$ NMR spectrum (**Figure 3.3.13**), but the corresponding ^{1}H-^{19}F coupling is not well resolved in the ^{1}H NMR spectrum.

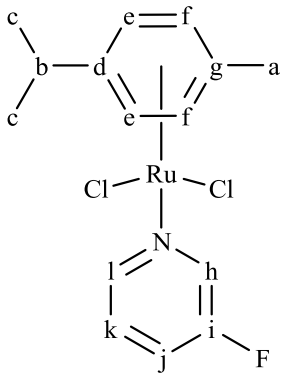

Figure 3.3.12 Labelled diagram of complex **3.8**

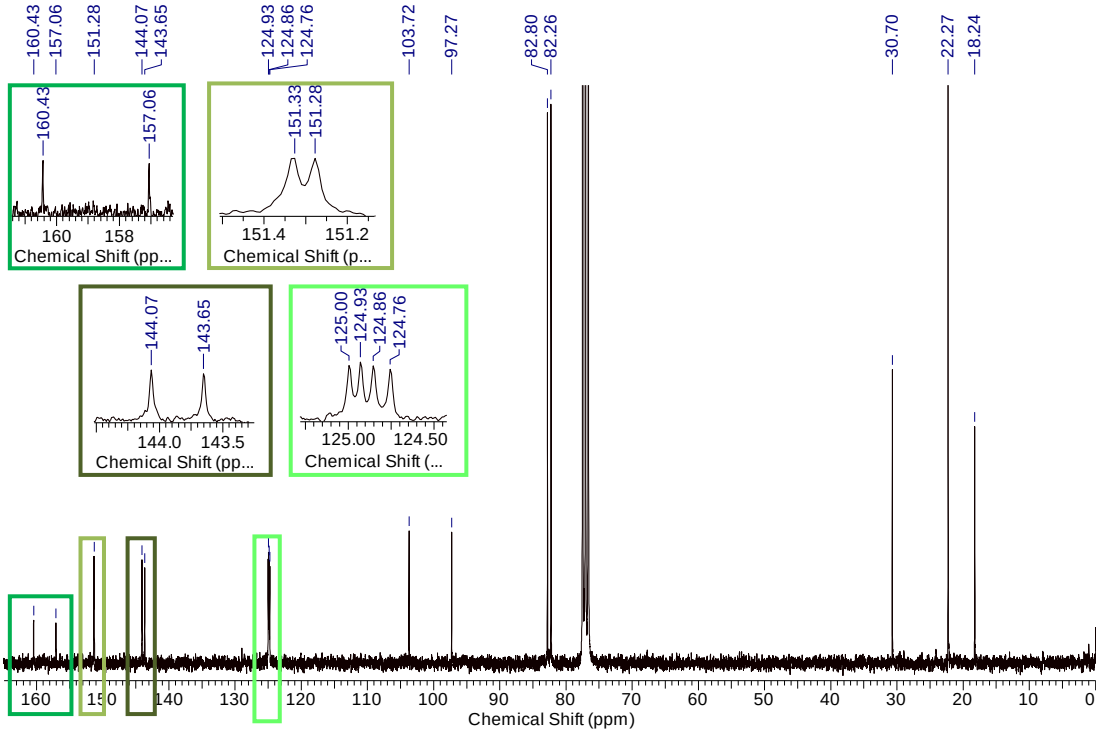

Figure 3.3.13 $^{13}C\{^{1}H\}$ NMR spectrum of **3.8** in $CDCl_3$ at 75.47 MHz and 300.1 K

^{1}H Chemical Shift, δ (ppm)	**Assignment**
8.99 (br. s, 1H)	h
8.90 (d, $^{3}J_{(H-H)}$ = 4.8 Hz, 1H)	l
7.50 (m, 1H)	j
7.33 (m, 1H)	k
5.46 (d, $^{3}J_{(H-H)}$ = 5.2 Hz, 2H)	e
5.25 (d, $^{3}J_{(H-H)}$ = 5.2 Hz, 2H)	f
2.98 (m, 1H)	b
2.10 (s, 3H)	a
1.31 (d, $^{3}J_{(H-H)}$ = 6.8 Hz, 6H)	c
^{13}C{^{1}H} Chemical Shift, δ (ppm)	**Assignment**
158.7 (d, $^{1}J_{(C-F)}$ = 254.3 Hz, Q)	i
151.3 (d, $^{4}J_{(C-F)}$ = 3.8 Hz, CH)	l
143.9 (d, $^{2}J_{(C-F)}$ = 31.7 Hz, CH)	h
124.9 (m, CH)	j & k
103.7 (s, Q)	d
97.3 (s, Q)	g
82.8 (s, CH)	e
82.3 (s, CH)	f
30.7 (s, CH)	b
22.3 (s, CH_3)	c
18.2 (s, CH_3)	a

Table 3.3.5 ^{1}H and ^{13}C{^{1}H} chemical shift assignment for complex **3.8**

3.3.2.5 X-Ray Crystallographic Analysis of Compound 3.8

Orange prisms of complex **3.8** suitable for X-ray crystallography were obtained by vapour diffusion of pentane into a saturated solution of the complex in chloroform. Compound **3.8** crystallised in a monoclinic cell, and structural solution was performed in the space group $P2_1/c$. The molecular structure of this complex is shown in **Figure 3.3.14** and selected bond lengths and angles are given in **Table 3.3.6**. The average Ru-$C_{(arene)}$ distance for this complex is 2.187 Å and the distance between the metal atom and the arene ring centroid is 1.662 Å. The distance Ru-N(1) is 2.1397(13) Å.

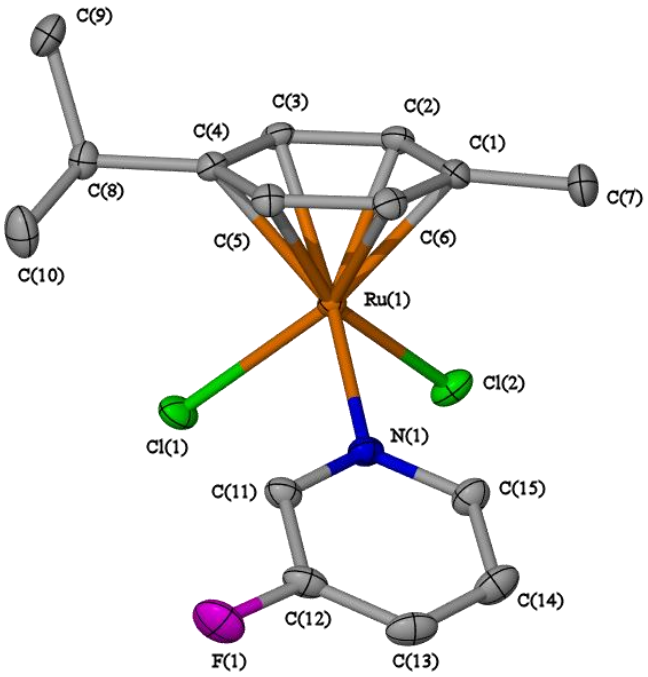

Figure 3.3.14 Molecular structure of complex **3.8**. Displacement ellipsoids are at the 50% probability level. Hydrogen atoms are omitted for clarity

Bond	**Distance (Å)**	**Bond**	**Distance (Å)**
Ru(1)-N(1)	2.1397(13)	C(4)-C(8)	1.514(2)
Ru(1)-Cl(1)	2.4174(4)	C(8)-C(9)	1.536(2)
Ru(1)-Cl(2)	2.4009(4)	C(8)-C(10)	1.523(2)
C(1)-C(2)	1.426(2)	N(1)-C(11)	1.345(2)
C(2)-C(3)	1.411(2)	C(11)-C(12)	1.383(2)
C(1)-C(7)	1.502(2)	F(1)-C(12)	1.350(2)
Ru(1)-Ring	1.662	Ru(1)-$C_{(arene)}$	2.187
Bond	**Angle (°)**	**Bond**	**Angle (°)**
Cl(2)-Ru(1)-Cl(1)	87.344(15)	C(6)-Ru(1)-C(1)	37.96(6)
N(1)-C(11)-C(12)	120.50(16)	C(6)-C(1)-C(2)	117.24(13)
C(11)-N(1)-Ru(1)	118.96(11)	C(5)-C(4)-C(8)	123.11(13)
N(1)-Ru(1)-Cl(1)	85.70(4)	C(10)-C(8)-C(9)	110.91(15)
N(1)-Ru(1)-Cl(2)	86.33(4)	F(1)-C(12)-C(11)	117.92(16)

Table 3.3.6 Selected interatomic distances and angles for compound **3.8** with s.u.s. shown in parenthesis

3.3.2.6 X-Ray Crystallographic Analysis of Compound 3.10

Orange needles of complex **3.10** suitable for X-ray crystallography were obtained by vapour diffusion of pentane into a saturated solution of the complex in

dichloromethane. Compound **3.10** crystallised in a monoclinic cell, and structural solution was performed in the space group $P2_1/c$. The molecular structure of this complex is shown in **Figure 3.3.15**. Selected bond lengths and angles are given in **Table 3.3.7**. The average Ru-$C_{(arene)}$ distance for this complex is 2.189 Å and the separation from the metal atom to the arene ring centroid is 1.670 Å. The distance Ru-N(1) is 2.1371(17) Å.

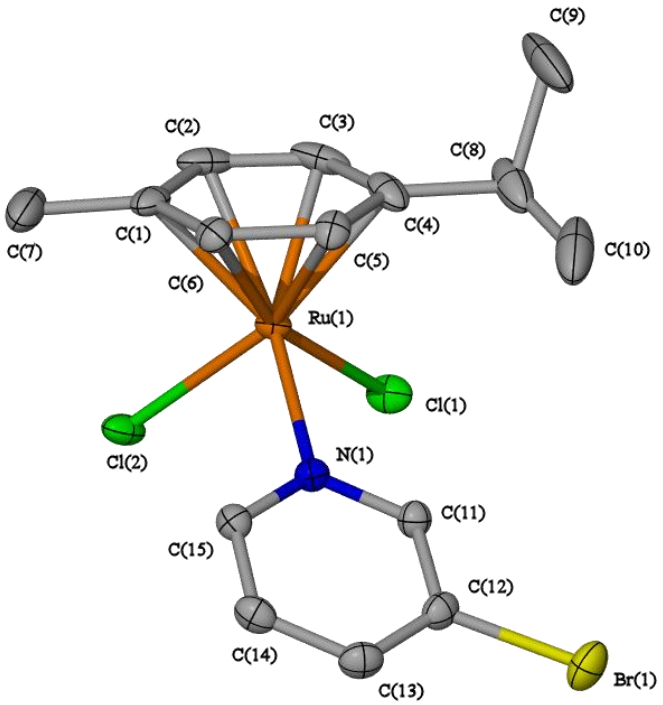

Figure 3.3.15 Molecular structure of complex **3.10**. Displacement ellipsoids are at the 50% probability level. Hydrogen atoms are omitted for clarity

Bond	Distance (Å)	Bond	Distance (Å)
Ru(1)-N(1)	2.1371(17)	C(4)-C(8)	1.510(4)
Ru(1)-Cl(1)	2.4165(5)	C(8)-C(9)	1.540(4)
Ru(1)-Cl(2)	2.4083(5)	C(8)-C(10)	1.522(5)
C(1)-C(2)	1.425(4)	N(1)-C(11)	1.346(3)
C(2)-C(3)	1.394(4)	C(11)-C(12)	1.385(3)
C(1)-C(7)	1.506(3)	Br(1)-C(12)	1.895(2)
Ru(1)-Ring	1.670	Ru(1)-$C_{(arene)}$	2.189
Bond	**Angle (°)**	**Bond**	**Angle (°)**
Cl(2)-Ru(1)-Cl(1)	87.97(2)	C(6)-Ru(1)-C(1)	37.19(8)
N(1)-C(11)-C(12)	121.3(2)	C(6)-C(1)-C(2)	118.7(2)
C(11)-N(1)-Ru(1)	122.34(14)	C(5)-C(4)-C(8)	123.9(3)
N(1)-Ru(1)-Cl(1)	86.34(5)	C(10)-C(8)-C(9)	110.9(3)
N(1)-Ru(1)-Cl(2)	84.99(5)	C(11)-C(12)-Br(1)	118.05(17)

Table 3.3.7 Selected interatomic distances and angles for compound **3.10** with s.u.s. shown in parenthesis

3.3.2.7 X-Ray Crystallographic Analysis of Compound 3.12

Orange crystals of complex **3.12** suitable for X-ray crystallography were obtained by vapour diffusion of diethyl ether into a saturated solution of the complex in dichloromethane. Compound **3.12** crystallised in a monoclinic cell, and structural solution was performed in the space group $P2_1/n$. The molecular structure of this complex is shown in **Figure 3.3.16**. Selected bond lengths and angles are given in **Table 3.3.8**. The average Ru-$C_{(arene)}$ distance for this complex is 2.189 Å and the separation from the metal atom to the arene ring centroid is 1.663 Å. The ruthenium and the pyridine nitrogen atoms are separated by 2.1348(16) Å. All of this data is comparable to the other complexes reported in this chapter that have been analysed by X-ray crystallography.

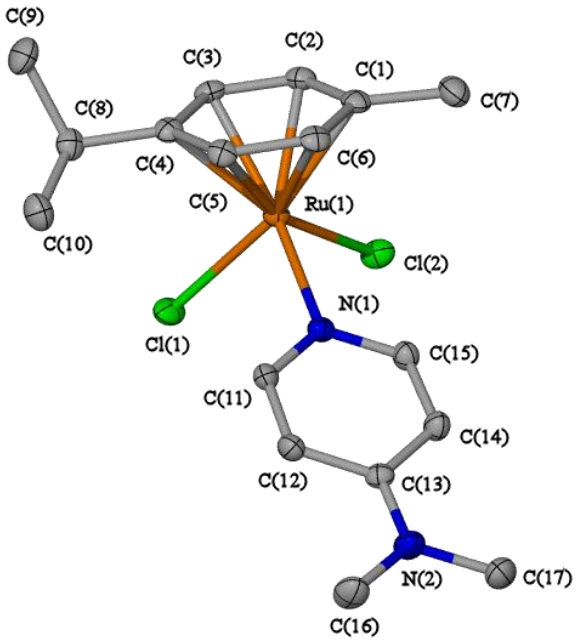

Figure 3.3.16 Molecular structure of complex **3.12**. Displacement ellipsoids are at the 50% probability level. Hydrogen atoms are omitted for clarity

Bond	**Distance (Å)**	**Bond**	**Distance (Å)**
Ru(1)-N(1)	2.1348(16)	C(4)-C(8)	1.519(3)
Ru(1)-Cl(1)	2.4254(5)	C(8)-C(9)	1.542(3)
Ru(1)-Cl(2)	2.4198(5)	C(8)-C(10)	1.531(3)
C(1)-C(2)	1.440(3)	N(1)-C(11)	1.363(2)
C(2)-C(3)	1.399(3)	C(13)-N(2)	1.353(2)
C(1)-C(7)	1.504(3)	N(2)-C(16)	1.460(3)
Ru(1)-Ring	1.663	Ru(1)-$C_{(arene)}$	2.189
Bond	**Angle (°)**	**Bond**	**Angle (°)**
Cl(2)-Ru(1)-Cl(1)	88.858(18)	C(6)-Ru(1)-C(1)	37.85(7)
N(1)-C(11)-C(12)	124.14(18)	C(6)-C(1)-C(2)	117.00(17)
C(11)-N(1)-Ru(1)	120.91(13)	C(10)-C(8)-C(9)	111.08(18)
N(1)-Ru(1)-Cl(1)	85.40(4)	N(2)-C(13)-C(12)	123.37(17)
N(1)-Ru(1)-Cl(2)	86.87(4)	C(17)-N(2)-C(16)	118.18(16)

Table 3.3.8 Selected interatomic distances and angles for compound **3.12** with s.u.s. shown in parenthesis

3.3.3 Synthesis of $[RuCl(C_{10}H_{14})(NC_5H_5)_2][SbF_6]$ (3.14)

Compound **3.14** was obtained in 100% yield from complex **3.4**, pyridine and $NaSbF_6$ in refluxing methanol (**Scheme 3.3.3**). It was originally an orange oil which crystallised out as orange needles over the course of a month. Different versions of

compound **3.14** had been previously synthesised by Dixneuf *et al*. (with BF_4 as counterion)[13] and Stephenson and co-workers (with PF_6 as counterion).[14]

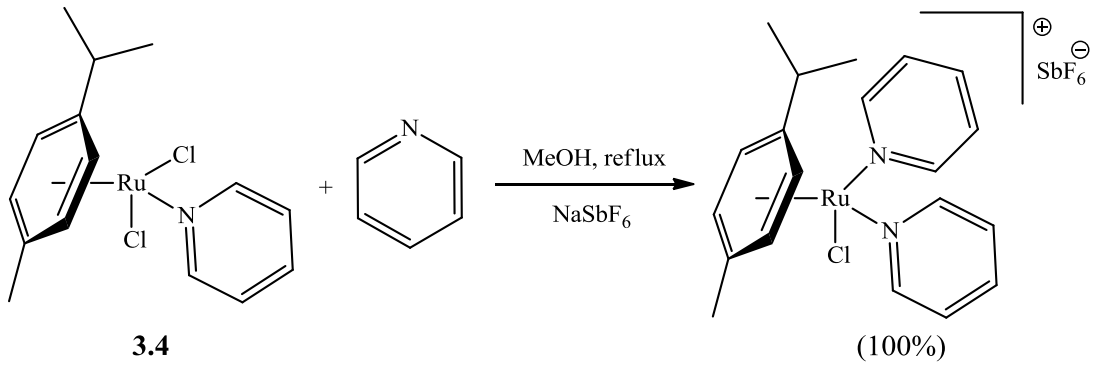

Scheme 3.3.3 Synthesis of complex **3.14** $[RuCl(C_{10}H_{14})(NC_5H_5)_2][SbF_6]$

3.3.3.1 NMR Data for Compound 3.14

A labelled diagram of complex **3.14** is shown in **Figure 3.3.17**. ^1H and $^{13}C\{^1H\}$ NMR spectra are given in **Figure 3.3.18** and **Figure 3.3.19**. The chemical shift assignment for this compound is summarised in **Table 3.3.9**.

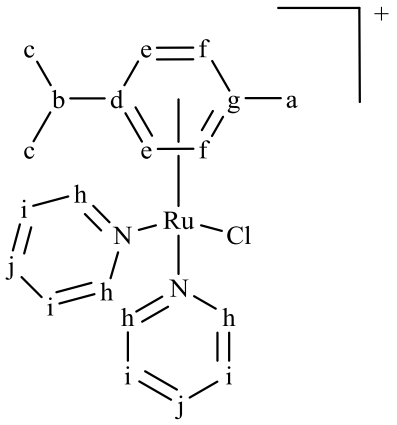

Figure 3.3.17 Labelled diagram of complex **3.14**

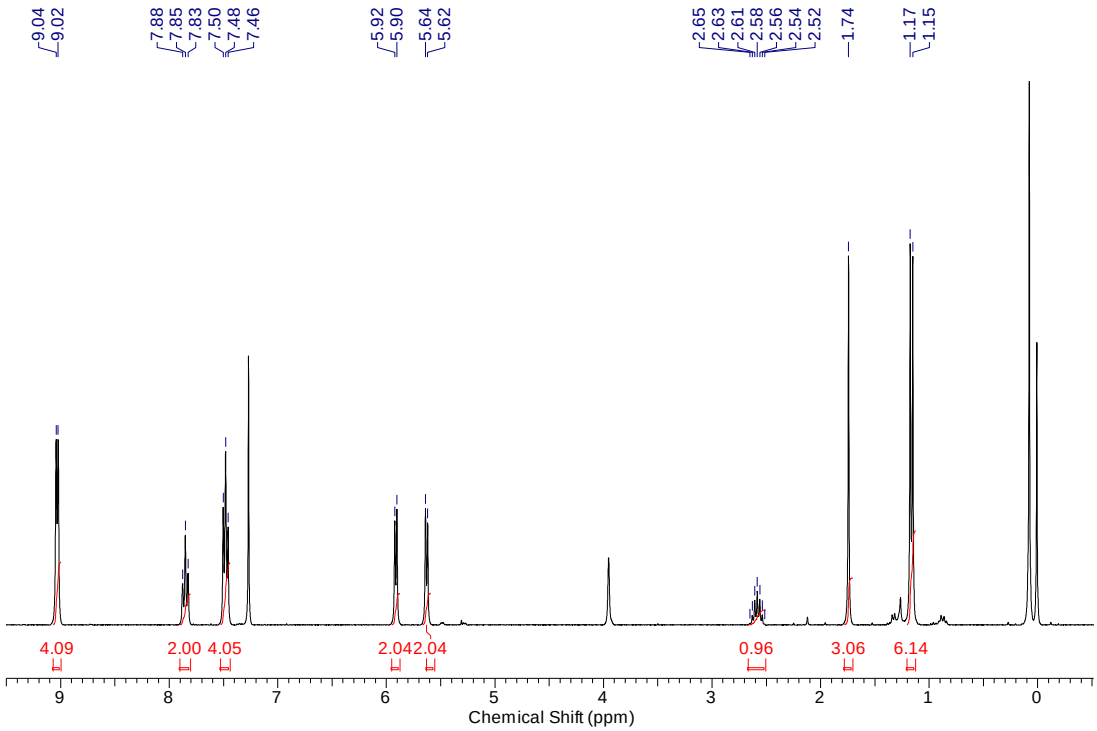

Figure 3.3.18 ^{1}H NMR spectrum of **3.14** in $CDCl_3$ at 300.13 MHz and 300.0 K

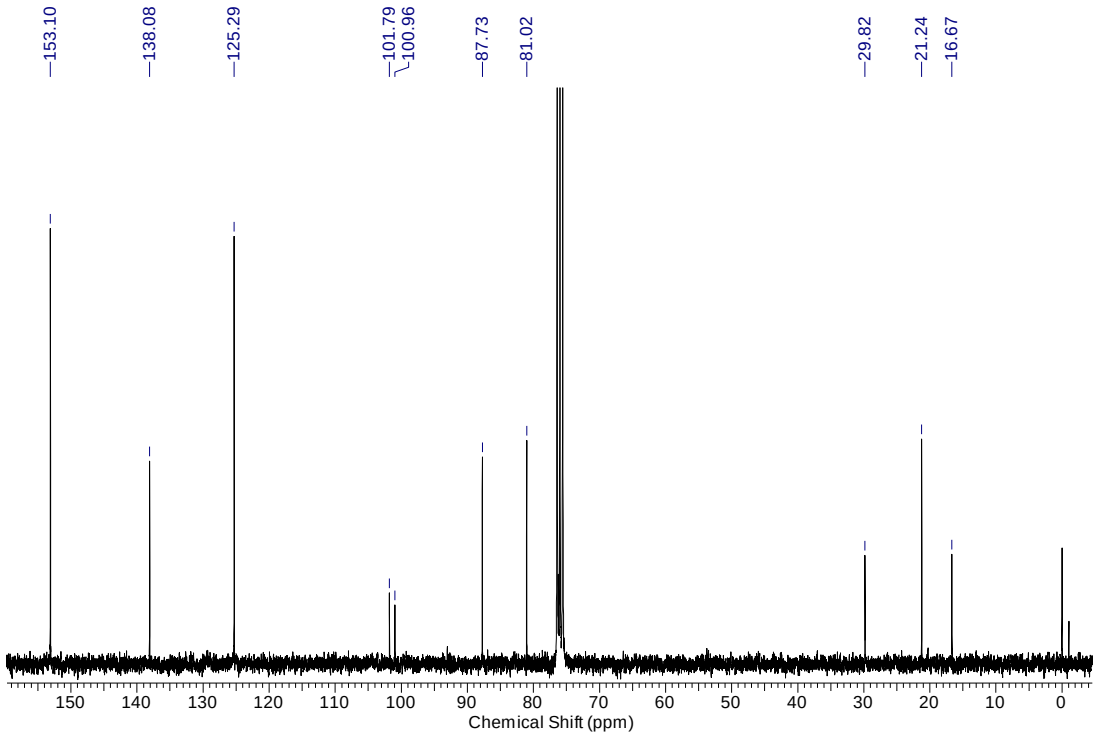

Figure 3.3.19 $^{13}C\{^{1}H\}$ NMR spectrum of **3.14** in $CDCl_3$ at 75.47 MHz and 300.1 K

^{1}H Chemical Shift, δ (ppm)	**Assignment**
9.03 (d, $^{3}J_{(H-H)}$ = 5.3 Hz, 4H)	h
7.85 (t, $^{3}J_{(H-H)}$ = 7.6 Hz, 2H)	j
7.48 (t, $^{3}J_{(H-H)}$ = 6.9 Hz, 4H)	i
5.91 (d, $^{3}J_{(H-H)}$ = 6.0 Hz, 2H)	e
5.63 (d, $^{3}J_{(H-H)}$ = 5.9 Hz, 2H)	f
2.58 (m, 1H)	b
1.74 (s, 3H)	a
1.16 (d, $^{3}J_{(H-H)}$ = 6.8 Hz, 6H)	c
^{13}C{^{1}H} Chemical Shift, δ (ppm)	**Assignment**
153.1 (CH)	h
138.1 (CH)	j
125.3 (CH)	i
101.8 (Q)	d
101.0 (Q)	g
87.7 (CH)	e
81.0 (CH)	f
29.8 (CH)	b
21.2 (CH_3)	c
16.7 (CH_3)	a

Table 3.3.9 ^{1}H and ^{13}C{^{1}H} chemical shift assignment for complex **3.14**

3.3.3.2 X-Ray Crystallographic Analysis of Compound 3.14

Yellow needles of complex **3.14** suitable for X-ray crystallography were obtained by vapour diffusion of pentane into a saturated solution of the complex in dichloromethane. Compound **3.14** crystallised in an orthorhombic cell, and structural solution was performed in the space group *Pbca*. A large residual electron density was found at the anion SbF_6, but the disorder could not be completely modelled. The structure of the cation is shown in **Figure 3.3.20**. Selected bond lengths and angles are given in **Table 3.3.10**. The distances Ru-N(1) and Ru-N(2) are 2.183(3) and 2.146(3) Å respectively, both in the range of Ru-N(pyridine) distances observed for the rest of the complexes in this project. The average Ru-$C_{(arene)}$ distance for this complex is 2.232 Å and the separation between the arene ring centroid and the ruthenium atom is 1.709 Å.

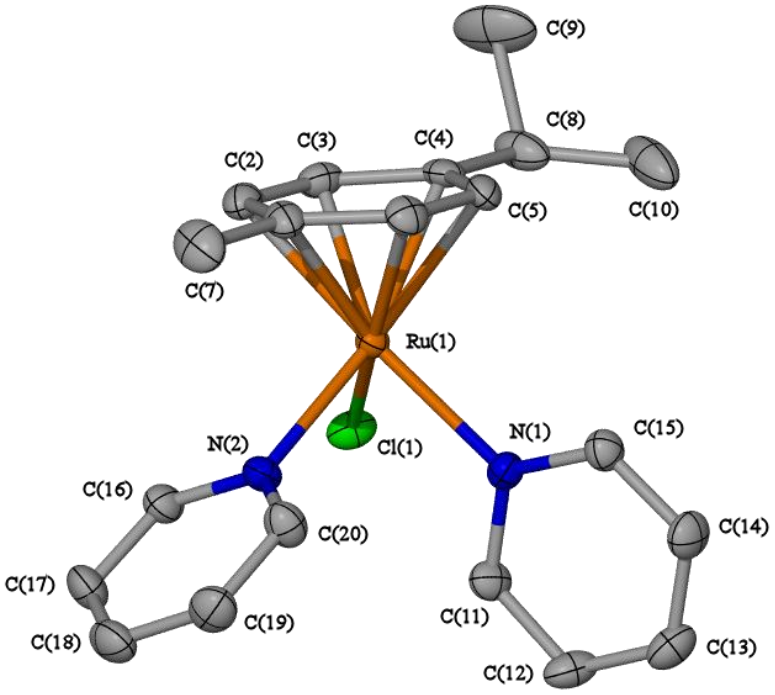

Figure 3.3.20 Structure of the cation of complex **3.14**. Displacement ellipsoids are at the 50% probability level. The counterion SbF_6 and hydrogen atoms are omitted for clarity

Bond	**Distance (Å)**	**Bond**	**Distance (Å)**
Ru(1)-N(1)	2.183(3)	C(8)-C(9)	1.558(6)
Ru(1)-N(2)	2.146(3)	C(8)-C(10)	1.551(7)
Ru(1)-Cl(1)	2.4342(9)	N(1)-C(11)	1.371(5)
C(1)-C(2)	1.444(5)	N(2)-C(16)	1.365(5)
C(1)-C(7)	1.516(5)	C(16)-C(17)	1.409(5)
C(4)-C(8)	1.537(5)	C(11)-C(12)	1.406(5)
Ru(1)-Ring	1.709	Ru(1)-$C_{(arene)}$	2.232
Bond	**Angle (°)**	**Bond**	**Angle (°)**
N(2)-Ru(1)-N(1)	82.56(11)	C(3)-Ru(1)-C(2)	37.22(14)
N(2)-Ru(1)-Cl(1)	88.02(9)	C(6)-C(1)-C(2)	118.7(3)
N(1)-Ru(1)-Cl(1)	85.81(8)	C(10)-C(8)-C(9)	111.3(4)

Table 3.3.10 Selected interatomic distances and angles for compound **3.14** with s.u.s. shown in parenthesis

The packing of complex **3.14** in the solid state shows intramolecular hydrogen bonds between C(11)-H and Cl(1) with a C...Cl distance of 3.158(4) Å, and intermolecular hydrogen bonds between C(14)-H and F(4) with a C...F distance of 3.274(5) Å, between C(16)-H and F(4) with a C...F distance of 3.234(4) Å and between C(18)-H and F(5) with a C...F distance of 3.180(10) Å.

3.4 Conclusions

A library of ten pyridine η^6-*p*-cymene ruthenium monomers and one *tert*-butylamine η^6-*p*-cymene ruthenium monomer has been prepared. These neutral complexes have been obtained in dichloromethane at room temperature, very mild conditions as opposed to reflux or ultrasound methods used and published previously for the synthesis of some of them. A charged η^6-*p*-cymene ruthenium complex with two pyridines has also been obtained. Characterisation by X-ray crystallography of some of these compounds showed similar structures; all of them seem to present the typical "half-sandwich" or "piano stool" disposition, with comparable bond lengths and angles.

The objective of these syntheses was the study of new potential homogeneous catalysts with labile monodentate ligands for hydrogen transfer reactions. An influence from the different substitutions in the pyridines on lability and activity was expected. The catalytic results will be presented in **Chapter 5**.

3.5 References

1. M. A. Bennett and A. K. Smith, *Journal of the Chemical Society, Dalton Transactions*, 1974, 233-241.
2. S. B. Jensen, S. J. Rodger and M. D. Spicer, *Journal of Organometallic Chemistry*, 1998, **556**, 151-158.
3. M. G. Mendoza-Ferri, C. G. Hartinger, A. A. Nazarov, R. E. Eichinger, M. A. Jakupec, K. Severin and B. K. Keppler, *Organometallics*, 2009, **28**, 6260-6265.
4. M. H. S. A. Hamid and J. M. J. Williams, *Chemical Communications*, 2007, 725-727.
5. X. Li, J. Blacker, I. Houson, X. Wu and J. Xiao, *Synlett*, 2006, **2006**, 1155-1160.
6. R. Noyori and S. Hashiguchi, *Accounts of Chemical Research*, 1997, **30**, 97-102.
7. K.-I. Fujita, N. Tanino and R. Yamaguchi, *Organic Letters*, 2006, **9**, 109-111.
8. Z. Almodares, *PhD Thesis*, University of Leeds, 2010.

9. T. Screen, *Personal communication*.
10. R. S. Bates, M. J. Begley and A. H. Wright, *Polyhedron*, 1990, **9**, 1113-1118.
11. R. Aronson, M. R. J. Elsegood, J. W. Steed and D. A. Tocher, *Polyhedron*, 1991, **10**, 1727-1732.
12. I. Özdemir, B. Çetinkaya, T. Seçkin and S. Köytepe, *Journal of Molecular Catalysis A: Chemical*, 2002, **179**, 263-270.
13. R. Mahe, Y. Sasaki, C. Bruneau and P. H. Dixneuf, *The Journal of Organic Chemistry*, 1989, **54**, 1518-1523.
14. T. Arthur and T. A. Stephenson, *Journal of Organometallic Chemistry*, 1981, **208**, 369-387.

Chapter 4

η^5-Pentamethylcyclopentadienyl and (5-Hydroxypentyl)-tetramethylcyclopentadienyl Ruthenium Complexes

4.1 Introduction

This chapter includes the synthesis and characterisation of η^5-pentamethylcyclopentadienyl (Cp*) and η^5-(5-hydroxypentyl)-tetramethylcyclopentadienyl ($Cp^{\#}$) ruthenium complexes (**4.3** to **4.12**), and the corresponding η^5-coordinating ligands employed for their syntheses (**4.1** and **4.2**). Compounds **4.3** and **4.4** have the general structure $[RuCl_2Cp^{*/\#}]_n$ and were synthesised as starting materials for compounds **4.5** to **4.11**, which contain diverse commercially available diphosphines as ligands and have the general structure [RuClCp*/#(PP)]. The PP ligands used were 1,1'-bis(diphenylphosphino)methane (dppm), 1,1'-bis(diphenylphosphino)ferrocene (dppf), bis(2-diphenylphosphinophenyl)ether (DPEphos) and 4,5-bis(diphenylphosphino)-9,9-dimethylxanthene (Xantphos) (**Figure 4.1.1**). Complex **4.12** was synthesised from compound **4.5** by reaction with $NaSbF_6$ and acetonitrile in methanol. Two tetramethylfulvene ruthenium(II) complexes (**4.13** and **4.14**) were obtained from reactions of **4.3** with diphenylacac. All of the species discussed in this chapter are shown in **Figure 4.1.2**.

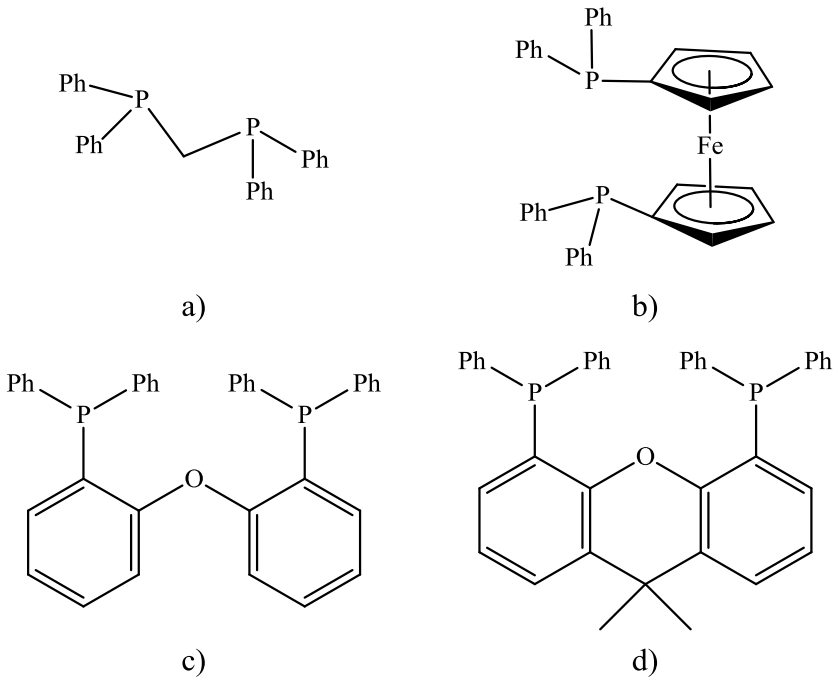

Figure 4.1.1 Diphosphine ligands used for the synthesis of complexes **4.5** to **4.11**. a) dppm, b) dppf, c) DPEphos, d) Xantphos

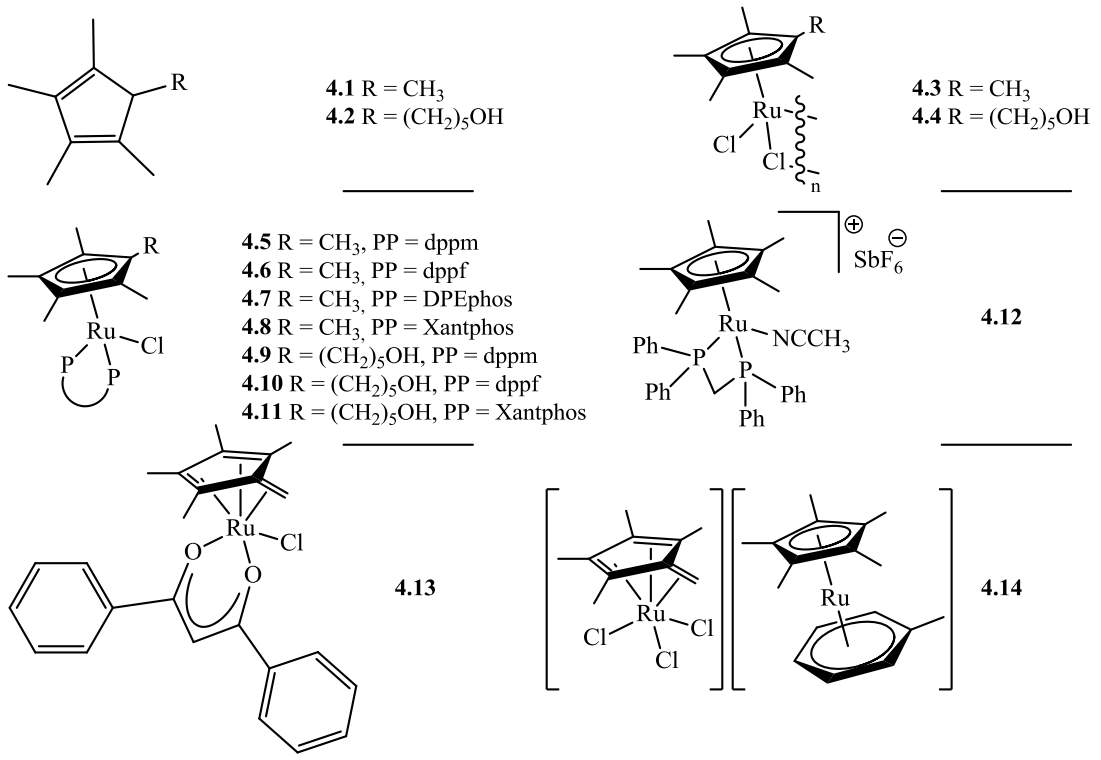

Figure 4.1.2 General structures of the complexes discussed in Chapter 4

Compounds **4.4**, **4.7** and **4.9** to **4.14** are all novel. This includes all of the η^5-(5-hydroxypentyl)-tetramethylcyclopentadienyl ($Cp^{\#}$) ruthenium complexes. The rest of the compounds have been previously synthesised with different methods and details will be given throughout the chapter.

After demonstrating the instability of the functionalised η^6-arene ruthenium complexes in **Chapter 2**, the search for new heterogeneous catalysts continued with the syntheses of complexes with η^5-coordinating ligands, which are expected to present higher coordination stabilities. The $Cp^{\#}$ complexes, with a $(CH_2)_5OH$ pendant chain, could offer good possibilities for flexible immobilisation by covalent reaction of the –OH group, while the equivalent Cp* complexes were synthesised, in principle, for homogeneous activity comparison.

4.2 Pentamethylcyclopentadiene and (5-Hydroxypentyl)-Tetramethylcyclopentadiene Ligands

The general synthesis of ligands **4.1** and **4.2** consisted of a lithiation of 2-bromo-2-butene and then reaction of the product with an ester (ethyl acetate for **4.1**) or lactone (caprolactone for **4.2**) whose number of carbons (excluding the carboxylic

one and the OCH_2CH_3 fragment in ethyl acetate, which acts as a leaving group) determined the length of the resulting pendant chain. The last step was performed in acidic media to yield the cyclisation, facilitated by the good leaving $–OH_2^+$ group. A general mechanism is shown in **Scheme 4.2.1**.

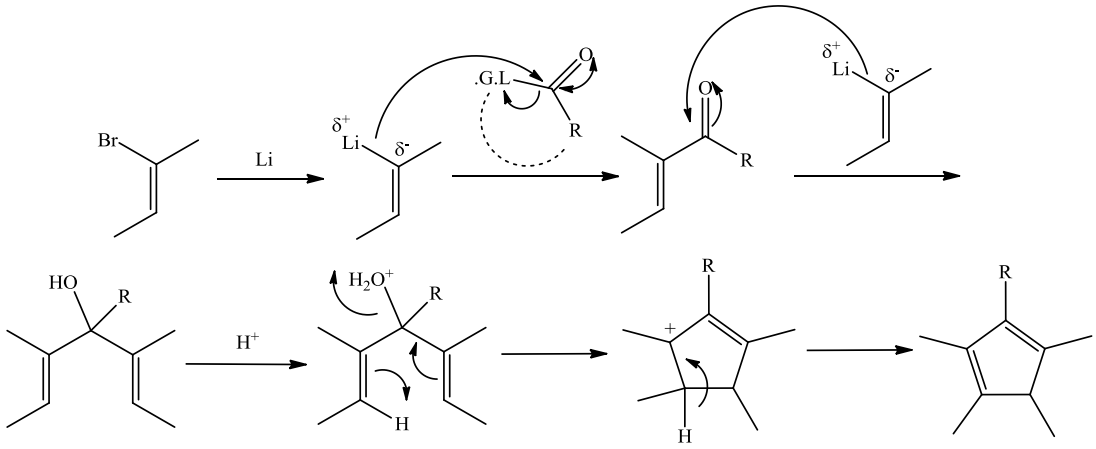

Scheme 4.2.1 General mechanism for the formation of the η^5 ligands

Both **4.1** and **4.2** were obtained as yellow oils in 58 and 55% yields respectively. To prevent Diels-Alder reactions, these ligands were kept in the freezer at -20ºC approx. The assignment of **4.2** was made considering just one of the three isomers that can be observed in the NMR spectrum (**Figure 4.2.1**). When these ligands are η^5-coordinated to a metal centre, they form $C_5(CH_3)_5$ or $C_5(CH_3)_4(CH_2)_5OH$, and these species are abbreviated as Cp* and $Cp^{\#}$ respectively.

Ligand **4.1** had been previously synthesised by Bergman *et al.*[1] and ligand **4.2** had been reported by Blacker and co-workers.[2] Both of the ligands have been used extensively as coordinating ligands to rhodium(III) or iridium(III), for instance, in the formation of the SCRAM transfer hydrogenation catalyst $[IrI_2Cp^*]_2$, and its functionalised derivative $[IrI_2Cp^{\#}]_2$, which has been attached to poly(ethyleneglycol).[2] The use of Cp* with ruthenium is less common, mainly due to more complicated synthetic processes, but some examples are presented within this chapter. The coordination of $Cp^{\#}$ to ruthenium had not been reported so far.

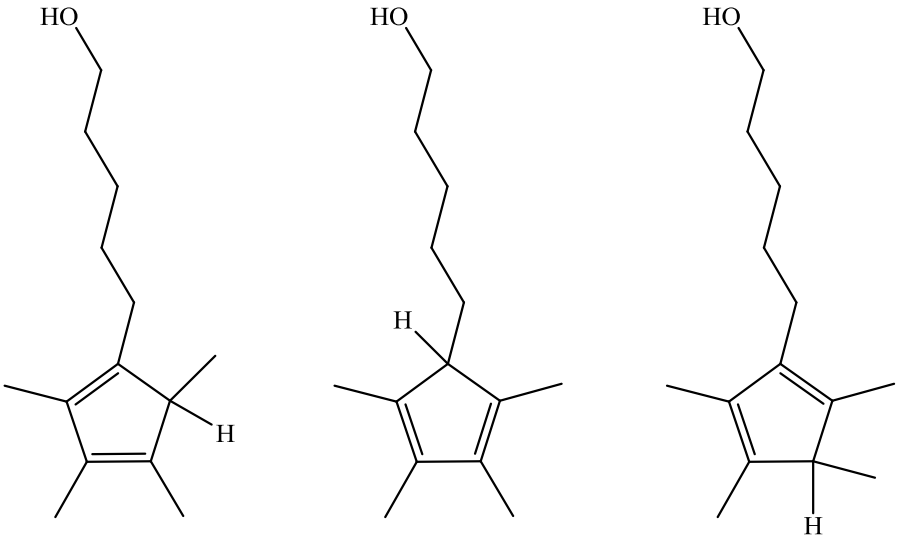

Figure 4.2.1 Three regioisomers of compound **4.2**

4.3 Cp* and Cp$^{\#}$ Ruthenium(III) Oligomers

4.3.1 Synthesis of $[RuCl_2Cp^{*/\#}]_n$ (4.3 and 4.4)

The reaction of ligands **4.1** or **4.2** with $RuCl_3 \cdot 3H_2O$ produced air sensitive Cp* or Cp$^{\#}$ Ru(III) complexes (**4.3** and **4.4**), with the general structure $[RuCl_2Cp^{*/\#}]_n$ (**Scheme 4.3.1**). They were obtained as dark red or orange solids in 74 and 48% yields respectively, and kept in the glove box. According to Suzuki and co-workers, the reaction could proceed in boiling methanol, ethanol or isopropanol, but whereas the product from the reaction in ethanol is soluble in dichloromethane and chloroform, those from the reactions in methanol or isopropanol are almost insoluble in such solvents, indicating higher molecular weights, *i.e.* longer oligomers.[3] Thus, ethanol was the solvent used in the present work. Koelle and Kossakowski also published that structures of this type of compounds in the solid state are formed by dimers.[4] Complex **4.3** had been previously synthesised by Suzuki[3] and Bercaw.[5]

Both compounds **4.3** and **4.4** are paramagnetic because the ruthenium centre is in the oxidation state +3, containing one unpaired electron. This is reflected in their ^{1}H NMR spectra, which present very broad peaks and unusual chemical shifts for the methyl groups. For **4.3**, the ^{1}H NMR spectrum consists of only one broad singlet at 4.67 ppm.

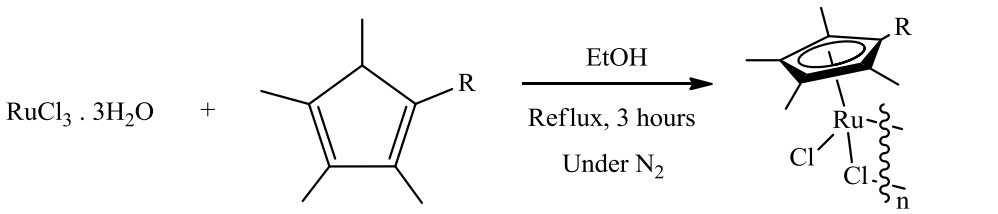

4.1 or **4.2**

4.3 R = CH_3 (74%)
4.4 R = $(CH_2)_5OH$ (48%)

Scheme 4.3.1 General scheme for the synthesis of the complexes $[RuCl_2Cp^{*/\#}]_n$

4.3.1.1 NMR Data for Compound 4.4

Figure 4.3.1 shows a labelled diagram of complex **4.4**. The ^1H and $^{13}C\{^1H\}$ NMR spectra for this compound are given in **Figure 4.3.2** and **Figure 4.3.3** respectively. **Table 4.3.1** summarises the chemical shift assignment for this complex.

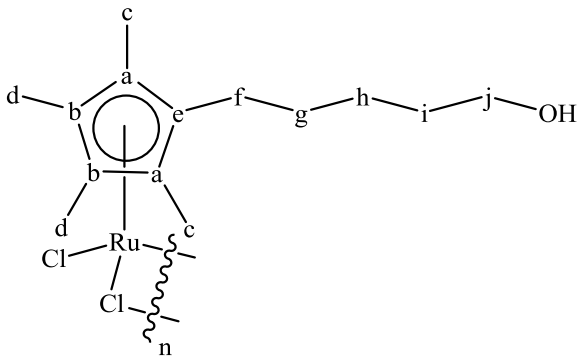

Figure 4.3.1 Labelled diagram of complex **4.4**

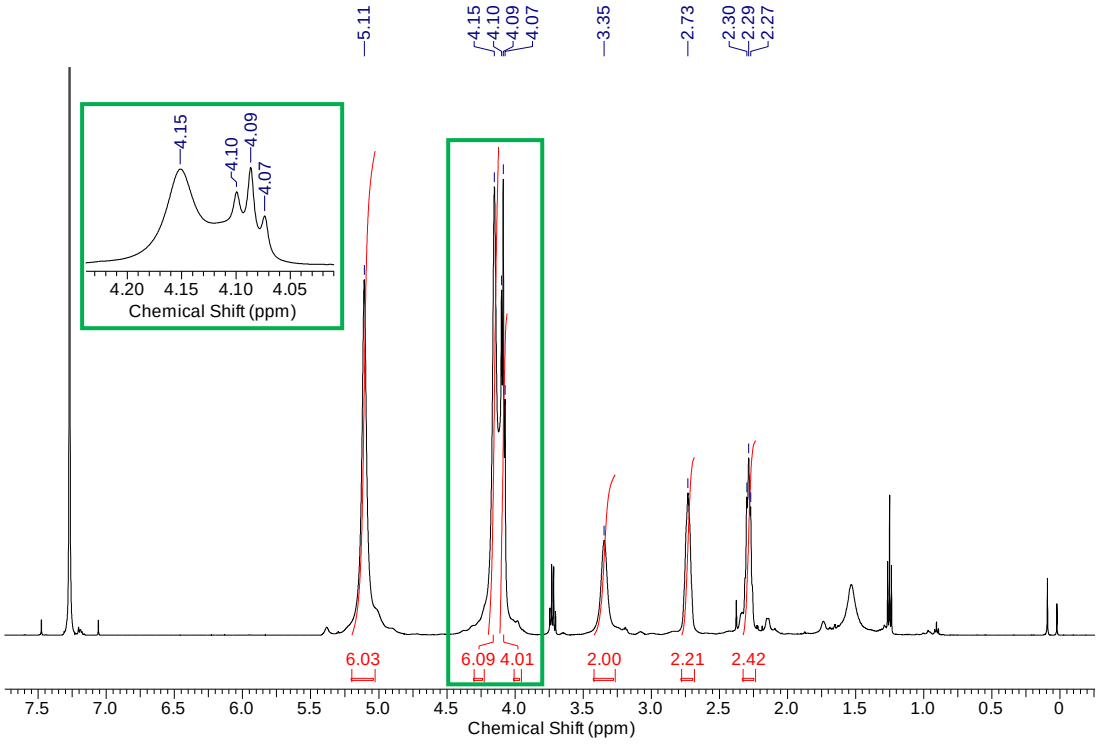

Figure 4.3.2 ^{1}H NMR spectrum of **4.4** in $CDCl_3$ at 500.57 MHz and 300.0 K

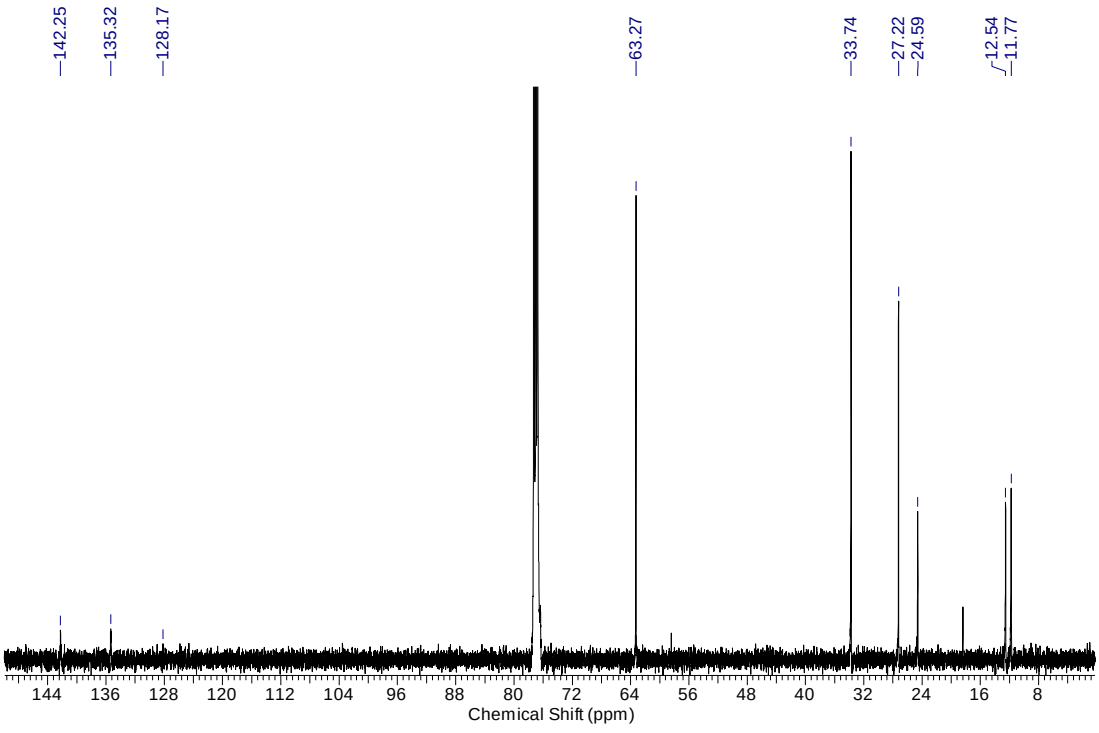

Figure 4.3.3 $^{13}C\{^{1}H\}$ NMR spectrum of **4.4** in $CDCl_3$ at 125.77 MHz and 299.2 K

^{1}H Chemical Shift, δ (ppm)	Assignment
5.11 (br. s, 6H)	c or d
4.15 (br. s, 6H)	c or d
4.09 (m, 4H)	f & j
3.35 (br. s, 2H)	i
2.73 (br. s, 2H)	h
2.29 (m, 2H)	g
^{13}C{^{1}H} Chemical Shift, δ (ppm)	**Assignment**
142.3 (Q)	a or b
135.3 (Q)	a or b
128.2 (Q)	e
63.3 (CH_2)	j
33.7 (CH_2)	f & g
27.2 (CH_2)	h
24.6 (CH_2)	i
12.5 (CH_3)	c or d
11.8 (CH_3)	c or d

Table 4.3.1 ^{1}H and ^{13}C{^{1}H} chemical shift assignment for complex **4.4**

4.4 Cp* and Cp$^{\#}$ Diphosphine Ruthenium(II) Monomers

4.4.1 Synthesis of [RuClCp*$^{/\#}$(PP)] (4.5-4.11)

The unstable and paramagnetic ruthenium(III) complexes **4.3** and **4.4** were easily reduced to air stable diamagnetic ruthenium(II) compounds (**4.5** to **4.11**) by reaction with commercially available diphosphines. The diphosphines used include 1,1'-bis(diphenylphosphino)methane (dppm), 1,1'-bis(diphenylphosphino)ferrocene (dppf), bis(2-diphenylphosphinophenyl)ether (DPEphos) and 4,5-bis(diphenylphosphino)-9,9-dimethylxanthene (Xantphos) (**Figure 4.1.1**), which were chosen as the most promising by one of the project's industrial partners after some screening of conditions for redox neutral alkylations with Ru(*p*-cymene) complexes. The reaction between the phosphine and $[RuCl_2Cp^{*/\#}]_n$ is a redox reaction where ruthenium is reduced and the diphosphine is believed to act as both ligand and, at the same time, reducing agent (**Scheme 4.4.1**). Thus, to facilitate this, 1.5 equivalents of the diphosphine were used for 1 equivalent of Ru. This resulted in better yields than stoichiometric 1 : 1 mixtures. The complexes **4.5** to **4.11** were obtained as either yellow or orange solids in yields ranging from 19 to 86%.

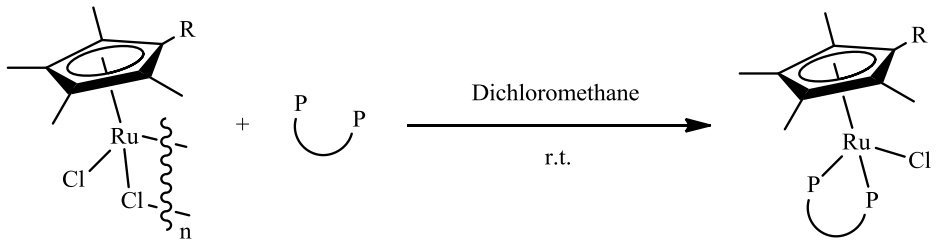

4.3 or **4.4**

4.5 R = CH_3, PP = dppm (71%)
4.6 R = CH_3, PP = dppf (21%)
4.7 R = CH_3, PP = DPEphos (26%)
4.8 R = CH_3, PP = Xantphos (49%)
4.9 R = $(CH_2)_5OH$, PP = dppm (33%)
4.10 R = $(CH_2)_5OH$, PP = dppf (86%)
4.11 R = $(CH_2)_5OH$, PP = Xantphos (19%)

Scheme 4.4.1 General scheme for the synthesis of the complexes [RuClCp*/#(PP)]

All of the [RuClCp#(PP)] complexes (**4.9** to **4.11**), *i.e.* those with the $C_5(CH_3)_4(CH_2)_5OH$ ligand, are novel to the best of the knowledge of the author. Among the [RuClCp*(PP)] complexes, **4.7** is novel. Compound **4.5** had been previously synthesised by White,[6] Kollipara[7] and Heinekey[8] from $[RuCp^*(PPh_3)_2Cl]$, by Girolami[9] from $[RuCp^*Cl]_4$, by Nolan[10] from [RuCp*(cod)Cl] and by Koelle[4] and co-workers from $[Ru_2Cp^*_2(\mu\text{-}Cl)_3]$, and characterised by X-ray crystallography by White *et al.*[6] Compound **4.6** had been prepared by Day,[11] Asai[12] and Moret[13] from either $[RuCp^*(PPh_3)_2Cl]$, $[RuCp^*(PMe_3)_2Cl]$ or $[RuCp^*Cl_2]_n$/Zn. Complex **4.8** was reported by Nozaki *et al.*[14] These types of compounds were employed mainly as starting materials to other complexes and in redox/electrochemical studies.[11, 13] The simple and straightforward synthetic method presented in this chapter had not been used before, which involved reactions at room temperature in dichloromethane under inert atmosphere.

4.4.1.1 NMR Data for Compound 4.9

A labelled diagram of compound **4.9** is given in **Figure 4.4.1**. ^1H and $^{13}C\{^1H\}$ NMR spectra are presented in **Figure 4.4.2** and **Figure 4.4.3** respectively. The most characteristic feature in the ^1H NMR spectrum is the appearance of two doublets of triplets for the CH_2 in dppm, due to the two protons having different environments and the coupling to the two phosphorus atoms, which is also observed in some peaks of the $^{13}C\{^1H\}$ NMR. The chemical shifts assignment is given in **Table 4.4.1**.

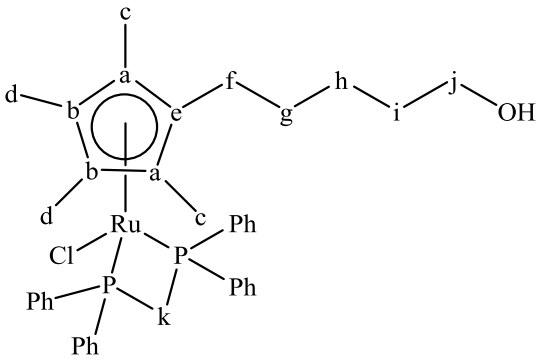

Figure 4.4.1 Labelled diagram of complex **4.9**

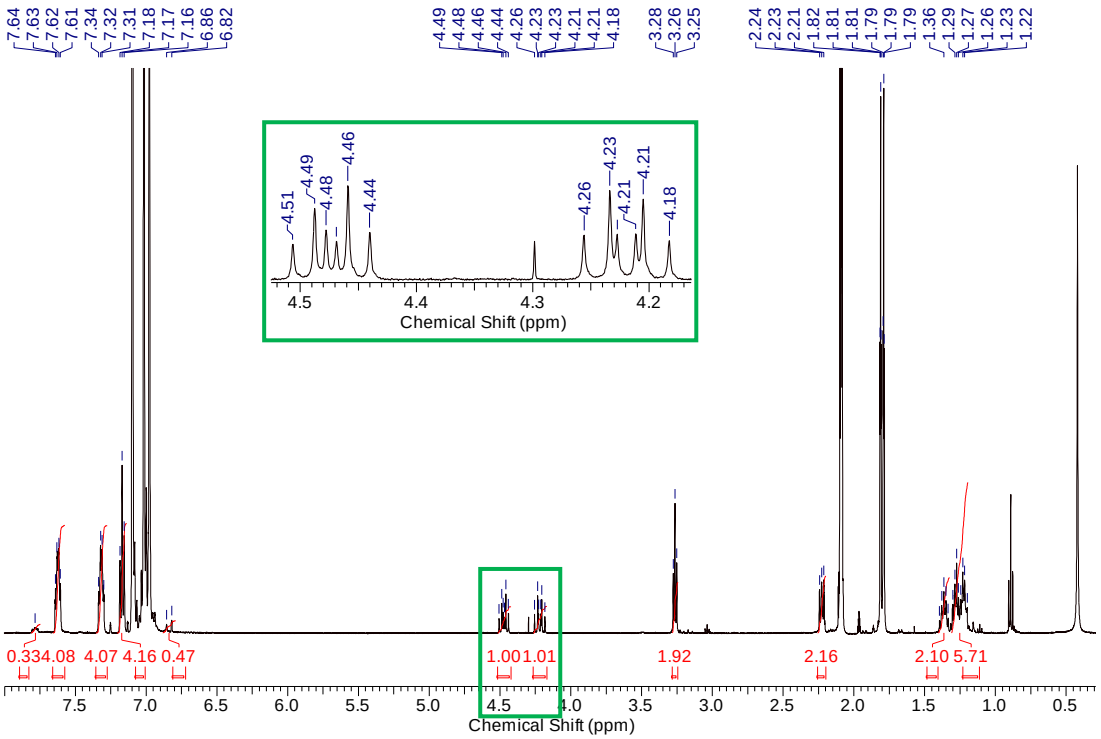

Figure 4.4.2 ^{1}H NMR spectrum of **4.9** in toluene-d_8 at 500.57 MHz and 300.0 K

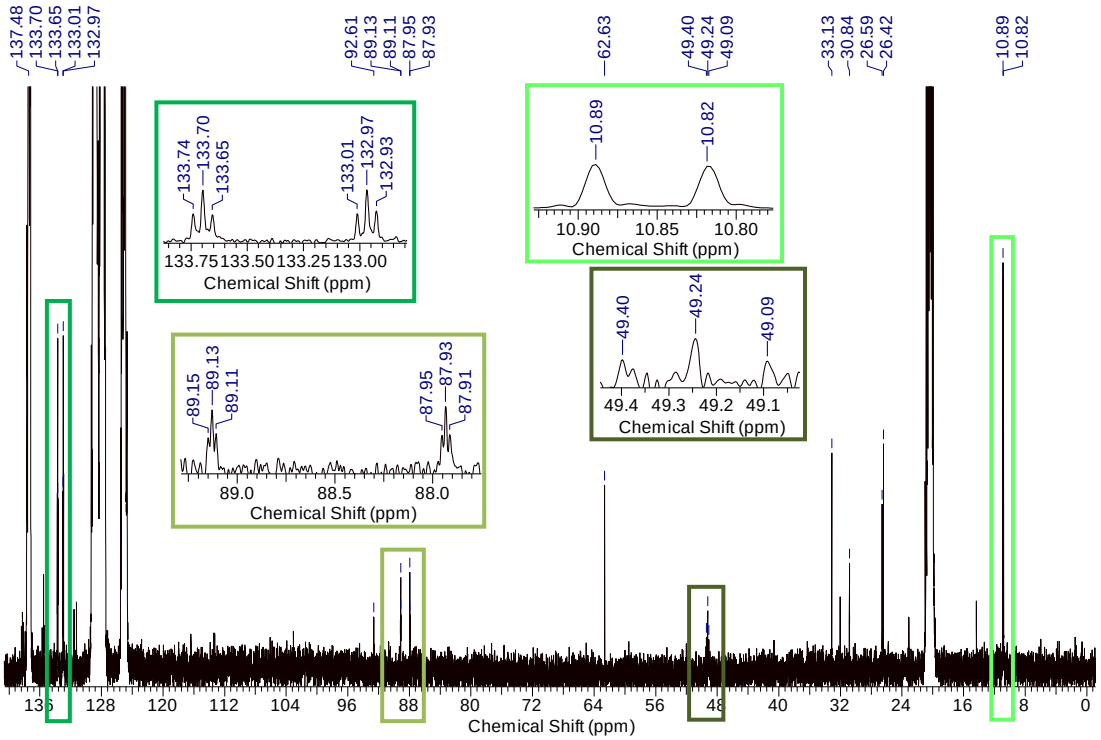

Figure 4.4.3 $^{13}C\{^{1}H\}$ NMR spectrum of **4.9** in toluene-d_8 at 125.77 MHz and 299.2 K

^{1}H Chemical Shift, δ (ppm)	**Assignment**
7.64-6.82 (20H)	Aromatics
4.47 (dt, $^{2}J_{(H-H)}$ = 14.5 Hz, $^{2}J_{(H-P)}$ = 9.4 Hz, 1H)	k
4.22 (dt, $^{2}J_{(H-H)}$ = 14.2 Hz, $^{2}J_{(H-P)}$ = 11.3 Hz, 1H)	k
3.26 (t, $^{3}J_{(H-H)}$ = 6.2 Hz, 2H)	j
2.23 (m, 2H)	f, g, h or i
1.81 (t, $^{4}J_{(H-P)}$ = 1.9 Hz, 6H)	c or d
1.79 (t, $^{4}J_{(H-P)}$ = 2.0 Hz, 6H)	c or d
1.36 (quint, $^{3}J_{(H-H)}$ = 7.6 Hz, 2H)	f, g, h or i
1.25 (m, 4H)	f, g, h or i
^{13}C{^{1}H} Chemical Shift, δ (ppm)	**Assignment**
137.5 (s, Q)	Aromatics
133.7 (t, $^{2,3}J_{(C-P)}$ = 5.4 Hz, CH)	Aromatics
133.0 (t, $^{2,3}J_{(C-P)}$ = 5.4 Hz, CH)	Aromatics
92.6 (m, Q)	a, b or e
89.1 (t, $^{2}J_{(C-P)}$ = 2.6 Hz, Q)	a, b or e
87.9 (t, $^{2}J_{(C-P)}$ = 2.6 Hz, Q)	a, b or e
62.6 (s, CH_2)	j
49.2 (t, $^{1}J_{(C-P)}$ = 19.2 Hz, CH_2)	k
33.1 (s, CH_2)	f, g, h or i
30.8 (s, CH_2)	f, g, h or i
26.6 (s, CH_2)	f, g, h or i
26.4 (s, CH_2)	f, g, h or i
10.9 (s, CH_3)	c or d
10.8 (s, CH_3)	c or d

Table 4.4.1 ^{1}H and ^{13}C{^{1}H} chemical shift assignment for complex **4.9**

4.4.2 Synthesis of [Ru(CH$_3$CN)(C$_{10}$H$_{15}$)(C$_{25}$H$_{22}$P$_2$)][SbF$_6$] (4.12)

Compound **4.12** was prepared from complex **4.5**, acetonitrile and $NaSbF_6$ in methanol at room temperature (**Scheme 4.4.2**). The bright yellow solid, which is air stable, was obtained in 77% yield.

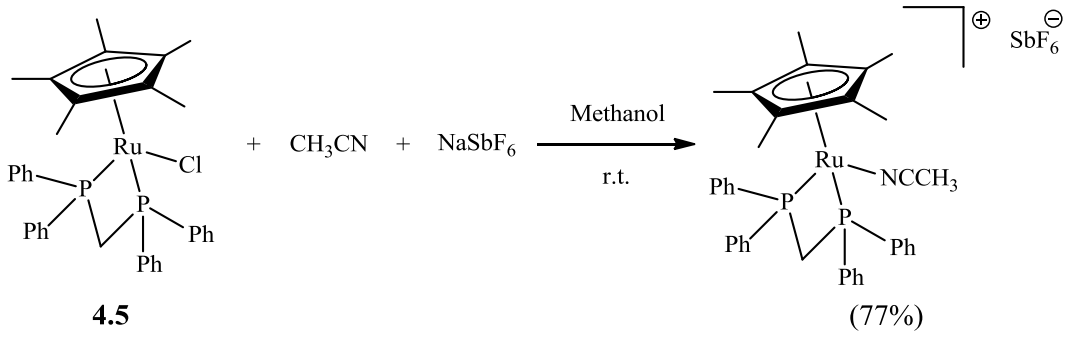

4.5 (77%)

Scheme 4.4.2 Synthesis of complex **4.12** [Ru(CH$_3$CN)(C$_{10}$H$_{15}$)(C$_{25}$H$_{22}$P$_2$)][SbF$_6$]

Similar complexes with different diphosphine ligands have been previously synthesised by Moret *et al*., using NH_4PF_6 instead of $NaSbF_6$.[13] Sato and Asai also published the synthesis of $[RuCp^*(CH_3CN)(dppf)][BF_4]$.[12]

4.4.2.1 NMR Data for Compound 4.12

A labelled diagram of compound **4.12** is given in **Figure 4.4.4**. The ^1H and $^{13}C\{^1H\}$ NMR spectra are shown in **Figure 4.4.5** and **Figure 4.4.6** respectively. The complete assignment is given in **Table 4.4.2**.

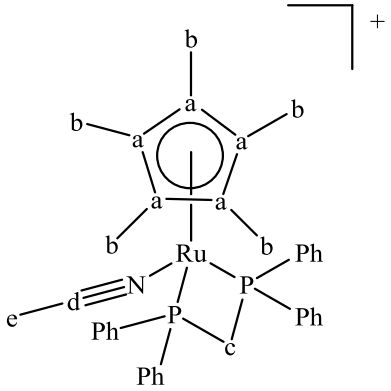

Figure 4.4.4 Labelled diagram of complex **4.12**

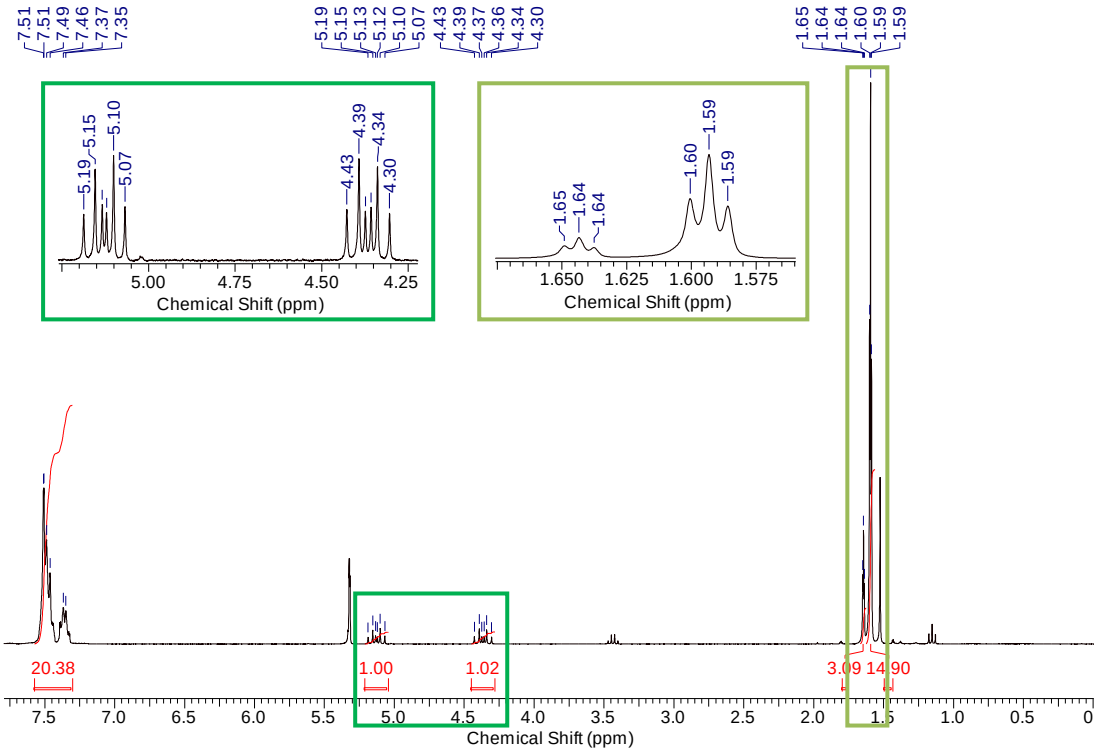

Figure 4.4.5 ^1H NMR spectrum of **4.12** in CD_2Cl_2 at 300.13 MHz and 300.0 K

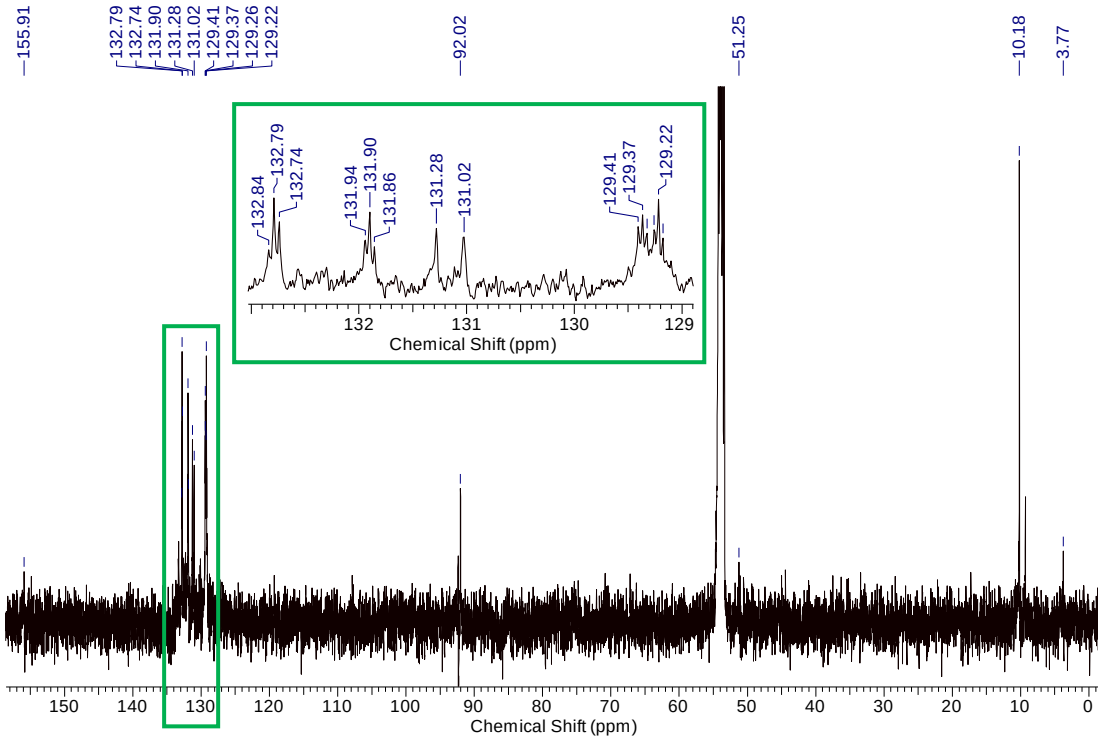

Figure 4.4.6 $^{13}C\{^{1}H\}$ NMR spectrum of **4.12** in CD_2Cl_2 at 125.88 MHz and 300.0 K

^{1}H Chemical Shift, δ (ppm)	**Assignment**
7.49 (m, 16H)	Aromatics
7.36 (m, 4H)	Aromatics
5.13 (dt, $^{2}J_{(H-H)}$ = 16 Hz, $^{2}J_{(H-P)}$ = 9.8 Hz, 1H)	c
4.37 (dt, $^{2}J_{(H-H)}$ = 16 Hz, $^{2}J_{(H-P)}$ = 10.5 Hz, 1H)	c
1.64 (t, $^{5}J_{(H-P)}$ = 1.7 Hz, 3H)	e
1.59 (t, $^{4}J_{(H-P)}$ = 2.2 Hz, 15H)	b
$^{13}C\{^{1}H\}$ Chemical Shift, δ (ppm)	**Assignment**
155.9 (s, Q)	d
132.8 (m, CH)	Aromatics
131.9 (t, $^{2,3}J_{(C-P)}$ = 5.2 Hz, CH)	Aromatics
131.2 (d, $^{1}J_{(C-P)}$ = 32.7 Hz, Q)	Aromatics
129.3 (dt, $^{2,3}J_{(C-P)}$ = 18.7, 5.2 Hz, CH)	Aromatics
92.0 (s, Q)	a
51.3 (s, CH_2)	c
10.2 (s, CH_3)	b
3.8 (s, CH_3)	e

Table 4.4.2 ^{1}H and $^{13}C\{^{1}H\}$ chemical shift assignment for complex **4.12**

4.4.2.2 X-Ray Crystallographic Analysis of Compound 4.12

Yellow crystalline prisms of compound **4.12** suitable for X-ray crystallography were obtained by vapour diffusion of pentane into a saturated solution of the complex in chloroform. This compound crystallised in a triclinic cell, and structural solution was performed in the space group $P\bar{1}$. The asymmetric unit comprises one molecule of compound **4.12**, including the counterion SbF_6. The molecular structure is shown in **Figure 4.4.7** and selected bond lengths and angles are given in **Table 4.4.3**.

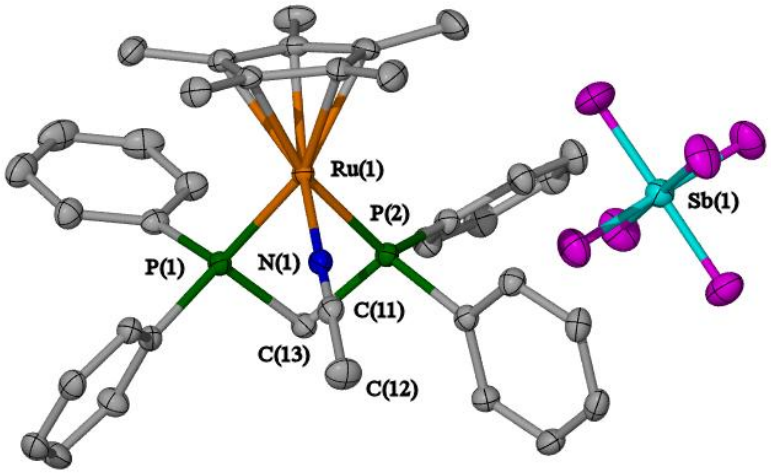

Figure 4.4.7 Molecular structure of complex **4.12**. Displacement ellipsoids are at the 50% probability level. Hydrogen atoms are omitted for clarity

Bond	**Distance (Å)**	**Bond**	**Distance (Å)**
Ru(1)-N(1)	2.0775(16)	P(2)-C(13)	1.8719(19)
Ru(1)-P(1)	2.3201(6)	N(1)-C(11)	1.153(2)
Ru(1)-P(2)	2.3503(6)	C(11)-C(12)	1.481(3)
P(1)-C(13)	1.8792(18)	Sb(1)-F(1)	1.9047(12)
Ru(1)-Ring	1.884	Ru(1)-$C_{(Cp^*)}$	2.25226
Bond	**Angle (°)**	**Bond**	**Angle (°)**
P(1)-Ru(1)-P(2)	71.626(19)	N(1)-Ru(1)-P(1)	90.22(5)
N(1)-C(11)-C(12)	178.5(2)	N(1)-Ru(1)-P(2)	87.10(4)
C(11)-N(1)-Ru(1)	178.90(16)	P(2)-C(13)-P(1)	93.53(8)

Table 4.4.3 Selected interatomic distances and angles for compound **4.12** with s.u.s. shown in parenthesis

The distance between the ruthenium centre and the η^5-ring centroid is 1.884 Å, which is longer than the usual distance between a ruthenium atom and the centre of an η^6-arene ligand coordinated to it (values ranging from 1.662 to 1.709 Å in **Chapter 2** and **Chapter 3**). However, the average length between the ruthenium atom and the carbon atoms in the Cp* ring, 2.2523 Å, is comparable to the results for η^6-arene complexes. If the structure of **4.12** (charged, with acetonitrile and dppm) is compared to that of **4.5** (neutral, with chloride and dppm), which was published by White *et al.*,[6] there is a very small variation in the distances between the ruthenium centre and the phosphorus atoms, with those in **4.5** being approximately 2.29 Å. The angle formed by the two phosphorus atoms and the carbon in between them in dppm is 93.53(8)º in the structure of **4.12** and 92.7(3)º in **4.5**, which are approximately equal values within a confidence interval. When packed, compound **4.12** does not show any π-π stacking interaction of the aromatic rings, but there is non-classical hydrogen bonding between C(9)-H and F(6) from the counterion, with a C...F distance of 3.198 Å (**Figure 4.4.8**).

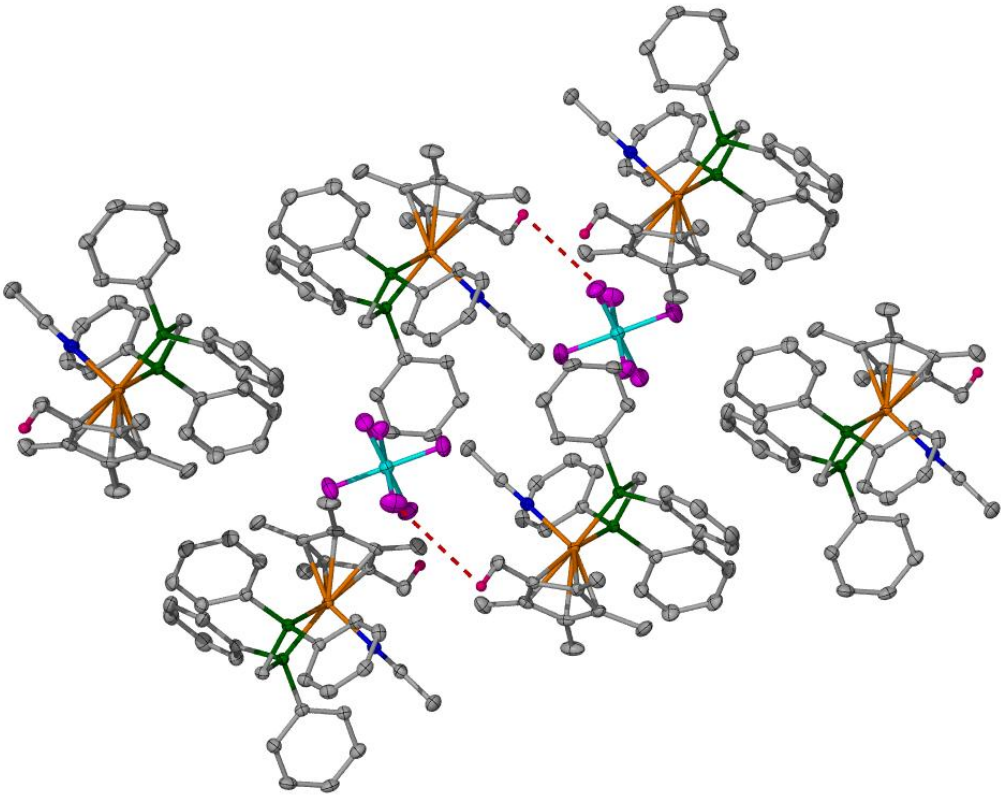

Figure 4.4.8 Compound **4.12** viewed along the a axis showing hydrogen bonding interactions (3.198 Å). Only the hydrogen atoms involved in these interactions are shown.

4.5 Tetramethylfulvene Ruthenium(II) Complexes

4.5.1 Introduction

Koelle and co-workers have reported the synthesis of Cp*Ru(acac) complexes (acac = $CH_3COCHCOCH_3$) by two different methods. In the first, the mixture of $[RuCp^*Cl_2]_2$ with 2 equivalents of acacH and triethylamine in dichloromethane produced the monomer $[RuCp^*Cl(acac)]$[4] (a in **Figure 4.5.1**), and in the second, the reaction of $[RuCp^*Cl_2]_2$ with 2 equivalents of acacH and K_2CO_3 in 2-propanol resulted in the formation of the dimeric species $[RuCp^*(acac)]_2$[15] (b in **Figure 4.5.1**). During this project, some attempts to synthesise similar Cp* ruthenium complexes to those aforementioned but with a diphenylacac ligand (PhCOCHCOPh) instead gave, unexpectedly, very different structures, which correspond to tetramethylfulvene complexes of ruthenium.

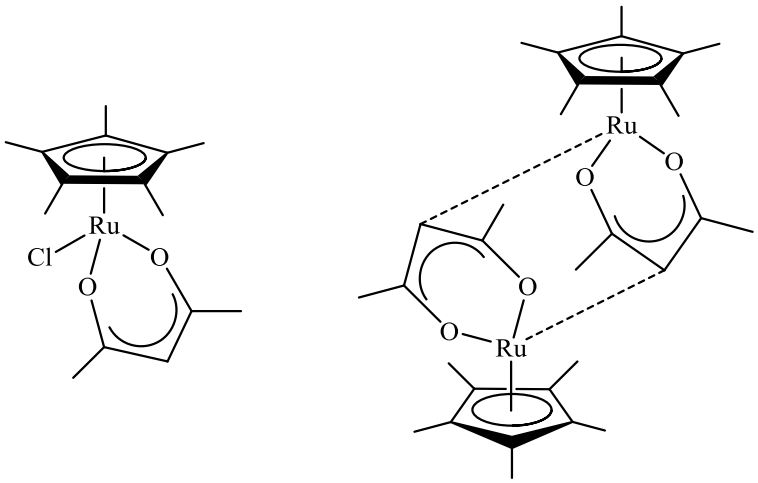

a) b)

Figure 4.5.1 RuCp*(acac) complexes synthesised by Koelle *et al*.[4, 15]

The tetramethylfulvene ligand is obtained by abstraction of one of the methyl hydrogens in the pentamethylcyclopentadienyl (Cp*) group, which normally occurs under the influence of strong bases or thermally. It is generally considered to bind in an η^2,η^4-fashion to metals (a in **Figure 4.5.2**), but some groups have described it as a methylenetetramethylcyclopentadienyl ligand instead, and considered an η^1,η^5-coordination (b in **Figure 4.5.2**).[16, 17]

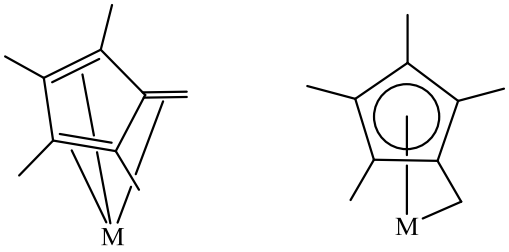

a) b)

Figure 4.5.2 a) Tetramethylfulvene and b) methylenetetramethylcyclopentadienyl ligands

The two modes of coordination can be distinguished mainly by three features:

- Bond length distribution inside the C_5 ring. In η^1,η^5-ligands, the bonds are all equal, whereas in η^2,η^4-ligands it is normally possible to differentiate between the single and the double bonds.[18]
- In the crystal structures of those complexes with η^2,η^4-ligands, the metal does not lie in the centre of the C_5 ring. There is a displacement of the metal centre towards the *exo* double bond.[19]
- The sp^2 character of the carbons in the *exo* double bond of η^2,η^4-tetramethylfulvene complexes *vs*. the sp^3 character of the methylene carbon in η^1,η^5-methylenetetramethylcyclopentadienyl complexes. This can be determined from NMR spectroscopy analyses.[20, 21]

There are several examples of fulvene complexes with ruthenium reported in the literature, such as the dimer $[RuCl_2(\eta^6\text{-}C_5Me_4CH_2)]_2$, which is obtained by oxidation of $[RuCp^*Cl_2]_2$ with O_2 followed by dehydration.[22-24] Complex $[RuCl(\eta^2\text{-}{}^tBuNSPh)(\eta^6\text{-}C_5Me_4CH_2)]$ can also be prepared from $[RuCp^*Cl_2]_2$ when Li(^{t}BuNSPh) is added at -78ºC.[25] Other examples also involve molecular oxygen or strong bases.[26, 27]

Fulvene complexes are more common with other metals, principally early transition metals[28-30] and lanthanides,[31] and they are most commonly obtained by thermolysis or photolysis. There are also some examples with rhenium, such as the complex $[Re(CO)_2(\eta^6\text{-}C_5Me_4CH_2)(C_6F_5)]$[32] or with iridium, like $[Ir(dppe)Me(\eta^6\text{-}C_5Me_4CH_2)]$[33] (dppe = 1,1'-bis(diphenylphosphino)ethane).

The reactions of complex **4.3** with diphenylacac and triethylamine in either dichloromethane at room temperature or toluene at reflux gave the novel complexes **4.13** and **4.14** respectively. Both have been identified as η^2,η^4-tetramethylfulvene complexes by NMR spectroscopy and X-ray crystallography analyses.

4.5.2 Synthesis of [RuCl($C_{10}H_{14}$)($C_{15}H_{11}O_2$)] (4.13)

Compound **4.13** was synthesised as a brown solid in 44% yield from complex **4.3** with one equivalent of diphenylacac and two equivalents of triethylamine, by stirring in dry dichloromethane at room temperature overnight (**Scheme 4.5.1**).

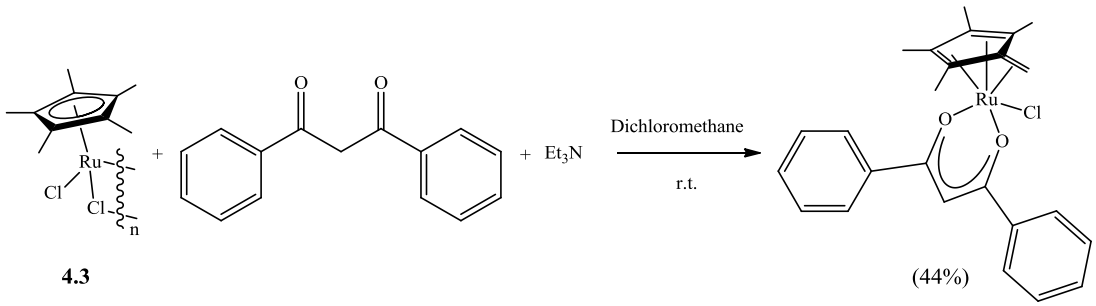

Scheme 4.5.1 Synthesis of complex **4.13** [RuCl($C_{10}H_{14}$)($C_{15}H_{11}O_2$)]

4.5.2.1 NMR Data for Compound 4.13

A labelled diagram of complex **4.13** is given in **Figure 4.5.3** and the ^{1}H, ^{13}C{^{1}H} and ^{1}J ^{1}H-^{13}C{^{1}H} HMQC NMR spectra for this complex are shown in **Figure 4.5.4**, **Figure 4.5.5** and **Figure 4.5.6** respectively. The chemical shift assignment is summarised in **Table 4.5.1**.

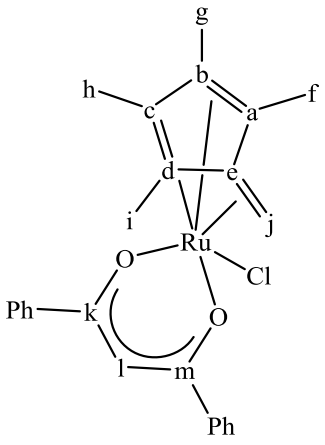

Figure 4.5.3 Labelled diagram of complex **4.13**

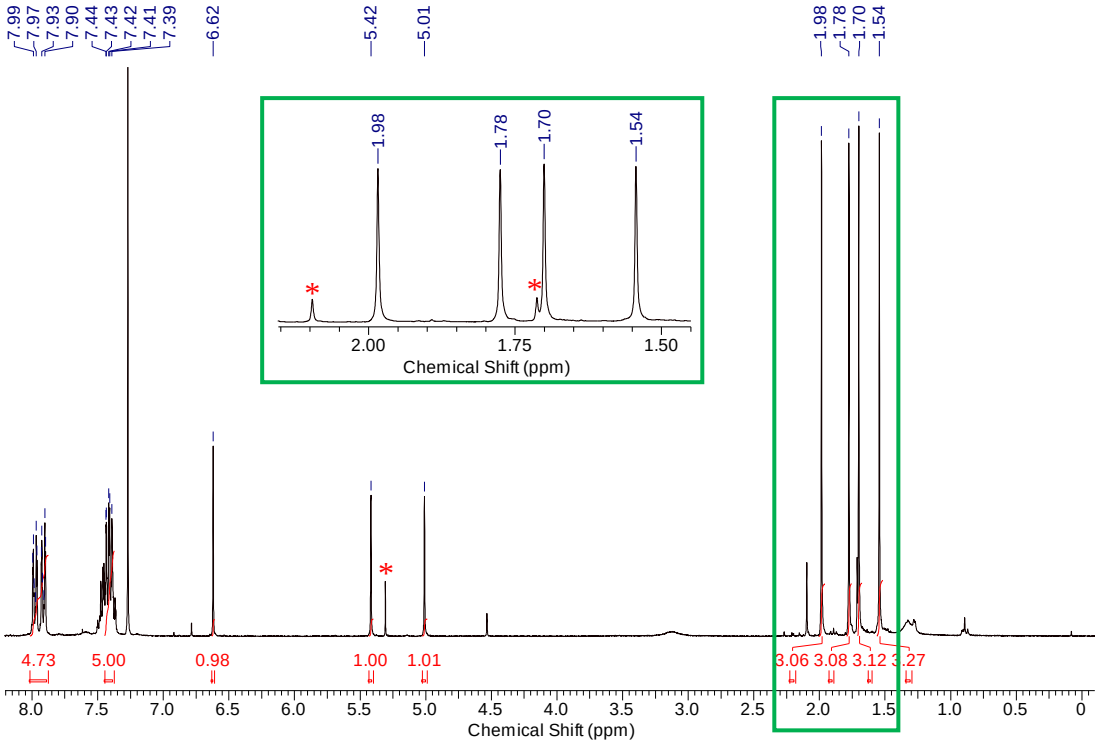

Figure 4.5.4 ^{1}H NMR spectrum of **4.13** in $CDCl_3$ at 300.13 MHz and 299.9 K

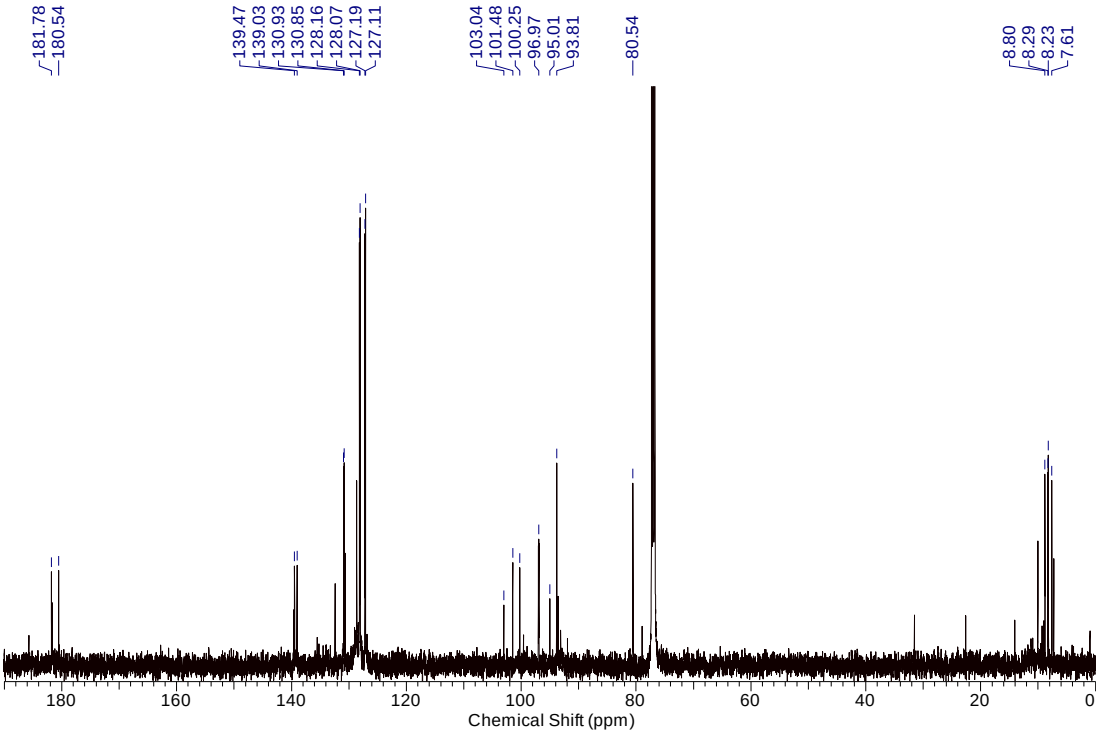

Figure 4.5.5 $^{13}C\{^{1}H\}$ NMR spectrum of **4.13** in $CDCl_3$ at 125.88 MHz and 300.0 K

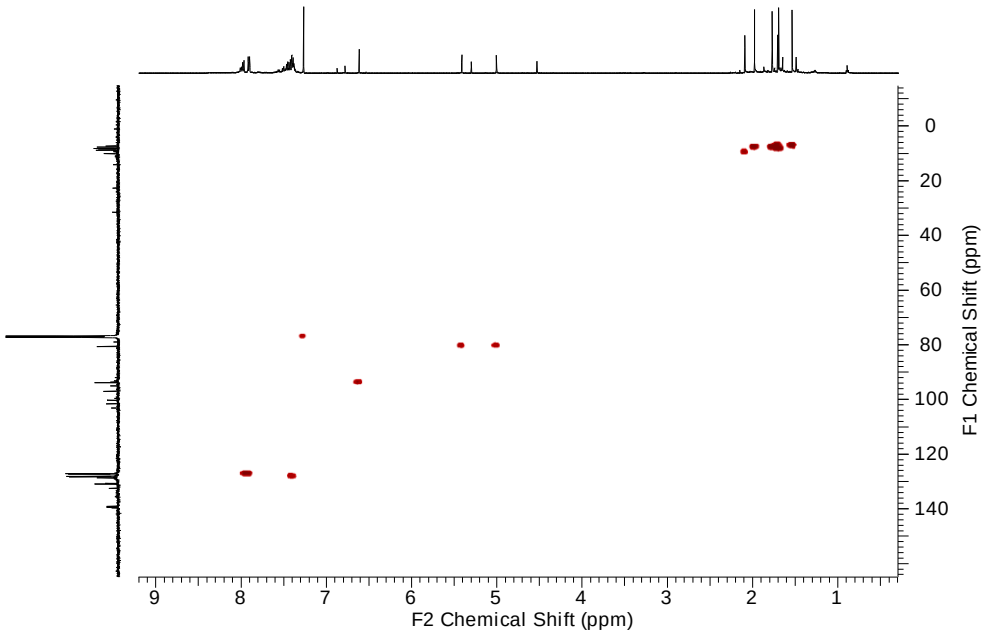

Figure 4.5.6 ^{1}J ^{1}H-^{13}C{^{1}H} HMQC spectrum of **4.13** in $CDCl_3$ at 300.0 K

It can be seen from both the ^{1}H and the ^{13}C{^{1}H} NMR spectra that compound **4.13** shows a high degree of asymmetry; the four methyl groups appear as four singlets and the two protons in the *exo* double bond also show different chemical environments. However, those peaks marked with * in the ^{1}H NMR spectrum are believed to belong to a higher symmetry isomer of the complex where the two $=CH_2$ protons are equivalent and there are only two peaks for the methyl groups. The ^{1}J ^{1}H-^{13}C{^{1}H} HMQC NMR spectrum shows that the two inequivalent protons in the *exo* double bond correspond to the same carbon at 80.5 ppm. This chemical shift implies a sp^2-hybridised character for that carbon atom. This is confirmed by the fact that no coupling constant is seen between the two protons on that carbon. Coupling constants for geminal hydrogens attached to sp^2 carbons are expected to lie between 0 and 3 Hz, whereas geminal hydrogens attached to sp^3 carbons have larger coupling constants around 12 Hz.[34] An η^2,η^4-tetramethylfulvene coordination is deduced for complex **4.13** from these data.

^{1}H Chemical Shift, δ (ppm)	**Assignment**
7.96 (m, 5H)	Aromatics
7.42 (m, 5H)	Aromatics
6.62 (s, 1H)	l
5.42 (s, 1H)	j
5.01 (s, 1H)	j
1.98 (s, 3H)	f, g, h or i
1.78 (s, 3H)	f, g, h or i
1.70 (s, 3H)	f, g, h or i
1.54 (s, 3H)	f, g, h or i
^{13}C{^{1}H} Chemical Shift, δ (ppm)	**Assignment**
181.8 (Q)	k or m
180.5 (Q)	k or m
139.5 (Q)	Aromatics
139.0 (Q)	Aromatics
130.9 (CH)	Aromatics
130.8 (CH)	Aromatics
128.2 (CH)	Aromatics
128.1 (CH)	Aromatics
127.2 (CH)	Aromatics
127.1 (CH)	Aromatics
103.0 (Q)	a, b, c, d or e
101.5 (Q)	a, b, c, d or e
100.3 (Q)	a, b, c, d or e
97.0 (Q)	a, b, c, d or e
95.0 (Q)	a, b, c, d or e
93.8 (CH)	l
80.5 (CH_2)	j
8.8 (CH_3)	f, g, h or i
8.3 (CH_3)	f, g, h or i
8.2 (CH_3)	f, g, h or i
7.6 (CH_3)	f, g, h or i

Table 4.5.1 ^{1}H and ^{13}C{^{1}H} chemical shift assignment for complex **4.13**

4.5.2.2 X-Ray Crystallographic Analysis of Compound 4.13

Orange prisms of compound **4.13** suitable for X-ray crystallography were obtained by vapour diffusion of pentane into a saturated solution of the complex in chloroform. This compound crystallised in an orthorhombic cell, and structural solution was performed in the space group $P2_12_12_1$. The molecular structure is shown in **Figure 4.5.7** and selected bond lengths and angles are given in **Table 4.5.2**.

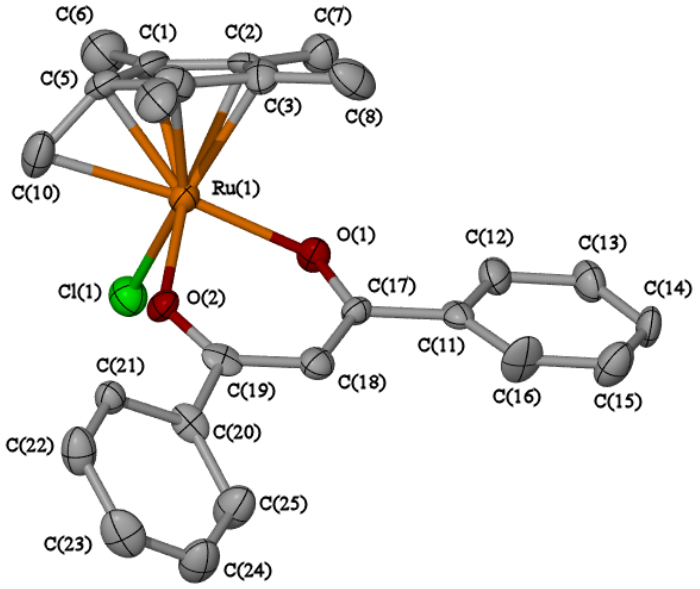

Figure 4.5.7 Molecular structure of complex **4.13**. Displacement ellipsoids are at the 50% probability level. Hydrogen atoms are omitted for clarity

Bond	**Distance (Å)**	**Bond**	**Distance (Å)**
Ru(1)-Cl(1)	2.428(2)	C(3)-C(4)	1.435(12)
Ru(1)-O(1)	2.085(6)	C(4)-C(5)	1.485(12)
Ru(1)-O(2)	2.072(6)	C(1)-C(5)	1.467(12)
Ru(1)-C(10)	2.241(9)	C(1)-C(6)	1.523(14)
Ru(1)-C(1)	2.157(10)	C(2)-C(7)	1.503(12)
Ru(1)-C(2)	2.212(8)	C(3)-C(8)	1.480(12)
Ru(1)-C(3)	2.227(9)	C(4)-C(9)	1.493(13)
Ru(1)-C(4)	2.196(9)	C(5)-C(10)	1.373(12)
Ru(1)-C(5)	2.048(9)	O(2)-C(19)	1.264(11)
C(1)-C(2)	1.386(12)	O(1)-C(17)	1.288(10)
C(2)-C(3)	1.462(12)	C(17)-C(18)	1.397(11)
Bond	**Angle (°)**	**Bond**	**Angle (°)**
O(2)-Ru(1)-O(1)	86.3(2)	O(1)-Ru(1)-C(10)	172.4(3)
O(1)-Ru(1)-Cl(1)	86.69(18)	O(2)-Ru(1)-C(10)	87.4(3)
O(2)-Ru(1)-Cl(1)	88.12(17)	C(5)-Ru(1)-C(10)	37.0(3)
C(10)-Ru(1)-Cl(1)	89.0(3)	C(10)-C(5)-Ru(1)	79.2(6)

Table 4.5.2 Selected interatomic distances and angles for compound **4.13** with s.u.s. shown in parenthesis

The distances from the ruthenium atom to the carbons in the C_5 ring vary significantly. The longer distances are those to C(2) (2.212(8) Å) and C(3) (2.227(9) Å), and the shorter distance is the one to C(5) (2.048(9) Å), indicating that the metal

is not exactly in the centre of the ring, but displaced towards the *exo* double bond, *i.e.* towards C(5). The distance between C(1) and C(2) (1.386(12) Å) is comparable to the distance between C(5) and C(10) (1.373(12) Å), and both correspond to double bonds. The distances between C(2) and C(3) (1.462(12) Å) and between C(4) and C(5) (1.485(12) Å) are the largest C-C distances within the ring. The bond length distribution which is typical of fulvenes cannot be completely observed. The Ru-C(10) bond length equals 2.241(9) Å. This solid state data reinforces the observations from the NMR studies, and an η^2,η^4-tetramethylfulvene coordination is concluded for complex **4.13**. The molecules of compound **4.13** present intramolecular hydrogen bonding between C(12)-H and O(1), with a C...O distance of 2.715 Å (**Figure 4.5.8**).

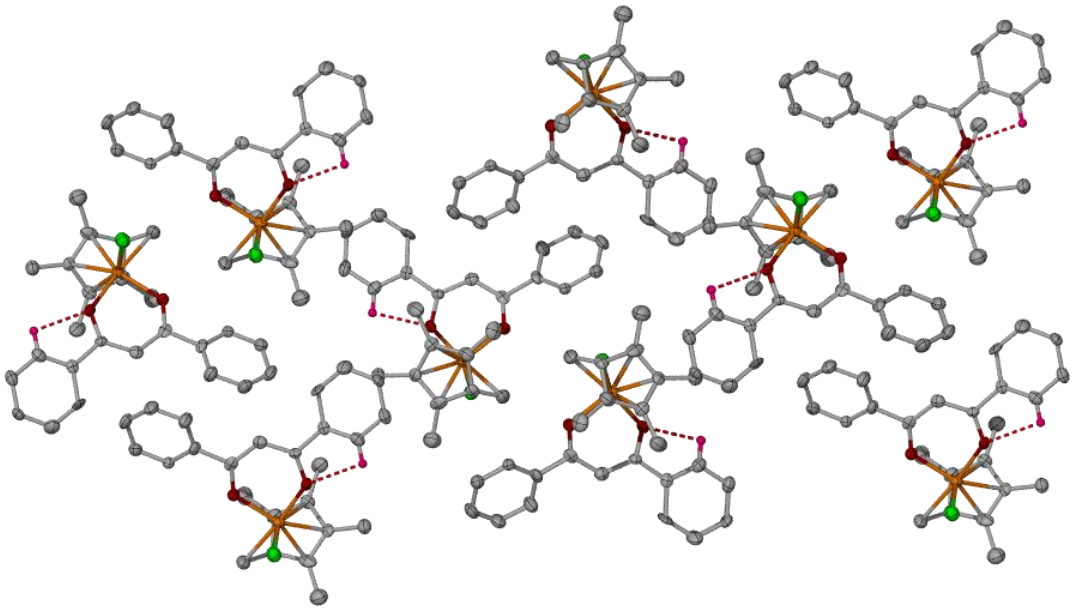

Figure 4.5.8 Compound **4.13** viewed along the a axis showing hydrogen bonding interactions (2.715 Å). Only the hydrogen atoms involved in these interactions are shown.

4.5.3 Synthesis of $[RuCl_3(C_{10}H_{14})][Ru(C_{10}H_{15})(C_7H_8)]$ (4.14)

Compound **4.14** was obtained as dark orange crystals from complex **4.3** with one equivalent of diphenylacac and one equivalent of triethylamine, which were heated to reflux in dry toluene over two hours (**Scheme 4.5.2**). Diphenylacac does not form part of the final complex.

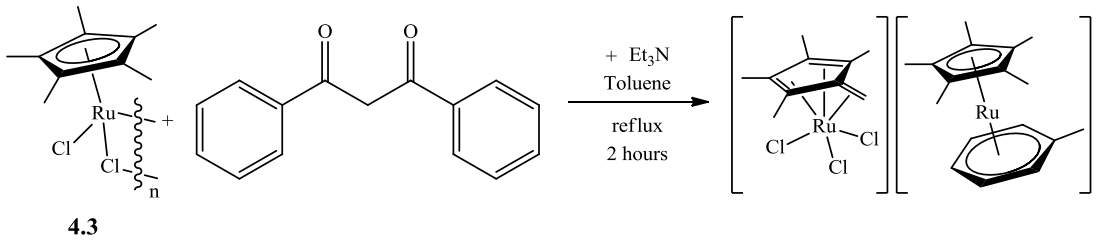

Scheme 4.5.2 Synthesis of complex **4.14** $[RuCl_3(C_{10}H_{14})][Ru(C_{10}H_{15})(C_7H_8)]$

4.5.3.1 X-Ray Crystallographic Analysis of Compound 4.14

Orange prisms of compound **4.14** suitable for X-ray crystallography were obtained at -20ºC after adding diethyl ether into a saturated solution of the reaction mixture in dichloromethane. This compound crystallised in a monoclinic cell, and structural solution was performed in the space group $P2_1/c$. The compound is formed by a cation of Cp*-ruthenium(II) which has incorporated a molecule of toluene in an η^6-arene coordination mode and an anionic tetramethylfulvene ruthenium(II) counterion. The structure is shown in **Figure 4.5.9** and selected bond lengths and angles are given in **Table 4.5.3**.

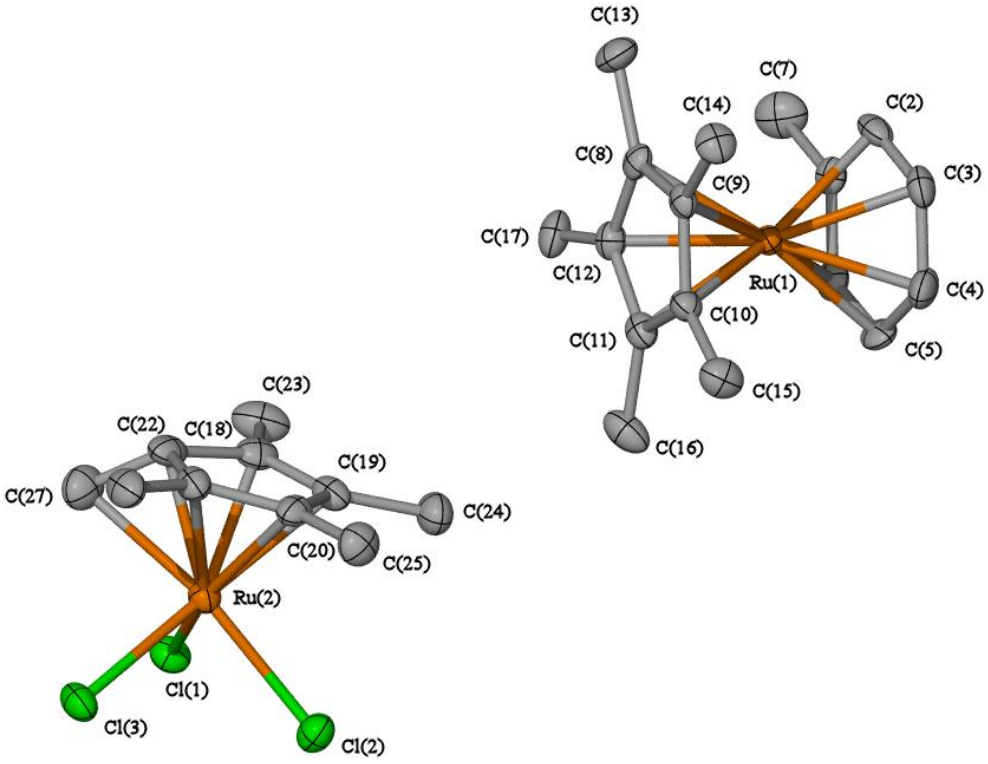

Figure 4.5.9 Structure of complex **4.14**. Displacement ellipsoids are at the 50% probability level. Hydrogen atoms are omitted for clarity

The distances from Ru(2) to the carbons in the C_5 fulvene ring vary in the same way as those in complex **4.13**, so the metal is again displaced towards the *exo* double bond. The only two clear double bonds in the fulvene ligand are those between C(22) and C(27) (1.372(8) Å) and C(18) and C(19) (1.398(8) Å), which is also similar to what was observed in complex **4.13**. An η^2,η^4-tetramethylfulvene structure is considered for the anion in **4.14**. The distance Ru(2)-C(27) is 2.253(6) Å. Compound **4.14** shows π-π stacking interactions (3.309 Å) between the tetramethylfulvene ligands of the anionic substructures in the solid state (**Figure 4.5.10**).

Bond	**Distance (Å)**	**Bond**	**Distance (Å)**
Ru(1)-Cp* centroid	1.806	Ru(2)-C(21)	2.179(5)
Ru(1)-$C_{(Cp*)}$	2.180	Ru(2)-C(22)	2.061(5)
Ru(1)-Arene centroid	1.708	C(18)-C(19)	1.398(8)
Ru(1)-$C_{(arene)}$	2.214	C(19)-C(20)	1.450(7)
C(1)-C(7)	1.506(8)	C(20)-C(21)	1.420(7)
Cl(1)-Ru(2)	2.4345(13)	C(21)-C(22)	1.455(8)
Ru(2)-Cl(2)	2.4123(15)	C(18)-C(22)	1.486(8)
Ru(2)-Cl(3)	2.4203(14)	C(18)-C(23)	1.472(8)
Ru(2)-C(27)	2.253(6)	C(19)-C(24)	1.489(7)
Ru(2)-C(18)	2.172(5)	C(20)-C(25)	1.494(8)
Ru(2)-C(19)	2.229(5)	C(21)-C(26)	1.493(7)
Ru(2)-C(20)	2.245(5)	C(22)-C(27)	1.372(8)
Bond	**Angle (°)**	**Bond**	**Angle (°)**
Cl(2)-Ru(2)-Cl(1)	87.53(5)	C(27)-Ru(2)-Cl(2)	170.40(15)
Cl(2)-Ru(2)-Cl(3)	86.96(5)	C(27)-Ru(2)-Cl(3)	85.93(17)
Cl(3)-Ru(2)-Cl(1)	91.16(5)	C(22)-Ru(2)-C(27)	36.7(2)
C(27)-Ru(2)-Cl(1)	86.18(16)	C(27)-C(22)-Ru(2)	79.3(4)

Table 4.5.3 Selected interatomic distances and angles for compound **4.14** with s.u.s. shown in parenthesis

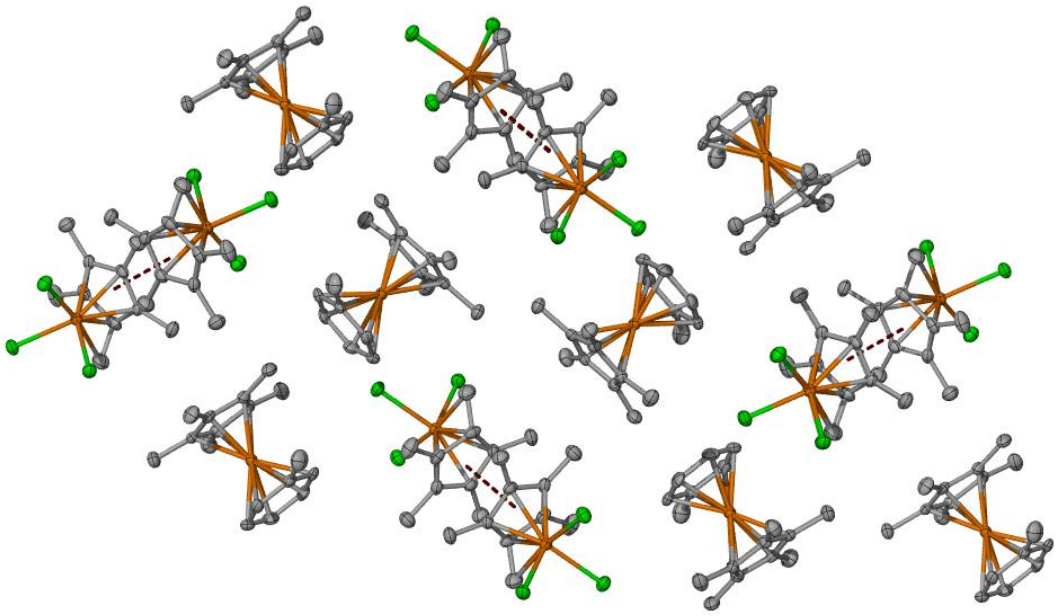

Figure 4.5.10 Compound **4.14** viewed along the a axis showing π-π stacking interactions (3.309 Å) between tetramethylfulvene ligands. Hydrogen atoms are omitted for clarity

4.6 Conclusions

A series of η^5-Cp* (Cp* = $C_5(CH_3)_5$) and η^5-Cp$^{\#}$ (Cp$^{\#}$ = $C_5(CH_3)_4(CH_2)_5OH$) complexes of ruthenium have been obtained and successfully characterised. The starting materials for these syntheses have been pentamethylcyclopentadiene (**4.1**) and (5-hydroxypentyl)-tetramethylcyclopentadiene (**4.2**), two potential η^5-coordinating ligands which were prepared following established methods. The reactions of these ligands with $RuCl_3 \cdot 3H_2O$ gave the initial complexes with general structure $[RuCl_2Cp^{*/\#}]_n$ (**4.3** and **4.4**), and these were later used to synthesise various diphosphine $RuCp^{*/\#}$ neutral complexes with chloride (**4.5** to **4.11**) and a charged complex where chloride was substituted by acetonitrile (**4.12**). All of the complexes with Cp$^{\#}$ are novel, and also some of those with Cp*. The crystal structure of $[RuCp^*(CH_3CN)(dppm)][SbF_6]$ (**4.12**) is reported.

The processes to synthesise these compounds were more complicated than those employed for η^6-arene ruthenium complexes in previous chapters. This is in part due to the pronounced air sensitivity of the $[RuCl_2Cp^{*/\#}]_n$ species, which need to be stored in a glove box, but mainly due to difficult work-ups and purifications, even though the diphosphine complexes are all air stable. This fact probably explains the higher relative abundance of published η^6-arene ruthenium complexes compared

to η^5-Cp*$^{/\#}$ complexes. The Cp* and Cp$^{\#}$ compounds presented in this chapter have been tested as catalysts for hydrogen transfer reactions under homogeneous conditions (**Chapter 5**).

Two tetramethylfulvene ruthenium(II) complexes (**4.13** and **4.14**) have been synthesised from $[RuCl_2Cp^*]_n$ (**4.3**) and diphenylacac, and characterised including crystal structures.

4.7 References

1. R. S. Threlkel, J. E. Bercaw, P. F. Seidler, J. M. Stryker and R. G. Bergman, in *Organic Syntheses*, 1987, vol. 65, p. 42.
2. A. J. Blacker, S. Brown, B. Clique, B. Gourlay, C. E. Headley, S. Ingham, D. Ritson, T. Screen, M. J. Stirling, D. Taylor and G. Thompson, *Organic Process Research & Development*, 2009, **13**, 1370-1378.
3. N. Oshima, H. Suzuki and Y. Moro-Oka, *Chemistry Letters*, 1984, **13**, 1161-1164.
4. U. Koelle and J. Kossakowski, *Journal of Organometallic Chemistry*, 1989, **362**, 383-398.
5. T. D. Tilley, R. H. Grubbs and J. E. Bercaw, *Organometallics*, 1984, **3**, 274-278.
6. M. I. Bruce, B. G. Ellis, P. J. Low, B. W. Skelton and A. H. White, *Organometallics*, 2003, **22**, 3184-3198.
7. K. S. Singh, C. Thöne and M. R. Kollipara, *Journal of Organometallic Chemistry*, 2005, **690**, 4222-4231.
8. J. K. Law, H. Mellows and D. M. Heinekey, *Journal of the American Chemical Society*, 2002, **124**, 1024-1030.
9. W. Lin, S. R. Wilson and G. S. Girolami, *Organometallics*, 1997, **16**, 2987-2994.
10. L. Luo, N. Zhu, N.-J. Zhu, E. D. Stevens and S. P. Nolan, *Organometallics*, 1994, **13**, 669-675.
11. R. T. Hembre, J. S. McQueen and V. W. Day, *Journal of the American Chemical Society*, 1996, **118**, 798-803.
12. M. Sato and M. Asai, *Journal of Organometallic Chemistry*, 1996, **508**, 121-127.

13. F. Morandini, A. Dondana, I. Munari, G. Pilloni, G. Consiglio, A. Sironi and M. Moret, *Inorganica Chimica Acta*, 1998, **282**, 163-172.
14. K. Takahashi, M. Yamashita, Y. Tanaka and K. Nozaki, *Angewandte Chemie International Edition*, 2012, **51**, 4383-4387.
15. U. Koelle, C. Rietmann and G. Raabe, *Organometallics*, 1997, **16**, 3273-3281.
16. Y. A. Borisov, M. I. Rybinskaya, Y. S. Nekrasov, A. Z. Kreindlin, A. A. Kamyshova and P. V. Petrovskii, *Journal of Organometallic Chemistry*, 2002, **645**, 87-93.
17. L. E. Schock, C. P. Brock and T. J. Marks, *Organometallics*, 1987, **6**, 232-241.
18. J. M. Meredith, K. I. Goldberg, W. Kaminsky and D. M. Heinekey, *Organometallics*, 2012, **31**, 8459-8462.
19. C. Li, L. Luo, S. P. Nolan, W. Marshall and P. J. Fagan, *Organometallics*, 1996, **15**, 3456-3462.
20. C. McDade, J. C. Green and J. E. Bercaw, *Organometallics*, 1982, **1**, 1629-1634.
21. J. W. Pattiasina, C. E. Hissink, J. L. De Boer, A. Meetsma, J. H. Teuben and A. L. Spek, *Journal of the American Chemical Society*, 1985, **107**, 7758-7759.
22. L. Fan, C. Wei, F. I. Aigbirhio, M. L. Turner, O. V. Gusev, L. N. Morozova, D. R. T. Knowles and P. M. Maitlis, *Organometallics*, 1996, **15**, 98-104.
23. L. Fan, M. L. Turner, M. B. Hursthouse, K. M. A. Malik, O. V. Gusev and P. M. Maitlis, *Journal of the American Chemical Society*, 1994, **116**, 385-386.
24. J. Román Torres-Lubián, M. Esther Sánchez-Castro, P. Juárez-Saavedra, J. Hernández-Martínez, B. Gordillo-Román and M. Angeles Paz-Sandoval, *Journal of Organometallic Chemistry*, 2002, **663**, 127-133.
25. D. M. Hankin, A. A. Danopoulos, G. Wilkinson, T. K. N. Sweet and M. B. Hursthouse, *Journal of the Chemical Society, Dalton Transactions*, 1996, 4063-4069.
26. C. Gemel, K. Mereiter, R. Schmid and K. Kirchner, *Organometallics*, 1997, **16**, 5601-5603.
27. U. Kölle, B.-S. Kang and U. Thewalt, *Journal of Organometallic Chemistry*, 1990, **386**, 267-273.

28. F. D. Miller and R. D. Sanner, *Organometallics*, 1988, **7**, 818-825.
29. F. G. N. Cloke, J. P. Day, J. C. Green, C. P. Morley and A. C. Swain, *Journal of the Chemical Society, Dalton Transactions*, 1991, 789-796.
30. G. A. Luinstra and J. H. Teuben, *Journal of the American Chemical Society*, 1992, **114**, 3361-3367.
31. M. Booij, A. Meetsma and J. H. Teuben, *Organometallics*, 1991, **10**, 3246-3252.
32. A. H. Klahn, M. H. Moore and R. N. Perutz, *Journal of the Chemical Society, Chemical Communications*, 1992, 1699-1701.
33. D. S. Glueck and R. G. Bergman, *Organometallics*, 1990, **9**, 2862-2863.
34. E. Rüba, K. Mereiter, R. Schmid, K. Kirchner, E. Bustelo, M. C. Puerta and P. Valerga, *Organometallics*, 2002, **21**, 2912-2920.

Chapter 5

Homogeneous Hydrogen Transfer Catalysis

5.1 Introduction

This chapter describes the catalytic results obtained with the ruthenium complexes presented in **Chapters 2-4** for homogeneous hydrogen transfer reactions. Two particular transformations were selected as representatives and studied in detail: the redox neutral alkylation of *tert*-butylamine with phenethyl alcohol and the reduction of benzaldehyde.

The redox neutral alkylation of *tert*-butylamine with phenethyl alcohol has been previously investigated by Williams and co-workers with different ruthenium catalytic systems, including $[RuCl_2(p\text{-cymene})]_2$, $[RuCl_2(benzene)]_2$ or $Ru(PPh_3)_3Cl_2$ and the bidentate phosphines DPEphos, Xantphos, BINAP, dppf, dippf, dppe or dppp (**Figure 5.1.1**), or the monodentate phosphine PPh_3. They suggested that the best combination was that of $[RuCl_2(p\text{-cymene})]_2$ with either dppf or DPEphos. The stoichiometry of ruthenium to the diphosphine ligand was always 1 : 1.[1, 2] The conditions reported for the N-alkylation involved reactions under an inert atmosphere with dry toluene and molecular sieves, and the use of K_2CO_3.[1] During optimisation processes (with different bases and temperatures) with $[RuCl_2(p\text{-cymene})]_2$ and dppf for the same reaction in this project, it was observed that the presence of molecular sieves and a base had a detrimental effect on the outcome of the catalysis. Thus, this reaction has been carried out without these additives and under non-inert atmosphere (**Scheme 5.1.1**).

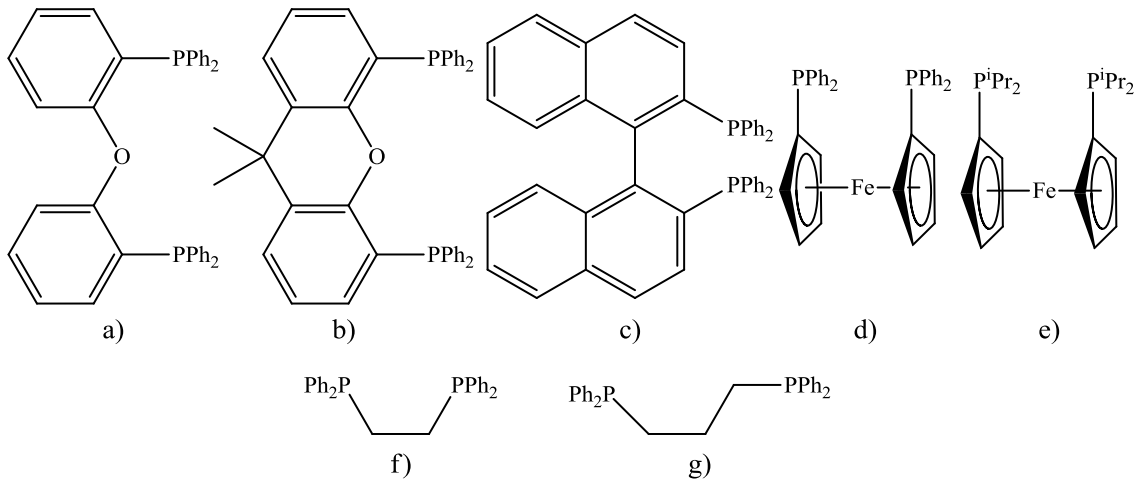

Figure 5.1.1 Diphosphine ligands: a) DPEphos, b) Xantphos, c) BINAP, d) dppf, e) dippf, f) dppe, g) dppp

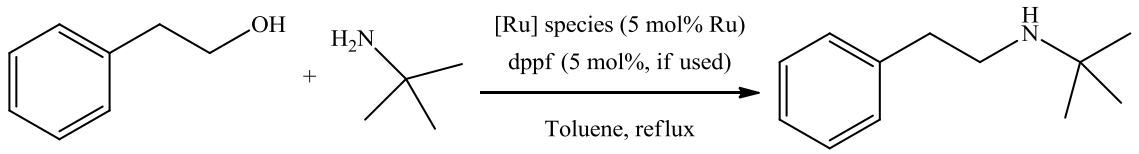

Scheme 5.1.1 Conditions used for the redox neutral alkylation of *tert*-butylamine with phenethyl alcohol after optimisation. [Substrates] = 0.3 M in 10 ml of toluene

After some optimisation work using $[RuCl_2(p\text{-cymene})]_2$ and dppf for the reduction of benzaldehyde, the conditions used henceforth for the study of this reaction are presented in **Scheme 5.1.2**.

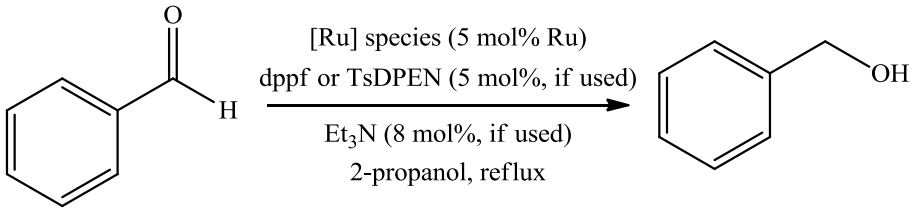

Scheme 5.1.2 Conditions used for the benzaldehyde reduction after optimisation. [Substrate] = 0.1 M in 10 ml of 2-propanol

All of the complexes tested in this chapter for the two model reactions are η^6-arene or η^5-$C_5(CH_3)_4R$ (R = CH_3 or $(CH_2)_5OH$) ruthenium complexes, with the same half-sandwich structure, bearing either two X- and one L-type ligands or one X- and two L-type ligands (X = one electron donor ligand, L = two electron donor ligand) (**Figure 5.1.2**). The possible nature of the pre-catalyst species formed after addition of the relevant ligands has been investigated in some of the cases.

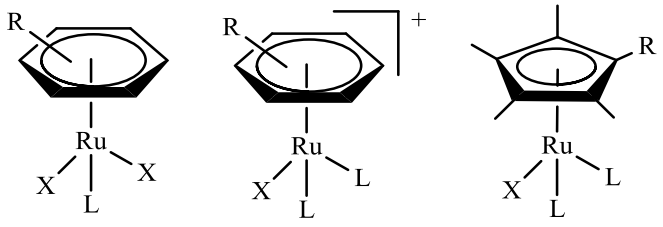

Figure 5.1.2 General structures of the ruthenium complexes tested for hydrogen transfer reactions

All of the catalytic reactions have been monitored over 24 hours by either Gas Chromatography (GC) or ^{1}H NMR spectroscopy (in this latter case the analyses were performed only on the final reaction mixtures after one day). The conversion percentages obtained by GC were calculated from the areas of both the starting substrate (phenethyl alcohol or benzaldehyde) and product peaks with the formula: [(area product)/(area product + area substrate)] × 100.

5.2 Nature of the Pre-Catalyst

After their studies on the redox neutral alkylation of *tert*-butylamine with phenethyl alcohol using [$RuCl_2$(*p*-cymene)]$_2$ and diphosphines, Williams and co-workers proposed the formation of a [RuCl(*p*-cymene)(P−P)][Cl] species as pre-catalyst for the transformation.[2] In consequence, they always reported the use of twice the amount of the correspondent diphosphine, this is, a stoichiometric relationship of [1:2] for [$RuCl_2$(*p*-cymene)]$_2$ and the diphosphine, which results in [1:1] Ru : diphosphine.[1, 2] The complex [RuCl(*p*-cymene)(dppf)][Cl] (**5.1**) was synthesised and isolated during this project by Mr. Joel Fonseca (**Scheme 5.2.1**).[3]

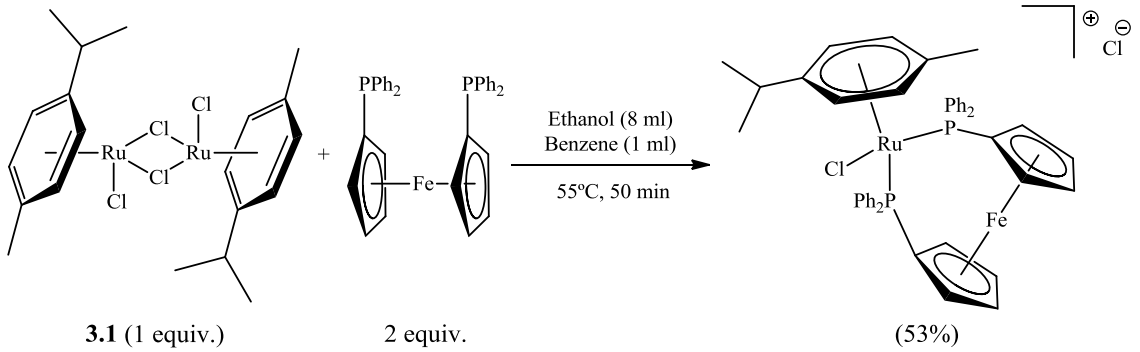

Scheme 5.2.1 Synthesis of complex **5.1** [RuCl($C_{10}H_{14}$)($C_{34}H_{28}FeP_2$)][Cl]

Complex **5.1** could only be prepared using an alcohol (ethanol or 2-propanol) as the solvent. The mixture of 1 equivalent of [$RuCl_2$(*p*-cymene)]$_2$ (**3.1**) with 2 equivalents of dppf in refluxing 2-propanol, which are the conditions employed for the reduction of benzaldehyde, produced this yellow compound **5.1**. A similar charged monomer with PF_6 or $SnCl_3$ as the counterion had been reported before,[4-8] including its crystal structure,[4, 8] where the most characteristic feature is the eclipsed conformation of the cyclopentadienyl rings. The ^{1}H NMR spectrum of complex **5.1** presents two broad

peaks at 5.89 and 5.19 ppm for the aromatic protons of the *p*-cymene ring, and four singlets at 5.07, 4.36, 4.27 and 4.08 ppm for the protons in the cyclopentadienyl rings.

When the solvent employed was changed to dichloromethane, chloroform or toluene, complex **5.2** was obtained, with the formula $[(RuCl_2(p\text{-cymene}))_2(dppf)]$ (**Scheme 5.2.2**).

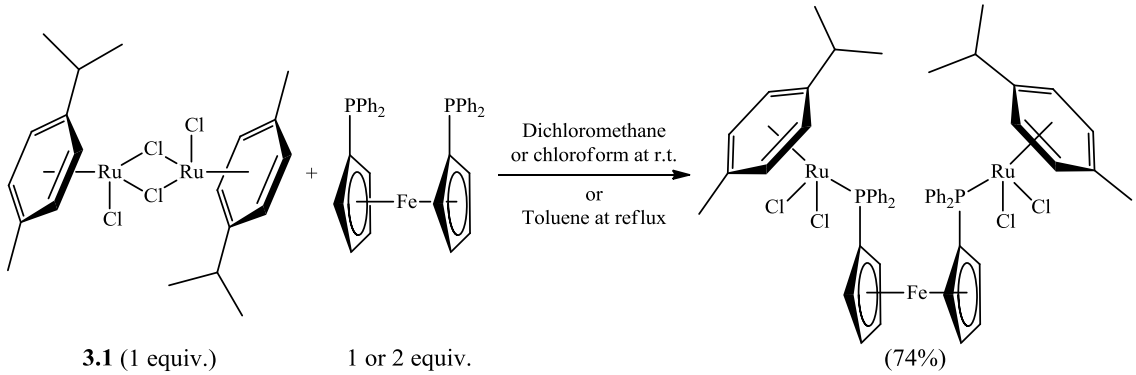

3.1 (1 equiv.) 1 or 2 equiv. (74%)

Scheme 5.2.2 Synthesis of complex **5.2** $[Ru_2Cl_4(C_{10}H_{14})_2(C_{34}H_{28}FeP_2)]$

The ^{1}H NMR spectrum of compound **5.2** is characterised by the presence of a broad singlet at 5.07 ppm, which is the peak for the aromatic protons in the *p*-cymene rings. This is different to the usual two doublets observed for the rest of the *p*-cymene complexes studied during this project. The protons of the cyclopentadienyl rings in the dppf bridge are represented by two singlets at 4.17 and 3.89 ppm. This matches previous publications of the synthesis and characterisation of complex **5.2**. The groups of Sieiro,[9] Yamamoto[5] and Kaim[7] have reported this compound, prepared from a 1 : 1 mixture of $[RuCl_2(p\text{-cymene})]_2$ and dppf, but not its crystal structure.

The structure of complex **5.2** was determined by X-ray crystallography. Orange single crystals were obtained by vapour diffusion of pentane into a saturated solution of the compound in dichloromethane. It crystallised in a triclinic cell, and the structural solution was performed in the space group $P\bar{1}$. The asymmetric unit contains half of a molecule and two co-crystallised molecules of water. The molecular structure of this complex is shown in **Figure 5.2.1** and selected bond lengths and angles are given in **Table 5.2.1**.

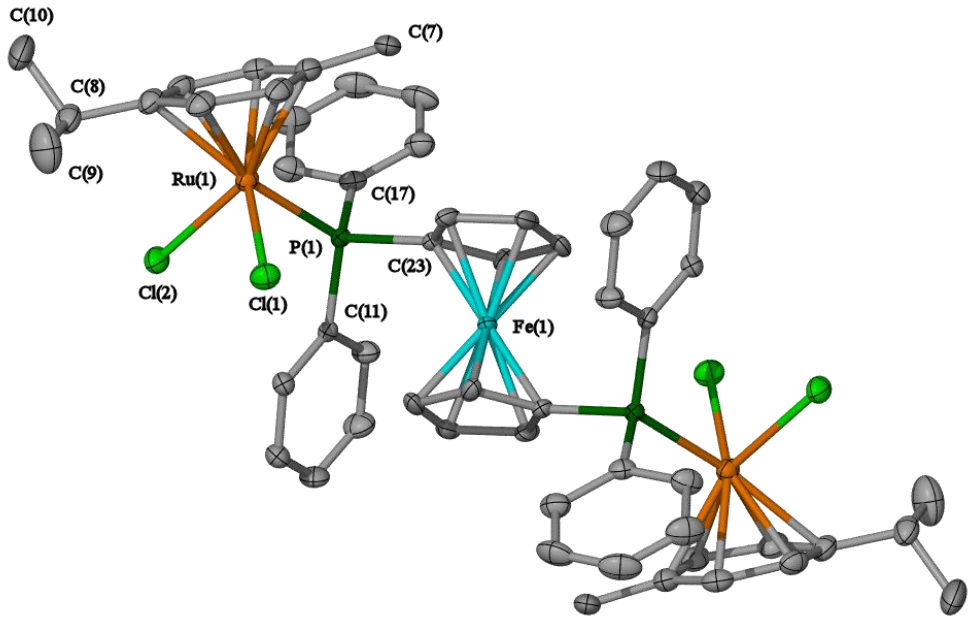

Figure 5.2.1 Molecular structure of complex **5.2**. Displacement ellipsoids are at the 50% probability level. Hydrogen atoms and the water molecules are omitted for clarity

Bond	**Distance (Å)**	**Bond**	**Distance (Å)**
Ru(1)-P(1)	2.3726(10)	C(8)-C(9)	1.540(8)
Ru(1)-Cl(1)	2.4259(10)	C(8)-C(10)	1.501(7)
Ru(1)-Cl(2)	2.4414(10)	P(1)-C(11)	1.840(4)
C(1)-C(2)	1.418(6)	P(1)-C(17)	1.844(4)
C(1)-C(8)	1.517(6)	P(1)-C(23)	1.826(4)
C(4)-C(7)	1.508(6)	C(23)-C(24)	1.449(5)
Ru(1)-Ring	1.724	Ru(1)-$C_{(arene)}$	2.2395
Fe(1)-Ring	1.667	Fe(1)-$C_{(Cp)}$	2.0702
Bond	**Angle (°)**	**Bond**	**Angle (°)**
Cl(1)-Ru(1)-Cl(2)	88.83(4)	C(6)-Ru(1)-C(1)	37.59(16)
P(1)-Ru(1)-Cl(1)	88.10(3)	C(10)-C(8)-C(9)	110.0(5)
P(1)-Ru(1)-Cl(2)	87.93(3)	C(2)-C(1)-C(6)	117.3(4)
C(23)-P(1)-Ru(1)	115.11(13)	C(11)-P(1)-C(17)	101.86(17)
P(1)-C(23)-Fe(1)	131.86(19)	C(24)-C(23)-C(27)	107.4(3)

Table 5.2.1 Selected interatomic distances and angles for compound **5.2** with s.u.s. shown in parenthesis

Both the distance between the ruthenium atom and the arene ring centroid (1.724 Å) and the average distance between ruthenium and all the carbons in the ring (2.2395 Å) are comparable to those observed in the other Ru(*p*-cymene) complexes reported in this document (approximately 1.69 and 2.20 Å respectively). Both ruthenium centres

present the typical piano-stool geometry, and the cyclopentadienyl rings are in a staggered conformation. No classic hydrogen bonds were found for complex **5.2** in the solid state.

A series of control experiments were performed in order to find out what Ru-dppf species is formed under the specific conditions employed for both the redox neutral alkylation and the reduction of benzaldehyde. The complexes were detected based on their different ^{1}H NMR spectra. **Figure 5.2.2** shows the ^{1}H NMR spectra of complexes **5.1** and **5.2**. A summary of the results obtained is presented in **Figure 5.2.3**. The reaction of 1 equivalent of **3.1** with only 1 equivalent of dppf produces exclusively compound **5.2**, both at reflux of toluene and at reflux of 2-propanol. The reaction of 1 equivalent of **3.1** with 2 equivalents of dppf also produces **5.2** in toluene, even in the presence of a 0.3 M alcohol. This was tested because phenethyl alcohol is used as the substrate for the N-alkylation, and it is at a 0.3 M concentration under catalytic conditions. Ethanol was employed instead of phenethyl alcohol, so it could be easily evaporated before recording the ^{1}H NMR spectrum. The analysis only revealed the presence of **5.2**. Complex **5.1** has only been observed under the conditions employed for the reduction of benzaldehyde, *i.e.* using 1 equivalent of **3.1** with 2 equivalents of dppf in refluxing 2-propanol.

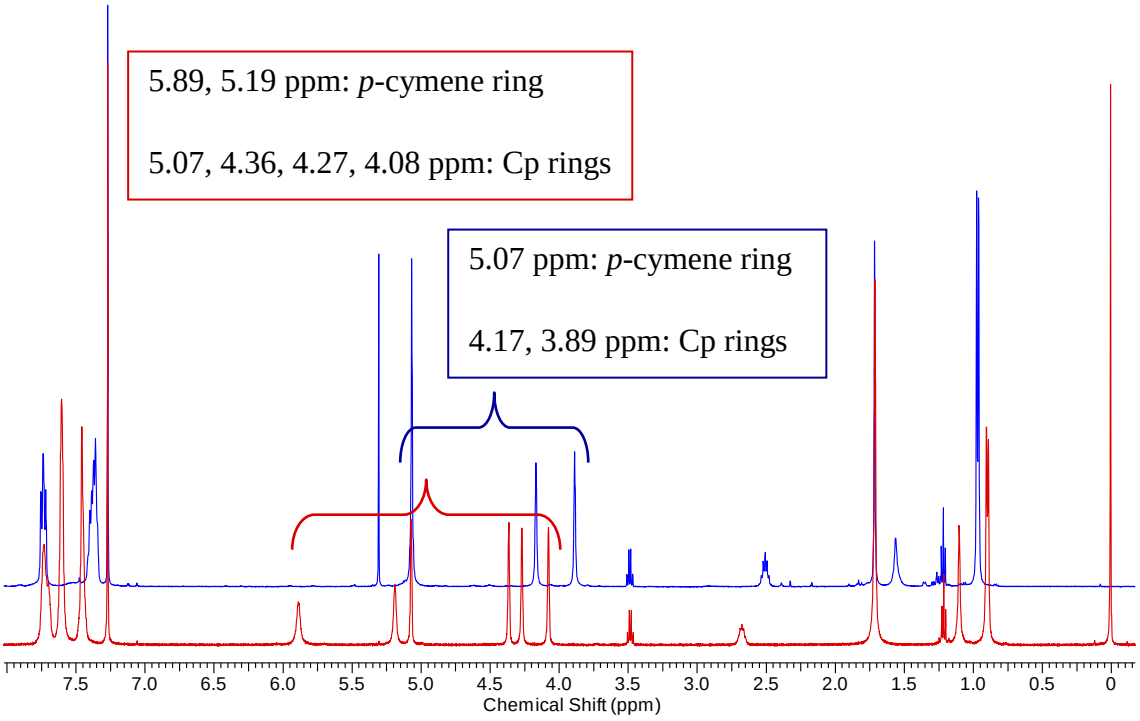

Figure 5.2.2 ^{1}H NMR spectra of complexes **5.1** (red) and **5.2** (blue)

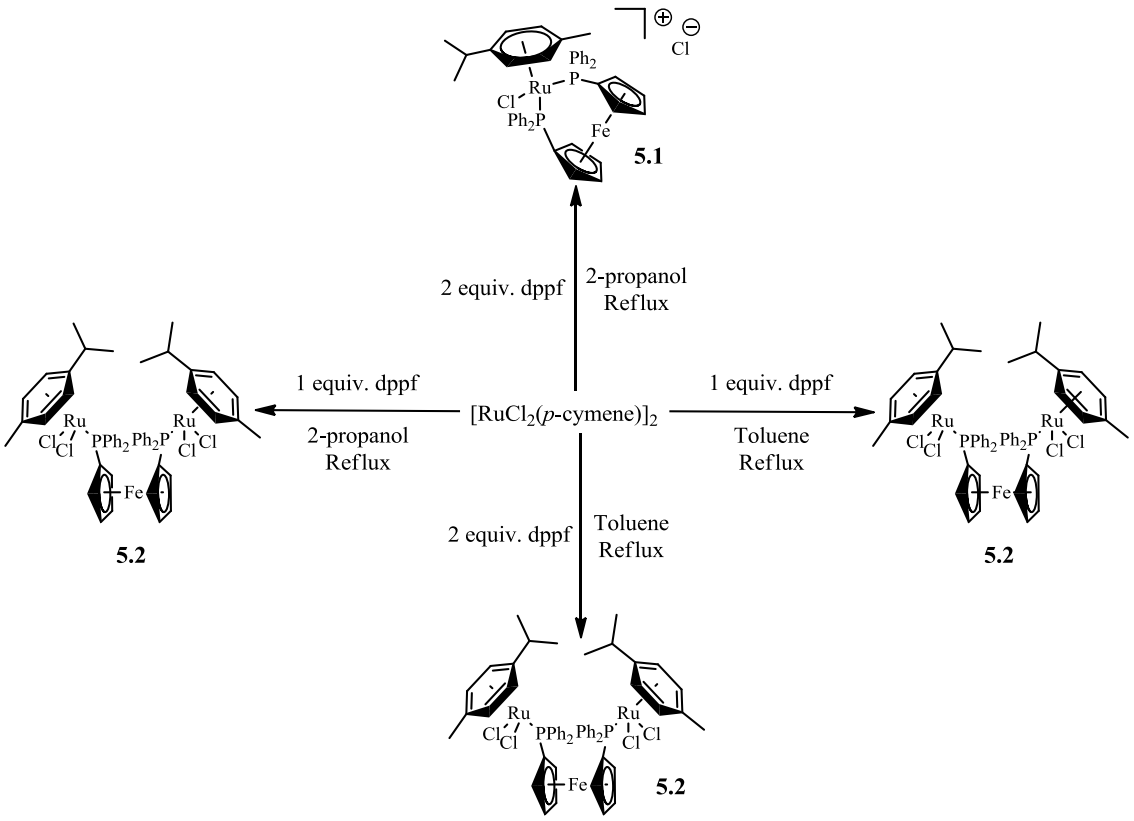

Figure 5.2.3 Summary of control experiments with the conditions employed for the redox neutral alkylation of *tert*-butylamine with phenethyl alcohol and the reduction of benzaldehyde, and the Ru-dppf species obtained

Compound **5.2** was tested for the redox neutral alkylation of *tert*-butylamine with phenethyl alcohol and the reduction of benzaldehyde, both with and without an extra equivalent of dppf, and the activities compared to those obtain with the *in situ* mixture of $[RuCl_2(p\text{-cymene})]_2$ + 2 equivalents of dppf.

For the redox neutral alkylation, the results are presented in **Figure 5.2.4** and summarised in **Table 5.2.2**. In all of the cases the loading of ruthenium was 5 mol%. The complex $[RuCl(p\text{-cymene})(dppf)][BF_4]$, which was synthesised by Mr. Joel Fonseca and is equivalent to **5.1** but with BF_4 as the counterion, was also tested for comparison. It can be observed that compound **5.2** is active, giving 55% conversion after 24 hours (entry 2 in **Table 5.2.2**). When 1 equivalent of dppf was added to **5.2** (2.5 mol% of dppf), the catalytic activity improved considerably, and matched that obtained with $[RuCl(p\text{-cymene})(dppf)][BF_4]$, indicating the possible formation of the monomer **5.1** (entries 3 and 4), which contradicts the previous control experiments. Curiously, the activity obtained with $[RuCl_2(p\text{-cymene})]_2$ + 2 equivalents of dppf was still the best

(entry 1). This likely implies a better performance of the catalyst when it is formed *in situ*.

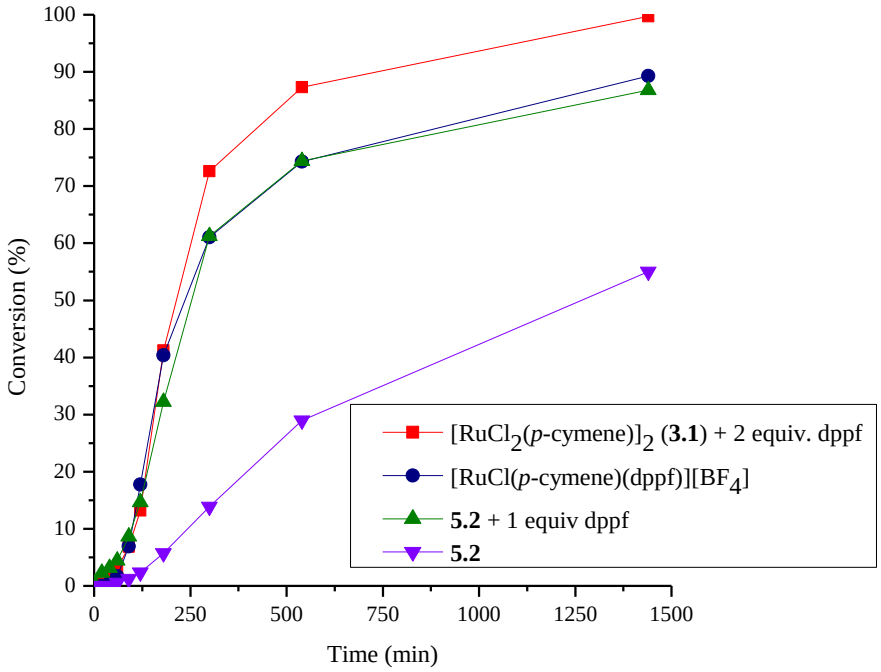

Figure 5.2.4 Catalytic activity of complexes **3.1**, [RuCl(*p*-cymene)(dppf)][BF_4] and **5.2** (5 mol% Ru) with different number of equivalents of dppf against the redox neutral alkylation of *tert*-butylamine with phenethyl alcohol in toluene at 110°C, monitored over 24 hours by GC

			Conv. % after:		
Entry	**Ru species**	**dppf equiv.**	**3 h**	**9 h**	**24 h**
1	**3.1**	2	41.2	87.3	99.7
2	**5.2**	0	5.7	29.0	55.0
3	**5.2**	1	32.2	74.4	86.8
4	[RuCl(*p*-cymene)(dppf)][BF_4]	0	40.4	74.3	89.3

Table 5.2.2 Summary of conversions obtained with complexes **3.1**, [RuCl(*p*-cymene)(dppf)][BF_4] and **5.2** with different number of equivalents of dppf after 3, 9 and 24 hours for the N-alkylation of *tert*-butylamine with phenethyl alcohol. The reactions were carried out using 5 mol% Ru in toluene at 110°C

For the reduction of benzaldehyde, the results with 5 mol% of ruthenium are shown in **Figure 5.2.5** and summarised in **Table 5.2.3**. Compound **5.2** is much more active by itself for this reaction, affording almost 95% conversion after only 2 hours (entry 2 in **Table 5.2.3**), but again the addition of 1 equivalent of dppf made the reaction slightly faster (entry 3), even though the final conversions after 24 hours were similar.

With 2 equivalents of dppf, the monomer **5.1** is formed under the benzaldehyde reduction conditions (see **Figure 5.2.3**), so it can be concluded that both **5.1** and **5.2** are very active for this reaction, but **5.1** is faster. The activity obtained with [$RuCl_2$(*p*-cymene)]$_2$ + 2 equivalents of dppf was also the best for this reaction (entry 1).

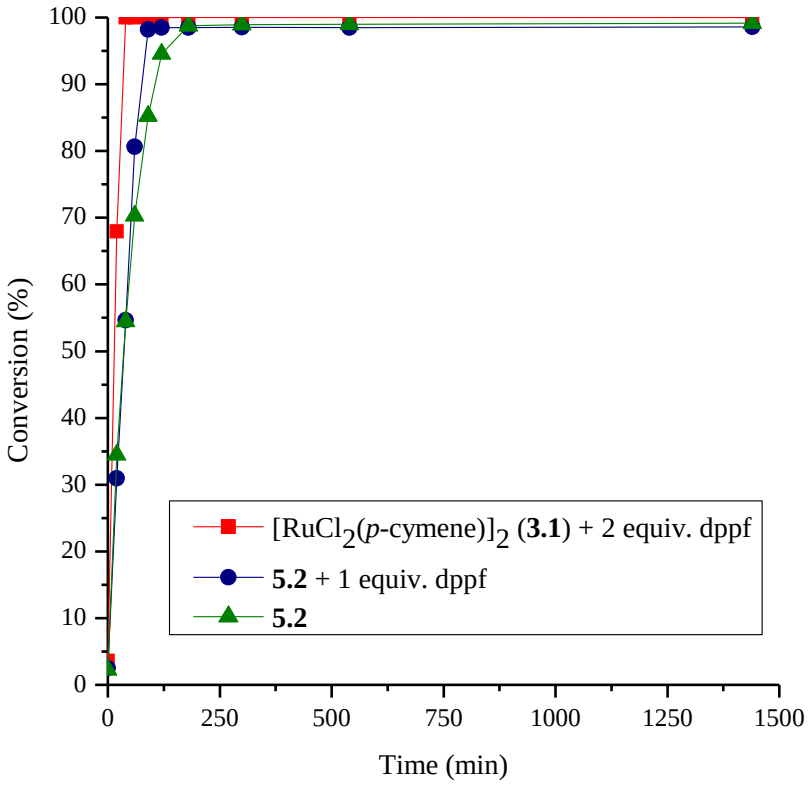

Figure 5.2.5 Catalytic activity of complexes **3.1** and **5.2** (5 mol% Ru) with different number of equivalents of dppf against the reduction of benzaldehyde in 2-propanol at 85°C, monitored over 24 hours by GC

			Conv. % after:		
Entry	**Ru species**	**dppf equiv.**	**1 h**	**1.5 h**	**2 h**
1	**3.1**	2	100	100	100
2	**5.2**	0	70.3	85.2	94.6
3	**5.2**	1	80.6	98.2	98.5

Table 5.2.3 Summary of conversions obtained with complexes **3.1** and **5.2** with different number of equivalents of dppf after 1, 1.5 and 2 hours for the reduction of benzaldehyde. The reactions were carried out using 5 mol% Ru in 2-propanol at 85°C

In conclusion, species **5.1** is believed to act as pre-catalyst for the reduction of benzaldehyde in 2-propanol, and **5.2** as pre-catalyst for the redox neutral alkylation of *tert*-butylamine with phenethyl alcohol in toluene. However, the best conversions were

observed with the use of $[RuCl_2(p\text{-cymene})]_2$ (**3.1**) + 2 equivalents of dppf, so this mixture was employed as reference in subsequent investigations.

5.3 Functionalised η^6-Arene Ruthenium Complexes

The acid- and ester-functionalised η^6-arene ruthenium complexes presented in **Chapter 2** were originally synthesised so that they could be potentially immobilised by covalent bonding onto a modified support and used as heterogeneous catalysts for hydrogen transfer reactions. As discussed in that chapter, their attachment to a solid support failed after some attempts, but several of those complexes have been tested as catalysts for the homogeneous N-alkylation of *tert*-butylamine with phenethyl alcohol.

The results discussed in this section correspond to the complexes **2.3** to **2.7** shown in **Figure 5.3.1**, together with $[RuCl_2(p\text{-cymene})]_2$ (**3.1**) and $RuCl_3 \cdot 3H_2O$, used as references. When $[RuCl_2(p\text{-cymene})]_2$ or $RuCl_3 \cdot 3H_2O$ were tested without the presence of dppf, the conversions obtained in both cases did not exceed 3% for the formation of N-phenethyl-*tert*-butylamine. Consequently, dppf was used as ligand, and it was confirmed that it is not catalytically active by itself.

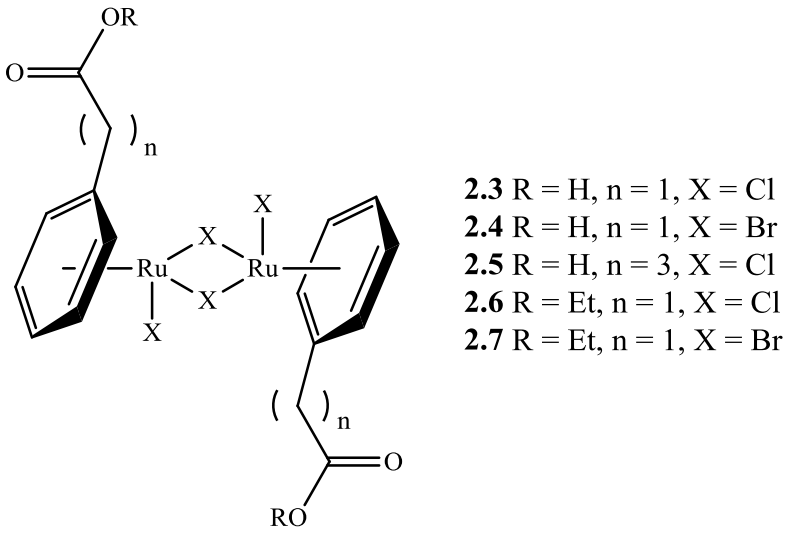

2.3 R = H, n = 1, X = Cl
2.4 R = H, n = 1, X = Br
2.5 R = H, n = 3, X = Cl
2.6 R = Et, n = 1, X = Cl
2.7 R = Et, n = 1, X = Br

Figure 5.3.1 Functionalised η^6-arene ruthenium complexes tested for the homogeneous N-alkylation of *tert*-butylamine with phenethyl alcohol

A loading of 5 mol% of Ru and 5 mol% of dppf was employed in all cases. The reactions were monitored by GC over a period of 24 hours, and the catalytic activities are illustrated in **Figure 5.3.2** and summarised in **Table 5.3.1**.

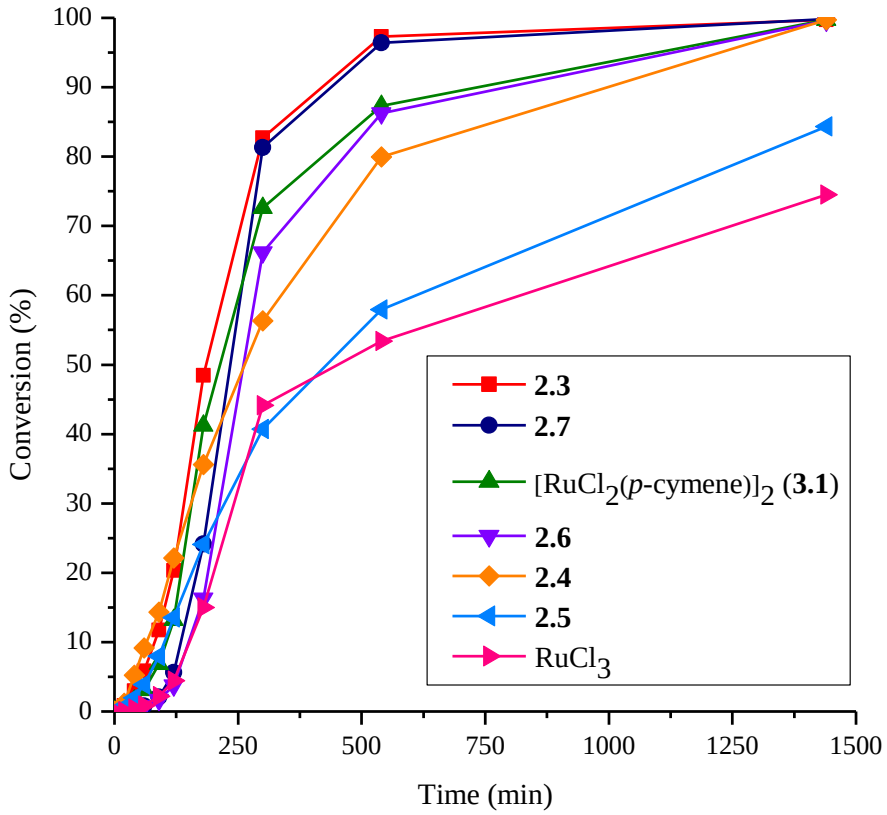

Figure 5.3.2 Catalytic activity of functionalised η^6-arene ruthenium complexes **2.3** to **2.7**, $[RuCl_2(p\text{-cymene})]_2$ (**3.1**) and $RuCl_3 \cdot 3H_2O$ (5 mol% Ru and 5 mol% dppf) against the redox neutral alkylation of *tert*-butylamine with phenethyl alcohol, monitored over 24 hours by GC

		Conversion % after:		
Entry	**Ruthenium species**	**3 hours**	**9 hours**	**24 hours**
1	**2.3**	48.5	97.3	99.7
2	**2.4**	35.6	80.0	99.7
3	**2.5**	24.1	57.9	84.4
4	**2.6**	16.3	86.2	99.6
5	**2.7**	24.1	96.4	99.8
6	$[RuCl_2(p\text{-cymene})]_2$ (**3.1**)	41.2	87.3	99.7
7	$RuCl_3 \cdot 3H_2O$	15.0	53.4	74.5

Table 5.3.1 Summary of conversions obtained with complexes **2.3** to **2.7**, $[RuCl_2(p\text{-cymene})]_2$ (**3.1**) and $RuCl_3 \cdot 3H_2O$ after 3, 9 and 24 hours for the N-alkylation of *tert*-butylamine with phenethyl alcohol. The reactions were carried out using 5 mol% Ru and 5 mol% dppf in toluene at 110°C

Complexes **2.3**, **2.4**, **2.6**, **2.7** and $[RuCl_2(p\text{-cymene})]_2$ all provided very high conversions above 99.5% after 24 hours, but at different rates. The fastest complexes

were **2.3** and **2.7**, which gave conversions above 96% after 9 hours, improving the catalytic activity of $[RuCl_2(p\text{-cymene})]_2$ (entries 1, 5 and 6 in **Table 5.3.1**). The reaction with complex **2.3** remarkably achieved almost 50% conversion after 3 hours (entry 1). It is noticeable that between the chloride complexes **2.3** and **2.6**, the one with an acid (**2.3**) was the most active, whereas between the bromide complexes **2.4** and **2.7**, complex **2.7** (an ester) showed a faster reaction rate. In fact, complexes **2.4** and **2.6** behaved as slightly worse catalysts than $[RuCl_2(p\text{-cymene})]_2$ (entries 2 and 4). Compound **2.5** reached only 84.4% conversion after 24 hours, which might derive from possible decomposition due to its longer chain (entry 3). Interestingly, $RuCl_3 \cdot 3H_2O$ also gave a moderate activity (74.5% after 24 hours) in the presence of dppf (entry 7). The complexes **2.3** and $[RuCl_2(p\text{-cymene})]_2$ (**3.1**) were also tested with a lower loading of 1 mol% Ru and 1 mol% dppf, but the activity in both cases did not surpass 3% after 24 hours.

5.4 η^6-*p*-Cymene Ruthenium Dimers and Monomers

The results discussed in this section correspond to the complexes **3.1** to **3.13**, which were introduced in **Chapter 3** (**Figure 5.4.1**). All of these complexes have an η^6-*p*-cymene unit coordinated to ruthenium in common, and compounds **3.3** to **3.13** have a labile N-ligand (pyridine or *tert*-butylamine) where the nitrogen atom acts as a two electron donor. Their activities against the N-alkylation of *tert*-butylamine with phenethyl alcohol have been investigated. Some studies on the reduction of benzaldehyde with complex **3.1** are also presented in this section.

The higher activities against the N-alkylation of t*ert*-butylamine with phenethyl alcohol in the absence of dppf were obtained with complexes **3.2** and **3.5**, which reached conversions of 11.8% and 8.7% respectively after 24 hours. With the chloride species (**3.1**, **3.3**, **3.4** and **3.6** to **3.13**), on the other hand, no more than a final conversion of 4% was observed in any case. Therefore, the use of dppf was proven necessary to make an effective catalyst. The results obtained with complexes **3.1** to **3.13** (5 mol% of Ru and 5 mol% of dppf) are summarised in **Table 5.4.1**.

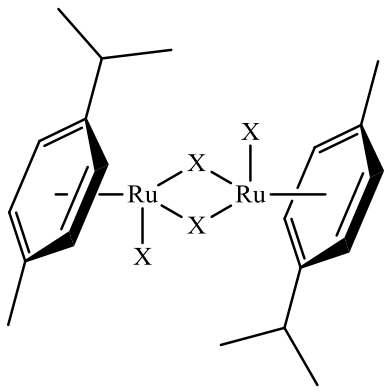

3.1 X = Cl
3.2 X = I

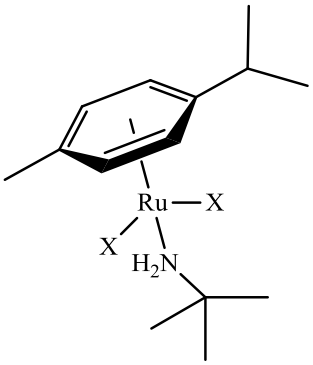

3.3

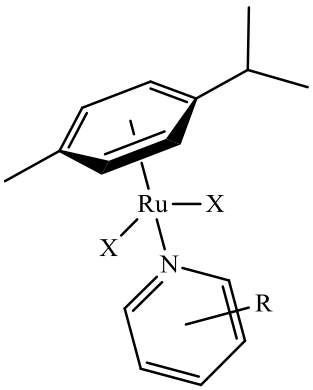

3.4 R = H, X = Cl
3.5 R = H, X = I
3.6 R = 2-NH_2, X = Cl
3.7 R = 3-OH, X = Cl
3.8 R = 3-F, X = Cl
3.9 R = 3-Cl, X = Cl
3.10 R = 3-Br, X = Cl
3.11 R = 3-I, X = Cl
3.12 R = 4-NMe_2, X = Cl
3.13 R = 4-Br, X = Cl

Figure 5.4.1 η^6-*p*-Cymene ruthenium complexes tested for the homogeneous N-alkylation of *tert*-butylamine with phenethyl alcohol using 5 mol% Ru and 5 mol% dppf

		Conversion % after:		
Entry	**Ruthenium species**	**3 hours**	**9 hours**	**24 hours**
1	**3.1**	41.2	87.3	99.7
2	**3.2**	75.3	93.3	99.7
	3.2 (without dppf)	4.7	10.2	11.8
3	**3.3**	19.3	85.3	99.5
4	**3.4**	25.3	86.5	99.7
5	**3.5**	87.5	99.7	99.7
	3.5 (without dppf)	3.1	5.6	8.7
6	**3.6**	31.5	50.1	73.4
7	**3.7**	54.5	78.0	95.2
8	**3.8**	45.1	71.7	97.2
9	**3.9**	33.5	78.0	98.9
10	**3.10**	39.1	80.5	99.3
11	**3.11**	36.8	91.9	99.8
12	**3.12**	17.3	64.1	93.5
13	**3.13**	15.4	87.7	99.0

Table 5.4.1 Summary of conversions obtained with complexes **3.1** to **3.13** after 3, 9 and 24 hours for the N-alkylation of *tert*-butylamine with phenethyl alcohol. The reactions were carried out using 5 mol% Ru and 5 mol% dppf (unless otherwise indicated) in toluene at 110°C

Complexes **3.2** and **3.5** gave the best results also in the presence of dppf. Even though many chloride complexes reached similar conversions after 24 hours, the iodide compounds **3.2** and **3.5** were characterised by much higher reaction rates, affording product yields above 75% after 3 hours (entries 2 and 5 in **Table 5.4.1**). A comparison between these two complexes and their chloride equivalents **3.1** and **3.4**, which only gave 41.2% and 25.3% conversions respectively after the same period of time (entries 1 and 4), can be best seen in **Figure 5.4.2**. Varying the halide ligands in transition metal complexes may indeed change their activity and properties due to the combination of both steric and electronic factors.[10] Examples of bromide complexes being more active than the analogous chloride ones had previously been observed within the McGowan group in anticancer trials.[11]

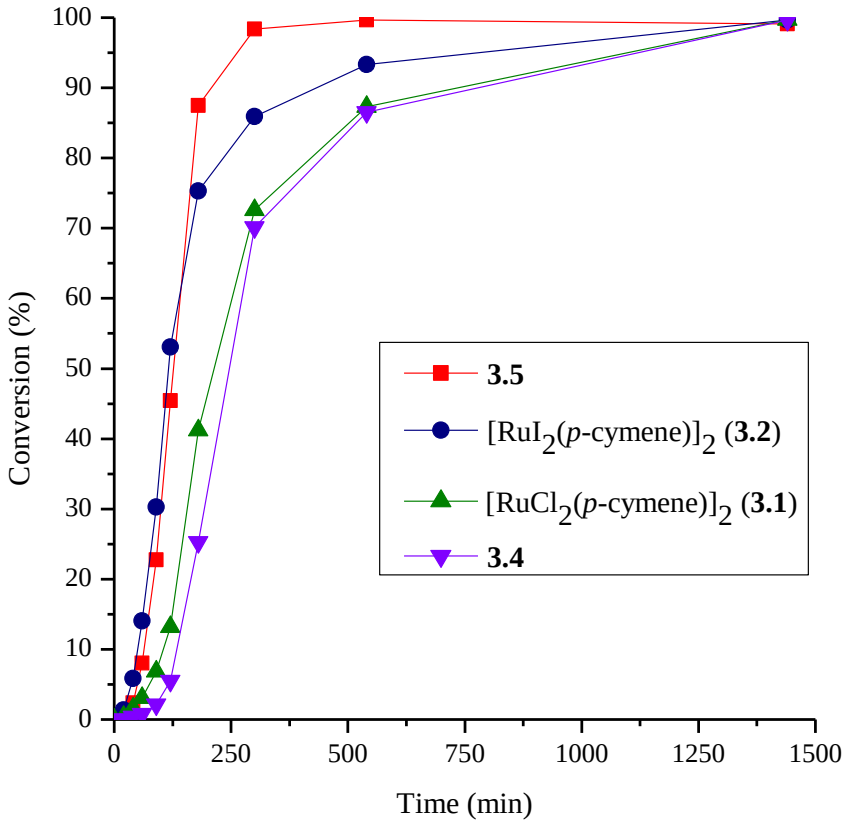

Figure 5.4.2 Catalytic activity of complexes **3.1** vs. **3.2** and **3.4** vs. **3.5** (5 mol% Ru and 5 mol% dppf) against the redox neutral alkylation of *tert*-butylamine with phenethyl alcohol, monitored over 24 hours by GC

Between the two iodide complexes, the dimer **3.2** dropped activity before the monomer **3.5**, so after 3 hours **3.5** seemed to be the only species maintaining its fast rate

(entries 2 and 5 in **Table 5.4.1** and **Figure 5.4.2**). Clear differences can also be noticed for the chloride compounds; complexes **3.6** and **3.12** were particularly slow and gave low conversions even after 24 hours (entries 6 and 12), whereas **3.11** reached almost 92% conversion after 9 hours, being the fastest complex among the chloride ones (entry 11). These variations could be due to the presence of different pyridines in the reaction media, after de-coordination from ruthenium to allow the formation of the active species with dppf.

For instance, one notable case is that of the 3-halopyridine complexes (**3.8** to **3.11**). For these four compounds, the activity decreased in the order **3.11** > **3.10** > **3.9** > **3.8**, mainly in the range between 300 and 1440 minutes, as shown in **Figure 5.4.3**. In other words, the iodide substitution in the pyridine resulted in a better performance than, successively, the bromide, chloride and fluoride substitutions at the same position. The catalytic activity of these complexes was related to several properties of their halides such as electronegativity or covalent radii, and to the pK_a of their pyridines. **Figure 5.4.4** shows these three features plotted against the areas under the curves from **Figure 5.4.3** for each complex, as a rough relative indicator of catalytic activity. These areas were approximated using the "trapezoid rule". There is no straight correlation in any of the cases, which probably indicates a combination of factors (sterics and electronics) influencing the effect of the pyridines on the catalytic activity.

For the reductions of benzaldehyde with complex **3.1**, the reactions were carried out with either dppf or TsDPEN, and sometimes in the presence of the base triethylenediamine (Et_3N). The results are presented in **Figure 5.4.5** and summarised in **Table 5.4.2**. 100% conversions were obtained in the presence of Et_3N with the two ligands after 24 hours, but the addition of dppf instead of TsDPEN gave much faster reactions, both with and without Et_3N (entries 1-4 in **Table 5.4.2**) Despite this, TsDPEN presents a different advantage, which is that it could be used for asymmetric transformations, although in the case of benzaldehyde that is not a concern. When no ligand was used, complex **3.1** still gave moderate activities, as opposed to the case of the N-alkylation, and it is noteworthy that the single presence of Et_3N improved the activity substantially (entries 5 and 6). Some control experiments without any ruthenium species were also performed, and benzaldehyde was recovered unchanged after 24 hours, indicating that the ligands are not active by themselves.

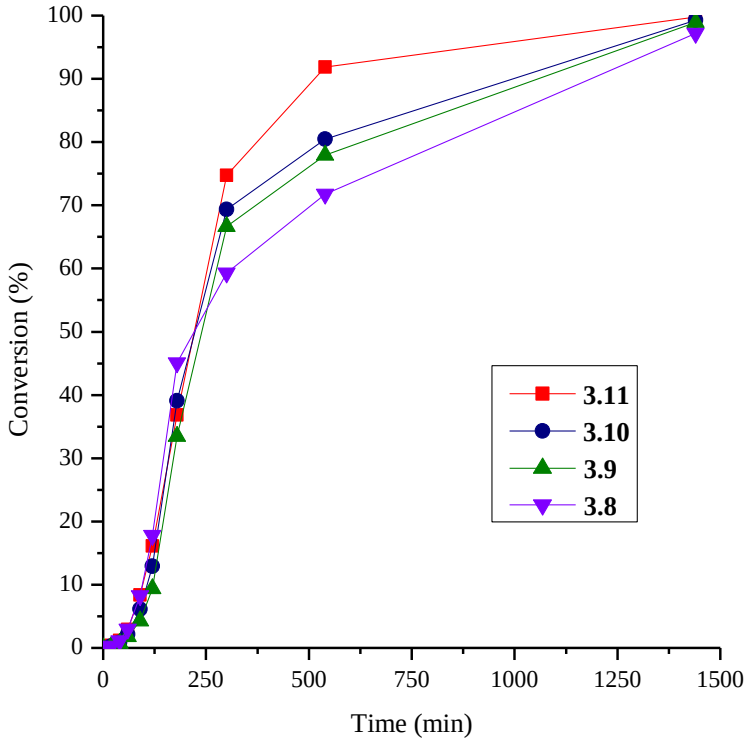

Figure 5.4.3 Catalytic activity of complexes **3.8** to **3.11** (5 mol% Ru and 5 mol% dppf) against the redox neutral alkylation of *tert*-butylamine with phenethyl alcohol, monitored over 24 hours by GC

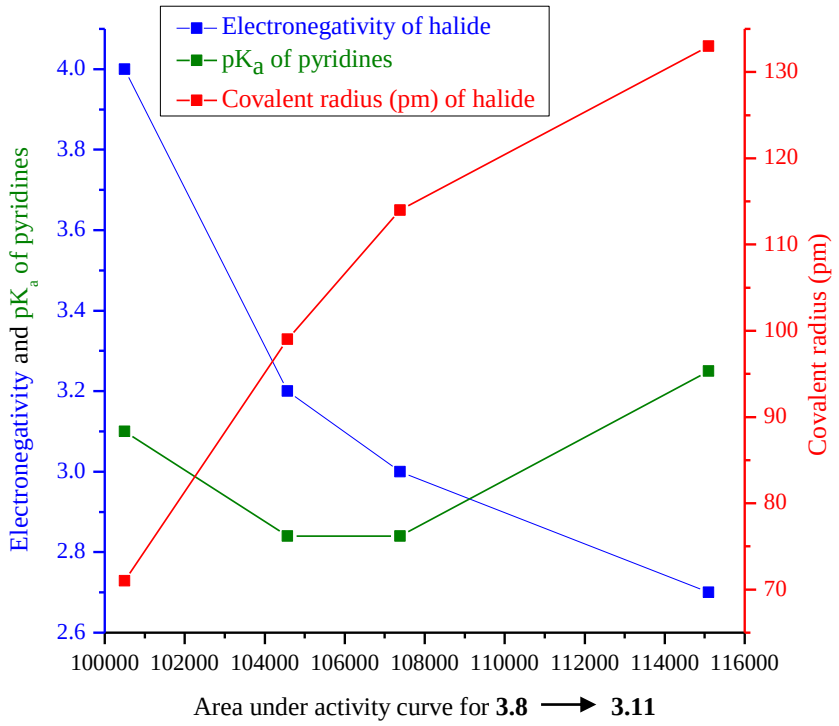

Figure 5.4.4 Electronegativity of halides,[12] pK_a of pyridines[13] and covalent radii of halides[12] against the areas under the catalytic activity curves for complexes **3.8**, **3.9**, **3.10** and **3.11**

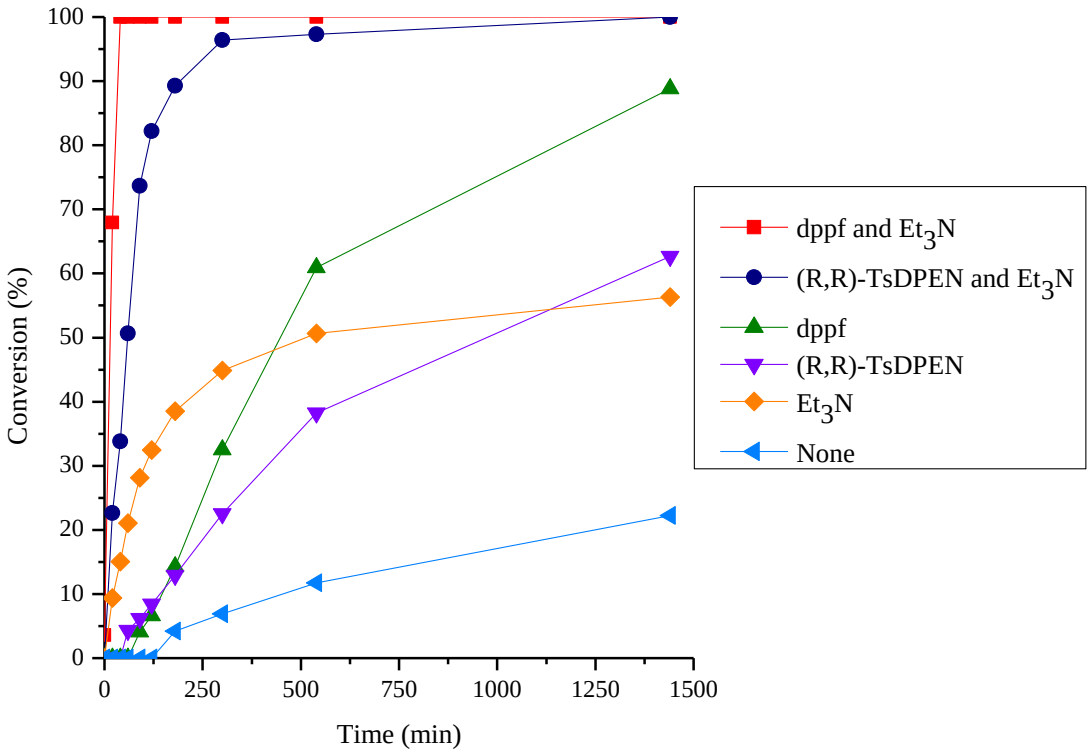

Figure 5.4.5 Catalytic activity of complex **3.1** (5 mol% of Ru) against the reduction of benzaldehyde in refluxing 2-propanol. The additives used in each case are indicated in the legend. The reactions were monitored over 24 hours by GC

				Conv. % after:		
Entry	**Ru species**	**Ligand (5 mol%)**	**Base (8 mol%)**	**3 h**	**9 h**	**24 h**
1	**3.1**	(R,R)-TsDPEN	Et_3N	89.3	97.3	100
2	**3.1**	(R,R)-TsDPEN	-	12.9	38.3	62.7
3	**3.1**	dppf	Et_3N	100	100	100
4	**3.1**	dppf	-	14.3	60.9	88.8
5	**3.1**	-	Et_3N	38.5	50.6	56.3
6	**3.1**	-	-	4.2	11.8	22.2

Table 5.4.2 Summary of conversions obtained with complex **3.1** (5 mol% of Ru) after 3, 9 and 24 hours for the reduction of benzaldehyde in 2-propanol at 85°C in the presence of different additives

5.5 Cp* and Cp$^{\#}$ Ruthenium Complexes

The homogeneous results discussed in this section correspond to the complexes **4.5**, **4.8** to **4.10** and **4.12**, which were introduced in **Chapter 4** (**Figure 5.5.1**). Of those, the Ru-Cp$^{\#}$ compounds (Cp$^{\#}$ = $C_5(CH_3)_4(CH_2)_5OH$) were prepared with the possibility of a covalent attachment to a support in mind.

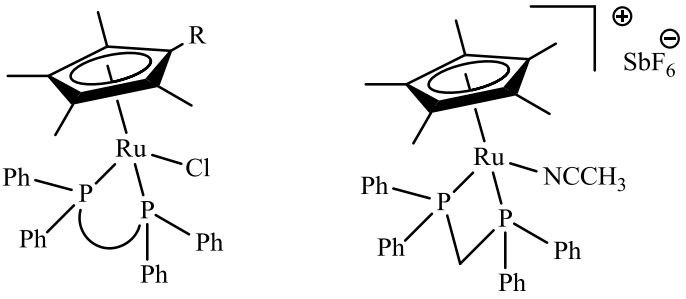

4.5 R = CH_3, PP = dppm
4.8 R = CH_3, PP = Xantphos
4.9 R = $(CH_2)_5OH$, PP = dppm
4.10 R = $(CH_2)_5OH$, PP = dppf

4.12

Figure 5.5.1 Cp* and Cp$^{\#}$ ruthenium complexes tested for the homogeneous N-alkylation of *tert*-butylamine with phenethyl alcohol and the reduction of benzaldehyde

Unfortunately, none of the Ru-Cp* or Ru-Cp$^{\#}$ complexes were active for either the reduction of benzaldehyde or the redox neutral alkylation of *tert*-butylamine with phenethyl alcohol under the catalytic conditions used so far. This is true not only for the neutral complexes (**4.5** and **4.8** to **4.10**), but also for the charged complex **4.12**.

In view of this, another hydrogen transfer reaction was tried: the racemisation of (R,R)-(+)-hydrobenzoin. This was kindly carried out by Mr. Peter Baldwin at the Institute of Process Research and Development (iPRD) at the University of Leeds. The two complexes tested were **4.5** and **4.12** and the conditions used were those shown in **Scheme 5.5.1**. No conversions were observed by Gas Chromatography for this transformation, even though the reaction conditions had been optimised for similar Ru-indenyl complexes.[14] Indenyl and Cp*, which are both η^5-coordination ligands, are considered comparable in size (**Figure 5.5.2**), but it has been generally observed that substitution reactions proceeding by an associative mechanism are faster in metal-indenyl than in metal-Cp/Cp* complexes. Leaving a vacant coordination site around the metal is more favourable for indenyl complexes because they can form η^3-indenyl intermediates that generate a fully aromatic benzene ring.[15-17]

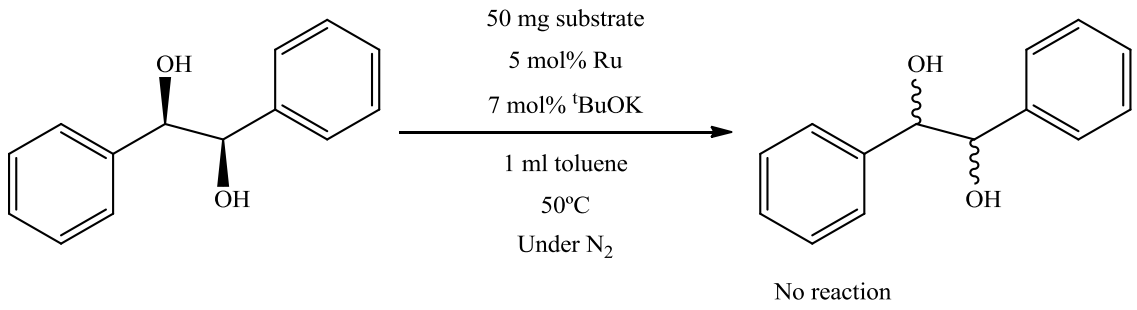

Scheme 5.5.1 Conditions used for the homogeneous racemisation of (R,R)-(+)-hydrobenzoin

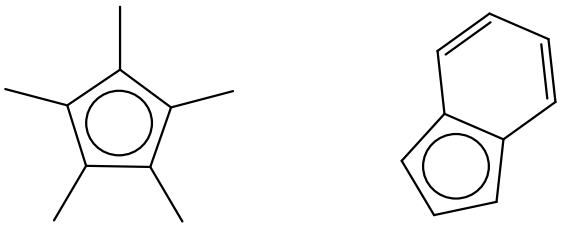

a) b)

Figure 5.5.2 a) Pentamethylcyclopentadienyl and b) indenyl ligands

In order to investigate other related reactions, the complexes **4.5**, **4.6**, **4.7** and **4.8** shown in **Figure 5.5.3** were tested for the homogeneous hydrogenation of N-benzylphthalimide. This transformation needs molecular hydrogen, so it is not a hydrogen transfer reaction like the previous ones. The experiments were carried out at Reaxa Ltd. in a hydrogen pressure vessel, and the conditions used were those depicted in **Scheme 5.5.2**. ^{1}H NMR spectra were taken for each experiment after 24 hours, and they corresponded entirely to the starting N-benzylphthalimide. No conversion was observed for any of the Ru-Cp* complexes tested.

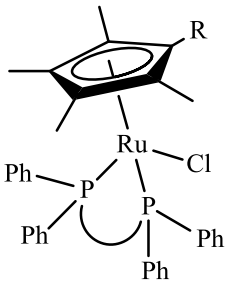

4.5 R = CH_3, PP = dppm
4.6 R = CH_3, PP = dppf
4.7 R = CH_3, PP = DPEphos
4.8 R = CH_3, PP = Xantphos

Figure 5.5.3 Cp* ruthenium complexes tested for the homogeneous hydrogenation of N-benzylphthalimide

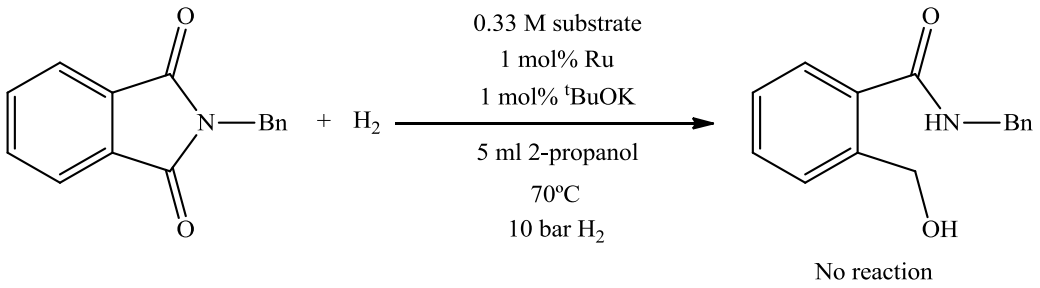

Scheme 5.5.2 Conditions used for the homogeneous hydrogenation of N-benzylphthalimide

The homogeneous hydrogenation of N-benzylphthalimide and other similar transformations has been successfully performed by Ikariya *et al*. using [RuClCp*(P−NH_2)] complexes.[18-20] They claim that P−NH_2 ligands like, for example, $Ph_2P(CH_2)_2NH_2$, and also P−NRH ligands to a lesser extent, are able to accelerate the reaction, as opposed to P−NMe_2 ligands, which are completely ineffective.

5.6 Conclusions

Different functionalised η^6-arene, η^6-*p*-cymene and η^5-Cp* or $Cp^{\#}$ ruthenium complexes have been tested as potential catalysts for homogeneous hydrogen transfer reactions such as the redox neutral alkylation of *tert*-butylamine with phenethyl alcohol, the reduction of benzaldehyde or the racemisation of (R,R)-(+)-hydrobenzoin.

It has been observed that a 1 : 2 mixture of $[RuCl_2(p\text{-cymene})]_2$ and dppf in alcoholic solvents produces the monomer **5.1**, and this is probably the pre-catalyst in the reductions of benzaldehyde, which have been carried out in 2-propanol. On the other hand, 1 : 1 or 1 : 2 mixtures of $[RuCl_2(p\text{-cymene})]_2$ and dppf in toluene yield the dimer **5.2**, where dppf acts as a monodentate bridging ligand. **5.2** is believed to act as pre-catalyst in the N-alkylation studied.

The functionalised η^6-arene ruthenium complexes were active for the N-alkylation of *tert*-butylamine with phenethyl alcohol in the presence of dppf ligand, with **2.3** and **2.7** being particularly good, better than $[RuCl_2(p\text{-cymene})]_2$ (**3.1**). Complex **2.5**, on the other hand, gave the worst conversion.

Among the η^6-*p*-cymene ruthenium pyridine complexes, those containing Ru-I bonds performed much better than those with Ru-Cl bonds for the N-alkylation of *tert*-butylamine with phenethyl alcohol in the presence of dppf. The different pyridines seem to affect the catalytic activity by combinations of steric and electronic factors.

Complex $[RuCl_2(p\text{-cymene})]_2$ was able to catalyse the reduction of benzaldehyde in the presence of Et_3N with either dppf or TsDPEN, but it was much faster with dppf. However, TsDPEN would be the ligand chosen if asymmetric transformations were desired.

The $[RuClCp^{*/\#}(PP)]$ and $[Ru(CH_3CN)Cp^*(PP)]^+$ complexes tested for hydrogen transfer reactions did not give any conversion to the expected products, and the same unfavourable results were obtained when the homogeneous hydrogenation of N-benzylphthalimide with molecular hydrogen was attempted.

5.7 Future Work

Future work in this area of catalysis could include:

- Exploration of the scope for the reactions studied with a range of different other substrates.
- Mechanistic studies for the hydrogen transfer reactions, possibly by isolation or detection of intermediate species, mainly looking out for 16 electron species or metal hydride bonds, which could be detected by ^1H NMR spectroscopy.
- Synthesis of $[RuClCp^{\#}(PPh_3)_2]$ complexes, to check if the presence of a chelating diphosphine is affecting the catalytic activity.
- Synthesis of $[RuClCp^{\#}(P{-}NH_2)]$ complexes, which are long chain analogues of the $[RuClCp^*(P{-}NH_2)]$ compounds that, according to Ikariya and co-workers, are active for hydrogenations,[18-20] and would offer an –OH tethered arm for later immobilisation.
- Study of new reactions that could be performed with Ru-Cp* and Ru-Cp$^{\#}$ complexes, like the Kharasch-type reactions, which are atom-transfer radical additions (ATRA) of halogenated compounds to olefins, and have been successfully carried out with $[Ru^{III}Cp^*Cl_2PPh_3]$ and $[Ru^{II}Cp^*Cl(PPh_3)_2]$ complexes.[21]

5.8 References

1. M. H. S. A. Hamid and J. M. J. Williams, *Chemical Communications*, 2007, 725-727.

2. M. H. S. A. Hamid, C. L. Allen, G. W. Lamb, A. C. Maxwell, H. C. Maytum, A. J. A. Watson and J. M. J. Williams, *Journal of the American Chemical Society*, 2009, **131**, 1766-1774.
3. J. Fonseca and P. C. McGowan, *Unpublished results*.
4. S. B. Jensen, S. J. Rodger and M. D. Spicer, *Journal of Organometallic Chemistry*, 1998, **556**, 151-158.
5. J.-F. Mai and Y. Yamamoto, *Journal of Organometallic Chemistry*, 1998, **560**, 223-232.
6. T. Sixt, J. Fiedler and W. Kaim, *Inorganic Chemistry Communications*, 2000, **3**, 80-82.
7. T. Sixt, M. Sieger, M. J. Krafft, D. Bubrin, J. Fiedler and W. Kaim, *Organometallics*, 2010, **29**, 5511-5516.
8. L. A. Paim, F. M. Dias, H. G. L. Siebald, J. Ellena, J. D. Ardisson, M. M. da Silva and A. A. Batista, *Polyhedron*, 2012, **42**, 110-117.
9. F. Estevan, P. Lahuerta, J. Latorre, A. Sánchez and C. Sieiro, *Polyhedron*, 1987, **6**, 473-478.
10. K. Fagnou and M. Lautens, *Angewandte Chemie International Edition*, 2002, **41**, 26-47.
11. A. Hebden, B. Crossley and P. C. McGowan, *Personal communication*.
12. C. E. Housecroft and E. C. Constable, *Chemistry*, 2nd edn., 2002.
13. *http://research.chem.psu.edu/brpgroup/pka_compilation.pdf, accessed on December 2012*.
14. P. Baldwin and J. Blacker, *Personal communication*.
15. J. W. Faller, R. H. Crabtree and A. Habib, *Organometallics*, 1985, **4**, 929-935.
16. J. M. O'Connor and C. P. Casey, *Chemical Reviews*, 1987, **87**, 307-318.
17. L. F. Veiros, *Organometallics*, 2000, **19**, 3127-3136.
18. M. Ito, A. Sakaguchi, C. Kobayashi and T. Ikariya, *Journal of the American Chemical Society*, 2007, **129**, 290-291.
19. M. Ito, C. Kobayashi, A. Himizu and T. Ikariya, *Journal of the American Chemical Society*, 2010, **132**, 11414-11415.
20. M. Ito, T. Ootsuka, R. Watari, A. Shiibashi, A. Himizu and T. Ikariya, *Journal of the American Chemical Society*, 2011, **133**, 4240-4242.
21. M. A. Fernández-Zúmel, K. Thommes, G. Kiefer, A. Sienkiewicz, K. Pierzchala and K. Severin, *Chemistry – A European Journal*, 2009, **15**, 11601-11607.

Chapter 6

Anticancer Activity Evaluation

6.1 Introduction

Some diphosphines have demonstrated cytotoxicity against various cell lines, and their activity seems to be related to their autoxidation capabilities.[1] For example, ethyl-substituted phosphines oxidise much more rapidly than phenyl-substituted phosphines, and, while the latter show anticancer potency, the former are inactive.[1] It has been observed that, upon coordination to metals (principally gold), diphosphines produce complexes with improved anticancer activity compared to the free ligands. A general hypothesis considers that gold protects the ligands from oxidation before they interact with the corresponding biological target.[2] A few groups have reported gold(I) complexes of the types $[(AuX)_2L]$ and $[AuL_2]X$ (L = diphosphine, commonly 1,2-bis(diphenylphosphino)ethane (dppe), X = Cl or a deprotonated N-heterocyclic ring system), which have been tested both *in vitro* and *in vivo* with promising results.[3-5]

Hetero tri- and bimetallic complexes where the diphosphine is a titanocene dichloride species coordinated to either gold, platinum or palladium have also been reported (**Figure 6.1.1**), and their cytotoxicity said to be higher than that of Cp_2TiCl_2.[6]

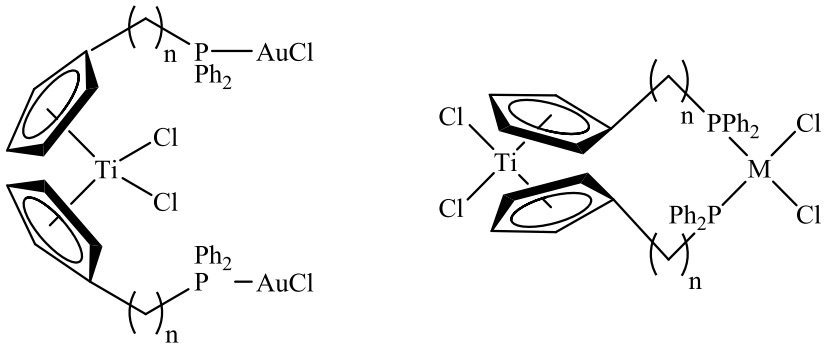

Figure 6.1.1 Cytotoxic tri- and bimetallic $TiAu_2$ and TiM (M = Pd or Pt) complexes

The cytotoxicity of complexes of ruthenium with diphosphines has not been so widely studied. Samuelson and co-workers have published the use of η^6-*p*-cymene ruthenium complexes with different diphosphines acting as either monodentate or chelating ligands, which showed good growth inhibitions against several cancer cell lines (IC_{50} values against the lung cancerous H460 cell line ranged from 1.6 to 22.1 μM, compared to 1.7 μM for cisplatin, after 48 hours)[7] This investigation proved

again that partial oxidation of the diphosphines reduces their anticancer activity, while coordination generally has the opposite effect.

Among the (η^6-arene)-ruthenium complexes screened as anticancer agents, two principal groups stand out as the most promising, which are the [(η^6-arene)Ru(NN)Cl]$^+$ complexes (NN = chelating σ-donor nitrogen ligands, especially ethylenediamine (en)), initially developed by Sadler's group,[8] and the [(η^6-arene)Ru(pta)Cl_2] (RAPTA) complexes (pta = 1,3,5-triaza-7-phosphatricyclo [3.3.1.1] decane), largely studied by Dyson and co-workers[9] (**Figure 6.1.2**). For [(η^6-arene)Ru(en)Cl]$^+$ complexes, it has been observed that more hydrophobic and larger arenes, especially fused systems, such as tetrahydroanthracene, improve cytotoxicity results to a large degree.[10, 11] In the case of the RAPTA complexes, their activity has been demonstrated to be pH-dependent. The pK_a of [(η^6-*p*-cymene)Ru(pta)Cl_2] is approximately 6.5, which means that the predominant species at physiological pH is neutral and can easily be transported through the lipid membranes, but the pH is generally lower in cancer cells, where the pta ligand will be protonated, and electrophoresis has shown that protonated species induce DNA damage more rapidly than their neutral analogues.[12] In the McGowan group, several Ru-arene complexes containing different N,N- or N,O-coordinating picolinamide or ketoiminate ligands have been tested, which resulted in promising activities that vary with the binding mode adopted by the corresponding ligand.[13-15]

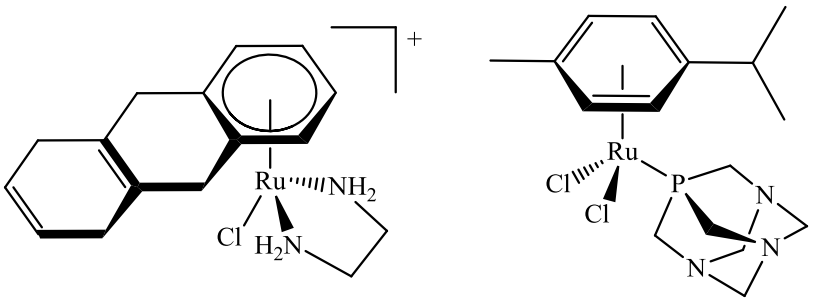

a) b)

Figure 6.1.2 Structures of a) [(η^6-tetrahydroanthracene)Ru(en)Cl]$^+$ and b) [(η^6-*p*-cymene)Ru(pta)Cl_2] (RAPTA-C)

In contrast to the numerous efforts in the evaluation of η^6-arene ruthenium complexes as anticancer agents, fewer examples have been studied with

cyclopentadienyl (Cp) or pentamethylcyclopentadienyl (Cp*) compounds. For instance, the group of Sava reported the synthesis of the compounds [(η^5-C_5H_5)Ru(pta)$_2$Cl] and [(η^5-C_5Me_5)Ru(pta)$_2$Cl], as equivalents to the RAPTA complexes, and observed that, while the Cp* complex inhibits the proliferation of TS/A murine adenocarcinoma tumour cells, the Cp analogue does not.[16] Compounds of the type [(η^5-C_5H_5)Ru(PP)L][X], where PP = 2 × PPh_3 or dppe, L = planar nitrogen σ-bonded ligand and X = CF_3SO_3 or PF_6, have been synthesised by Moreno *et al*. and some of them show better cytotoxicities (IC_{50} = 0.38-2.26 μM against leukaemia HL-60 cancer cells after 72 hours) than cisplatin (IC_{50} = 2.15 μM).[17-19] Other examples with Cp* include the complexes of rhodium [(η^5-C_5Me_5)Rh(pta)Cl_2] and [(η^5-C_5Me_5)Rh(pta)$_2$Cl]$^+$, which even surpass the activity of [(η^6-*p*-cymene)M(pta)Cl_2] (M = Ru or Os) against certain cell lines.[20]

It has been observed that ruthenium compounds are, in general, less toxic than platinum drugs, *i.e.* more selective towards cancer cells.[9] Ruthenium normally accumulates in rapidly dividing cells, such as tumour cells, because it mimics the behaviour of iron and binds transferrin, which is the protein responsible for delivering iron to cells and is over-expressed in cancerous cells due to their higher iron requirements for fast proliferation.[9] The other speculative explanation is that ruthenium(III) species (such as NAMI-A or KP1019), which are less active, can be reduced *in vivo* in the hypoxic environment of tumours to produce ruthenium(II) species (with increased lability of Ru(II)-Cl bonds).[21]

There are some common features in the aqueous chemistry of organometallic ruthenium(II) and diamine platinum(II) chloride anticancer complexes. Organometallic ruthenium complexes also tend to bind DNA, and this interaction is stabilised through hydrogen-bonding and π-π stacking of the arene or cyclopentadienyl ligands with nucleobases (favoured with big fused arene systems).[11] For this to happen, the Ru-Cl species needs to be "activated" by hydrolysis, so the Cl^- labile ligand(s) is replaced by H_2O, because Ru-OH_2 complexes react faster than their Ru-Cl analogues with the corresponding biological targets. This hydrolysis is greatly suppressed in media with high chloride concentrations, like blood plasma, where [Cl^-] is approximately 100 mM, but is favoured in the intracellular medium, with [Cl^-] of 23 mM in the cytoplasm and 4 mM inside the nucleus.[22, 23]

Compounds of iron, in particular, ferrocene-derivatives, also show exploitable properties as anticancer agents, and some examples include ferrocifen, which was firstly synthesised by Jaouen and co-workers as an alternative to tamoxifen[24], and ferricenium ions.[25] As with ruthenium, iron has the advantage of low general toxicity, and these two metals have in fact been combined in complexes tested by Dyson's group with moderate cytotoxicity results.[21, 26]

This chapter presents the results from cell line assays carried out with ruthenium complexes of general structures [RuCp*(PP)X], [RuCp$^{\#}$(PP)X] (Cp$^{\#}$ = $C_5Me_4(CH_2)_5OH$) or [RuCp*(PP)L][Z], where X = Cl, Z = SbF_6, L = CH_3CN and PP are diphosphine ligands, one of them being the ferrocene-derivative dppf (1,1'-bis(diphenylphosphino)ferrocene).

6.2 Cytotoxicity Screening Assays

The MTT colorimetric assay was developed by T. Mosmann as a quantitative way of measuring mammalian cell survival and proliferation.[27] It is based on the pale yellow salt 3-(4,5-dimethylthiazol-2-yl)-2,5-diphenyl tetrazolium bromide (MTT), which accepts electrons from substrates such as NADH or NADPH, producing a reduced formazan product, which is dark blue (**Scheme 6.2.1**).[28] It has been suggested that MTT reduction occurs mainly at the mitochondria, but it might take place at multiple active cellular sites.[29] This assay only detects living cells, and is still one of the most commonly used for determination of cell survival in drug screening protocols *in vitro*.

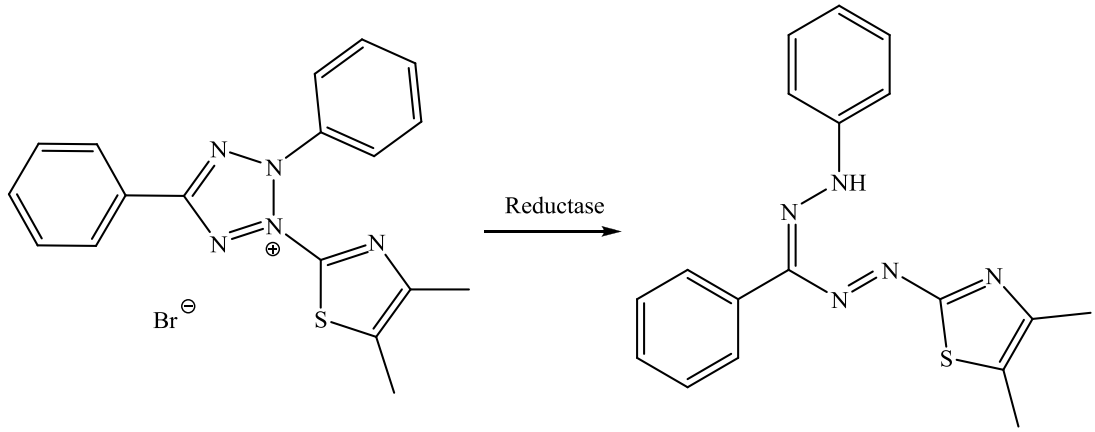

Scheme 6.2.1 Reduction of MTT to formazan

The drugs tested during this project were incubated with the cancer cells for five days at 37ºC, at concentrations ranging from 250 to 0.49 μM. MTT was added as a solution in distilled water (5 mg/ml) to each well plate after drug exposure, and incubated for a further three hours, when the reduction to formazan occurred. The cell medium was then removed and the formazan crystals dissolved in dimethylsulfoxide (DMSO), and these solutions used to measure the absorbance at a wavelength of 540 nm to determine cell survival. The results are expressed as IC_{50} values, which are the half maximal inhibitory concentrations, *i.e.* the concentration of each complex needed to kill half of the cells. These values were obtained from plots of percentage cell survival against drug concentration (μM), like the example in **Figure 6.2.1**. Each IC_{50} number was obtained as the average from three assays, which were performed by Miss Rianne Lord (HT-29) and Miss Aida Basri (A2780).

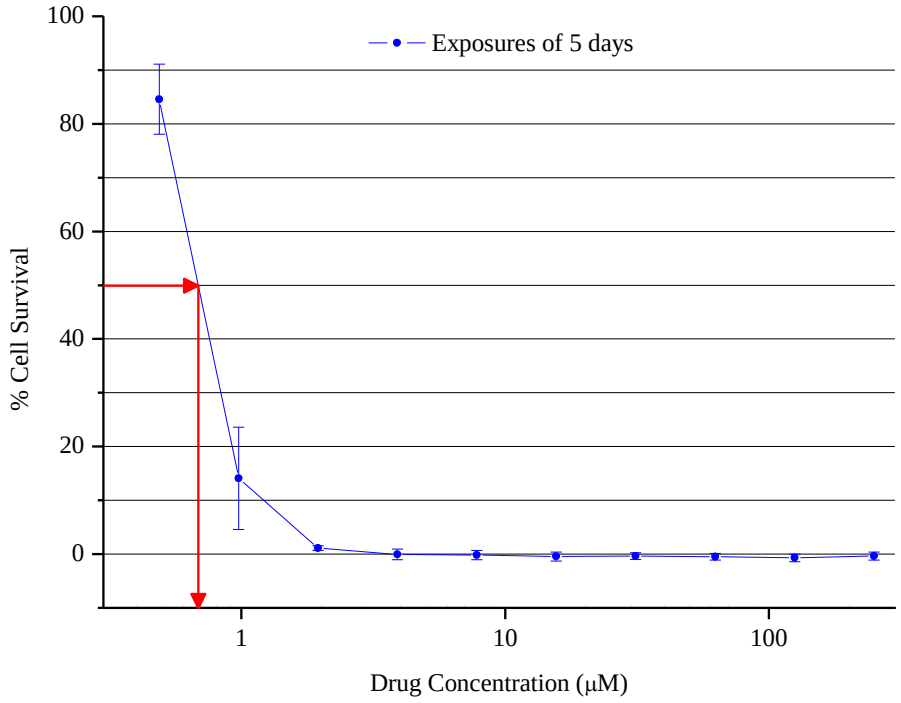

Figure 6.2.1 % Cell survival versus drug concentration (logarithmic scale) for complex **4.5** against the cell line HT-29 after exposures of five days

No reaction between the complexes tested and DMSO has been observed by ^{1}H NMR spectroscopy in deuterated DMSO after a period of five days, but some of the compounds did not dissolve completely in the DMSO/media mixture used for the cell line assays. This is detailed later on in the results section.

6.3 Results and Discussion

6.3.1 Introduction

Some of the Cp* and Cp$^{\#}$ diphosphine-ruthenium(II) complexes (**4.5**, **4.6** and **4.8** to **4.12**) presented in **Chapter 4** (**Figure 6.3.1**), together with the corresponding free diphosphines (**Figure 6.3.2**) and cisplatin as a reference have been tested as potential anticancer agents against the cell lines HT-29 (colon cancerous cells) and A2780 (ovarian cancerous cells), with exposures of five days at 37ºC. This allows for a comparison of the activities of free and coordinated diphosphines. The effect of the $-(CH_2)_5OH$ chain in the Cp$^{\#}$ ruthenium complexes is also analysed. Complexes **4.5** and **4.12** have been used for NMR spectroscopy studies in mixtures of 90% deuterated dimethylsulfoxide and 10% deuterium oxide to determine the extent of ligand-exchange reactions from either chloride or acetonitrile ligands to yield a hydrolysed product, and how this is related to their anticancer activity.

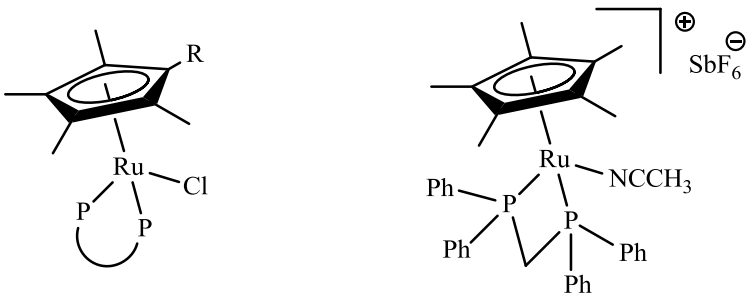

4.5 R = CH_3, PP = dppm
4.6 R = CH_3, PP = dppf
4.8 R = CH_3, PP = Xantphos
4.9 R = $(CH_2)_5OH$, PP = dppm
4.10 R = $(CH_2)_5OH$, PP = dppf
4.11 R = $(CH_2)_5OH$, PP = Xantphos

4.12

Figure 6.3.1 Cp* and Cp$^{\#}$ ruthenium complexes tested as anticancer agents against the cell lines HT-29 and A2780

6.3.2 Cytotoxicity IC_{50} Values

The IC_{50} results for cisplatin, dppm, dppf, Xantphos and the ruthenium complexes after five-day exposures are presented in **Table 6.3.1**, **Figure 6.3.3** and **Figure 6.3.4**. Although the cytotoxicity trends are repeated in both cell lines, the

compounds tested gave, in general, better results against the A2780 ovarian cancerous cells.

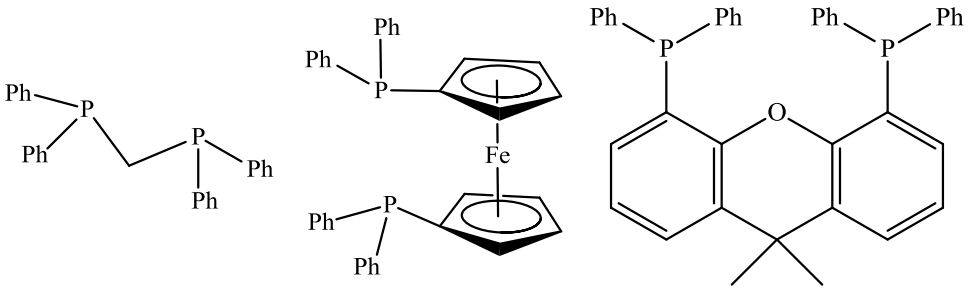

Figure 6.3.2 Structures of a) dppm, b) dppf and c) Xantphos

	IC_{50} Values After 5-Day Exposures (μM)			
Compound	**HT-29 (Colon)**	**±**	**A2780 (Ovarian)**	**±**
Cisplatin	2.52	0.09	1.4	0.3
dppm	1.47	0.02	1	1
4.5	0.73	0.05	1.1	0.2
4.9	0.791	0.007	0.9	0.1
4.12	0.61	0.01	0.70	0.02
dppf	11.6	0.7	0.4	0.4
4.6	>250	-	40	10
4.10	20	1	11.9	0.3
Xantphos	>250	-	>250	-
4.8	10.1	0.5	3.6	0.4
4.11	11.9	0.7	4.0	0.3

Table 6.3.1 IC_{50} values for Cp* and $Cp^{\#}$ diphosphine-ruthenium complexes, cisplatin, dppm, dppf and Xantphos against the HT-29 and A2780 cell lines after exposures of five days

Dppf and the complexes **4.6** and **4.10**, formed with this ligand, had very low solubilities in the mixture DMSO/media used for the cell line assays, and precipitation was observed in the plates used for the *in vitro* studies, which implies less accuracy in those particular IC_{50} concentrations. Despite not having been quantified, complex **4.6** seemed less soluble than **4.10**, probably because of the –OH polar group in **4.10**. All of the values have been calculated from an average of three assays.

The most active complexes were those with the ligand dppm (**4.5**, **4.9** and **4.12**), all with better cytotoxicities than cisplatin for both HT-29 and A2780 cell

lines. It can be seen that dppm is very active by itself and it is still unclear whether the activity of the aforementioned complexes comes mostly from the ligand. However, ^{1}H and ^{31}P NMR spectroscopy experiments in deuterated DMSO showed no de-coordination of dppm from complexes **4.5** and **4.12** after five days. Compounds **4.8** and **4.11** with the ligand Xantphos presented moderate to good activities, despite the ligand not being active in this case, but they did not improve on cisplatin. This shows that the coordination of Xantphos to ruthenium increases the anticancer activity to a large degree. Complexes **4.6** and **4.10** did not seem to surpass the activity of dppf alone, but the lack of solubility makes these results hardly comparable.

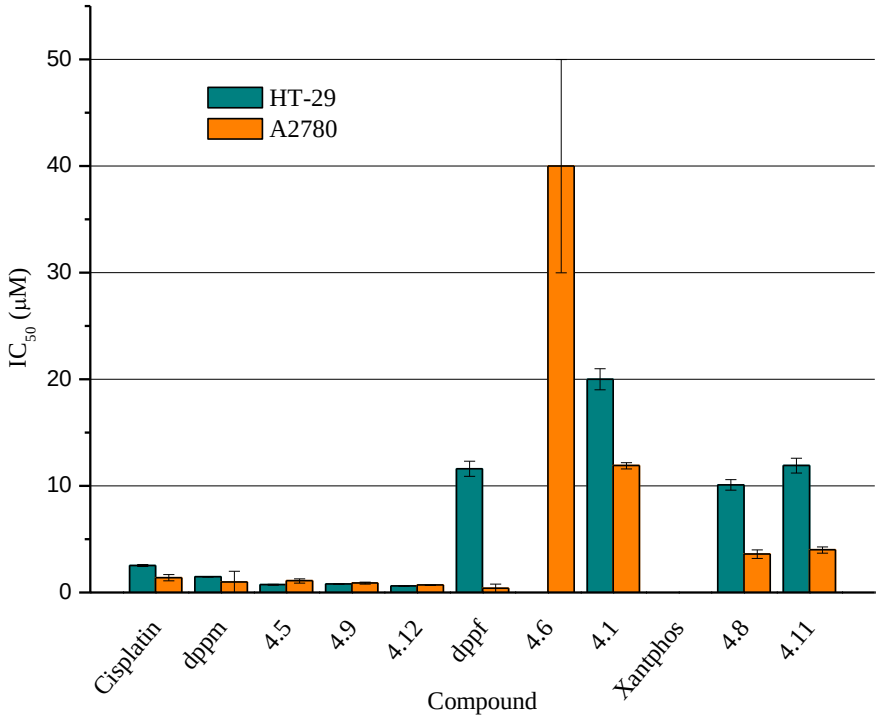

Figure 6.3.3 IC_{50} values for Cp* and $Cp^{\#}$ diphosphine-ruthenium complexes, cisplatin, dppm, dppf and Xantphos against the HT-29 and A2780 cell lines after exposures of five days. The blank spaces indicate no activity

Except in the case of the dppf complexes **4.6** and **4.10** where solubility might be an issue, the $–(CH_2)_5OH$ chain in the $Cp^{\#}$ compounds produced no great effect on the anticancer activity, as can be seen within the couples **4.5**-**4.9** and **4.8**-**4.11**. The presence of CH_3CN in complex **4.12**, on the other hand, improved considerably its cytotoxicity in comparison to that of **4.5**. This may be either the result of faster

hydrolysis of the CH_3CN group (see below) or better solubility of **4.12**, which is a charged (monocationic) species.

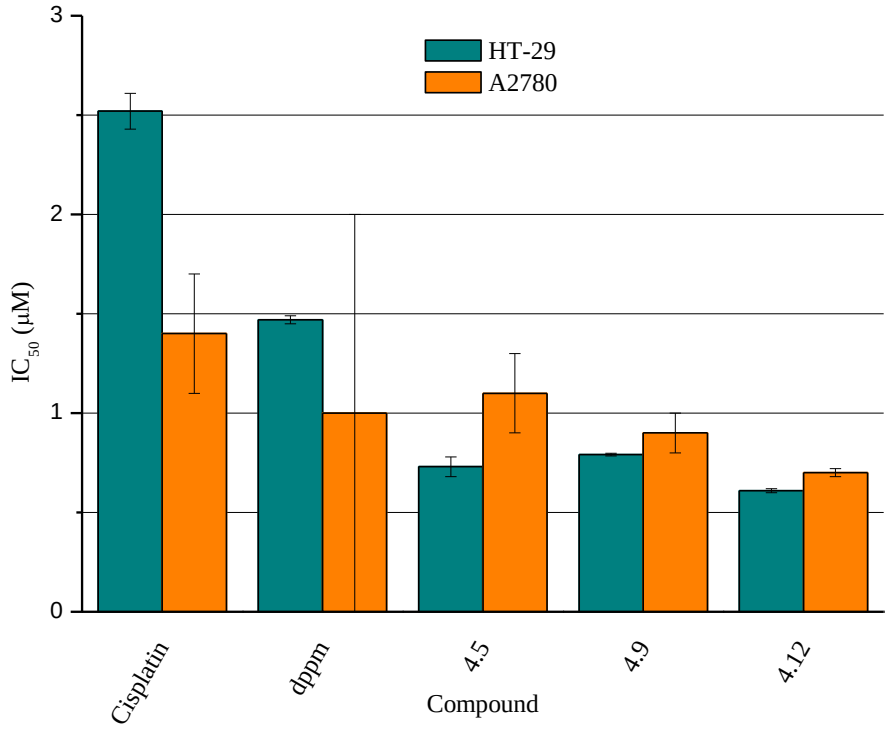

Figure 6.3.4 Enlargement of **Figure 6.3.3** for the compounds with better activities than cisplatin

6.3.3 Hydrolysis Studies

10 μM samples of complex **4.5** and complex **4.12** in 0.6 ml of deuterated solvent (90% deuterated DMSO + 10% deuterium oxide) were prepared in NMR tubes and analysed by ^1H NMR spectroscopy every 24 hours during five days at room temperature. The results are shown in **Figure 6.3.5** and **Figure 6.3.8** respectively, with enlargements of different sections of the spectra in **Figure 6.3.6**, **Figure 6.3.7**, **Figure 6.3.9** and **Figure 6.3.10**. The peaks at 2.50 and 3.68 ppm are residual DMSO and H_2O. When higher percentages of deuterium oxide were tried in the mixture, complex **4.5** could not be dissolved or, with a 20% of D_2O, it crystallised in the NMR tube after one day, indicating a lower solubility than that of the cationic complex **4.12**.

Complex **4.5** gave, initially, a triplet at 1.56 ppm for the Cp* methyl protons and two doublets of triplets at 3.95 and 5.15 ppm for the CH_2 protons of dppm

(**Figure 6.3.5**). After five days, a new set of peaks at 5.14 and 1.61 ppm appeared (**Figure 6.3.6** and **Figure 6.3.7**). The fresh sample of complex **4.12** gave peaks at 1.50 ppm for the Cp* methyl protons, at 1.76 ppm for the CH_3 protons in the coordinated acetonitrile and at 4.52 and 5.33 ppm for the CH_2 protons of dppm (**Figure 6.3.8**). After five days, a new set of peaks at 5.14, 2.03 (free acetonitrile) and 1.61 ppm appeared (**Figure 6.3.9** and **Figure 6.3.10**). The new peaks coincide in both experiments, and they belong to the hydrolysed species $[RuCp^*(dppm)(OH_2)]^+$ (**6.1**, further characterisation in **Chapter 7**). From integrations of the NMR peaks, this new species forms, after five days, in 48% yield from complex **4.5** and in 67% yield from complex **4.12**, which hydrolyses to a higher extent under the same conditions, and this coincides with the higher anticancer activity of compound **4.12**. **Figure 6.3.11** shows a plot of the IC_{50} values of **4.5** and **4.12** for both cell lines against the percentages of hydrolysed complex **6.1** obtained during these experiments.

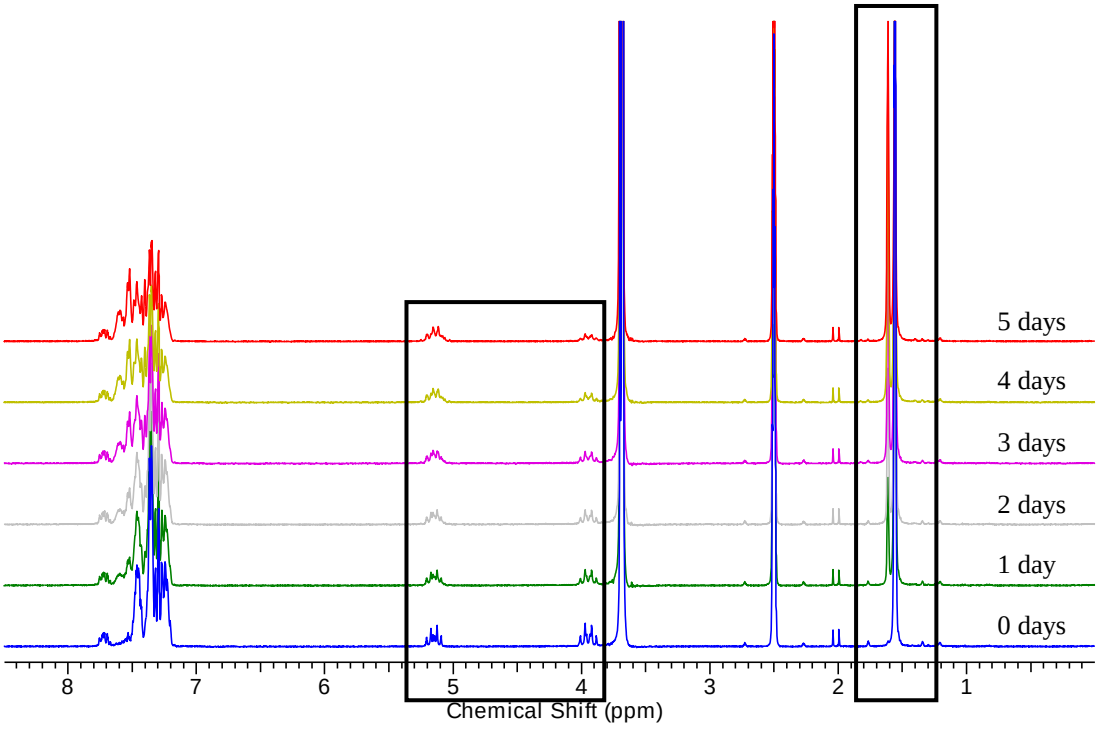

Figure 6.3.5 ^1H NMR spectra of complex **4.5** (10 μM) in 90% deuterated DMSO + 10% D_2O after 0, 1, 2, 3, 4 and 5 days at room temperature

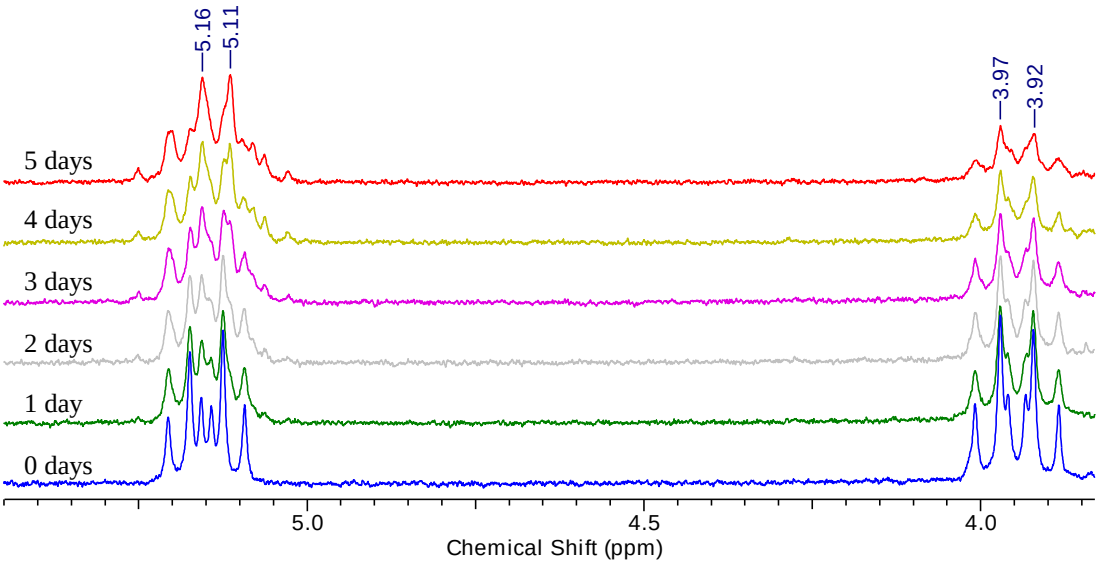

Figure 6.3.6 Enlargement of **Figure 6.3.5** in the CH_2 area

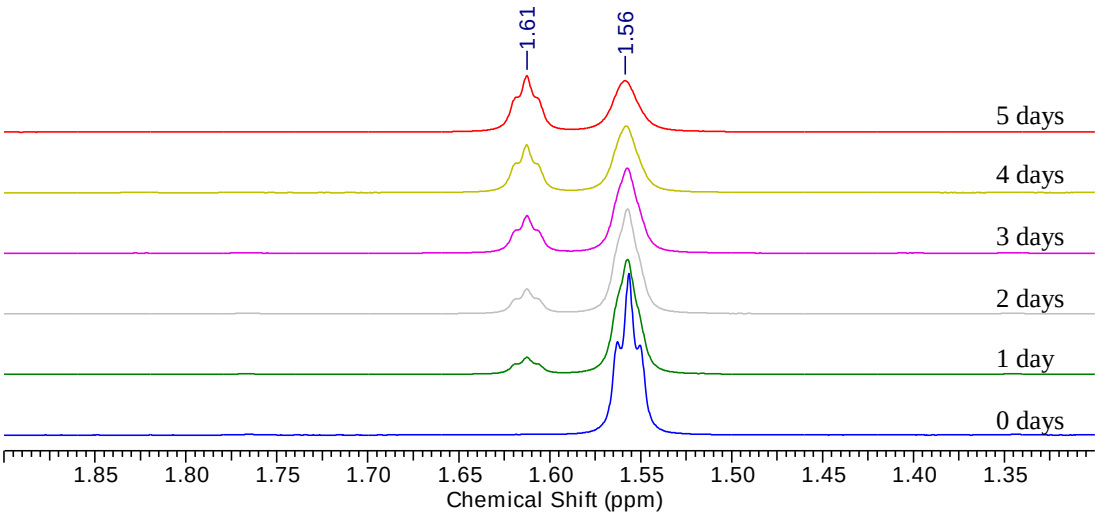

Figure 6.3.7 Enlargement of **Figure 6.3.5** in the Cp* area

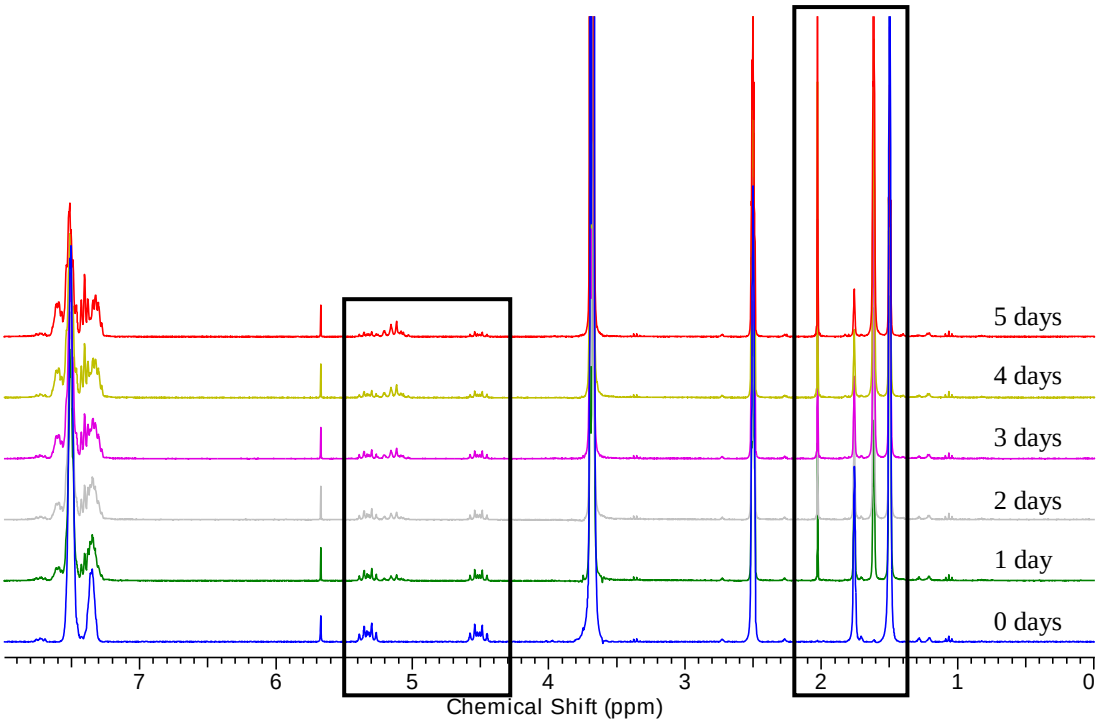

Figure 6.3.8 ^{1}H NMR spectra of complex **4.12** (10 μM) in 90% deuterated DMSO + 10% D_2O after 0, 1, 2, 3, 4 and 5 days at room temperature

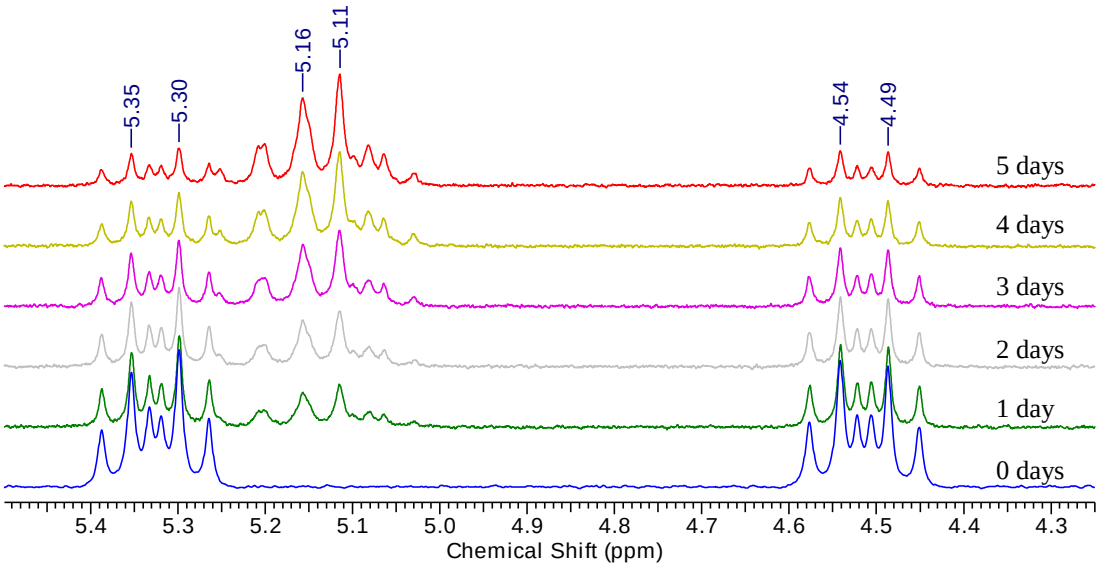

Figure 6.3.9 Enlargement of **Figure 6.3.8** in the CH_2 area

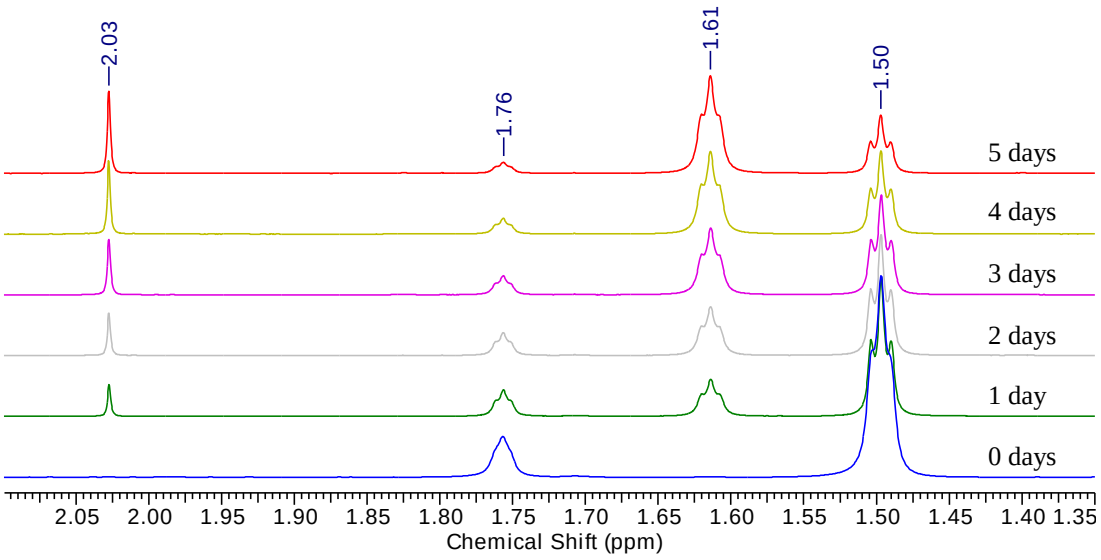

Figure 6.3.10 Enlargement of **Figure 6.3.8** in the Cp* and CH_3 (acetonitrile) area

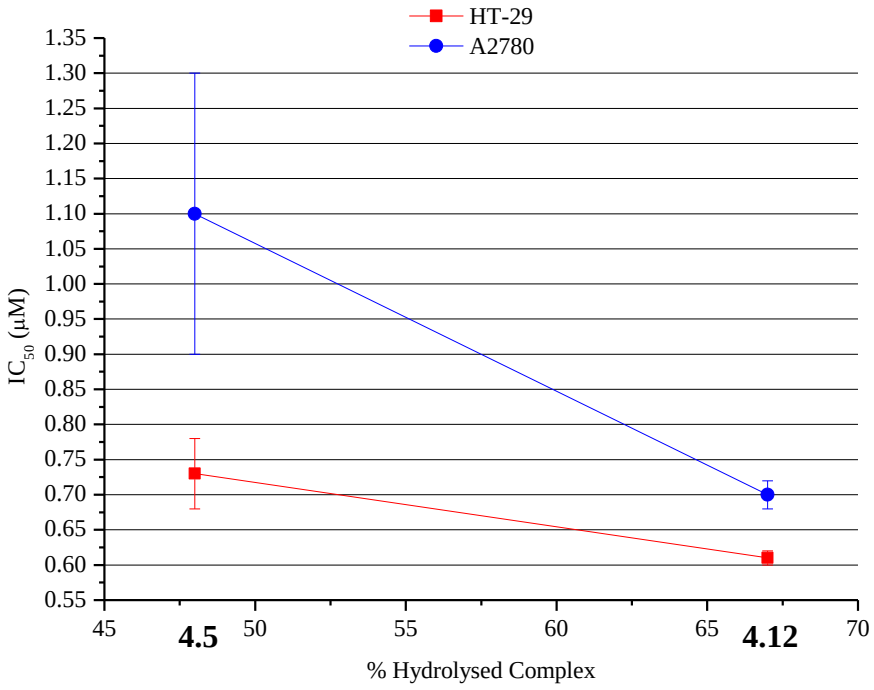

Figure 6.3.11 IC_{50} values of compounds **4.5** and **4.12** for the cell lines HT-29 and A2780 against the percentages of hydrolysed species **6.1** obtained from each complex in the NMR experiments

6.4 Conclusions

A series of RuCp* and RuCp$^{\#}$ (Cp$^{\#}$ = $C_5Me_4(CH_2)_5OH$) complexes bearing diphosphines as chelating ligands have been tested *in vitro* against the cancerous cell lines HT-29 and A2780, and the corresponding cytotoxicity values obtained using the MTT colorimetric assay after exposures of five days.

The complexes with the ligand dppm showed the best anticancer activities, probably due to the intrinsic cytotoxicity of free dppm. All of these complexes improved on the performance of cisplatin. On the other hand, it was demonstrated that the coordination of the diphosphine Xantphos reduces the IC_{50} values very significantly, because this compound is not cytotoxic by itself. The complexes with the ligand dppf showed very low solubilities in the mixture DMSO/media used for the assays and so the results cannot really be compared with those of the other PP ligands.

The complexes with Cp$^{\#}$ did not introduce any appreciable improvement with respect to those with Cp*. However, changing the chloride ligands for acetonitrile resulted in a slight increase in cytotoxicity, and hydrolysis studies by ^{1}H NMR spectroscopy showed that the bond Ru-$NCCH_3$ is hydrolysed to a higher extent than Ru-Cl over the same period of time. Complexes **4.5** and **4.12** were converted to different extents to the aqua species $[RuCp^*(dppm)(OH_2)]^+$ (**6.1**) in 90% deuterated DMSO/10% D_2O solutions.

6.5 Future Work

Future work in this area of anticancer agents could include:

- Further studies of hydrolysis reactions for the rest of the compounds and comparison of hydrolysis rates/percentages with the cytotoxicities shown by the different complexes.
- Lipophilicity studies in water/octanol to elucidate relative solubilities and how they might have affected the cell line results.
- Synthesis and testing of other CH_3CN charged analogues which may, as **4.12**, give better activities due to increased aquation rates. The use of

counteranions different to SbF_6 could also provide a range of various solubilities.

- Investigation of the anticancer activity exhibited by other complexes synthesised during this project, for example, the functionalised η^6-arene complexes presented in **Chapter 2**.

6.6 References

1. S. J. Berners-Price, R. E. Norman and P. J. Sadler, *Journal of Inorganic Biochemistry*, 1987, **31**, 197-209.
2. S. J. Berners-Price, C. K. Mirabelli, R. K. Johnson, M. R. Mattern, F. L. McCabe, L. F. Faucette, C.-M. Sung, S.-M. Mong, P. J. Sadler and S. T. Crooke, *Cancer Research*, 1986, **46**, 5486-5493.
3. C. K. Mirabelli, D. T. Hill, L. F. Faucette, F. L. McCabe, G. R. Girard, D. B. Bryan, B. M. Sutton, J. O. L. Barus, S. T. Crooke and R. K. Johnson, *Journal of Medicinal Chemistry*, 1987, **30**, 2181-2190.
4. C. Wetzel, P. C. Kunz, M. U. Kassack, A. Hamacher, P. Bohler, W. Watjen, I. Ott, R. Rubbiani and B. Spingler, *Dalton Transactions*, 2011, **40**, 9212-9220.
5. U. E. I. Horvath, L. Dobrzańska, C. E. Strasser, W. Bouwer, G. Joone, C. E. J. van Rensburg, S. Cronje and H. G. Raubenheimer, *Journal of Inorganic Biochemistry*, 2012, **111**, 80-90.
6. J. F. González-Pantoja, M. Stern, A. A. Jarzecki, E. Royo, E. Robles-Escajeda, A. Varela-Ramírez, R. J. Aguilera and M. Contel, *Inorganic Chemistry*, 2011, **50**, 11099-11110.
7. S. Das, S. Sinha, R. Britto, K. Somasundaram and A. G. Samuelson, *Journal of Inorganic Biochemistry*, 2010, **104**, 93-104.
8. R. E. Morris, R. E. Aird, P. del Socorro Murdoch, H. Chen, J. Cummings, N. D. Hughes, S. Parsons, A. Parkin, G. Boyd, D. I. Jodrell and P. J. Sadler, *Journal of Medicinal Chemistry*, 2001, **44**, 3616-3621.
9. W. Han Ang and P. J. Dyson, *European Journal of Inorganic Chemistry*, 2006, **2006**, 4003-4018.
10. A. Habtemariam, M. Melchart, R. Fernández, S. Parsons, I. D. H. Oswald, A. Parkin, F. P. A. Fabbiani, J. E. Davidson, A. Dawson, R. E. Aird, D. I.

Jodrell and P. J. Sadler, *Journal of Medicinal Chemistry*, 2006, **49**, 6858-6868.

11. S. J. Dougan and P. J. Sadler, *CHIMIA International Journal for Chemistry*, 2007, **61**, 704-715.
12. C. S. Allardyce, P. J. Dyson, D. J. Ellis and S. L. Heath, *Chemical Communications*, 2001, 1396-1397.
13. S. H. van Rijt, A. J. Hebden, T. Amaresekera, R. J. Deeth, G. J. Clarkson, S. Parsons, P. C. McGowan and P. J. Sadler, *Journal of Medicinal Chemistry*, 2009, **52**, 7753-7764.
14. K. D. Camm, A. El-Sokkary, A. L. Gott, P. G. Stockley, T. Belyaeva and P. C. McGowan, *Dalton Transactions*, 2009, 10914-10925.
15. S. J. Lucas, R. M. Lord, R. L. Wilson, R. M. Phillips, V. Sridharan and P. C. McGowan, *Dalton Transactions*, 2012, **41**, 13800-13802.
16. D. N. Akbayeva, L. Gonsalvi, W. Oberhauser, M. Peruzzini, F. Vizza, P. Bruggeller, A. Romerosa, G. Sava and A. Bergamo, *Chemical Communications*, 2003, 264-265.
17. M. H. Garcia, T. S. Morais, P. Florindo, M. F. M. Piedade, V. Moreno, C. Ciudad and V. Noe, *Journal of Inorganic Biochemistry*, 2009, **103**, 354-361.
18. V. Moreno, J. Lorenzo, F. X. Avilés, M. H. Garcia, J. P. Ribeiro, T. S. Morais, P. Florindo and M. P. Robalo, *Bioinorganic Chemistry and Applications*, 2010, **2010**, 1-11.
19. V. Moreno, M. Font-Bardia, T. Calvet, J. Lorenzo, F. X. Avilés, M. H. Garcia, T. S. Morais, A. Valente and M. P. Robalo, *Journal of Inorganic Biochemistry*, 2011, **105**, 241-249.
20. A. Dorcier, W. H. Ang, S. Bolaño, L. Gonsalvi, L. Juillerat-Jeannerat, G. Laurenczy, M. Peruzzini, A. D. Phillips, F. Zanobini and P. J. Dyson, *Organometallics*, 2006, **25**, 4090-4096.
21. J. Tauchman, G. Süss-Fink, P. Štěpnička, O. Zava and P. J. Dyson, *Journal of Organometallic Chemistry*, 2013, **723**, 233-238.
22. F. Wang, H. Chen, S. Parsons, I. D. H. Oswald, J. E. Davidson and P. J. Sadler, *Chemistry – A European Journal*, 2003, **9**, 5810-5820.
23. C. Scolaro, A. Bergamo, L. Brescacin, R. Delfino, M. Cocchietto, G. Laurenczy, T. J. Geldbach, G. Sava and P. J. Dyson, *Journal of Medicinal Chemistry*, 2005, **48**, 4161-4171.

24. S. Top, B. Dauer, J. Vaissermann and G. Jaouen, *Journal of Organometallic Chemistry*, 1997, **541**, 355-361.
25. P. Köpf-Maier, H. Köpf and E. W. Neuse, *Journal of Cancer Research and Clinical Oncology*, 1984, **108**, 336-340.
26. M. Auzias, B. Therrien, G. Süss-Fink, P. Štěpnička, W. H. Ang and P. J. Dyson, *Inorganic Chemistry*, 2007, **47**, 578-583.
27. T. Mosmann, *Journal of Immunological Methods*, 1983, **65**, 55-63.
28. R. D. Lillie, *H. J. Conn's Biological Stains*, 9th edn., Williams and Wilkins, Baltimore, 1977.
29. D. T. Vistica, P. Skehan, D. Scudiero, A. Monks, A. Pittman and M. R. Boyd, *Cancer Research*, 1991, **51**, 2515-2520.

Chapter 7

Experimental Details and Characterisation

7.1 Experimental Techniques

7.1.1 General Procedures

All of the manipulations for the syntheses of the 2,5-dihydrophenyl carboxy ligands (**2.1** and **2.2**), the pentamethylcyclopentadiene and (5-hydroxypentyl)-tetramethylcyclopentadiene ligands (**4.1** and **4.2**), the η^5-pentamethylcyclopentadienyl and η^5-(5-hydroxypentyl)-tetramethylcyclopentadienyl ruthenium complexes (**4.3** to **4.12**) and the tetramethylfulvene complexes (**4.13** and **4.14**) were conducted using standard Schlenk line techniques under an inert atmosphere of dry dinitrogen in a dual vacuum/dinitrogen line. Dry dinitrogen was obtained by passing dinitrogen gas through a double column with phosphorus pentoxide and activated 4 Å molecular sieves.

Dry diethyl ether, toluene, methanol, ethanol, dichloromethane and hexane were collected from the stills in the Department of Chemistry, using a Pure Solvent MD Solvent Purification System, and were subsequently stored in ampoules under dinitrogen. Glassware, cannulae and filter papers were stored in an oven at 100-150°C prior to use. A Braun Labmaster 100 glove box was used to store all of the air sensitive compounds.

The liquid ammonia needed for the synthesis of the 2,5-dihydrophenyl carboxy ligands (**2.1** and **2.2**) was transferred to the reaction flask from a gas ammonia cylinder and condensed using an acetone/dry ice bath that maintained a constant temperature of -78ºC.

All of the η^6-arene ruthenium complexes were synthesised under non-inert atmosphere, with non pre-dried solvents. All of the catalytic reactions were also performed in non-dry conditions, unless otherwise stated.

Chemicals were supplied by Sigma-Aldrich Chemicals Co., Alfa Aesar, Fisher Scientific, SAFC Supply Solutions, Fluka Analytical, Acros Organics, VWR International Ltd. and the Department of Chemistry breached bottle store, and they were used without further purification.

Deuterated NMR solvents were purchased from Sigma-Aldrich Chemicals Co. The deuterated chloroform used in the glove box was degassed using freeze-pump-thaw cycles and stored over molecular sieves.

7.1.2 Instrumentation

All of the NMR spectra were recorded either by the author using a Bruker DPX 300 MHz spectrometer, a Bruker Avance 400 MHz spectrometer or a Bruker DRX 500 MHz spectrometer, or by Mr. Simon Barrett using a Bruker DRX 500 MHz spectrometer. Microanalyses were obtained by Mr. Ian Blakely at the University of Leeds Microanalytical Service. Mass spectra were obtained by Ms. Tanya Marinko-Covell at the University of Leeds Mass Spectrometry Service. Solid state infrared spectra were obtained by the author on a PerkinElmer Spectrum One FT-IR spectrometer. Gas chromatography analyses were obtained by the author using a Hewlett Packard Agilent HP6890 Series GC system with a HP7683 Series injector and a capillary column HP-5 (5% phenyl methyl siloxane) HP 19091J-413, with a length of 30 m, a diameter of 0.32 mm and a film thickness of 0.25 μm. The solvent used was acetonitrile.

7.1.3 X-Ray Crystallography

X-Ray diffraction data were collected either by the author or Mr. Colin Kilner. Suitable single crystals were selected under the microscope and immersed in inert oil. The crystals were mounted on a glass capillary and attached to a goniometer head on a Bruker X8 Apex diffractometer using graphite monochromated Mo-Kα radiation (λ = 0.71073 Å) and 1.0° Φ-rotation frames. The crystals were cooled to 150 K by an Oxford cryostream low temperature device.[1] The full data sets were recorded and the images processed using the Apex2 software, Bruker Nonius 2004. The structures were resolved by the author, Mr. Colin Kilner and Dr. Christopher Pask.

Structure solution by direct methods was achieved through the use of the SHELXS-97 program,[2] and the structural model refined by full matrix least squares on F2 using SHELXL-97.[2] Molecular graphics were plotted using POV-Ray *via* the XSeed program.[3] Editing of Crystallographic Information Files (CIFs) and construction of tables of bond lengths and angles were achieved using WC.[4]

Hydrogen atoms were placed using idealised geometric positions (with free rotation for methyl groups), allowed to move in a "riding model" along with the atoms to which they were attached, and refined isotropically.

7.2 2,5-Dihydrophenyl Carboxy Ligands

The ligands in this section (**2.1** and **2.2**) were synthesised following a route based on previous work by Sheldrick *et al*.[5] ^{1}H NMR spectra were recorded for each of them to confirm product formation, but further characterisation was not completed.

7.2.1 Preparation of $C_8H_{10}O_2$ (2.1)

Phenylacetic acid (4.08 g, 30 mmol) in diethyl ether (50 ml) was added to a mixture of sodium (6.9 g, 300 mmol) in liquid ammonia (200 ml) at -78°C under N_2. Ethanol (100 ml) was added dropwise at -78°C and the mixture stirred until the dark blue colour disappeared. The ammonia was left to evaporate overnight, water (100 ml) added and then HCl was added dropwise until pH 2. The product was extracted in diethyl ether, dried ($MgSO_4$) and the solvent removed *in vacuo* to afford a white solid that was recrystallised from petrol (40-60ºC).

Yield: 3.4 g, 24.6 mmol (82%).

Characterisation:

^{1}H NMR ($CDCl_3$, 400.13 MHz, 293.8 K)

δ 5.70 [m, 2H, $(CH(CH_2)_2(C\underline{H})_2C)CH_2CO_2H$], 5.64 [br. s, 1H, $(C\underline{H}(CH_2)_2(CH)_2C)CH_2CO_2H$], 3.03 [s, 2H, $(CH(CH_2)_2(CH)_2C)C\underline{H_2}CO_2H$], 2.73 [m, 4H, $(CH(C\underline{H_2})_2(CH)_2C)CH_2CO_2H$].

7.2.2 Preparation of $C_{10}H_{14}O_2$ (2.2)

4-Phenylbutyric acid (4.93 g, 30 mmol) in diethyl ether (50 ml) was added to a mixture of sodium (6.9 g, 300 mmol) in liquid ammonia (200 ml) at -78°C under N_2. Ethanol (100 ml) was added dropwise at -78°C and the mixture stirred until the dark blue colour disappeared. The ammonia was left to evaporate overnight, water (150 ml) added and then HCl was added dropwise until pH 2. The product was

extracted in diethyl ether, dried ($MgSO_4$) and the solvent removed *in vacuo* to afford a dark solid.

Yield: 4.39 g, 26.4 mmol (88%).

Characterisation:

^{1}H NMR ($CDCl_3$, 400.13 MHz, 300.0 K)

δ 5.62 [m, 2H, $(CH(CH_2)_2(C\underline{H})_2C)CH_2CH_2CH_2CO_2H$], 5.36 [br. s, 1H, $(C\underline{H}(CH_2)_2(CH)_2C)CH_2CH_2CH_2CO_2H$], 2.55 [m, 4H, $(CH(C\underline{H_2})_2(CH)_2C)CH_2CH_2CH_2CO_2H$], 2.27 [m, 2H, $(CH(CH_2)_2(CH)_2C)CH_2CH_2C\underline{H_2}CO_2H$], 2.21 [m, 2H, $(CH(CH_2)_2(CH)_2C)C\underline{H_2}CH_2CH_2CO_2H$], 1.69 [m, 2H, $(CH(CH_2)_2(CH)_2C)CH_2C\underline{H_2}CH_2CO_2H$].

7.3 Functionalised η^6-Arene Ruthenium Complexes

Most of these complexes (**2.3** to **2.8**) were synthesised by a method developed by Sheldrick *et al.*[5] and used previously within the McGowan group.[6] Complex **2.9** was synthesised by a slight modification of the procedures used by Keppler *et al.*[7] and some partners of this project in similar transformations.[8] Complexes **2.3**, **2.5** and **2.6** were known[5] and their formation was confirmed by ^{1}H NMR and elemental analysis. The rest of the complexes are novel.

7.3.1 Preparation of $[RuCl_2C_6H_5CH_2COOH]_2$ (2.3)

Ligand **2.1** (4.5 g, 32.6 mmol) was added to a round bottom flask with $RuCl_3 \cdot 3H_2O$ (2.13 g, 8.14 mmol) in acetone/water (5:1 v/v, 54 ml). The mixture was heated under reflux for 5.5 hours, concentrated *in vacuo*, and the precipitate filtered, washed with diethyl ether and dried under vacuum to afford an orange solid.

Yield: 2.19 g, 3.56 mmol (87%).

Characterisation:

Calculated for $C_{16}H_{16}Cl_4O_4Ru_2$ (616.27 g mol^{-1}): C 31.2; H 2.6; Cl 23.0%

Found: C 31.3; H 2.6; Cl 22.8%

^{1}H NMR (CD_3CN, 400.13 MHz, 293.9 K)

δ 5.76 [m, 4H, *meta*-CH of $C_6\underline{H_5}CH_2CO_2H$], 5.69 [m, 2H, *para*-CH of $C_6\underline{H_5}CH_2CO_2H$], 5.56 [d, $^{3}J_{(H-H)}$ = 5.8 Hz, 4H, *ortho*-CH of $C_6\underline{H_5}CH_2CO_2H$], 3.61 [s, 4H, $C_6H_5C\underline{H_2}CO_2H$].

7.3.2 Preparation of $[RuBr_2C_6H_5CH_2COOH]_2$ (2.4)

Ligand **2.1** (0.5 g, 3.6 mmol) was added to a round bottom flask with $RuBr_3$ (0.31 g, 0.9 mmol) in acetone/water (5:1 v/v, 6 ml). The mixture was heated under reflux for 3 days, concentrated *in vacuo*, and the precipitate filtered, washed with diethyl ether and dried under vacuum to afford a red solid.

Yield: 0.30 g, 0.37 mmol (82%).

Characterisation:

Calculated for $C_{16}H_{16}Br_4O_4Ru_2$ (793.86 g mol^{-1}): C 24.2; H 2.0; Br 40.3%

Found: C 24.2; H 2.1; Br 40.0%

^{1}H NMR (CD_3CN, 400.13 MHz, 294.6 K)

δ 5.77 [m, 6H, *meta* & *para*-CH of $C_6\underline{H_5}CH_2CO_2H$], 5.64 [d, $^{3}J_{(H-H)}$ = 2.9 Hz, 4H, *ortho*-CH of $C_6\underline{H_5}CH_2CO_2H$], 3.64 [s, 4H, $C_6H_5C\underline{H_2}CO_2H$];

^{13}C{^{1}H} NMR (CD_3CN, 100.62 MHz, 295.6 K)

δ 157.6 [$C_6H_5CH_2\underline{C}O_2H$], 116.4 [Quaternary C of $\underline{C_6}H_5CH_2CO_2H$], 84.6 [*ortho*-CH of $\underline{C_6}H_5CH_2CO_2H$], 84.5 [*meta*-CH of $\underline{C_6}H_5CH_2CO_2H$], 83.0 [*para*-CH of $\underline{C_6}H_5CH_2CO_2H$], 38.3 [$C_6H_5\underline{C}H_2CO_2H$].

7.3.3 Preparation of $[RuCl_2C_6H_5(CH_2)_3COOH]_2$ (2.5)

Ligand **2.2** (6.2 g, 37 mmol) was added to a round bottom flask with $RuCl_3{\cdot}3H_2O$ (2.42 g, 9.25 mmol) in acetone/water (5:1 v/v, 60 ml). The mixture was heated under reflux for 3 days, concentrated *in vacuo*, and the precipitate filtered, washed with diethyl ether and dried under vacuum to afford an orange solid.

Yield: 1.80 g, 2.67 mmol (58%).

Characterisation:

Calculated for $C_{20}H_{24}Cl_4O_4Ru_2$ (672.33 g mol^{-1}): C 35.7; H 3.6; Cl 21.1%

Found: C 36.0; H 3.6; Cl 21.0%

^{1}H NMR (CD_3CN, 400.13 MHz, 300.0 K)

δ 5.69 [t, $^3J_{(H-H)}$ = 5.7 Hz, 4H, *meta*-CH of $C_6\underline{H_5}CH_2CH_2CH_2CO_2H$], 5.62 [t, $^3J_{(H-H)}$ = 5.6 Hz, 2H, *para*-CH of $C_6\underline{H_5}CH_2CH_2CH_2CO_2H$], 5.45 [d, $^3J_{(H-H)}$ = 5.6 Hz, 4H, *ortho*-CH of $C_6\underline{H_5}CH_2CH_2CH_2CO_2H$], 2.57 [m, 4H, $C_6H_5C\underline{H_2}CH_2CH_2CO_2H$], 2.39 [t, $^3J_{(H-H)}$ = 7.5 Hz, 4H, $C_6H_5CH_2CH_2C\underline{H_2}CO_2H$], 1.91 [m, 4H, $C_6H_5CH_2C\underline{H_2}CH_2CO_2H$].

7.3.4 Preparation of $[RuCl_2C_6H_5CH_2COOCH_2CH_3]_2$ (2.6)

Ligand **2.1** (0.83 g, 6 mmol) was added to a round bottom flask with $RuCl_3 \cdot 3H_2O$ (0.52 g, 2 mmol) in ethanol (30 ml). The mixture was heated under reflux for 2 hours, concentrated *in vacuo*, and the precipitate filtered, washed with ethanol and dried under vacuum to afford an orange solid.

Yield: 0.37 g, 0.56 mmol (56%).

Characterisation:

Calculated for $C_{20}H_{24}Cl_4O_4Ru_2$ (672.33 g mol^{-1}): C 35.7; H 3.6; Cl 21.1%

Found: C 35.8; H 3.5; Cl 21.4%

^{1}H NMR ($CDCl_3$, 400.13 MHz, 300.0 K)

δ 5.68 [m, 6H, *meta* & *para*-CH of $C_6\underline{H_5}CH_2CO_2CH_2CH_3$], 5.50 [d, $^3J_{(H-H)}$ = 5.6 Hz, 4H, *ortho*-CH of $C_6\underline{H_5}CH_2CO_2CH_2CH_3$], 4.16 [q, $^3J_{(H-H)}$ = 7.0 Hz, 4H, $C_6H_5CH_2CO_2C\underline{H_2}CH_3$], 3.66 [s, 4H, $C_6H_5C\underline{H_2}CO_2CH_2CH_3$], 1.26 [t, $^3J_{(H-H)}$ = 7.2 Hz, 6H, $C_6H_5CH_2CO_2CH_2C\underline{H_3}$].

7.3.5 Preparation of $[RuBr_2C_6H_5CH_2COOCH_2CH_3]_2$ (2.7)

Ligand **2.1** (0.5 g, 3.6 mmol) was added to a round bottom flask with $RuBr_3$ (0.31 g, 0.9 mmol) in ethanol (30 ml). The mixture was heated under reflux for 24

hours, concentrated *in vacuo*, and the precipitate filtered, washed with ethanol and dried under vacuum to afford an orange solid.

Yield: 0.12 g, 0.14 mmol (31%).

Characterisation:

Calculated for $C_{20}H_{24}Br_4O_4Ru_2$ (849.93 g mol^{-1}): C 28.2; H 2.9; Br 37.6%

Found: C 28.1; H 2.8; Br 37.4%

^{1}H NMR ($CDCl_3$, 400.13 MHz, 294.4 K)

δ 5.77 [m, 2H, *para*-CH of $C_6\underline{H_5}CH_2CO_2CH_2CH_3$], 5.67 [t, $^3J_{(H-H)}$ = 5.6 Hz, 4H, *meta*-CH of $C_6\underline{H_5}CH_2CO_2CH_2CH_3$], 5.54 [d, $^3J_{(H-H)}$ = 5.6 Hz, 4H, *ortho*-CH of $C_6\underline{H_5}CH_2CO_2CH_2CH_3$], 4.16 [q, $^3J_{(H-H)}$ = 7.0 Hz, 4H, $C_6H_5CH_2CO_2C\underline{H_2}CH_3$], 3.68 [s, 4H, $C_6H_5C\underline{H_2}CO_2CH_2CH_3$], 1.26 [t, $^3J_{(H-H)}$ = 7.2 Hz, 6H, $C_6H_5CH_2CO_2CH_2C\underline{H_3}$];

^{13}C{^{1}H} NMR ($CDCl_3$, 125.76 MHz, 300.0 K)

δ 169.4 [$C_6H_5CH_2\underline{C}O_2CH_2CH_3$], 92.6 [Quaternary C of $\underline{C_6}H_5CH_2CO_2CH_2CH_3$], 83.8 [*ortho*-CH of $\underline{C_6}H_5CH_2CO_2CH_2CH_3$], 83.1 [*meta*-CH of $\underline{C_6}H_5CH_2CO_2CH_2CH_3$], 82.4 [*para*-CH of $\underline{C_6}H_5CH_2CO_2CH_2CH_3$], 61.7 [$C_6H_5CH_2CO_2\underline{C}H_2CH_3$], 39.7 [$C_6H_5\underline{C}H_2CO_2CH_2CH_3$], 14.1 [$C_6H_5CH_2CO_2CH_2\underline{C}H_3$].

7.3.6 Preparation of $[RuCl_2C_6H_5(CH_2)_3COOCH_2CH_3]_2$ (2.8)

Ligand **2.2** (1 g, 6 mmol) was added to a round bottom flask with $RuCl_3{\cdot}3H_2O$ (0.52 g, 2 mmol) in ethanol (30 ml). The mixture was heated under reflux for 4 days, concentrated *in vacuo*, and the precipitate filtered, washed with ethanol and dried under vacuum to afford an orange solid.

Yield: 0.04 g, 0.05 mmol (5%).

Characterisation:

Calculated for $C_{24}H_{32}Cl_4O_4Ru_2$ (728.37 g mol^{-1}): C 39.5; H 4.4; Cl 19.5%

Found: C 39.5; H 4.4; Cl 19.2%

^{1}H NMR ($CDCl_3$, 400.13 MHz, 300.0 K)

δ 5.66 [t, $^{3}J_{(H-H)}$ = 5.4 Hz, 4H, *meta*-CH of $C_6\underline{H_5}CH_2CH_2CH_2CO_2CH_2CH_3$], 5.61 [t, $^{3}J_{(H-H)}$ = 5.3 Hz, 2H, *para*-CH of $C_6\underline{H_5}CH_2CH_2CH_2CO_2CH_2CH_3$], 5.39 [d, $^{3}J_{(H-H)}$ = 5.6 Hz, 4H, *ortho*-CH of $C_6\underline{H_5}CH_2CH_2CH_2CO_2CH_2CH_3$], 4.12 [q, $^{3}J_{(H-H)}$ = 7.1 Hz, 4H, $C_6H_5CH_2CH_2CH_2CO_2C\underline{H_2}CH_3$], 2.60 [m, 4H, $C_6H_5C\underline{H_2}CH_2CH_2CO_2CH_2CH_3$], 2.37 [t, $^{3}J_{(H-H)}$ = 7.3 Hz, 4H, $C_6H_5CH_2CH_2C\underline{H_2}CO_2CH_2CH_3$], 1.92 [quintet, $^{3}J_{(H-H)}$ = 7.5 Hz, 4H, $C_6H_5CH_2C\underline{H_2}CH_2CO_2CH_2CH_3$], 1.26 [t, $^{3}J_{(H-H)}$ = 7.0 Hz, 6H, $C_6H_5CH_2CH_2CH_2CO_2CH_2C\underline{H_3}$];

^{13}C{^{1}H} NMR ($CDCl_3$, 100.61 MHz, 300.0 K)

δ 172.7 [$C_6H_5CH_2CH_2CH_2\underline{C}O_2CH_2CH_3$], 100.5 [Quaternary C of $\underline{C_6}H_5CH_2CH_2CH_2CO_2CH_2CH_3$], 84.1 [*meta*-CH of $\underline{C_6}H_5CH_2CH_2CH_2CO_2CH_2CH_3$], 80.5 [*ortho*-CH of $\underline{C_6}H_5CH_2CH_2CH_2CO_2CH_2CH_3$], 80.0 [*para*-CH of $\underline{C_6}H_5CH_2CH_2CH_2CO_2CH_2CH_3$], 60.6 [$C_6H_5CH_2CH_2CH_2CO_2\underline{C}H_2CH_3$], 33.5 [$C_6H_5CH_2CH_2\underline{C}H_2CO_2CH_2CH_3$], 32.9 [$C_6H_5\underline{C}H_2CH_2CH_2CO_2CH_2CH_3$], 24.8 [$C_6H_5CH_2\underline{C}H_2CH_2CO_2CH_2CH_3$], 14.3 [$C_6H_5CH_2CH_2CH_2CO_2CH_2\underline{C}H_3$].

7.3.7 Preparation of $[RuI_2C_6H_5CH_2COOCH_2CH_3]_2$ (2.9)

NaI (0.23 g, 1.525 mmol) was added to a solution of complex **2.6** (33.6 mg. 0.05 mmol) in chloroform (10 ml). The mixture was stirred for three days and then filtered and washed with chloroform. The washings were collected and the solvent was evaporated to give a red solid that was recrystallised from dichloromethane/hexane.

Yield: 0.0071 g, 0.0068 mmol (14%).

Characterisation:

Calculated for $C_{20}H_{24}I_4O_4Ru_2$ (1037.93 g mol^{-1}): C 23.1; H 2.3%

Found: C 23.8; H 2.3%

^{1}H NMR ($CDCl_3$, 500.23 MHz, 298.4 K)

δ 5.84 [t, $^{3}J_{(H-H)}$ = 5.4 Hz, 2H, *para*-CH of $C_6\underline{H_5}CH_2CO_2CH_2CH_3$], 5.67 [t, $^{3}J_{(H-H)}$ = 5.6 Hz, 4H, *meta*-CH of $C_6\underline{H_5}CH_2CO_2CH_2CH_3$], 5.61 [d, $^{3}J_{(H-H)}$ = 5.6 Hz, 4H, *ortho*-

CH of $C_6\underline{H_5}CH_2CO_2CH_2CH_3$], 4.16 [q, $^3J_{(H-H)}$ = 7.2 Hz, 4H, $C_6H_5CH_2CO_2C\underline{H_2}CH_3$], 3.69 [s, 4H, $C_6H_5C\underline{H_2}CO_2CH_2CH_3$], 1.27 [t, $^3J_{(H-H)}$ = 7.2 Hz, 6H, $C_6H_5CH_2CO_2CH_2C\underline{H_3}$];

$^{13}C\{^1H\}$ NMR ($CDCl_3$, 125.77 MHz, 300.2 K)

δ 170.0 [$C_6H_5CH_2\underline{C}O_2CH_2CH_3$], 96.8 [Quaternary C of $\underline{C_6}H_5CH_2CO_2CH_2CH_3$], 86.1 [*ortho*-CH of $\underline{C_6}H_5CH_2CO_2CH_2CH_3$], 84.0 [*para*-CH of $\underline{C_6}H_5CH_2CO_2CH_2CH_3$], 83.0 [*meta*-CH of $\underline{C_6}H_5CH_2CO_2CH_2CH_3$], 61.7 [$C_6H_5CH_2CO_2\underline{C}H_2CH_3$], 40.6 [$C_6H_5\underline{C}H_2CO_2CH_2CH_3$], 14.1 [$C_6H_5CH_2CO_2CH_2\underline{C}H_3$].

ES MS (+): m/z 912.69 $[M - I]^+$.

7.3.8 Preparation of $[RuCl_2(C_6H_5CH_2COOCH_2CH_3)(NC_5H_5)]$ (2.10)

Complex **2.6** (67 mg, 0.1 mmol) was dissolved in dichloromethane (10 ml) and pyridine (16 µl, 0.2 mmol) was added. The mixture was stirred overnight to give an orange solution and the solvent was evaporated to give an orange/yellow product.

Yield: 0.0592 g, 0.14 mmol (71 %).

Characterisation:

Calculated for $C_{15}H_{17}Cl_2NO_2Ru$ (415.83 g mol^{-1}): C 43.3; H 4.1; N 3.4; Cl 17.1%

Found: C 43.2; H 4.1; N 3.3; Cl 16.9%

^1H NMR ($CDCl_3$, 500.23 MHz, 298.6 K)

δ 9.05 [d, $^3J_{(H-H)}$ = 5.2 Hz, 2H, 2,6-CH of $NC_5\underline{H_5}$], 7.77 [t, $^3J_{(H-H)}$ = 7.4 Hz, 1H, 4-CH of $NC_5\underline{H_5}$], 7.33 [t, $^3J_{(H-H)}$ = 6.8 Hz, 2H, 3,5-CH of $NC_5\underline{H_5}$], 5.64 [t, $^3J_{(H-H)}$ = 5.4 Hz, 2H, *meta*-CH of $C_6\underline{H_5}CH_2CO_2CH_2CH_3$], 5.58 [t, $^3J_{(H-H)}$ = 5.2 Hz, 1H, *para*-CH of $C_6\underline{H_5}CH_2CO_2CH_2CH_3$], 5.54 [d, $^3J_{(H-H)}$ = 5.6 Hz, 2H, *ortho*-CH of $C_6\underline{H_5}CH_2CO_2CH_2CH_3$], 4.20 [q, $^3J_{(H-H)}$ = 7.2 Hz, 2H, $C_6H_5CH_2CO_2C\underline{H_2}CH_3$], 3.67 [s, 2H, $C_6H_5C\underline{H_2}CO_2CH_2CH_3$], 1.29 [t, $^3J_{(H-H)}$ = 7.2 Hz, 3H, $C_6H_5CH_2CO_2CH_2C\underline{H_3}$];

$^{13}C\{^1H\}$ NMR ($CDCl_3$, 75.47 MHz, 300.0 K)

δ 169.6 [$C_6H_5CH_2\underline{C}O_2CH_2CH_3$], 155.3 [2,6-CH of $N\underline{C_5}H_5$], 138.0 [4-CH of $N\underline{C_5}H_5$], 124.9 [3,5-CH of $N\underline{C_5}H_5$], 94.8 [Quaternary C of $\underline{C_6}H_5CH_2CO_2CH_2CH_3$], 85.9

[*meta*-CH of $\underline{C_6}H_5CH_2CO_2CH_2CH_3$], 83.8 [*ortho*-CH of $\underline{C_6}H_5CH_2CO_2CH_2CH_3$], 82.1 [*para*-CH of $\underline{C_6}H_5CH_2CO_2CH_2CH_3$], 61.7 [$C_6H_5CH_2CO_2\underline{C}H_2CH_3$], 38.8 [$C_6H_5\underline{C}H_2CO_2CH_2CH_3$], 14.2 [$C_6H_5CH_2CO_2CH_2\underline{C}H_3$].

ES MS (+): m/z 379.99 $[M - Cl]^+$; 300.95 $[M - Cl - py]^+$.

7.4 η^6-*p*-Cymene Ruthenium Dimers

Compound **3.1** was synthesised according to a method already utilised in the McGowan group,[9] and compound **3.2** was synthesised from the previous one by modification of some existing treatments.[7, 8]

7.4.1 Preparation of $[RuCl_2(C_{10}H_{14})]_2$ (3.1)

α-Terpinene (19 ml, 116.7 mmol) was added to a solution of $RuCl_3 \cdot 3H_2O$ (2.51 g, 9.6 mmol) in absolute ethanol (150 ml) and heated under reflux for two days. After that, the volume was reduced *in vacuo* and the solution stored in the freezer for three days. The red precipitate formed was filtered off, washed with ice cold diethyl ether and dried to yield a red crystalline powder.

Yield: 2.61 g, 4.27 mmol (89%).

Characterisation:

Calculated for $C_{20}H_{28}Cl_4Ru_2$ (612.36 g mol^{-1}): C 39.2; H 4.6; Cl 23.2%

Found: C 39.4; H 4.6; Cl 23.1%

^{1}H NMR ($CDCl_3$, 500.23 MHz, 300.0 K)

δ 5.47 [d, $^3J_{(H-H)}$ = 6.0 Hz, 4H, $CH_3C(CH)_2(C\underline{H})_2CCH(CH_3)_2$], 5.34 [d, $^3J_{(H-H)}$ = 6.0 Hz, 4H, $CH_3C(C\underline{H})_2(CH)_2CCH(CH_3)_2$], 2.92 [sep, $^3J_{(H-H)}$ = 6.9 Hz, 2H, $CH_3C(CH)_2(CH)_2CC\underline{H}(CH_3)_2$], 2.16 [s, 6H, $C\underline{H_3}C(CH)_2(CH)_2CCH(CH_3)_2$], 1.28 [d, $^3J_{(H-H)}$ = 6.8 Hz, 12H, $CH_3C(CH)_2(CH)_2CCH(C\underline{H_3})_2$];

^{13}C{^{1}H} NMR ($CDCl_3$, 75.47 MHz, 299.9 K)

δ 101.2 [$CH_3C(CH)_2(CH)_2\underline{C}CH(CH_3)_2$], 96.7 [$CH_3\underline{C}(CH)_2(CH)_2CCH(CH_3)_2$], 81.3 [$CH_3C(CH)_2(\underline{C}H)_2CCH(CH_3)_2$], 80.6 [$CH_3C(\underline{C}H)_2(CH)_2CCH(CH_3)_2$], 30.6

$[CH_3C(CH)_2(CH)_2C\underline{C}H(CH_3)_2]$, 22.1 $[CH_3C(CH)_2(CH)_2CCH(\underline{C}H_3)_2]$, 18.9 $[\underline{C}H_3C(CH)_2(CH)_2CCH(CH_3)_2]$.

ES MS (+): m/z 575.9 $[M - H - Cl]^+$.

7.4.2 Preparation of $[RuI_2(C_{10}H_{14})]_2$ (3.2)

A solution of NaI (3.7 g, 24.4 mmol) in water (25 ml) was added to a solution of complex **3.1** (0.49 g, 0.8 mmol) in chloroform (20 ml), and the mixture was stirred overnight. The two phases were separated and the organic layer was washed with water and brine, dried over Na_2SO_4 and filtered, and the solvent removed to give a dark red solid, which was recrystallised from dichloromethane/hexane.

Yield: 0.68 g, 0.69 mmol (86%).

Characterisation:

Calculated for $C_{20}H_{28}I_4Ru_2$ (977.98 g mol^{-1}): C 24.5; H 2.9; I 51.9%

Found: C 24.3; H 2.8; I 51.9%

^{1}H NMR ($CDCl_3$, 400.13 MHz, 294.4 K)

δ 5.54 [d, $^3J_{(H-H)}$ = 6.0 Hz, 4H, $CH_3C(CH)_2(C\underline{H})_2CCH(CH_3)_2$], 5.44 [d, $^3J_{(H-H)}$ = 5.6 Hz, 4H, $CH_3C(C\underline{H})_2(CH)_2CCH(CH_3)_2$], 3.02 [sep, $^3J_{(H-H)}$ = 6.8 Hz, 2H, $CH_3C(CH)_2(CH)_2CC\underline{H}(CH_3)_2$], 2.37 [s, 6H, $C\underline{H}_3C(CH)_2(CH)_2CCH(CH_3)_2$], 1.26 [d, $^3J_{(H-H)}$ = 6.8 Hz, 12H, $CH_3C(CH)_2(CH)_2CCH(C\underline{H}_3)_2$];

^{13}C{^{1}H} NMR ($CDCl_3$, 100.62 MHz, 295.2 K)

δ 104.3 $[CH_3C(CH)_2(CH)_2\underline{C}CH(CH_3)_2]$, 97.6 $[CH_3\underline{C}(CH)_2(CH)_2CCH(CH_3)_2]$, 82.5 $[CH_3C(CH)_2(\underline{C}H)_2CCH(CH_3)_2]$, 82.1 $[CH_3C(\underline{C}H)_2(CH)_2CCH(CH_3)_2]$, 31.5 $[CH_3C(CH)_2(CH)_2C\underline{C}H(CH_3)_2]$, 22.8 $[CH_3C(CH)_2(CH)_2CCH(\underline{C}H_3)_2]$, 20.3 $[\underline{C}H_3C(CH)_2(CH)_2CCH(CH_3)_2]$.

ES MS (+): m/z 852.7 $[MH - I]^+$.

7.5 η^6-*p*-Cymene Ruthenium Monomers

Compounds **3.3** to **3.13** were synthesised in dichloromethane at room temperature from complexes **3.1** or **3.2** and the correspondent pyridine or amine.

Compounds **3.3**, **3.4**, **3.6** and **3.12** had been previously synthesised in high temperatures or ultrasound conditions.[10-12]

Compound **3.14** was synthesised by variation of some experiments already performed within the McGowan group which, in turn, were adapted from published work.[13]

7.5.1 Preparation of $[RuCl_2(C_{10}H_{14})(NH_2C(CH_3)_3)]$ (3.3)

Complex **3.1** (0.15 g, 0.25 mmol) was dissolved in dichloromethane (10 ml), and *tert*-butylamine (0.1 ml, 1 mmol) was added. The mixture was stirred overnight to give an orange solution and the solvent was evaporated to give an orange solid.

Yield: 0.14 g, 0.37 mmol (74%).

Characterisation:

Calculated for $C_{14}H_{25}Cl_2NRu$ (379.27 g mol^{-1}): C 44.3; H 6.6; N 3.7; Cl 18.7%

Found: C 44.4; H 6.7; N 3.6; Cl 18.9%

^{1}H NMR ($CDCl_3$, 500.23 MHz, 300.0 K)

δ 5.51 [d, $^3J_{(H-H)}$ = 6.0 Hz, 2H, $CH_3C(CH)_2(C\underline{H})_2CCH(CH_3)_2$], 5.46 [d, $^3J_{(H-H)}$ = 5.6 Hz, 2H, $CH_3C(C\underline{H})_2(CH)_2CCH(CH_3)_2$], 3.07 [sep, $^3J_{(H-H)}$ = 6.8 Hz, 1H, $CH_3C(CH)_2(CH)_2CC\underline{H}(CH_3)_2$], 2.28 [s, 3H, $C\underline{H_3}C(CH)_2(CH)_2CCH(CH_3)_2$], 1.35 [s, 9H, $NH_2C(C\underline{H_3})_3$], 1.30 [d, $^3J_{(H-H)}$ = 6.8 Hz, 6H, $CH_3C(CH)_2(CH)_2CCH(C\underline{H_3})_2$];

^{13}C{^{1}H} NMR ($CDCl_3$, 75.47 MHz, 300.1 K)

δ 103.4 [$CH_3C(CH)_2(CH)_2\underline{C}CH(CH_3)_2$], 95.0 [$CH_3\underline{C}(CH)_2(CH)_2CCH(CH_3)_2$], 81.6 [$CH_3C(CH)_2(\underline{C}H)_2CCH(CH_3)_2$], 79.1 [$CH_3C(\underline{C}H)_2(CH)_2CCH(CH_3)_2$], 53.2 [$NH_2\underline{C}(CH_3)_3$], 31.1 [$NH_2C(\underline{C}H_3)_3$], 30.7 [$CH_3C(CH)_2(CH)_2C\underline{C}H(CH_3)_2$], 22.1 [$CH_3C(CH)_2(CH)_2CCH(\underline{C}H_3)_2$], 18.6 [$\underline{C}H_3C(CH)_2(CH)_2CCH(CH_3)_2$].

ES MS (+): m/z 344.1 $[M - Cl]^+$.

7.5.2 Preparation of $[RuCl_2(C_{10}H_{14})(NC_5H_5)]$ (3.4)

Complex **3.1** (0.6 g, 1 mmol) was dissolved in dichloromethane (30 ml), and pyridine (0.32 ml, 4 mmol) was added. The mixture was stirred overnight to give an orange solution and the solvent was evaporated to give an orange solid.

Yield: 0.689 g, 1.79 mmol (89%).

Characterisation:

Calculated for $C_{15}H_{19}Cl_2NRu$ (385.22 g mol^{-1}): C 46.7; H 5.0; N 3.6; Cl 18.4%

Found: C 46.6; H 5.0; N 3.5; Cl 18.8%

^{1}H NMR ($CDCl_3$, 500.23 MHz, 300.0 K)

δ 9.06 [d, $^3J_{(H-H)}$ = 5.1 Hz, 2H, 2,6-CH of $NC_5\underline{H}_5$], 7.75 [t, $^3J_{(H-H)}$ = 7.7 Hz, 1H, 4-CH of $NC_5\underline{H}_5$], 7.32 [t, $^3J_{(H-H)}$ = 6.8 Hz, 2H, 3,5-CH of $NC_5\underline{H}_5$], 5.45 [d, $^3J_{(H-H)}$ = 6.0 Hz, 2H, $CH_3C(CH)_2(C\underline{H})_2CCH(CH_3)_2$], 5.23 [d, $^3J_{(H-H)}$ = 5.1 Hz, 2H, $CH_3C(C\underline{H})_2(CH)_2CCH(CH_3)_2$], 3.01 [m, 1H, $CH_3C(CH)_2(CH)_2CC\underline{H}(CH_3)_2$], 2.11 [s, 3H, $C\underline{H}_3C(CH)_2(CH)_2CCH(CH_3)_2$], 1.32 [d, $^3J_{(H-H)}$ = 6.8 Hz, 6H, $CH_3C(CH)_2(CH)_2CCH(C\underline{H}_3)_2$];

^{13}C{^{1}H} NMR ($CDCl_3$, 75.47 MHz, 300.1 K)

δ 154.9 [2,6-CH of NC_5H_5], 137.6 [4-CH of NC_5H_5], 124.6 [3,5-CH of NC_5H_5], 103.6 [$CH_3C(CH)_2(CH)_2CCH(CH_3)_2$], 97.1 [$CH_3C(CH)_2(CH)_2CCH(CH_3)_2$], 82.8 [$CH_3C(CH)_2(CH)_2CCH(CH_3)_2$], 82.3 [$CH_3C(CH)_2(CH)_2CCH(CH_3)_2$], 30.7 [$CH_3C(CH)_2(CH)_2CCH(CH_3)_2$], 22.3 [$CH_3C(CH)_2(CH)_2CCH(CH_3)_2$], 18.2 [$CH_3C(CH)_2(CH)_2CCH(CH_3)_2$].

ES MS (+): m/z 350.0 $[M - Cl]^+$.

7.5.3 Preparation of $[RuI_2(C_{10}H_{14})(NC_5H_5)]$ (3.5)

Complex **3.2** (0.15 g, 0.15 mmol) was dissolved in dichloromethane (10 ml), and pyridine (49 μl, 0.6 mmol) was added. The mixture was stirred overnight to give a dark red solution and the solvent was evaporated to give a brown solid.

Yield: 0.15 g, 0.26 mmol (88%).

Characterisation:

Calculated for $C_{15}H_{19}I_2NRu$ (568.02 g mol^{-1}): C 31.7; H 3.4; N 2.5; I 44.7%

Found: C 32.1; H 3.5; N 2.5; I 44.6%

^{1}H NMR ($CDCl_3$, 300.13 MHz, 299.9 K)

δ 9.48 [m, 2H, 2,6-CH of $NC_5\underline{H}_5$], 7.72 [t, $^3J_{(H-H)}$ = 6.8 Hz, 1H, 4-CH of $NC_5\underline{H}_5$], 7.20 [t, $^3J_{(H-H)}$ = 5.6 Hz, 2H, 3,5-CH of $NC_5\underline{H}_5$], 5.69 [d, $^3J_{(H-H)}$ = 4.8 Hz, 2H, $CH_3C(CH)_2(C\underline{H})_2CCH(CH_3)_2$], 5.32 [d, $^3J_{(H-H)}$ = 4.8 Hz, 2H, $CH_3C(C\underline{H})_2(CH)_2CCH(CH_3)_2$], 3.05 [m, 1H, $CH_3C(CH)_2(CH)_2CC\underline{H}(CH_3)_2$], 1.89 [br. s, 3H, $C\underline{H}_3C(CH)_2(CH)_2CCH(CH_3)_2$], 1.26 [d, $^3J_{(H-H)}$ = 6.8 Hz, 6H, $CH_3C(CH)_2(CH)_2CCH(C\underline{H}_3)_2$];

^{13}C{^{1}H} NMR ($CDCl_3$, 75.47 MHz, 299.9 K)

δ 160.0 [2,6-CH of $N\underline{C}_5H_5$], 137.4 [4-CH of $N\underline{C}_5H_5$], 124.4 [3,5-CH of $N\underline{C}_5H_5$], 103.3 [$CH_3C(CH)_2(CH)_2\underline{C}CH(CH_3)_2$], 97.9 [$CH_3\underline{C}(CH)_2(CH)_2CCH(CH_3)_2$], 83.9 [$CH_3C(CH)_2(\underline{C}H)_2CCH(CH_3)_2$], 83.2 [$CH_3C(\underline{C}H)_2(CH)_2CCH(CH_3)_2$], 31.8 [$CH_3C(CH)_2(CH)_2C\underline{C}H(CH_3)_2$], 22.9 [$CH_3C(CH)_2(CH)_2CCH(\underline{C}H_3)_2$], 18.8 [$\underline{C}H_3C(CH)_2(CH)_2CCH(CH_3)_2$].

ES MS (+): m/z 442.0 $[MH - I]^+$.

7.5.4 Preparation of $[RuCl_2(C_{10}H_{14})(2\text{-}NH_2NC_5H_4)]$ (3.6)

Complex **3.1** (0.15 g, 0.25 mmol) was dissolved in dichloromethane (10 ml), and 2-aminopyridine (47 mg, 0.5 mmol) was added. The mixture was stirred overnight to give a red/orange solution and the solvent was evaporated to give a brown/orange solid.

Yield: 0.169 g, 0.42 mmol (85%).

Characterisation:

Calculated for $C_{15}H_{20}Cl_2N_2Ru$ (400.23 g mol^{-1}): C 45.0; H 5.0; N 7.0%

Found: C 44.7; H 5.0; N 6.7%

^{1}H NMR ($CDCl_3$, 500.23 MHz, 300.0 K)

δ 8.60 [d, $^{3}J_{(H-H)}$ = 6.0 Hz, 1H, 6-CH of 2-$NH_2NC_5\underline{H}_4$], 7.36 [br. t, $^{3}J_{(H-H)}$ = 7.3 Hz, 1H, 4-CH of 2-$NH_2NC_5\underline{H}_4$], 6.59 [m, 1H, 5-CH of 2-$NH_2NC_5\underline{H}_4$], 6.53 [d, $^{3}J_{(H-H)}$ = 7.7 Hz, 1H, 3-CH of 2-$NH_2NC_5\underline{H}_4$], 5.54 [d, $^{3}J_{(H-H)}$ = 5.1 Hz, 2H, $CH_3C(CH)_2(C\underline{H})_2CCH(CH_3)_2$], 5.33 [d, 2H, $^{3}J_{(H-H)}$ = 5.1 Hz, $CH_3C(C\underline{H})_2(CH)_2CCH(CH_3)_2$], 2.97 [m, 1H, $CH_3C(CH)_2(CH)_2CC\underline{H}(CH_3)_2$], 2.03 [s, 3H, $C\underline{H}_3C(CH)_2(CH)_2CCH(CH_3)_2$], 1.30 [d, $^{3}J_{(H-H)}$ = 6.8 Hz, 6H, $CH_3C(CH)_2(CH)_2CCH(C\underline{H}_3)_2$];

^{13}C{^{1}H} NMR ($CDCl_3$, 125.77 MHz, 299.2 K)

δ 162.6 [Quaternary C of 2-$NH_2N\underline{C}_5H_4$], 138.8 [6-CH of 2-$NH_2N\underline{C}_5H_4$], 129.0 [4-CH of 2-$NH_2N\underline{C}_5H_4$], 126.3 [5-CH of 2-$NH_2N\underline{C}_5H_4$], 114.5 [3-CH of 2-$NH_2N\underline{C}_5H_4$], 103.2 [$CH_3C(CH)_2(CH)_2\underline{C}CH(CH_3)_2$], 96.8 [$CH_3\underline{C}(CH)_2(CH)_2CCH(CH_3)_2$], 81.3 [$CH_3C(CH)_2(\underline{C}H)_2CCH(CH_3)_2$], 80.6 [$CH_3C(\underline{C}H)_2(CH)_2CCH(CH_3)_2$], 33.7 [$CH_3C(CH)_2(CH)_2C\underline{C}H(CH_3)_2$], 22.3 [$CH_3C(CH)_2(CH)_2CCH(\underline{C}H_3)_2$], 18.3 [$\underline{C}H_3C(CH)_2(CH)_2CCH(CH_3)_2$].

ES MS (+): m/z 365.0 $[M - Cl]^+$.

7.5.5 Preparation of $[RuCl_2(C_{10}H_{14})(3\text{-}OHNC_5H_4)]$ (3.7)

Complex **3.1** (0.15 g, 0.25 mmol) was dissolved in dichloromethane (10 ml), and 3-hydroxypyridine (47.6 mg, 0.5 mmol) was added. The mixture was stirred overnight and changed from a dark orange solution to an orange suspension that was filtered and washed with cold hexane to give a yellow solid.

Yield: 0.149 g, 0.37 mmol (74%).

Characterisation:

Calculated for $C_{15}H_{19}Cl_2NORu$ (401.22 g mol^{-1}): C 44.9; H 4.8; N 3.5; Cl 17.7%

Found: C 44.7; H 4.8; N 3.4; Cl 17.8%

^{1}H NMR ($CDCl_3$, 500.23 MHz, 300.0 K)

δ 8.63 [m, 1H, 2-CH of 3-$OHNC_5\underline{H}_4$], 8.34 [d, $^{3}J_{(H-H)}$ = 5.1 Hz, 1H, 6-CH of 3-$OHNC_5\underline{H}_4$], 7.02 [dd, $^{3}J_{(H-H)}$ = 8.3, 1.5 Hz, 1H, 4-CH of 3-$OHNC_5\underline{H}_4$], 6.89 [dd, $^{3}J_{(H-$

$_{H)}$ = 8.1, 5.6 Hz, 1H, 5-CH of 3-OHNC$_5$H$_4$], 5.47 [d, $^3J_{(H-H)}$ = 5.1 Hz, 2H, CH$_3$C(CH)$_2$(CH)$_2$CCH(CH$_3$)$_2$], 5.23 [d, $^3J_{(H-H)}$ = 6.0 Hz, 2H, CH$_3$C(CH)$_2$(CH)$_2$CCH(CH$_3$)$_2$], 2.98 [m, 1H, CH$_3$C(CH)$_2$(CH)$_2$CCH(CH$_3$)$_2$], 2.04 [s, 3H, CH$_3$C(CH)$_2$(CH)$_2$CCH(CH$_3$)$_2$], 1.31 [d, $^3J_{(H-H)}$ = 6.8 Hz, 6H, CH$_3$C(CH)$_2$(CH)$_2$CCH(CH$_3$)$_2$];

^{13}C{^{1}H} NMR (CDCl$_3$, 125.77 MHz, 299.2 K)

δ 153.3 [Quaternary C of 3-OHNC$_5$H$_4$], 146.1 [6-CH of 3-OHNC$_5$H$_4$], 144.2 [2-CH of 3-OHNC$_5$H$_4$], 126.3 [4-CH of 3-OHNC$_5$H$_4$], 124.6 [5-CH of 3-OHNC$_5$H$_4$], 103.5 [CH$_3$C(CH)$_2$(CH)$_2$CCH(CH$_3$)$_2$], 97.4 [CH$_3$C(CH)$_2$(CH)$_2$CCH(CH$_3$)$_2$], 83.1 [CH$_3$C(CH)$_2$(CH)$_2$CCH(CH$_3$)$_2$], 82.1 [CH$_3$C(CH)$_2$(CH)$_2$CCH(CH$_3$)$_2$], 30.7 [CH$_3$C(CH)$_2$(CH)$_2$CCH(CH$_3$)$_2$], 22.3 [CH$_3$C(CH)$_2$(CH)$_2$CCH(CH$_3$)$_2$], 18.2 [CH$_3$C(CH)$_2$(CH)$_2$CCH(CH$_3$)$_2$].

ES MS (+): m/z 366.0 [M – Cl]$^+$.

7.5.6 Preparation of [RuCl$_2$(C$_{10}$H$_{14}$)(3-FNC$_5$H$_4$)] (3.8)

Complex **3.1** (0.15 g, 0.25 mmol) was dissolved in dichloromethane (10 ml), and 3-fluoropyridine (86 μl, 1 mmol) was added. The mixture was stirred overnight to give an orange solution and the solvent was evaporated to give an orange solid.

Yield: 0.195 g, 0.48 mmol (97%).

Characterisation:

Calculated for C$_{15}$H$_{18}$Cl$_2$FNRu (403.21 g mol^{-1}): C 44.6; H 4.5; N 3.5; Cl 17.6%

Found: C 44.9; H 4.5; N 3.6; Cl 18.0%

^{1}H NMR (CDCl$_3$, 500.23 MHz, 300.0 K)

δ 8.99 [br. s, 1H, 2-CH of 3-FNC$_5$H$_4$], 8.90 [d, $^3J_{(H-H)}$ = 4.8 Hz, 1H, 6-CH of 3-FNC$_5$H$_4$], 7.50 [m, 1H, 4-CH of 3-FNC$_5$H$_4$], 7.33 [m, 1H, 5-CH of 3-FNC$_5$H$_4$], 5.46 [d, $^3J_{(H-H)}$ = 5.2 Hz, 2H, CH$_3$C(CH)$_2$(CH)$_2$CCH(CH$_3$)$_2$], 5.25 [d, $^3J_{(H-H)}$ = 5.2 Hz, 2H, CH$_3$C(CH)$_2$(CH)$_2$CCH(CH$_3$)$_2$], 2.98 [m, 1H, CH$_3$C(CH)$_2$(CH)$_2$CCH(CH$_3$)$_2$], 2.10 [s, 3H, CH$_3$C(CH)$_2$(CH)$_2$CCH(CH$_3$)$_2$], 1.31 [d, $^3J_{(H-H)}$ = 6.8 Hz, 6H, CH$_3$C(CH)$_2$(CH)$_2$CCH(CH$_3$)$_2$];

$^{13}C\{^{1}H\}$ NMR ($CDCl_3$, 75.47 MHz, 300.1 K)

δ 158.7 [d, $^{1}J_{(C-F)}$ = 254.3 Hz, Quaternary C of 3-FN$\underline{C}_5H_4$], 151.3 [d, $^{4}J_{(C-F)}$ = 3.8 Hz, 6-CH of 3-FN$\underline{C}_5H_4$], 143.9 [d, $^{2}J_{(C-F)}$ = 31.7 Hz, 2-CH of 3-FN$\underline{C}_5H_4$], 124.9 [m, 4- and 5-CH of 3-FN$\underline{C}_5H_4$], 103.7 [s, $CH_3C(CH)_2(CH)_2\underline{C}CH(CH_3)_2$], 97.3 [s, $CH_3\underline{C}(CH)_2(CH)_2CCH(CH_3)_2$], 82.8 [s, $CH_3C(CH)_2(\underline{C}H)_2CCH(CH_3)_2$], 82.3 [s, $CH_3C(\underline{C}H)_2(CH)_2CCH(CH_3)_2$], 30.7 [s, $CH_3C(CH)_2(CH)_2C\underline{C}H(CH_3)_2$], 22.3 [s, $CH_3C(CH)_2(CH)_2CCH(\underline{C}H_3)_2$], 18.2 [s, $\underline{C}H_3C(CH)_2(CH)_2CCH(CH_3)_2$].

ES MS (+): m/z 368.0 $[M - Cl]^+$.

7.5.7 Preparation of $[RuCl_2(C_{10}H_{14})(3\text{-}ClNC_5H_4)]$ (3.9)

Complex **3.1** (0.15 g, 0.25 mmol) was dissolved in dichloromethane (10 ml), and 3-chloropyridine (95 μl, 1 mmol) was added. The mixture was stirred overnight to give an orange solution and the solvent was evaporated to give an orange solid.

Yield: 0.201 g, 0.48 mmol (96%).

Characterisation:

Calculated for $C_{15}H_{18}Cl_3NRu$ (419.71 g mol^{-1}): C 42.9; H 4.3; N 3.3; Cl 25.4%

Found: C 42.8; H 4.3; N 3.2; Cl 25.3%

^{1}H NMR ($CDCl_3$, 500.23 MHz, 300.0 K)

δ 9.05 [m, 1H, 2-CH of 3-$ClNC_5\underline{H}_4$], 8.98 [d, $^{3}J_{(H-H)}$ = 5.1 Hz, 1H, 6-CH of 3-$ClNC_5\underline{H}_4$], 7.74 [d, $^{3}J_{(H-H)}$ = 7.7 Hz, 1H, 4-CH of 3-$ClNC_5\underline{H}_4$], 7.29 [m, 1H, 5-CH of 3-$ClNC_5\underline{H}_4$], 5.47 [d, $^{3}J_{(H-H)}$ = 6.0 Hz, 2H, $CH_3C(CH)_2(C\underline{H})_2CCH(CH_3)_2$], 5.25 [d, $^{3}J_{(H-H)}$ = 5.1 Hz, 2H, $CH_3C(C\underline{H})_2(CH)_2CCH(CH_3)_2$], 2.98 [sep, $^{3}J_{(H-H)}$ = 6.8 Hz, 1H, $CH_3C(CH)_2(CH)_2CC\underline{H}(CH_3)_2$], 2.11 [s, 3H, $C\underline{H}_3C(CH)_2(CH)_2CCH(CH_3)_2$], 1.32 [d, $^{3}J_{(H-H)}$ = 6.8 Hz, 6H, $CH_3C(CH)_2(CH)_2CCH(C\underline{H}_3)_2$];

$^{13}C\{^{1}H\}$ NMR ($CDCl_3$, 75.47 MHz, 300.0 K)

δ 153.7 [2-CH of 3-ClN$\underline{C}_5H_4$], 153.0 [6-CH of 3-ClN$\underline{C}_5H_4$], 137.7 [4-CH of 3-ClN$\underline{C}_5H_4$], 132.5 [Quaternary C of 3-ClN$\underline{C}_5H_4$], 124.7 [5-CH of 3-ClN$\underline{C}_5H_4$], 103.7 [$CH_3C(CH)_2(CH)_2\underline{C}CH(CH_3)_2$], 97.3 [$CH_3\underline{C}(CH)_2(CH)_2CCH(CH_3)_2$], 82.9 [$CH_3C(CH)_2(\underline{C}H)_2CCH(CH_3)_2$], 82.2 [$CH_3C(\underline{C}H)_2(CH)_2CCH(CH_3)_2$], 30.7

$[CH_3C(CH)_2(CH)_2C\underline{C}H(CH_3)_2]$, 22.3 $[CH_3C(CH)_2(CH)_2CCH(\underline{C}H_3)_2]$, 18.3 $[\underline{C}H_3C(CH)_2(CH)_2CCH(CH_3)_2]$.

ES MS (+): m/z 384.0 $[M - Cl]^+$.

7.5.8 Preparation of $[RuCl_2(C_{10}H_{14})(3\text{-}BrNC_5H_4)]$ (3.10)

Complex **3.1** (0.15 g, 0.25 mmol) was dissolved in dichloromethane (10 ml), and 3-bromopyridine (96.3 μl, 1 mmol) was added. The mixture was stirred overnight to give an orange solution and the solvent was evaporated to give an orange solid.

Yield: 0.209 g, 0.45 mmol (90%).

Characterisation:

Calculated for $C_{15}H_{18}BrCl_2NRu$ (464.12 g mol^{-1}): C 38.8; H 3.9; N 3.0%

Found: C 38.8; H 3.9; N 2.9%

^{1}H NMR ($CDCl_3$, 500.23 MHz, 300.0 K)

δ 9.15 [m, 1H, 2-CH of $3\text{-}BrNC_5\underline{H}_4$], 9.02 [d, $^3J_{(H\text{-}H)}$ = 5.6 Hz, 1H, 6-CH of $3\text{-}BrNC_5\underline{H}_4$], 7.89 [d, $^3J_{(H\text{-}H)}$ = 7.9 Hz, 1H, 4-CH of $3\text{-}BrNC_5\underline{H}_4$], 7.23 [dd, $^3J_{(H\text{-}H)}$ = 7.7, 5.8 Hz, 1H, 5-CH of $3\text{-}BrNC_5\underline{H}_4$], 5.47 [d, $^3J_{(H\text{-}H)}$ = 6.0 Hz, 2H, $CH_3C(CH)_2(C\underline{H})_2CCH(CH_3)_2$], 5.25 [d, $^3J_{(H\text{-}H)}$ = 6.0 Hz, 2H, $CH_3C(C\underline{H})_2(CH)_2CCH(CH_3)_2$], 2.98 [sep, $^3J_{(H\text{-}H)}$ = 6.9 Hz, 1H, $CH_3C(CH)_2(CH)_2CC\underline{H}(CH_3)_2$], 2.12 [s, 3H, $C\underline{H}_3C(CH)_2(CH)_2CCH(CH_3)_2$], 1.32 [d, $^3J_{(H\text{-}H)}$ = 6.8 Hz, 6H, $CH_3C(CH)_2(CH)_2CCH(C\underline{H}_3)_2$];

^{13}C{^{1}H} NMR ($CDCl_3$, 75.47 MHz, 300.0 K)

δ 155.7 [2-CH of $3\text{-}BrN\underline{C}_5H_4$], 153.4 [6-CH of $3\text{-}BrN\underline{C}_5H_4$], 140.5 [4-CH of $3\text{-}BrN\underline{C}_5H_4$], 125.1 [5-CH of $3\text{-}BrN\underline{C}_5H_4$], 120.4 [Quaternary C of $3\text{-}BrN\underline{C}_5H_4$], 103.7 $[CH_3C(CH)_2(CH)_2\underline{C}CH(CH_3)_2]$, 97.4 $[CH_3\underline{C}(CH)_2(CH)_2CCH(CH_3)_2]$, 82.9 $[CH_3C(CH)_2(\underline{C}H)_2CCH(CH_3)_2]$, 82.2 $[CH_3C(\underline{C}H)_2(CH)_2CCH(CH_3)_2]$, 30.7 $[CH_3C(CH)_2(CH)_2C\underline{C}H(CH_3)_2]$, 22.3 $[CH_3C(CH)_2(CH)_2CCH(\underline{C}H_3)_2]$, 18.3 $[\underline{C}H_3C(CH)_2(CH)_2CCH(CH_3)_2]$.

ES MS (+): m/z 429.9 $[M - Cl]^+$.

7.5.9 Preparation of [$RuCl_2(C_{10}H_{14})(3\text{-}INC_5H_4)$] (3.11)

Complex **3.1** (0.15 g, 0.25 mmol) was dissolved in dichloromethane (10 ml), and 3-iodopyridine (0.2 g, 1 mmol) was added. The mixture was stirred overnight to give an orange solution that formed a suspension after less than 5 minutes. This suspension was filtered and washed with cold hexane to give a yellow solid.

Yield: 0.19 g, 0.37 mmol (74%).

Characterisation:

Calculated for $C_{15}H_{18}Cl_2INRu$ (511.11 g mol^{-1}): C 35.2; H 3.6; N 2.7%

Found: C 35.5; H 3.5; N 2.7%

^{1}H NMR ($CDCl_3$, 500.23 MHz, 300.0 K)

δ 9.29 [m, 1H, 2-CH of 3-IN$C_5\underline{H}_4$], 9.06 [d, $^3J_{(H\text{-}H)}$ = 5.2 Hz, 1H, 6-CH of 3-IN$C_5\underline{H}_4$], 8.07 [d, $^3J_{(H\text{-}H)}$ = 7.9 Hz, 1H, 4-CH of 3-IN$C_5\underline{H}_4$], 7.10 [dd, $^3J_{(H\text{-}H)}$ = 7.9, 5.6 Hz, 1H, 5-CH of 3-IN$C_5\underline{H}_4$], 5.46 [d, $^3J_{(H\text{-}H)}$ = 6.0 Hz, 2H, $CH_3C(CH)_2(C\underline{H})_2CCH(CH_3)_2$], 5.24 [d, $^3J_{(H\text{-}H)}$ = 5.6 Hz, 2H, $CH_3C(C\underline{H})_2(CH)_2CCH(CH_3)_2$], 2.98 [m, 1H, $CH_3C(CH)_2(CH)_2CC\underline{H}(CH_3)_2$], 2.12 [s, 3H, $C\underline{H}_3C(CH)_2(CH)_2CCH(CH_3)_2$], 1.33 [d, $^3J_{(H\text{-}H)}$ = 6.8 Hz, 6H, $CH_3C(CH)_2(CH)_2CCH(C\underline{H}_3)_2$];

^{13}C{^{1}H} NMR ($CDCl_3$, 75.47 MHz, 300.1 K)

δ 160.3 [2-CH of 3-IN$\underline{C}_5H_4$], 153.7 [6-CH of 3-IN$\underline{C}_5H_4$], 146.0 [4-CH of 3-IN$\underline{C}_5H_4$], 125.4 [5-CH of 3-IN$\underline{C}_5H_4$], 103.6 [$CH_3C(CH)_2(CH)_2\underline{C}CH(CH_3)_2$], 97.3 [$CH_3\underline{C}(CH)_2(CH)_2CCH(CH_3)_2$], 91.8 [Quaternary C of 3-IN$\underline{C}_5H_4$], 82.9 [$CH_3C(CH)_2(\underline{C}H)_2CCH(CH_3)_2$], 82.2 [$CH_3C(\underline{C}H)_2(CH)_2CCH(CH_3)_2$], 30.7 [$CH_3C(CH)_2(CH)_2C\underline{C}H(CH_3)_2$], 22.3 [$CH_3C(CH)_2(CH)_2CCH(\underline{C}H_3)_2$], 18.3 [$\underline{C}H_3C(CH)_2(CH)_2CCH(CH_3)_2$].

ES MS (+): m/z 475.9 $[M - Cl]^+$.

7.5.10 Preparation of [$RuCl_2(C_{10}H_{14})(4\text{-}N(CH_3)_2NC_5H_4)$] (3.12)

Complex **3.1** (0.15 g, 0.25 mmol) was dissolved in dichloromethane (10 ml), and 4-(dimethylamino)pyridine (61.1 mg, 0.5 mmol) was added. The mixture was

stirred for two days to give an orange solution and the solvent was evaporated to give an orange solid.

Yield: 0.15 g, 0.35 mmol (70%).

Characterisation:

Calculated for $C_{17}H_{24}Cl_2N_2Ru$ (428.26 g mol^{-1}): C 47.6; H 5.7; N 6.5; Cl 16.6%

Found: C 47.2; H 5.6; N 6.4; Cl 17.1%

^{1}H NMR ($CDCl_3$, 300.13 MHz, 300.0 K)

δ 8.42 [dm, $^3J_{(H-H)}$ = 7.2 Hz, 2H, 2,6-CH of 4-N$(CH_3)_2NC_5\underline{H}_4$], 6.41 [dm, $^3J_{(H-H)}$ = 7.2 Hz, 2H, 3,5-CH of 4-N$(CH_3)_2NC_5\underline{H}_4$], 5.40 [d, $^3J_{(H-H)}$ = 5.7 Hz, 2H, $CH_3C(CH)_2(C\underline{H})_2CCH(CH_3)_2$], 5.17 [d, $^3J_{(H-H)}$ = 5.7 Hz, 2H, $CH_3C(C\underline{H})_2(CH)_2CCH(CH_3)_2$], 2.99 [s, 6H, 4-N$(C\underline{H}_3)_2NC_5H_4$], 2.97 [m, 1H, $CH_3C(CH)_2(CH)_2CC\underline{H}(CH_3)_2$], 2.09 [s, 3H, $C\underline{H}_3C(CH)_2(CH)_2CCH(CH_3)_2$], 1.29 [d, $^3J_{(H-H)}$ = 7.2 Hz, 6H, $CH_3C(CH)_2(CH)_2CCH(C\underline{H}_3)_2$];

^{13}C{^{1}H} NMR ($CDCl_3$, 75.47 MHz, 300.0 K)

δ 153.3 [2,6-CH of 4-N$(CH_3)_2N\underline{C}_5H_4$], 107.4 [3,5-CH of 4-N$(CH_3)_2N\underline{C}_5H_4$], 102.9 [$CH_3C(CH)_2(CH)_2\underline{C}CH(CH_3)_2$], 96.8 [$CH_3\underline{C}(CH)_2(CH)_2CCH(CH_3)_2$], 89.8 [Quaternary C of 4-N$(CH_3)_2N\underline{C}_5H_4$], 82.8 [$CH_3C(CH)_2(\underline{C}H)_2CCH(CH_3)_2$], 81.8 [$CH_3C(\underline{C}H)_2(CH)_2CCH(CH_3)_2$], 39.3 [4-N$(\underline{C}H_3)_2NC_5H_4$], 30.6 [$CH_3C(CH)_2(CH)_2C\underline{C}H(CH_3)_2$], 22.4 [$CH_3C(CH)_2(CH)_2CCH(\underline{C}H_3)_2$], 18.3 [$\underline{C}H_3C(CH)_2(CH)_2CCH(CH_3)_2$].

ES MS (+): m/z 393.1 $[M - Cl]^+$.

7.5.11 Preparation of $[RuCl_2(C_{10}H_{14})(4\text{-}BrNC_5H_4)]$ (3.13)

Complex **3.1** (0.15 g, 0.25 mmol) was dissolved in dichloromethane (10 ml), and 4-bromopyridine hydrochloride (97.23 mg, 0.5 mmol) was added. The mixture was stirred overnight to give an orange solution with some undissolved powder that was filtered, and the filtrate evaporated to give an orange solid.

Yield: 0.23 g, 0.5 mmol (100%).

Characterisation:

Calculated for $C_{15}H_{18}BrCl_2NRu$ (464.11 g mol^{-1}): C 38.8; H 3.9; N 3.0%

Found: C 39.1; H 3.9; N 2.9%

^{1}H NMR ($CDCl_3$, 500.23 MHz, 300.0 K)

δ 8.87 [d, $^3J_{(H-H)}$ = 5.2 Hz, 2H, 2,6-CH of 4-$BrNC_5\underline{H}_4$], 7.49 [d, $^3J_{(H-H)}$ = 5.6 Hz, 2H, 3,5-CH of 4-$BrNC_5\underline{H}_4$], 5.46 [d, $^3J_{(H-H)}$ = 4.8 Hz, 2H, $CH_3C(CH)_2(C\underline{H})_2CCH(CH_3)_2$], 5.25 [d, $^3J_{(H-H)}$ = 4.8 Hz, 2H, $CH_3C(C\underline{H})_2(CH)_2CCH(CH_3)_2$], 2.99 [m, 1H, $CH_3C(CH)_2(CH)_2CC\underline{H}(CH_3)_2$], 2.12 [s, 3H, $C\underline{H}_3C(CH)_2(CH)_2CCH(CH_3)_2$], 1.32 [d, $^3J_{(H-H)}$ = 6.8 Hz, 6H, $CH_3C(CH)_2(CH)_2CCH(C\underline{H}_3)_2$];

^{13}C{^{1}H} NMR ($CDCl_3$, 75.47 MHz, 300.0 K)

δ 155.3 [2,6-CH of 4-$BrN\underline{C}_5H_4$], 135.5 [Quaternary C of 4-$BrN\underline{C}_5H_4$], 128.1 [3,5-CH of 4-$BrN\underline{C}_5H_4$], 103.7 [$CH_3C(CH)_2(CH)_2\underline{C}CH(CH_3)_2$], 97.2 [$CH_3\underline{C}(CH)_2(CH)_2CCH(CH_3)_2$], 82.8 [$CH_3C(CH)_2(\underline{C}H)_2CCH(CH_3)_2$], 82.2 [$CH_3C(\underline{C}H)_2(CH)_2CCH(CH_3)_2$], 30.7 [$CH_3C(CH)_2(CH)_2C\underline{C}H(CH_3)_2$], 22.3 [$CH_3C(CH)_2(CH)_2CCH(\underline{C}H_3)_2$], 18.3 [$\underline{C}H_3C(CH)_2(CH)_2CCH(CH_3)_2$].

ES MS (+): m/z 429.9 $[M - Cl]^+$.

7.5.12 Preparation of $[RuCl(C_{10}H_{14})(NC_5H_5)_2][SbF_6]$ (3.14)

Complex **3.4** (57.8 mg, 0.15 mmol) and pyridine (24.3 µl, 0.3 mmol) were dissolved in methanol (5 ml) and $NaSbF_6$ (0.23 g, 0.9 mmol), dissolved in methanol (5 ml), was added. The mixture was stirred and heated to reflux. After four hours, the solvent was evaporated. Chloroform was added to the solid obtained to separate the product from the salts by filtering, and then the filtrate was evaporated and the resulting residue dissolved in the minimum quantity of dichloromethane. Hexane was added, which gave an orange oil. After approximately one month, crystals suitable for X-ray diffraction studies formed.

Yield: 0.1 g, 0.15 mmol (100%).

Characterisation:

Calculated for $[C_{20}H_{24}ClN_2Ru][F_6Sb]$ (664.51 g mol^{-1}): C 36.1; H 3.6; N 4.2; Cl 5.3%

Found: C 36.3; H 3.7; N 4.1; Cl 5.2%

^{1}H NMR ($CDCl_3$, 300.13 MHz, 300.0 K)

δ 9.03 [d, $^3J_{(H-H)}$ = 5.3 Hz, 4H, 2,6-CH of $NC_5\underline{H}_5$], 7.85 [t, $^3J_{(H-H)}$ = 7.6 Hz, 2H, 4-CH of $NC_5\underline{H}_5$], 7.48 [t, $^3J_{(H-H)}$ = 6.9 Hz, 4H, 3,5-CH of $NC_5\underline{H}_5$], 5.91 [d, $^3J_{(H-H)}$ = 6.0 Hz, 2H, $CH_3C(CH)_2(C\underline{H})_2CCH(CH_3)_2$], 5.63 [d, $^3J_{(H-H)}$ = 5.9 Hz, 2H, $CH_3C(C\underline{H})_2(CH)_2CCH(CH_3)_2$], 2.58 [m, 1H, $CH_3C(CH)_2(CH)_2CC\underline{H}(CH_3)_2$], 1.74 [s, 3H, $C\underline{H}_3C(CH)_2(CH)_2CCH(CH_3)_2$], 1.16 [d, $^3J_{(H-H)}$ = 6.8 Hz, 6H, $CH_3C(CH)_2(CH)_2CCH(C\underline{H}_3)_2$];

^{13}C{^{1}H} NMR ($CDCl_3$, 75.47 MHz, 300.1 K)

δ 153.1 [2,6-CH of NC_5H_5], 138.1 [4-CH of NC_5H_5], 125.3 [3,5-CH of NC_5H_5], 101.8 [$CH_3C(CH)_2(CH)_2CCH(CH_3)_2$], 101.0 [$CH_3C(CH)_2(CH)_2CCH(CH_3)_2$], 87.7 [$CH_3C(CH)_2(CH)_2CCH(CH_3)_2$], 81.0 [$CH_3C(CH)_2(CH)_2CCH(CH_3)_2$], 29.8 [$CH_3C(CH)_2(CH)_2CCH(CH_3)_2$], 21.2 [$CH_3C(CH)_2(CH)_2CCH(CH_3)_2$], 16.7 [$CH_3C(CH)_2(CH)_2CCH(CH_3)_2$].

ES MS (+): m/z 429.07 $[M - SbF_6]^+$.

7.6 Pentamethylcyclopentadiene and (5-Hydroxypentyl)-Tetramethylcyclopentadiene Ligands

Compound **4.1** was synthesised according to the method by Bergman *et al*.[14] Compound **4.2** had been synthesised previously by Blacker and co-workers with a similar procedure to that of ligand **4.1**, but changing ethyl acetate to caprolactone to obtain the long –OH tether.[15] Their synthetic method was the one employed here.

7.6.1 Preparation of $C_{10}H_{16}$ (4.1)

2-Bromo-2-butene (60.2 ml, 0.59 mol) was added dropwise from an addition funnel to lithium wire (7.92 g, 1.14 mol) in dry diethyl ether under a nitrogen atmosphere. The reaction started to reflux and was stirred for three hours. Ethyl

acetate (26.3 ml, 0.27 mol) diluted in diethyl ether was added through the addition funnel and stirred for one hour. The mixture was poured into 600 ml of saturated aqueous NH_4Cl. The layers were separated, and the aqueous layer extracted with diethyl ether (×3). The ether layers were combined, washed with water, dried over $MgSO_4$, filtered and concentrated to approx. 200 ml. This concentrate was added to *p*-toluensulphonic acid (4.91 g, 0.026 mol) in dry diethyl ether (300 ml) under nitrogen, maintaining a gentle reflux. The mixture was stirred for one hour and then saturated aqueous $NaHCO_3$ was added. The ether layer was separated and the aqueous layer extracted with diethyl ether (×3). The combined ether layers were washed with water, dried over Na_2SO_4, filtered and evaporated. The yellow oil obtained was purified by distillation (34°C) under reduced pressure and stored in the freezer.

Yield: 21.44 g, 0.157 mol (58%).

Characterisation:

^{1}H NMR ($CDCl_3$, 300.13 MHz, 300.0 K)

δ 2.52 [q, $^3J_{(H-H)}$ = 7.6 Hz, 1H, $(CCH_3)_4C\underline{H}CH_3$], 1.84 [s, 6H, $(CC\underline{H_3})_4CHCH_3$], 1.80 [s, 6H, $(CC\underline{H_3})_4CHCH_3$], 1.04 [d, $^3J_{(H-H)}$ = 7.7 Hz, 3H, $(CCH_3)_4CHC\underline{H_3}$].

ES MS (+): m/z 136.13 $[M]^+$.

7.6.2 Preparation of $C_{14}H_{24}O$ (4.2)

2-Bromo-2-butene (12.2 ml, 0.12 mol) was added dropwise from an addition funnel to lithium wire (1.6 g, 0.23 mol) in dry diethyl ether under a nitrogen atmosphere. The reaction started to reflux and was stirred for two hours. ε-Caprolactone (5.98 ml, 0.054 mol) was added from the dropping funnel and the reaction was stirred for one hour. The mixture was poured into a saturated aqueous solution of NH_4Cl. The ether layer was separated and the aqueous layer was extracted with *tert*-butyl-methyl ether (×3). The ether layers were combined, washed with brine, dried over $MgSO_4$ and concentrated to approx. 100 ml. A 10% solution of HCl (150 ml) was added to the concentrate and stirred for three hours. Two orange/dark yellow layers formed and the aqueous one was extracted with *tert*-butyl-methyl ether (×3) after separating the organic layer. The combined ether layers were

washed with water (×2), dried over Na_2SO_4, filtered and the solvent evaporated to give a dark orange oil, which was purified by column chromatography with silica and a solvent mixture of hexane : ethyl acetate (10 : 1). The resulting yellow oil was kept in the freezer.

Yield: 6.2 g, 0.0299 mol (55%).

Characterisation:

^{1}H NMR ($CDCl_3$, 500.23 MHz, 303.4 K)

δ 3.64 [t, $^3J_{(H-H)}$ = 6.4 Hz, 2H, $(CCH_3)_3(CHCH_3)C(C\underline{H}_2)_5OH$], 2.21 [m, 2H, $(CCH_3)_3(CHCH_3)C(C\underline{H}_2)_5OH$], 1.82 [br. s, 3H, $(CC\underline{H}_3)_3(CHCH_3)C(CH_2)_5OH$], 1.78 [br. s, 6H, $(CC\underline{H}_3)_3(CHCH_3)C(CH_2)_5OH$], 1.59 [m, 2H, $(CCH_3)_3(CHCH_3)C(C\underline{H}_2)_5OH$], 1.44 [br. s, 1H, $(CCH_3)_3(C\underline{H}CH_3)C(CH_2)_5OH$], 1.39 [m, 2H, $(CCH_3)_3(CHCH_3)C(C\underline{H}_2)_5OH$], 1.28 [m, 2H, $(CCH_3)_3(CHCH_3)C(C\underline{H}_2)_5OH$], 1.01 [dd, $^3J_{(H-H)}$ = 7.8, 4.6 Hz, 3H, $(CCH_3)_3(CHC\underline{H}_3)C(CH_2)_5OH$].

7.7 Cp* and Cp$^{\#}$ Ruthenium(III) Oligomers

Compound **4.3** was synthesised with a combination of the methods published by Suzuki[16] and Bercaw.[17] This procedure was also adapted for the preparation of the novel compound **4.4**.

7.7.1 Preparation of $[RuCl_2(C_{10}H_{15})]_n$ (4.3)

Cyclopentadiene (**4.1**) (2 g, 15.1 mmol) was added to a solution of $RuCl_3 \cdot 3H_2O$ (1.73 g, 6.62 mmol) in dry ethanol (50 ml). The mixture was stirred and heated to reflux under nitrogen for three hours. After that, it was concentrated and left in the freezer overnight, and the red/brown solid obtained was filtered and washed with dry hexane (×3). Once this was dried under vacuum, it was kept in the glove box.

Yield: 1.5 g, 4.90 mmol (74%).

Characterisation:

Calculated for $[C_{10}H_{15}Cl_2Ru]_n$ (307.19 g mol^{-1}): C 39.1; H 4.9; Cl 23.1%

Found: C 38.9; H 4.9; Cl 23.3%

^{1}H NMR ($CDCl_3$, 300.13 MHz, 300.1 K)

δ 4.67 [br. s, 15H, $C_5(C\underline{H}_3)_5$];

^{13}C{^{1}H} NMR ($CDCl_3$, 75.48 MHz, 300.0 K)

δ 138.1 [$\underline{C}_5(CH_3)_5$], 12.0 [$C_5(\underline{C}H_3)_5$].

7.7.2 Preparation of $[RuCl_2(C_{14}H_{23})]_n$ (4.4)

(5-Hydroxypentyl)-tetramethylcyclopentadiene (**4.2**) (3.14 g, 15.1 mmol) was added to a solution of $RuCl_3 \cdot 3H_2O$ (1.73 g, 6.62 mmol) in dry ethanol (50 ml) and the mixture was stirred and heated to reflux under nitrogen for three hours. After that, it was concentrated and left in the freezer overnight, which resulted in precipitation of an orange solid. This was filtered, washed with dry hexane (×3), dried under vacuum and kept in the glove box.

Yield: 1.214 g, 3.20 mmol (48%).

Characterisation:

Calculated for $[C_{14}H_{23}Cl_2Ru]_n$ (379.25 g mol^{-1}): C 44.3; H 6.1; Cl 18.7%

Found: C 44.7; H 6.3; Cl 18.3%

^{1}H NMR ($CDCl_3$, 500.57 MHz, 300.0 K)

δ 5.11 [br. s, 6H, $C_5(C\underline{H}_3)_4(CH_2)_5OH$], 4.15 [br. s, 6H, $C_5(C\underline{H}_3)_4(CH_2)_5OH$], 4.09 [m, 4H, $C_5(CH_3)_4(C\underline{H}_2)_5OH$], 3.35 [br. s, 2H, $C_5(CH_3)_4(C\underline{H}_2)_5OH$], 2.73 [br. s, 2H, $C_5(CH_3)_4(C\underline{H}_2)_5OH$], 2.29 [m, 2H, $C_5(CH_3)_4(C\underline{H}_2)_5OH$];

^{13}C{^{1}H} NMR ($CDCl_3$, 125.77 MHz, 299.2 K)

δ 142.3 [$\underline{C}_5(CH_3)_4(CH_2)_5OH$], 135.3 [$\underline{C}_5(CH_3)_4(CH_2)_5OH$], 128.2 [$\underline{C}_5(CH_3)_4(CH_2)_5OH$], 63.3 [$C_5(CH_3)_4(\underline{C}H_2)_5OH$], 33.7 [$C_5(CH_3)_4(\underline{C}H_2)_5OH$], 27.2 [$C_5(CH_3)_4(\underline{C}H_2)_5OH$], 24.6 [$C_5(CH_3)_4(\underline{C}H_2)_5OH$], 12.5 [$C_5(\underline{C}H_3)_4(CH_2)_5OH$], 11.8 [$C_5(\underline{C}H_3)_4(CH_2)_5OH$].

7.8 Cp* and Cp$^{\#}$ Diphosphine Ruthenium(II) Monomers

The compounds **4.5** to **4.11** were synthesised using the same general method adapted from those of Suzuki[16] and Bercaw.[17] Complexes **4.3** or **4.4** were used as starting materials, and the diphosphines were all commercially available. The solvent used was dichloromethane, and the reactions proceeded at room temperature. Compound **4.12** was synthesised from complex **4.5** by adapting the method published by Moret *et al*.[18]

7.8.1 Preparation of [RuCl($C_{10}H_{15}$)($C_{25}H_{22}P_2$)] (4.5)

1,1'-Bis(diphenylphosphino)methane (0.46 g, 1.2 mmol) was added to a solution of compound **4.3** (0.25 g, 0.8 mmol) in dry dichloromethane (100 ml) and the mixture was stirred under nitrogen overnight. The solvent was evaporated to give a dark yellow/brown residue, which was extracted with diethyl ether (×3). The solvent was evaporated from the extract and the orange residue was recrystallised from dichloromethane/hexane to give orange needles.

Yield: 0.3724 g, 0.568 mmol (71%).

Characterisation:

Calculated for $C_{35}H_{37}ClP_2Ru$ (655.80 g mol^{-1}): C 64.0; H 5.7; Cl 5.4%

Found: C 63.9; H 5.7; Cl 5.6%

^{1}H NMR ($C_6D_5CD_3$, 300.13 MHz, 299.9 K)

δ 7.61-6.71 [20H, ($C_6\underline{H}_5)_4P_2CH_2$], 4.45 [dt, $^2J_{(H-H)}$ = 14.2 Hz, $^2J_{(H-P)}$ = 9.4 Hz, 1H, ($C_6H_5)_4P_2C\underline{H}_2$], 4.21 [dt, $^2J_{(H-H)}$ = 14.2 Hz, $^2J_{(H-P)}$ = 11.2 Hz, 1H, ($C_6H_5)_4P_2C\underline{H}_2$], 1.74 [t, $^4J_{(H-P)}$ = 2.0 Hz, 15H, $C_5(C\underline{H}_3)_5$];

^{31}P{^{1}H} NMR ($C_6D_5CD_3$, 121.49 MHz, 300.0 K) δ 12.81 [s];

^{13}C{^{1}H} NMR ($C_6D_5CD_3$, 75.48 MHz, 300.0 K)

δ 137.5 [s, ($\underline{C}_6H_5)_4P_2CH_2$], 133.6 [m, ($\underline{C}_6H_5)_4P_2CH_2$], 132.9 [m, ($\underline{C}_6H_5)_4P_2CH_2$], 88.5 [t, $^2J_{(C-P)}$ = 2.5 Hz, $\underline{C}_5(CH_3)_5$], 49.1 [m, ($C_6H_5)_4P_2\underline{C}H_2$], 10.7 [s, $C_5(\underline{C}H_3)_5$].

ES MS (+): m/z 621.1 $[M - Cl]^+$.

7.8.2 Preparation of [RuCl($C_{10}H_{15}$)($C_{34}H_{28}FeP_2$)] (4.6)

1,1'-Bis(diphenylphosphino)ferrocene (0.42 g, 0.75 mmol) was added to a solution of compound **4.3** (0.15 g, 0.5 mmol) in dry dichloromethane (100 ml) and the mixture was stirred under nitrogen overnight. The solvent was evaporated to give a dark yellow residue, which was washed with diethyl ether (×4) and recrystallised from dichloromethane (filtered solution)/hexane to give a yellow microcrystalline solid.

Yield: 0.0856 g, 0.1036 mmol (21%).

Characterisation:

Calculated for $C_{44}H_{43}ClFeP_2Ru$ (825.77 g mol^{-1}) + CH_2Cl_2 (85.02 g mol^{-1}) : C 59.3; H 5.0; Cl 11.7%

Found: C 60.1; H 5.1; Cl 11.4%

^{1}H NMR ($C_6D_5CD_3$, 300.13 MHz, 300.1 K)

δ 8.12-6.70 [20H, $(C_6\underline{H}_5)_4P_2Fe(C_5H_4)_2$], 5.46 [s, 2H, $(C_6H_5)_4P_2Fe(C_5\underline{H}_4)_2$], 4.01 [s, 2H, $(C_6H_5)_4P_2Fe(C_5\underline{H}_4)_2$], 3.87 [s, 2H, $(C_6H_5)_4P_2Fe(C_5\underline{H}_4)_2$], 3.63 [s, 2H, $(C_6H_5)_4P_2Fe(C_5\underline{H}_4)_2$], 1.11 [t, $^4J_{(H-P)}$ = 1.5 Hz, 15H, $C_5(C\underline{H}_3)_5$];

^{31}P{^{1}H} NMR ($C_6D_5CD_3$, 121.49 MHz, 300.0 K) δ 42.37 [s];

^{13}C{^{1}H} NMR ($C_6D_5CD_3$, 125.77 MHz, 299.2 K)

δ 137.4 [m, $(\underline{C}_6H_5)_4P_2Fe(C_5H_4)_2$], 136.8 [t, $^{2,3}J_{(C-P)}$ = 4.8 Hz, $(\underline{C}_6H_5)_4P_2Fe(C_5H_4)_2$], 134.9 [t, $^{2,3}J_{(C-P)}$ = 4.8 Hz, $(\underline{C}_6H_5)_4P_2Fe(C_5H_4)_2$], 91.3 [m, $(C_6H_5)_4P_2Fe(\underline{C}_5H_4)_2$], 89.1 [s, $\underline{C}_5(CH_3)_5$], 77.8 [m, $(C_6H_5)_4P_2Fe(\underline{C}_5H_4)_2$], 72.8 [s, $(C_6H_5)_4P_2Fe(\underline{C}_5H_4)_2$], 72.2 [s, $(C_6H_5)_4P_2Fe(\underline{C}_5H_4)_2$], 67.3 [s, $(C_6H_5)_4P_2Fe(\underline{C}_5H_4)_2$], 9.2 [s, $C_5(\underline{C}H_3)_5$].

ES MS (+): m/z 791.1 $[M - Cl]^+$.

7.8.3 Preparation of [RuCl($C_{10}H_{15}$)($C_{36}H_{28}OP_2$)] (4.7)

Bis(2-diphenylphosphinophenyl)ether (0.4 g, 0.75 mmol) was added to a solution of compound **4.3** (0.15 g, 0.5 mmol) in dry dichloromethane (100 ml) and the mixture was stirred under nitrogen overnight. The solvent was evaporated to give

an orange/brown residue, which was extracted with diethyl ether (×4). The orange ether extract was evaporated and the residue was recrystallised from dichloromethane/hexane to give an orange solid.

Yield: 0.1033 g, 0.13 mmol (26%).

Characterisation:

Calculated for $C_{46}H_{43}ClOP_2Ru$ (809.85 g mol^{-1}): C 68.2; H 5.4; Cl 4.4%

Found: C 67.9; H 5.3; Cl 4.7%

^{1}H NMR ($C_6D_5CD_3$, 300.13 MHz, 300.0 K)

δ 9.04-5.91 [28H, $(C_6\underline{H}_5)_4P_2O(C_6\underline{H}_4)_2$], 1.23 [m, 15H, $C_5(C\underline{H}_3)_5$];

^{31}P{^{1}H} NMR ($C_6D_5CD_3$, 202.46 MHz, 299.2 K) δ 22.41 [s];

DEPT135 ^{13}C{^{1}H} NMR ($C_6D_5CD_3$, 125.77 MHz, 299.2 K)

δ 137.4-118.4 [$(\underline{C}_6H_5)_4P_2O(\underline{C}_6H_4)_2$], 8.2 [s, $C_5(\underline{C}H_3)_5$].

ES MS (+): m/z 775.2 $[M - Cl]^+$.

7.8.4 Preparation of $[RuCl(C_{10}H_{15})(C_{39}H_{32}OP_2)]$ (4.8)

4,5-Bis(diphenylphosphino)-9,9-dimethylxanthene (0.43 g, 0.75 mmol) was added to a solution of compound **4.3** (0.15 g, 0.5 mmol) in dry dichloromethane (100 ml) and the mixture was stirred under nitrogen overnight. The solvent was evaporated to give a brown residue, which was extracted with diethyl ether (×4). The yellow ether extract was evaporated and the residue was recrystallised from dichloromethane/hexane to give a yellow solid.

Yield: 0.2062 g, 0.24 mmol (49%).

Characterisation:

Calculated for $C_{49}H_{47}ClOP_2Ru$ (849.97 g mol^{-1}): C 69.2; H 5.6; Cl 4.2%

Found: C 70.9; H 5.7; Cl 4.3%

^{1}H NMR ($C_6D_5CD_3$, 300.13 MHz, 300.0 K)

δ 8.16-6.49 [26H, $(C_6\underline{H}_5)_4P_2OC(CH_3)_2(C_6\underline{H}_3)_2$], 1.58 [s, 6H, $(C_6H_5)_4P_2OC(C\underline{H}_3)_2(C_6H_3)_2$], 1.00 [t, $^{4}J_{(H-P)}$ = 1.6 Hz, 15H, $C_5(C\underline{H}_3)_5$];

^{31}P{^{1}H} NMR ($C_6D_5CD_3$, 121.49 MHz, 300.0 K) δ 34.02 [s];

^{13}C{^{1}H} NMR ($C_6D_5CD_3$, 125.77 MHz, 299.2 K)

δ 155.9-123.1 [$(\underline{C}_6H_5)_4P_2OC(CH_3)_2(\underline{C}_6H_3)_2$], 88.2 [s, $\underline{C}_5(CH_3)_5$], 36.8 [s, $(C_6H_5)_4P_2O\underline{C}(CH_3)_2(C_6H_3)_2$], 30.7 [s, $(C_6H_5)_4P_2OC(\underline{C}H_3)_2(C_6H_3)_2$], 22.5 [s, $(C_6H_5)_4P_2OC(\underline{C}H_3)_2(C_6H_3)_2$], 9.1 [s, $C_5(\underline{C}H_3)_5$].

ES MS (+): m/z 815.2 $[M - Cl]^+$.

7.8.5 Preparation of [RuCl($C_{14}H_{23}$)($C_{25}H_{22}P_2$)] (4.9)

1,1'-Bis(diphenylphosphino)methane (0.29 g, 0.75 mmol) was added to a solution of compound **4.4** (0.19 g, 0.5 mmol) in dry dichloromethane (100 ml) and the mixture was stirred under nitrogen overnight. The solvent was evaporated to give a brown residue, which was extracted with diethyl ether (×2). The orange ether extract was concentrated and left in the freezer. A precipitate formed, which was then filtered. The obtained filtrate was evaporated to give an orange solid, and this was recrystallised from dichloromethane/hexane.

Yield: 0.1184 g, 0.163 mmol (33%).

Characterisation:

Calculated for $C_{39}H_{45}ClOP_2Ru$ (727.87 g mol^{-1}): C 64.3; H 6.2; Cl 4.9%

Found: C 64.1; H 6.3; Cl 5.1%

^{1}H NMR ($C_6D_5CD_3$, 500.57 MHz, 300.0 K)

δ 7.64-6.82 [20H, $(C_6\underline{H}_5)_4P_2CH_2$], 4.47 [dt, $^{2}J_{(H-H)}$ = 14.5 Hz, $^{2}J_{(H-P)}$ = 9.4 Hz, 1H, $(C_6H_5)_4P_2C\underline{H}_2$], 4.22 [dt, $^{2}J_{(H-H)}$ = 14.2 Hz, $^{2}J_{(H-P)}$ = 11.3 Hz, 1H, $(C_6H_5)_4P_2C\underline{H}_2$], 3.26 [t, $^{3}J_{(H-H)}$ = 6.2 Hz, 2H, $C_5(CH_3)_4(CH_2)_4C\underline{H}_2OH$], 2.23 [m, 2H, $C_5(CH_3)_4(C\underline{H}_2)_4CH_2OH$], 1.81 [t, $^{4}J_{(H-P)}$ = 1.9 Hz, 6H, $C_5(C\underline{H}_3)_4(CH_2)_4CH_2OH$], 1.79

[t, $^{4}J_{(H-P)}$ = 2.0 Hz, 6H, $C_5(C\underline{H}_3)_4(CH_2)_4CH_2OH$], 1.36 [quint, $^{3}J_{(H-H)}$ = 7.6 Hz, 2H, $C_5(CH_3)_4(C\underline{H}_2)_4CH_2OH$], 1.25 [m, 4H, $C_5(CH_3)_4(C\underline{H}_2)_4CH_2OH$];

$^{31}P\{^{1}H\}$ NMR ($C_6D_5CD_3$, 121.49 MHz, 300.0 K) δ 12.38 [s];

$^{13}C\{^{1}H\}$ NMR ($C_6D_5CD_3$, 125.77 MHz, 299.2 K)

δ 137.5 [s, $(\underline{C}_6H_5)_4P_2CH_2$], 133.7 [t, $^{2,3}J_{(C-P)}$ = 5.4 Hz, $(\underline{C}_6H_5)_4P_2CH_2$], 133.0 [t, $^{2,3}J_{(C-P)}$ = 5.4 Hz, $(\underline{C}_6H_5)_4P_2CH_2$], 92.6 [m, $\underline{C}_5(CH_3)_4(CH_2)_4CH_2OH$], 89.1 [t, $^{2}J_{(C-P)}$ = 2.6 Hz, $\underline{C}_5(CH_3)_4(CH_2)_4CH_2OH$], 87.9 [t, $^{2}J_{(C-P)}$ = 2.6 Hz, $\underline{C}_5(CH_3)_4(CH_2)_4CH_2OH$], 62.6 [s, $C_5(CH_3)_4(CH_2)_4\underline{C}H_2OH$], 49.2 [t, $^{1}J_{(C-P)}$ = 19.2 Hz, $(C_6H_5)_4P_2\underline{C}H_2$], 33.1 [s, $C_5(CH_3)_4(\underline{C}H_2)_4CH_2OH$], 30.8 [s, $C_5(CH_3)_4(\underline{C}H_2)_4CH_2OH$], 26.6 [s, $C_5(CH_3)_4(\underline{C}H_2)_4CH_2OH$], 26.4 [s, $C_5(CH_3)_4(\underline{C}H_2)_4CH_2OH$], 10.9 [s, $C_5(\underline{C}H_3)_4(CH_2)_4CH_2OH$], 10.8 [s, $C_5(\underline{C}H_3)_4(CH_2)_4CH_2OH$].

ES MS (+): m/z 693.2 $[M - Cl]^+$.

7.8.6 Preparation of $[RuCl(C_{14}H_{23})(C_{34}H_{28}FeP_2)]$ (4.10)

1,1'-Bis(diphenylphosphino)ferrocene (0.42 g, 0.75 mmol) was added to a solution of compound **4.4** (0.19 g, 0.5 mmol) in dry dichloromethane (100 ml) and the mixture was stirred under nitrogen overnight. The solvent was evaporated to give an orange/brown residue, which was washed with diethyl ether (×4) and recrystallised from dichloromethane/hexane to give a dark yellow solid.

Yield: 0.3852 g, 0.43 mmol (86%).

Characterisation:

Calculated for $C_{48}H_{51}ClFeOP_2Ru$ (897.76 g mol^{-1}): C 64.2; H 5.7; Cl 4.0%

Found: C 64.1; H 5.6; Cl 4.4%

^{1}H NMR ($C_6D_5CD_3$, 500.13 MHz, 299.2 K)

δ 8.17-6.82 [20H, $(C_6\underline{H}_5)_4P_2Fe(C_5H_4)_2$], 5.48 [s, 2H, $(C_6H_5)_4P_2Fe(C_5\underline{H}_4)_2$], 4.01 [s, 2H, $(C_6H_5)_4P_2Fe(C_5\underline{H}_4)_2$], 3.88 [s, 2H, $(C_6H_5)_4P_2Fe(C_5\underline{H}_4)_2$], 3.64 [s, 2H, $(C_6H_5)_4P_2Fe(C_5\underline{H}_4)_2$], 3.22 [m, 2H, $C_5(CH_3)_4(CH_2)_4C\underline{H}_2OH$], 1.52 [m, 2H, $C_5(CH_3)_4(C\underline{H}_2)_4CH_2OH$], 1.35 [br. s, 2H, $C_5(CH_3)_4(C\underline{H}_2)_4CH_2OH$], 1.31 [m, 2H,

$C_5(CH_3)_4(C\underline{H}_2)_4CH_2OH]$, 1.24 [br. s, 6H, $C_5(C\underline{H}_3)_4(CH_2)_4CH_2OH]$, 1.20 [br. s, 6H, of $C_5(C\underline{H}_3)_4(CH_2)_4CH_2OH]$, 1.11 [t, $^3J_{(H-H)}$ = 7.0 Hz, 2H, $C_5(CH_3)_4(C\underline{H}_2)_4CH_2OH]$;

$^{31}P\{^1H\}$ NMR ($C_6D_5CD_3$, 121.49 MHz, 300.0 K) δ 40.86 [s];

$^{13}C\{^1H\}$ NMR ($C_6D_5CD_3$, 125.77 MHz, 299.2 K)

δ 137.5 [s, $(\underline{C}_6H_5)_4P_2Fe(C_5H_4)_2]$, 136.9 [m, $(\underline{C}_6H_5)_4P_2Fe(C_5H_4)_2]$, 134.9 [m, $(\underline{C}_6H_5)_4P_2Fe(C_5H_4)_2]$, 77.8 [s, $(C_6H_5)_4P_2Fe(\underline{C}_5H_4)_2]$, 72.8 [s, $(C_6H_5)_4P_2Fe(\underline{C}_5H_4)_2]$, 72.2 [s, $(C_6H_5)_4P_2Fe(\underline{C}_5H_4)_2]$, 67.3 [s, $(C_6H_5)_4P_2Fe(\underline{C}_5H_4)_2]$, 62.6 [s, $C_5(CH_3)_4(CH_2)_4\underline{C}H_2OH]$, 32.8 [s, $C_5(CH_3)_4(\underline{C}H_2)_4CH_2OH]$, 29.3 [s, $C_5(CH_3)_4(\underline{C}H_2)_4CH_2OH]$, 26.6 [s, $C_5(CH_3)_4(\underline{C}H_2)_4CH_2OH]$, 24.3 [s, $C_5(CH_3)_4(\underline{C}H_2)_4CH_2OH]$, 9.4 [s, $C_5(\underline{C}H_3)_4(CH_2)_4CH_2OH]$, 9.3 [s, $C_5(\underline{C}H_3)_4(CH_2)_4CH_2OH]$.

ES MS (+): m/z 863.2 $[M - Cl]^+$.

7.8.7 Preparation of $[RuCl(C_{14}H_{23})(C_{39}H_{32}OP_2)]$ (4.11)

4,5-Bis(diphenylphosphino)-9,9-dimethylxanthene (0.43 g, 0.75 mmol) was added to a solution of compound **4.4** (0.19 g, 0.5 mmol) in dry dichloromethane (100 ml) and the mixture was stirred under nitrogen overnight. The solvent was evaporated to give a brown residue, which was extracted with diethyl ether (×4). The yellow ether extract was concentrated and left in the freezer overnight. The precipitate formed was filtered, and the orange filtrate evaporated. The residue was recrystallised from dichloromethane/hexane to give a yellow solid.

Yield: 0.0897 g, 0.097 mmol (19%).

Characterisation:

Calculated for $C_{53}H_{55}ClO_2P_2Ru$ (921.94 g mol^{-1}): C 69.0; H 6.0; Cl 3.9%

Found: C 68.3; H 6.1; Cl 4.3%

^1H NMR ($C_6D_5CD_3$, 300.13 MHz, 300.0 K)

δ 8.20-6.49 [26H, $(C_6\underline{H}_5)_4P_2OC(CH_3)_2(C_6\underline{H}_3)_2]$, 3.15 [t, $^3J_{(H-H)}$ = 6.2 Hz, 2H, $C_5(CH_3)_4(CH_2)_4C\underline{H}_2OH]$, 1.64 [s, 3H, $(C_6H_5)_4P_2OC(C\underline{H}_3)_2(C_6H_3)_2]$, 1.59 [s, 3H, $(C_6H_5)_4P_2OC(C\underline{H}_3)_2(C_6H_3)_2]$, 1.57 [br. s, 6H, $C_5(C\underline{H}_3)_4(CH_2)_4CH_2OH]$, 1.29 [m, 2H,

$C_5(CH_3)_4(C\underline{H}_2)_4CH_2OH]$, 0.98 [br. s, 6H, $C_5(C\underline{H}_3)_4(CH_2)_4CH_2OH]$, 0.85 [m, 4H, $C_5(CH_3)_4(C\underline{H}_2)_4CH_2OH]$, 0.45 [m, 2H, $C_5(CH_3)_4(C\underline{H}_2)_4CH_2OH]$;

$^{31}P\{^1H\}$ NMR ($C_6D_5CD_3$, 202.63 MHz, 300.0 K) δ 33.26 [s];

$^{13}C\{^1H\}$ NMR ($C_6D_5CD_3$, 125.77 MHz, 299.2 K)

δ 137.5 [$(\underline{C}_6H_5)_4P_2OC(CH_3)_2(\underline{C}_6H_3)_2]$, 92.4 [s, $\underline{C}_5(CH_3)_4(CH_2)_4CH_2OH]$, 62.5 [s, $C_5(CH_3)_4(CH_2)_4\underline{C}H_2OH]$, 36.8 [s, $(C_6H_5)_4P_2O\underline{C}(CH_3)_2(C_6H_3)_2]$, 32.0 [s, $C_5(CH_3)_4(\underline{C}H_2)_4CH_2OH]$, 30.7 [s, $C_5(CH_3)_4(\underline{C}H_2)_4CH_2OH]$, 30.3 [s, $(C_6H_5)_4P_2OC(\underline{C}H_3)_2(C_6H_3)_2]$, 26.7 [s, $C_5(CH_3)_4(\underline{C}H_2)_4CH_2OH]$, 23.6 [s, $C_5(CH_3)_4(\underline{C}H_2)_4CH_2OH]$, 23.1 [s, $(C_6H_5)_4P_2OC(\underline{C}H_3)_2(C_6H_3)_2]$, 9.6 [s, $C_5(\underline{C}H_3)_4(CH_2)_4CH_2OH]$, 9.2 [s, $C_5(\underline{C}H_3)_4(CH_2)_4CH_2OH]$.

ES MS (+): m/z 922.2 $[M]^+$; 887.3 $[M\text{-}Cl]^+$.

7.8.8 Preparation of $[Ru(CH_3CN)(C_{10}H_{15})(C_{25}H_{22}P_2)][SbF_6]$ (4.12)

Dry methanol (80 ml) and dry acetonitrile (4 ml) were added to a mixture of complex **4.5** (0.15 g, 0.23 mmol) and $NaSbF_6$ (0.6 g, 2.3 mmol) under nitrogen. The initial orange suspension changed to a light yellow solution, and this was stirred overnight. The solvent was evaporated and the residue treated with dichloromethane and filtered. The filtrate was concentrated and, after adding diethyl ether and placing the mixture in the freezer for some hours, the light yellow precipitate formed was filtered off, washed with diethyl ether and dried.

Yield: 0.1597 g, 0.178 mmol (77%).

Characterisation:

Calculated for $C_{37}H_{40}F_6NP_2RuSb$ (897.07 g mol^{-1}): C 49.5; H 4.5; N 1.6%

Found: C 49.6; H 4.6; N 1.5%

^1H NMR (CD_2Cl_2, 300.13 MHz, 300.0 K)

δ 7.49 [m, 16H, $(C_6\underline{H}_5)_4P_2CH_2]$, 7.36 [m, 4H, $(C_6\underline{H}_5)_4P_2CH_2]$, 5.13 [dt, $^2J_{(H\text{-}H)}$ = 16 Hz, $^2J_{(H\text{-}P)}$ = 9.8 Hz, 1H, $(C_6H_5)_4P_2C\underline{H}_2]$, 4.37 [dt, $^2J_{(H\text{-}H)}$ = 16 Hz, $^2J_{(H\text{-}P)}$ = 10.5 Hz, 1H, $(C_6H_5)_4P_2C\underline{H}_2]$, 1.64 [t, $^5J_{(H\text{-}P)}$ = 1.7 Hz, 3H, $C\underline{H}_3CN]$, 1.59 [t, $^4J_{(H\text{-}P)}$ = 2.2 Hz 15H, $C_5(C\underline{H}_3)_5]$;

$^{31}P\{^{1}H\}$ NMR (CD_2Cl_2, 121.49 MHz, 300.0 K) δ 9.56 [s];

$^{13}C\{^{1}H\}$ NMR (CD_2Cl_2, 125.88 MHz, 300.0 K)

δ 155.9 [s, $CH_3\underline{C}N$], 132.8 [m, $(\underline{C_6}H_5)_4P_2CH_2$], 131.9 [t, $^{2,3}J_{(C-P)}$ = 5.2 Hz, $(\underline{C_6}H_5)_4P_2CH_2$], 131.2 [d, $^{1}J_{(C-P)}$ = 32.7 Hz, $(\underline{C_6}H_5)_4P_2CH_2$], 129.3 [dt, $^{2,3}J_{(C-P)}$ = 18.7, 5.2 Hz, $(\underline{C_6}H_5)_4P_2CH_2$], 92.0 [s, $\underline{C_5}(CH_3)_5$], 51.3 [s, $(C_6H_5)_4P_2\underline{C}H_2$], 10.2 [s, $C_5(C\underline{H_3})_5$], 3.8 [s, $\underline{C}H_3CN$].

ES MS (+): m/z 662.2 $[M\text{-}SbF_6]^+$.

7.9 Tetramethylfulvene Ruthenium(II) Complexes

The compounds **4.13** and **4.14** were obtained from complex **4.3** and commercial diphenylacac (dibenzoylmethane) using different amounts of triethylamine in dichloromethane or toluene respectively.

7.9.1 Preparation of $[RuCl(C_{10}H_{14})(C_{15}H_{11}O_2)]$ (4.13)

Complex **4.3** (0.2 g, 0.65 mmol) was dissolved in dry dichloromethane (50 ml) and diphenylacac (0.15 g, 0.65 mmol) and triethylamine (0.18 ml, 1.3 mmol) were added. The mixture was stirred at room temperature overnight, the solvent evaporated and the brown residue treated with dichloromethane and diethyl ether. Triethylamine hydrochloride precipitated. The filtrate was evaporated and the residue washed with pentane and recrystallised in a mixture of dichloromethane and hexane at -20ºC.

Yield: 0.142 g, 0.29 mmol (44%).

Characterisation:

Calculated for $C_{25}H_{25}ClO_2Ru$ (493.77 g mol^{-1}): C 60.8; H 5.1; Cl 7.2%

Found: C 60.3; H 5.2; Cl 6.7%

^{1}H NMR ($CDCl_3$, 300.13 MHz, 299.9 K)

δ 7.96 [m, 5H, $CH(COC_6\underline{H_5})_2$], 7.42 [m, 5H, $CH(COC_6\underline{H_5})_2$], 6.62 [s, 1H, $C\underline{H}(COC_6H_5)_2$], 5.42 [s, 1H, $C_5(CH_3)_4C\underline{H_2}$], 5.01 [s, 1H, $C_5(CH_3)_4C\underline{H_2}$], 1.98 [s, 3H,

$C_5(C\underline{H}_3)_4CH_2$], 1.78 [s, 3H, $C_5(C\underline{H}_3)_4CH_2$], 1.70 [s, 3H, $C_5(C\underline{H}_3)_4CH_2$], 1.54 [s, 3H, $C_5(C\underline{H}_3)_4CH_2$];

$^{13}C\{^1H\}$ NMR ($CDCl_3$, 125.88 MHz, 300.0 K)

δ 181.8 [$CH(\underline{C}OC_6H_5)_2$], 180.5 [$CH(\underline{C}OC_6H_5)_2$], 139.5 [Quaternary C of $CH(CO\underline{C}_6H_5)_2$], 139.0 [Quaternary C of $CH(CO\underline{C}_6H_5)_2$], 130.9 [$CH(CO\underline{C}_6H_5)_2$], 130.8 [$CH(CO\underline{C}_6H_5)_2$], 128.2 [$CH(CO\underline{C}_6H_5)_2$], 128.1 [$CH(CO\underline{C}_6H_5)_2$], 127.2 [$CH(CO\underline{C}_6H_5)_2$], 127.1 [$CH(CO\underline{C}_6H_5)_2$], 103.0 [$\underline{C}_5(CH_3)_4CH_2$], 101.5 [$\underline{C}_5(CH_3)_4CH_2$], 100.3 [$\underline{C}_5(CH_3)_4CH_2$], 97.0 [$\underline{C}_5(CH_3)_4CH_2$], 95.0 [$\underline{C}_5(CH_3)_4CH_2$], 93.8 [$\underline{C}H(COC_6H_5)_2$], 80.5 [$C_5(CH_3)_4\underline{C}H_2$], 8.8 [$C_5(\underline{C}H_3)_4CH_2$], 8.3 [$C_5(\underline{C}H_3)_4CH_2$], 8.2 [$C_5(\underline{C}H_3)_4CH_2$], 7.6 [$C_5(\underline{C}H_3)_4CH_2$].

ES MS (+): m/z 459.09 $[M\text{-}Cl]^+$.

7.9.2 Preparation of $[RuCl_3(C_{10}H_{14})][Ru(C_{10}H_{15})(C_7H_8)]$ (4.14)

Complex **4.3** (0.15 g, 0.5 mmol) was dissolved in dry toluene (50 ml) and diphenylacac (0.11 g, 0.5 mmol) and triethylamine (70 μl, 0.5 mmol) were added. The mixture was stirred at reflux for two hours, filtered, the solvent evaporated and the orange residue treated with dichloromethane and diethyl ether, from where dark orange crystals formed at -20ºC.

Characterisation:

Calculated for $C_{27}H_{37}Cl_3Ru_2$ (669.93 g mol^{-1}): C 48.4; H 5.6; Cl 15.9%

Found: C 48.2; H 5.6; Cl 16.0%

ES MS (+): m/z 329.1 $[C_{17}H_{23}Ru]^+$.

7.10 Dppf η^6-*p*-Cymene Ruthenium Complexes

Complex **5.1** was prepared and isolated by Mr. Joel Fonseca, former member of the McGowan group.[19]

7.10.1 Preparation of $[RuCl(C_{10}H_{14})(C_{34}H_{28}FeP_2)][Cl]$ (5.1)

A mixture of complex **3.1** (0.15 g, 0.25 mmol) and 1,1'-bis(diphenylphosphino)ferrocene (0.28 g, 0.5 mmol) in ethanol (8 ml) and benzene

(1 ml) was heated to 55°C for 50 minutes and then stirred overnight. After evaporating the solvent, dichloromethane was used to dissolve the residue and diethyl ether added to precipitate a dark yellow solid. This was recrystallised from methanol/diethyl ether.

Yield: 0.2295 g, 0.267 mmol (53%).

Characterisation:

Calculated for $C_{44}H_{42}Cl_2FeP_2Ru$ (860.09 g mol^{-1}): C 61.4; H 4.9; Cl 8.2%

Found: C 58.8; H 5.0; Cl 8.2%

^{1}H NMR ($CDCl_3$, 500.23 MHz, 300.0 K)

δ 7.73 [br. s, 6H, $(C_6\underline{H}_5)_4P_2Fe(C_5H_4)_2$], 7.61 [br. s, 8H, $(C_6\underline{H}_5)_4P_2Fe(C_5H_4)_2$], 7.46 [br. s, 6H, $(C_6\underline{H}_5)_4P_2Fe(C_5H_4)_2$], 5.89 [br. s, 2H, $CH_3C(C\underline{H})_2(CH)_2CCH(CH_3)_2$], 5.19 [br. s, 2H, $CH_3C(CH)_2(C\underline{H})_2CCH(CH_3)_2$], 5.07 [s, 2H, $(C_6H_5)_4P_2Fe(C_5\underline{H}_4)_2$], 4.36 [s, 2H, $(C_6H_5)_4P_2Fe(C_5\underline{H}_4)_2$], 4.27 [s, 2H, $(C_6H_5)_4P_2Fe(C_5\underline{H}_4)_2$], 4.08 [s, 2H, $(C_6H_5)_4P_2Fe(C_5\underline{H}_4)_2$], 2.68 [m, 1H, $CH_3C(CH)_2(CH)_2CC\underline{H}(CH_3)_2$], 1.10 [s, 3H, $C\underline{H}_3C(CH)_2(CH)_2CCH(CH_3)_2$], 0.90 [d, $^3J_{HH}$ = 6.4 Hz, 6H, $CH_3C(CH)_2(CH)_2CCH(C\underline{H}_3)_2$];

^{31}P{^{1}H} NMR ($CDCl_3$, 121.49 MHz, 300.0 K) δ 36.44 [s];

^{13}C{^{1}H} NMR ($CDCl_3$, 125.88 MHz, 300.0 K)

δ 183.3-128.6 [$(\underline{C}_6H_5)_4P_2Fe(C_5H_4)_2$], 99.4 [$CH_3C(CH)_2(CH)_2\underline{C}CH(CH_3)_2$], 96.9 [$CH_3\underline{C}(CH)_2(CH)_2CCH(CH_3)_2$], 90.9 [Quaternary C of $(C_6H_5)_4P_2Fe(\underline{C}_5H_4)_2$], 83.9 [$CH_3C(\underline{C}H)_2(CH)_2CCH(CH_3)_2$], 83.4 [$CH_3C(CH)_2(\underline{C}H)_2CCH(CH_3)_2$], 78.6 [$(C_6H_5)_4P_2Fe(\underline{C}_5H_4)_2$], 74.7 [$(C_6H_5)_4P_2Fe(\underline{C}_5H_4)_2$], 73.7 [$(C_6H_5)_4P_2Fe(\underline{C}_5H_4)_2$], 69.1 [$(C_6H_5)_4P_2Fe(\underline{C}_5H_4)_2$], 31.0 [$CH_3C(CH)_2(CH)_2C\underline{C}H(CH_3)_2$], 20.9 [$CH_3C(CH)_2(CH)_2CCH(\underline{C}H_3)_2$], 15.8 [$\underline{C}H_3C(CH)_2(CH)_2CCH(CH_3)_2$].

ES MS (+): m/z 825.1 $[M\text{-}Cl]^+$.

7.10.2 Preparation of $[Ru_2Cl_4(C_{10}H_{14})_2(C_{34}H_{28}FeP_2)]$ (5.2)

Complex **3.1** (0.2 g, 0.33 mmol) and 1,1'-bis(diphenylphosphino)ferrocene (0.18 g, 0.33 mmol) were dissolved in dichloromethane (20 ml) and stirred overnight

at room temperature. After that, the solution was concentrated, diethyl ether added and a precipitate formed. The mixture was kept in the freezer for 1 hour and then the orange precipitate was filtered, washed with diethyl ether and dried under vacuum.

Yield: 0.2866 g, 0.246 mmol (74%).

Characterisation:

Calculated for $C_{54}H_{56}Cl_4FeP_2Ru_2$ (1166.18 g mol^{-1}) + $\frac{1}{2}CH_2Cl_2$ (42.46 g mol^{-1}): C 54.1; H 4.8; Cl 14.7%

Found: C 54.0; H 4.8; Cl 14.5%

^{1}H NMR ($CDCl_3$, 300.13 MHz, 300.1 K)

δ 7.74 [t, $^3J_{(H-H)}$ = 7.9 Hz, 8H, $(C_6\underline{H}_5)_4P_2Fe(C_5H_4)_2$], 7.38 [br. s, 12H, $(C_6\underline{H}_5)_4P_2Fe(C_5H_4)_2$], 5.07 [br. s, 8H, $CH_3(C_6\underline{H}_4)CH(CH_3)_2$], 4.17 [br. s, 4H, $(C_6H_5)_4P_2Fe(C_5\underline{H}_4)_2$], 3.89 [br. s, 4H, $(C_6H_5)_4P_2Fe(C_5\underline{H}_4)_2$], 2.51 [m, 2H, $CH_3(C_6H_4)C\underline{H}(CH_3)_2$], 1.71 [s, 6H, $C\underline{H}_3(C_6H_4)CH(CH_3)_2$], 0.97 [d, $^3J_{(H-H)}$ = 6.6 Hz, 12H, $CH_3(C_6H_4)CH(C\underline{H}_3)_2$];

^{31}P{^{1}H} NMR ($CDCl_3$, 121.49 MHz, 299.8 K) δ 18.19 [s].

^{13}C{^{1}H} NMR ($CDCl_3$, 125.88 MHz, 300.0 K)

δ 136.3 [$(\underline{C}_6H_5)_4P_2Fe(C_5H_4)_2$], 136.0 [$(\underline{C}_6H_5)_4P_2Fe(C_5H_4)_2$], 134.0 [$(\underline{C}_6H_5)_4P_2Fe(C_5H_4)_2$], 130.0 [$(\underline{C}_6H_5)_4P_2Fe(C_5H_4)_2$], 127.5 [$(\underline{C}_6H_5)_4P_2Fe(C_5H_4)_2$], 109.6 [$CH_3C(CH)_2(CH)_2\underline{C}CH(CH_3)_2$], 95.3 [$CH_3\underline{C}(CH)_2(CH)_2CCH(CH_3)_2$], 90.0 [$CH_3C(\underline{C}H)_2(CH)_2CCH(CH_3)_2$], 85.9 [$CH_3C(CH)_2(\underline{C}H)_2CCH(CH_3)_2$], 75.7 [$(C_6H_5)_4P_2Fe(\underline{C}_5H_4)_2$], 74.3 [$(C_6H_5)_4P_2Fe(\underline{C}_5H_4)_2$], 29.9 [$CH_3C(C_4H_4)C\underline{C}H(CH_3)_2$], 21.8 [$CH_3C(C_4H_4)CCH(\underline{C}H_3)_2$], 17.0 [$\underline{C}H_3C(C_4H_4)CCH(CH_3)_2$].

ES MS (+): m/z 1131.0 $[M\text{-}Cl]^+$; 1191 $[M+Na]^+$.

7.11 Experimental Procedures for Homogeneous Catalysis

The procedures presented below are only general, and some variations may have been reported in **Chapter 5**.

7.11.1 Redox Neutral Alkylation of *tert*-Butylamine with Phenethyl Alcohol

Phenethyl alcohol (0.36 ml, 3 mmol) and toluene (10 ml) were added to a mixture of the corresponding ruthenium species (if used, 5 mol% Ru) and dppf (if used, 5 mol%) in a 25 ml round bottom flask with a suba-seal at the side-neck. The mixture was stirred at reflux for 10 minutes. After this time, *tert*-butylamine (0.32 ml, 3 mmol) was added and the first sample of 20 μl was taken with a micro syringe through the suba-seal, dissolved in 2 ml of acetonitrile and kept in the freezer. Samples were taken at 0, 20, 40, 60, 90, 120, 180, 300, 540 and 1440 min, thus maintaining the reflux for 24 hours.

All of the samples were analysed by gas chromatography. Injection volume = 1μl. The oven temperature ramped from 60ºC (hold for 3 minutes) to 280ºC (hold for 3 minutes) at 20ºC/min. Inlet pressure = 4.3 psi. The retention time for phenethyl alcohol is approximately 7.0 minutes, and the retention time for N-phenethyl-*tert*-butylamine is 8.8 minutes.

The solvent was evaporated from the final reaction mixture after 24 hours and the residue analysed by ^{1}H NMR:

^{1}H NMR of phenethyl alcohol ($CDCl_3$, 500.23 MHz, 300.0 K)

δ 7.36-7.17 [m, 5H, $C_6\underline{H}_5(CH_2)_2OH$], 3.85 [t, $^{3}J_{(H\text{-}H)}$ = 6.6 Hz, 2H, $C_6H_5(C\underline{H}_2)_2OH$], 2.87 [t, $^{3}J_{(H\text{-}H)}$ = 6.8 Hz, 2H, $C_6H_5(C\underline{H}_2)_2OH$].

^{1}H NMR of N-phenethyl-*tert*-butylamine ($CDCl_3$, 500.23 MHz, 300.0 K)

δ 7.36-7.17 [m, 5H, $C_6\underline{H}_5(CH_2)_2NHC(CH_3)_3$], 2.80 [m, 4H, $C_6H_5(C\underline{H}_2)_2NHC(CH_3)_3$], 1.07 [s, 9H, $C_6H_5(CH_2)_2NHC(C\underline{H}_3)_3$].

7.11.2 Benzaldehyde Reduction

Isopropanol (10 ml) was added to a mixture of the corresponding ruthenium species (if used, 5 mol% Ru) and the ligand (dppf or (R,R)-TsDPEN, if used, 5 mol%) in a 25 ml round bottom flask with a suba-seal at the side-neck. Triethylamine (5 μl, 0.08 mmol, 8 mol%) was added next and the mixture was stirred at reflux for half an hour. After this time, benzaldehyde (0.1 ml, 1 mmol) was added and the first sample of 20 μl was taken with a micro syringe through the suba-

seal, dissolved in 2 ml of acetonitrile and kept in the freezer. Samples were taken at 0, 20, 40, 60, 90, 120, 180, 300, 540 and 1440 min, thus maintaining the reflux for 24 hours.

All of the samples were analysed by gas chromatography. Injection volume = 1 µl. The oven temperature ramped from 60ºC (hold for 3 minutes) to 200ºC (hold for 3 minutes) at 20ºC/min. Inlet pressure = 4.3 psi. The retention time for benzaldehyde is 5.2 minutes and the retention time for benzylalcohol is approximately 6.2 minutes.

The solvent was evaporated from the final reaction mixture after 24 hours and the residue analysed by ^{1}H NMR:

^{1}H NMR of benzaldehyde ($CDCl_3$, 300.13 MHz, 294.4 K)

δ 9.88 [s, 1H, $C_6H_5CO\underline{H}$], 7.77 [d, $^{3}J_{(H-H)}$ = 7.0 Hz, 2H, $C_6\underline{H}_5COH$], 7.53 [t, $^{3}J_{(H-H)}$ = 7.4 Hz, 1H, $C_6\underline{H}_5COH$], 7.44 [d, $^{3}J_{(H-H)}$ = 7.6 Hz, 2H, $C_6\underline{H}_5COH$].

^{1}H NMR of benzyl alcohol ($CDCl_3$, 300.13 MHz, 294.4 K)

δ 7.25-7.23 [m, 5H, $C_6\underline{H}_5CH_2OH$], 4.54 [s, 2H, $C_6H_5C\underline{H}_2OH$], 2.91 [br. s, 1H, $C_6H_5CH_2O\underline{H}$].

7.12 Cp* Ruthenium Aqua Complex

7.12.1 Preparation of $[Ru(H_2O)(C_{10}H_{15})(C_{25}H_{22}P_2)][X]$ (6.1)

Compound **6.1** formed slowly inside NMR tubes from either complex **4.5** (X = Cl) or complex **4.12** (X = SbF_6) in solutions of 90% deuterated dimethylsulfoxide and 10% deuterium oxide, giving very light yellow solutions after 100% conversion.

Characterisation:

^{1}H NMR ($(CD_3)_2SO$, 500.57 MHz, 300.0 K)

δ 7.60 [q, $^{3}J_{(H-H)}$ = 5.8 Hz, 4H, $(C_6\underline{H}_5)_4P_2CH_2$], 7.51 [m, 8H, $(C_6\underline{H}_5)_4P_2CH_2$], 7.40 [t, $^{3}J_{(H-H)}$ = 7.5 Hz, 4H, $(C_6\underline{H}_5)_4P_2CH_2$], 7.30 [m, 4H, $(C_6\underline{H}_5)_4P_2CH_2$], 5.14 [m, 2H, $(C_6H_5)_4P_2C\underline{H}_2$], 1.61 [s, 15H, $C_5(C\underline{H}_3)_5$];

^{31}P{^{1}H} NMR ($(CD_3)_2SO$, 121.49 MHz, 300.0 K) δ 5.07 [s];

$^{13}C\{^{1}H\}$ NMR ($(CD_3)_2SO$, 125.88 MHz, 300.0 K)

δ 134.6 [m, ($\underline{C}_6H_5)_4P_2CH_2$], 132.3 [m, ($\underline{C}_6H_5)_4P_2CH_2$], 131.7 [t, $^{2,3}J_{(C-P)}$ = 4.9 Hz, ($\underline{C}_6H_5)_4P_2CH_2$], 130.8 [t, $^{2,3}J_{(C-P)}$ = 5.2 Hz, ($\underline{C}_6H_5)_4P_2CH_2$], 130.7 [s, ($\underline{C}_6H_5)_4P_2CH_2$], 130.5 [s, ($\underline{C}_6H_5)_4P_2CH_2$], 128.9 [t, $^{2,3}J_{(C-P)}$ = 4.7 Hz, ($\underline{C}_6H_5)_4P_2CH_2$], 128.5 [t, $^{2,3}J_{(C-P)}$ = 4.7 Hz, ($\underline{C}_6H_5)_4P_2CH_2$], 94.5 [s, $\underline{C}_5(CH_3)_5$], 44.5 [s, $(C_6H_5)_4P_2\underline{C}H_2$], 10.3 [s, $C_5(\underline{C}H_3)_5$].

ES MS (+): m/z 621.1 $[M\text{-}H_2O]^+$.

7.13 Experimental Procedure for Cell Line Assessments

The *in vitro* studies were performed at the Institute of Cancer Therapeutics, Bradford, on the cell lines A2780 (human ovarian carcinoma) and HT29 (human colon carcinoma) by Miss Aida Basri and Miss Rianne Lord respectively. Cells were incubated in 96-well plates at a cell concentration of 2.0 x 10^4 cells/mL. Complete cell media containing RPMI-1640, supplemented with 10% foetal calf serum, sodium pyruvate (1 mM) and L-glutamine (2 mM), was used to prepare the desired cell concentration and reference wells. Plates containing cells were incubated for 24 hours at 37 °C in an atmosphere of 5% CO_2, prior to drug exposure. All compounds were dissolved in dimethylsulfoxide to give an initial concentration of 25 mM and diluted further with cell media to obtain concentrations ranging from 250-0.49 μM. A final dimethylsulfoxide concentration of 0.1% (v/v) was obtained, which is non-toxic to cells. 100 μL of cell media was added to the reference cells and 100 μL of differing concentrations of drug solution were added to the remaining wells. The plates were incubated for a further 5 days at 37 °C in an atmosphere of 5% CO_2. 20 μL of 3-(4,5-dimethylthiazol-1-yl)-2,5-diphenyltetrazolium bromide (MTT) solution (5 mg/mL) was added to each well and incubated for a further 3 hours at 37 °C in an atmosphere of 5% CO_2. Upon completion all solutions were removed from the wells *via* pipette, and 150 μL of dimethylsulfoxide was added to each well to dissolve the purple formazan crystals. A Thermo Scientific Multiskan EX microplate photometer was used to measure the absorbance at 540 nm. Lanes containing 100% cell media and 100% cell solution were used as a blank and 100% cell survival respectively. Cell survival was determined as the absorbance of treated cells minus the blank cell media, divided by the absorbance of the 100% cell solution; this value was expressed

as a percentage. The IC_{50} values were determined from a plot of percentage cell survival against drug concentration (μM), and each experiment was carried out three times to obtain average IC_{50} values.

7.14 References

1. J. Cosier and A. M. Glazer, *Journal of Applied Crystallography*, 1986, **19**, 105-107.
2. G. M. Sheldrick, University of Gottingen, 1997, pp. 'SHELXL97', Program for Crystall Structure Refinement.
3. L. J. Barbour, University of Missouri, 1999, p. 'XSeed'.
4. M. Thomton-Pett, University of Leeds, 2000, pp. 'WC-A Windows CIF Processor'.
5. R. Stodt, S. Gencaslan, Iris M. Müller and William S. Sheldrick, *European Journal of Inorganic Chemistry*, 2003, **2003**, 1873-1882.
6. K. D. Camm, *PhD Thesis*, University of Leeds, 2004.
7. M. G. Mendoza-Ferri, C. G. Hartinger, A. A. Nazarov, R. E. Eichinger, M. A. Jakupec, K. Severin and B. K. Keppler, *Organometallics*, 2009, **28**, 6260-6265.
8. T. Screen, *Personal communication*.
9. Z. Almodares, *PhD Thesis*, University of Leeds, 2010.
10. R. S. Bates, M. J. Begley and A. H. Wright, *Polyhedron*, 1990, **9**, 1113-1118.
11. M. A. Bennett and A. K. Smith, *Journal of the Chemical Society, Dalton Transactions*, 1974, 233-241.
12. R. Aronson, M. R. J. Elsegood, J. W. Steed and D. A. Tocher, *Polyhedron*, 1991, **10**, 1727-1732.
13. T. Sixt, M. Sieger, M. J. Krafft, D. Bubrin, J. Fiedler and W. Kaim, *Organometallics*, 2010, **29**, 5511-5516.
14. R. S. Threlkel, J. E. Bercaw, P. F. Seidler, J. M. Stryker and R. G. Bergman, in *Organic Syntheses*, 1987, vol. 65, p. 42.
15. A. J. Blacker, S. Brown, B. Clique, B. Gourlay, C. E. Headley, S. Ingham, D. Ritson, T. Screen, M. J. Stirling, D. Taylor and G. Thompson, *Organic Process Research & Development*, 2009, **13**, 1370-1378.

16. N. Oshima, H. Suzuki and Y. Moro-Oka, *Chemistry Letters*, 1984, **13**, 1161-1164.
17. T. D. Tilley, R. H. Grubbs and J. E. Bercaw, *Organometallics*, 1984, **3**, 274-278.
18. F. Morandini, A. Dondana, I. Munari, G. Pilloni, G. Consiglio, A. Sironi and M. Moret, *Inorganica Chimica Acta*, 1998, **282**, 163-172.
19. J. Fonseca and P. C. McGowan, *Unpublished results*.

Appendix: Summary of Crystallographic Data

Compound **2.9**

Crystal system	Monoclinic		
Space group	$P2_1/c$		
Cell dimensions	a = 7.6638(9) Å	α = 90°	
	b = 23.150(3) Å	β = 90.124(5)°	V = 1306.0(3) Å^3
	c = 7.3612(8) Å	γ = 90°	
Z	2		
Goodness of fit	0.936		

Compound **2.10**

Crystal system	Triclinic		
Space group	$P\ \bar{1}$		
Cell dimensions	a = 8.7685(12) Å	α = 118.520(7)°	
	b = 10.2415(15) Å	β = 95.204(7)°	V = 799.0(2) Å^3
	c = 10.5473(15) Å	γ = 100.907(6)°	
Z	1		
Goodness of fit	1.125		

Compound **3.3**

Crystal system	Monoclinic		
Space group	$P2_1/c$		
Cell dimensions	a = 10.1336(8) Å	α = 90°	
	b = 18.1925(18) Å	β = 93.819(4)°	V = 2134.3(3) Å^3
	c = 11.6027(11) Å	γ = 90°	
Z	4		
Goodness of fit	1.037		

Compound **3.4**

Crystal system	Monoclinic		
Space group	$P2_1/c$		
Cell dimensions	a = 10.0953(15) Å	α = 90°	
	b = 7.9950(11) Å	β = 103.501(6)°	V = 1599.3(4) Å^3
	c = 20.377(3) Å	γ = 90°	
Z	4		
Goodness of fit	1.308		

Compound **3.7**

Crystal system	Monoclinic		
Space group	$P2_1/c$		
Cell dimensions	a = 7.8704(9) Å	α = 90°	
	b = 12.8864(16) Å	β = 103.467(5)°	V = 1564.7(3) Å^3
	c = 15.864(2) Å	γ = 90°	
Z	4		
Goodness of fit	1.32		

Compound **3.8**

Crystal system	Monoclinic		
Space group	$P2_1/c$		
Cell dimensions	a = 9.9656(5) Å	α = 90°	
	b = 7.9319(3) Å	β = 103.628(2)°	V = 1542.77(12) Å^3
	c = 20.0828(9) Å	γ = 90°	
Z	4		
Goodness of fit	1.084		

Compound **3.10**

Crystal system	Monoclinic		
Space group	$P2_1/c$		
Cell dimensions	a = 15.2457(5) Å	α = 90°	
	b = 14.8885(5) Å	β = 92.3380(10)°	V = 1666.05(9) Å^3
	c = 7.3460(2) Å	γ = 90°	
Z	4		
Goodness of fit	1.25		

Compound **3.12**

Crystal system	Monoclinic		
Space group	$P2_1/n$		
Cell dimensions	a = 15.0133(5) Å	α = 90°	
	b = 7.7940(2) Å	β = 92.9020(10)°	V = 1775.98(9) Å^3
	c = 15.1970(5) Å	γ = 90°	
Z	4		
Goodness of fit	1.15		

Compound **3.14**

Crystal system	Orthorhombic		
Space group	*Pbca*		
Cell dimensions	*a* = 12.1237(10) Å	α = 90°	V = 4870.2(7) Å^3
	b = 17.3704(15) Å	β = 90°	
	c = 23.126(2) Å	γ = 90°	
Z	8		
Goodness of fit	1.02		

Compound **4.12**

Crystal system	Triclinic		
Space group	$P\ \bar{1}$		
Cell dimensions	*a* = 10.8236(19) Å	α = 91.890(8)°	V = 1841.5(5) Å^3
	b = 11.4240(19) Å	β = 99.060(8)°	
	c = 15.162(3) Å	γ = 95.244(8)°	
Z	2		
Goodness of fit	1.06		

Compound **4.13**

Crystal system	Orthorhombic		
Space group	$P2_12_12_1$		
Cell dimensions	*a* = 7.5069(15) Å	α = 90°	V = 2194.7(7) Å^3
	b = 11.360(2) Å	β = 90°	
	c = 25.736(5) Å	γ = 90°	
Z	4		
Goodness of fit	1.078		

Compound **4.14**

Crystal system	Monoclinic		
Space group	$P2_1/c$		
Cell dimensions	*a* = 8.7750(14) Å	α = 90°	V = 2645.6(7) Å^3
	b = 24.948(4) Å	β = 124.722(7)°	
	c = 14.7032(18) Å	γ = 90°	
Z	4		
Goodness of fit	1.019		

Compound **5.2**

Crystal system	Triclinic		
Space group	$P\ \bar{1}$		
Cell dimensions	a = 9.6847(11) Å	α = 76.893(5)°	
	b = 11.8387(13) Å	β = 88.748(5)°	V = 1290.5(3) Å^3
	c = 12.4139(15) Å	γ = 68.900(5)°	
Z	2		
Goodness of fit	1.072		